INTERNATIONAL DOCTORAL
SCHOOL OF THE USC

Maite
López López

PhD Thesis

Tear proteomics and corneal biomechanics for identifying keratoconus at-risk stages: new insights into the early molecular networks and pathways.

Santiago de Compostela, 2024

Doctoral Programme in Vision Science

ESCOLA DE DOUTORAMENTO
INTERNACIONAL DA USC

DOCTORAL THESIS

Tear proteomics and corneal biomechanics for identifying keratoconus at-risk stages: new insights into the early molecular networks and pathways.

Author

Maite López López

Supervisors: María Isabel Lema Gesto and Uxía Regueiro Lorenzo

DOCTORAL PROGRAMME IN VISION SCIENCE

SANTIAGO DE COMPOSTELA

2024

Conflict of interest

The author, Maite López López, declares no conflict of interest in relation to this doctoral thesis.

Funding

This study was partially supported by grants from the Instituto de Salud Carlos III (ISCIII) co-financed by the European Union (UE) (PI18/00159, PI23/00323), and the Xunta de Galicia (IN607A2018/3, IN607A2022/03).

Furthermore, the PhD student Maite López López acknowledges the financial support from the Xunta de Galicia (Galician Innovation Agency GAIN: IN607A2018/3), the Spanish Research Network on Cerebrovascular Diseases INVICTUS PLUS (RD16/0019/0001), and the Universidade de Santiago de Compostela and Banco Santander predoctoral fellowship.

Research Stay

During the PhD period, the predoctoral student Maite López López conducted an international research stay at the Clinical & Experimental Optometry Research Laboratory (CEORLab), University of Minho, Braga, Portugal. This research stay was under the supervision of Professor José Manuel González-Meijome from September 19th to December 21st, 2022.

Agradecimientos

Este mogollón de palabras condensadas en un documento que pasaría rápidamente desapercibido entre la gran cantidad de bibliografía científica existente describe mucho más que un simple proyecto de tesis. Desde la ilusión de una estudiante que se adentraba en el camino del doctorado -tan apasionante como intimidante- intentando encontrarse un lugar en un mundo completamente desconocido, el despertar de la inquietud científica, la satisfacción del acierto, la desesperación del fracaso, el cuestionamiento constante, el pc en la mochila para todos lados, el temor a la ausencia del "*" en la pantalla de resultados del SPSS… Pero, sobre todo, describen un viaje que ha sido maravilloso gracias a todas las personas que lo han vivido conmigo.

Isa, recuerdo nítidamente aquella tarde en la que acudía a la facultad para hablar sobre la evolución de mi TFG. Había empezado mis prácticas clínicas y me invadía una sensación de incertidumbre característica del final de una etapa. Tu cercanía aún sin apenas conocerme hizo que verbalizara el mar de dudas que llevaba un tiempo persiguiéndome. Hasta aquel entonces, la posibilidad de sumergirme en una tesis ni se me había pasado por la cabeza, y mi concepción de la investigación era distante y escasa. Sin embargo, la ilusión con la que me hablabas de aquel proyecto de Queratocono que recientemente os habían concedido consiguió desbloquear aquella mente confundida y desorientada. Durante todos estos años has sido -y eres- mucho más que una directora de tesis. Me abriste las puertas del laboratorio y del INGO donde me acogisteis con gran cariño desde el primer día. Me has guiado y aconsejado en cada paso, me has escuchado y te has sentado conmigo millones de veces a poner orden a esas aturulladas ideas que invaden mi cabeza de vez en cuando. Me has transmitido calma cuando lo necesitaba y me has impulsado hacia nuevas metas. Siempre has valorado mis propuestas y has priorizado aquello que fuese mejor para mí, regalándome una confianza plena que me ha ayudado a ser quien soy hoy. Mas allá de lo puramente académico, me has enseñado lo importante que es no perder nunca la humanidad. La satisfacción de la amabilidad. El cariño que transmites a todos los que estamos a tu alrededor, tu amistad, sencillez, y tu disposición incondicional para ayudarnos y apoyarnos en todo cuanto necesitamos hacen que estas palabras se queden muy cortas para poder agradecerte todo lo que has hecho por mí durante estos años. Por todos estos motivos y muchos más, el primer gracias es para ti.

A Uxía. Podría pensar en este agradecimiento durante meses y seguiría sin encontrar las palabras para poder expresarlo. Conseguir transmitir la motivación y las ganas en todo cuanto haces, ser amiga, compañera, profe y directora de tesis no sería jamás fácil excepto por ser tú. Gracias por cada minuto que me has dedicado, tanto en lo personal como en lo científico. Gracias por cada consejo, por el millón de veces que me has explicado cada experimento, por tu paciencia, por tu implicación en cada uno de mis objetivos, por

enseñarme que la dedicación y el esfuerzo pasan por encima de cualquier otra aptitud, y por transmitirme esa voluntad insaciable para conseguir cada paso que te propones. Gracias por preocuparte tanto por mi casi como lo haces por ti misma. Por poner orden a mi desorganizado sistema. Por estar siempre en los momentos buenos y en los no tan buenos, especialmente por no soltarme nunca en estos últimos. Durante este recorrido he sido muy afortunada con todos aquellos y aquellas que me he encontrado en el camino, pero sin duda, tú ocupas el lugar más especial. Ojalá todos tuviesen la mitad de suerte que he tenido yo al encontrarte. Sobra decir que, sin ti, esta tesis no solo no hubiese estado a la altura, sino que tampoco habría reflejado ni una pequeña parte de toda la ilusión y el esfuerzo dedicado.

A mis niñas del Linc, Anti, Ana y Marta. Si bien es cierto que nunca es tarde para entablar nuevas amistades, a medida que pasa el tiempo las conexiones personales se reducen y sólo florecen y se mantienen las naturales y verdaderas. Antonieta, quien me iba a decir que del resquemor a vivir juntas por la posible incompatibilidad de nuestras personalidades ibas a terminar siendo uno de mis humanos favoritos. Quien te conoce bien sabe lo buena amiga que eres. Justa, honesta y siempre dispuesta a aconsejar y ayudar. Has celebrado conmigo en los momentos buenos, pero también has sido quien más me ha escuchado en los bajones. Gracias por ser uno de mis más sinceros apoyos durante toda esta etapa. Con el tiempo uno aprende lo difícil que es llegar a considerar a alguien como un amigo, y sin duda, tú eres una de las más reales que tengo. Aniña, poco se puede decir de ti más allá de todo lo que reflejas. Eres transparente, generosa, con un corazón inmenso. Defiendes las causas justas como la que más y no abandonas tus principios nunca. Describes todas las cualidades que hacen que este mundo se mueva en la dirección correcta. Eres amable, empática y cuidas de los demás con tanta naturalidad y cariño. Escuchas y ayudas incondicionalmente, y mientras muchos nos ahogamos en un vaso vacío, tú nos inspiras a reflexionar sobre lo realmente importante. Gracias por millones de razones, pero sobre todo gracias por ser el hombro amigable en el que apoyarse cuando la vida se nos hace bola. Y finalmente, Marti. Contagias tu ilusión por la vida y las ganas de exprimir las experiencias al máximo. Haces sitio a todo el mundo, no juzgas y compartes. Eres tan natural y auténtica que me sacas una risita incluso en los momentos más tristes. Siempre me has aconsejado desde un corazón sensible, totalmente ajeno a los prejuicios y estereotipos. Consigues sacar lo mejor de mí aun cuando asoma mi carácter reservado y hermético. Gracias por tus palabras amables en los momentos regulares, por tu generosidad, por llorar y por reír conmigo, gracias por ser tan de verdad.

Marquiños, llegaste como un soplo de aire fresco y te integraste tan bien que parece que lleves aquí toda la vida. Gracias por tus cariñosos buenos días, por compartir conmigo el amor al café y la sobremesas, y, especialmente, por tu desinteresadas ganas de echar un cable en todo cuanto puedes. Eres único. Gracias también a las nuevas chicas de ojos, Yaiza y Tania. Llegasteis cargadas de entusiasmo y contagiándonos la ilusión de los nuevos comienzos. En muy poco tiempo ya habéis conseguido ser indispensables, y la verdad es que este pequeño grupo ha tenido una suerte inmensa de que lo hayáis escogido. Gracias por ayudarme siempre y por vuestra calidez detrás de una sencilla sonrisa.

A mi querido Manolo. Detrás de una apariencia distante y seria se encuentra una de las personas más acogedoras y bondadosas que conozco. Gracias por cada broma seguida de una risa amable que consigue quitarle hierro a cualquier situación, eres maravilloso. Al carismático Andresiño da Silva, gracias por integrarme en el laboratorio desde el primer minuto con tu naturalidad, tus ingeniosas preguntas incómodas, los post-it anónimos, tu gran habilidad para reírte de mí y conmigo, y por patrocinar muchos de los mejores momentos que he vivido durante estos años en el LINC. Mentiría si no dijera que a tu marcha dejaste un lab más triste y menos vivo. Dopi, a ti te doy las gracias por cada risa después de nuestros consejos nefastos sobre el amor y las relaciones, y también por esos diarios e increpantes "que, ¿ya está la tesis?" de estos últimos 3 meses, con el único objetivo de escuchar mis quejidos durante diez minutos. Por último, llegó el momento del grandísimo Paulinho Da Sousa. Comprensivo, atento, cariñoso, siempre con unas palabras amables y una disposición absoluta para ayudar a quien te lo pide. Al mismo tiempo perseverante, trabajador y entregado con todo cuanto te propones. Estaba segura de que conseguirías todos tus objetivos, siendo un orgullo para todos los que compartimos el turbulento camino de la tesis contigo. Gracias por tus conocimientos informáticos, por cada instalación del SPSS, por tu inglés brillante, pero, sobre todo, gracias por escucharme y por cada abrazo asfixiante que hizo sentirte amigo desde el principio.

Por supuesto, gracias a todos mis compañeros del LINC. María Pérez, Teresa, Mari Luz, Dani, Alberto, Esteban, Ana Sampedro, Clara, Lara, Sabela, Mónica, Mariña, Lucía, María Muros, Sara, Nuria, Manuel, Pelayo y Crhistian, sois un ejemplo de dedicación y trabajo en grupo, muchas gracias por formar parte de este equipo.

Gracias también a Tomás, Fran y Ramón por haberme facilitado cuanto he necesitado para la realización de esta tesis y por transmitirnos vuestra implicación y compromiso con este trabajo. A Pepe. Porque desde aquel saludo tímido y las presentaciones en los miércoles LINC con las pulsaciones a mil por hora creció una chica más segura, perseverante y cabezota. Gracias por inculcarnos la importancia de la tenacidad, el empeño y el sacrificio. Por motivarnos en los momentos bajos y por regañarnos cuando bajamos la guardia. Por preocuparte por todos nosotros genuinamente. Por tu humanidad y por tu cercanía. Gracias de corazón por haberme acogido en esta segunda casa de la que me siento tan afortunada de pertenecer. Al Dr. Hervellis, gracias por tu buena disposición, tu ayuda, la alegría incondicional, las risas, el "¿qué che fixen eu?" seguido instantáneamente de una carcajada; pero, sobre todo, por ser capaz de alegrarte tanto por nuestros logros como por los tuyos propios, y saber transmitirnos que de eso va la ciencia. Gracias también a ti Joserra, por la enorme paciencia que tienes con todos nosotros y tu capacidad para resolver todo tipo de contratiempos siempre con una sonrisa.

Gracias también a la Unidad de proteómica del IDIS por haberse implicado tanto en esta tesis. Especialmente, gracias Susana por haberme acercado al mundo de la espectrometría de masas y la proteómica, que pensé que jamás llegaría a comprender. Gracias por contestar a mis mails instantáneamente, por hacerme un hueco en tu despacho millones de veces, por encontrar las palabras exactas para que una estudiante con poca o ninguna

idea de química analítica hoy entienda -en términos generales- las diferencias entre los modos de adquisición de datos. Muchas gracias por guiarme tan bien durante estos años y por poder contar contigo siempre.

Mucho antes de comenzar en el LINC, mi experiencia se abría camino en el INGO, un lugar que me fascinaba donde las horas se pasaban rapidísimo y en el que tenía la sensación de que conseguía dar lo mejor de mí. A todos mis compañeros del INGO, no sabría como agradeceros el trato, el aprendizaje y la confianza que habéis depositado en mí durante todo este tiempo. Gracias Elío por apoyarnos en todo, por tu optimismo, tu cercanía y por dar los mejores consejos antes de mi primera clase como predoc. Gracias Consu por tu cariño, por tu buen carácter, por el trato inmejorable que nos hace sentir tan a gusto a todos los que estamos a tu alrededor, tus amables "gracias miña reina" aunque sólo te hubiese sacado una copia de la impresora, muchas gracias de corazón por haberme hecho sentir una más durante este tiempo. Cope, gracias por tu confianza, por enseñarme desde la ilusión, por tus buenas palabras al llegar cada mañana y por ofrecerme tu ayuda siempre que lo que necesitado. A Miriam, gracias por tu paciencia, por estar disponible para echar una mano en lo que haga falta, por tu polivalencia y por tu cariñosa forma de ponerme las pilas de vez en cuando. Gracias también a Pedro, Belén, Marta, María José y María por vuestro apoyo y cariño durante estos años. Óscar y Gema, no podría olvidarme de vosotros. Gracias por vuestra dulzura y serenidad, y por poner tanta ilusión y empeño en mis estudios.

Gracias a todos los pacientes por ser el corazón de esta tesis. Por vuestra generosidad, interés, entusiasmo y buena voluntad. Sin vosotros nada de esto se hubiese podido llevar a cabo.

Aos meus colegas do CEORLab. Iñaki, María, Sarinha, Ana, Rute, Filipa e André. O que começou por ser uma aventura sozinha acabou por se tornar numa casa para onde queria sempre voltar. Não podem imaginar a sorte que sinto por vos ter encontrado. Gostaria também de agradecer aos professores António Queirós, Paulo e Miguel pela proximidade e carinho, ajudando-me em tudo quando precisei. Tenho também de agradecer ao Professor José Manuel não só pela sua atenção e apoio, mas também por me ter dado a oportunidade de estar com um grupo tão bom, tanto a nível pessoal como científico.

A mis amigas. Aniña y Alba, no llegasteis desde el principio, pero sí para quedaros hasta el final. Gracias por darle vuestra amistad sincera a aquella niña que se colaba en todas vuestras excursiones. Lu, sin duda fuiste la mejor sorpresa que me regaló la uni. Gracias por nuestras conversaciones eternas, por transmitirme tu fuerza y tu cordura, y, en definitiva, por seguir aquí durante todos estos años. También a vosotras, Lau y Ana Amor, por compartir tantos buenos momentos juntas y por seguir creciendo a mi lado. Palomi, la que mejor entiende mis olvidos a contestar por WhatsApp, a vivir sin demasiados planes, a disfrutar de estar en casa simplemente contándonos la vida, a disfrutar de las cosas más sencillas. Siento que siempre estás cerca aun pasando meses sin vernos. Y finalmente apareciste tú, Meri. Con un corazoncito tan grande, siempre atenta a los

detalles y tan preocupada por todos los tuyos. Con personalidades tan diferentes, pero tan compatibles al mismo tiempo. Durante este último año te has convertido en mi mejor compañera de aventuras, y como siempre te digo y te diré, eres lo mejor que me dio Coru y no puedo tener más suerte de haberte encontrado.

Llegando ya casi al final de este monólogo infinito, estáis vosotras. Las de siempre. Susi, Ele, Nere y Lau. Las que camináis a mi lado incondicionalmente y estáis presentes en cada uno de mis recuerdos. Parece increíble pensar que unas niñas de tres años consiguieran establecer lazos tan fuertes que veintipico años después sigan tan sólidos e inquebrantables como al principio. Sin apenas demandar nada, florecemos año tras año. Desde distintos lugares del mundo, la conexión siempre permanece intacta. Con cada anécdota volvemos a ser niñas y os siento siempre conmigo sin importar el tiempo que pase desde la última vez que nos vimos. Todo lo que me quedaría por deciros sólo se podría resumir con otra tesis doctoral, por lo que lo voy a dejar en un sincero "gracias".

Por último, a mi familia. Sin vosotros nada de esto sería posible. Gracias por vuestro apoyo, por hacerme sentir libre para tomar el camino que considero adecuado y por anteponer mi felicidad siempre. A mis abuelos, quienes me muestran día tras día la importancia de la gratitud a través de una visión del mundo sencilla y humilde. A papá, por creer en mí desde el principio. Por apoyarme. Por enseñarme el valor del trabajo bien hecho. Gracias también por decirme lo que no me gusta tanto escuchar, y por bajarme a la tierra de vez en cuando. A mamá. Cada domingo, al despedirnos en la estación no puedo evitar pensar en la inmensa suerte que tengo contigo. Creo que ninguna sensación se podría acercar a la gran admiración que siento al hablar de ti. Gracias por conocerme tan bien y estar siempre, incluso cuando seguramente solo me merezco un buen tirón de orejas. Gracias por cada viaje a Santiago, por cada llamada antes de cualquier reunión, seminario, o presentación importante. Gracias por no olvidarte nunca. Por apoyarme, por escucharme, por animarme… Pero, sobre todo, gracias también por cuestionarme, reñirme y por enseñarme a enfrentar los giros inesperados y el gran poder de la frustración.

Aquí termina una etapa de mi vida inolvidable, llena de aprendizaje y con una gran satisfacción y motivación que estoy segura de que me empujarán hacia los siguientes desafíos con la mayor de las ilusiones.

“Todos somos gotas del mismo océano”

Isabel Allende

“The important thing is not to stop questioning.

Curiosity has its own reason for existing.”

Albert Einstein

Index

Resumo ..... **I**
Abbreviations ..... **X**
Introduction **1**
Keratoconus **1**
1.1 Definition and main remarks **1**
1.2 Delving deeper into corneal ectasias **2**
1.3 Epidemiology **3**
1.4 Aetiology **4**
1.4.1 Genetics and inheritance 4
Genetics *4*
Inheritance *5*
1.4.2 Mechanical and environmental factors 6
1.5 Pathophysiology **6**
1.5.1 Oxidative stress 7
1.5.2 Inflammation 8
1.5.3 Innate immunity 8
1.5.4 Extracellular matrix degradation 11
1.5.5 Hormonal factors 12
1.6 Histology and semiology **12**
1.6.1 Histology 12
1.6.2 Semiology 13
1.7 Diagnosis and classification **13**
1.7.1 Corneal biomechanics 14
1.7.2 Corneal topography and tomography 17
1.7.3 Classification 18
1.8 Treatment **19**
Tear fluid in the diagnosis and prognosis of KC disease. **20**
2.1 Production, release, and delivery of the tear fluid **20**
2.2 Composition **21**
2.3 Tear fluid as a biomarker source in KC disease **22**
2.3.1 The KC tear proteome 23
2.3.2 New tools and recent advances for proteomic profiling 24
Justification and hypothesis **27**
Objectives **29**

Methodology **32**
Clinical studies **32**
3.1 Study design and participants **32**
3.2 Clinical measurements and protocols **33**
3.2.1 Anamnesis 33
3.2.2 Ocular health 34
3.2.3 Corneal biomechanics 34
3.2.4 Corneal tomography 36
Molecular analysis **36**
4.1 Sample extraction **36**
4.1.1 Tear fluid 36
4.1.2 Blood 36
4.2 Sample preparation **36**
4.2.1 Tear samples processing 36
4.2.2 Blood samples processing 37
4.3 Sample analysis **37**
4.3.1 Mass spectrometry analysis by TripleTOF 6600 LC-MS/MS system 37
Tryptic digestion *37*
Data-dependent acquisition (DDA) *37*
Relative quantification by Sequential Window Acquisition for All Theoretical Mass Spectra (SWATH-MS) *38*
4.3.2 ELISA 40
4.4 Gene Ontology analysis: Protein interaction networks and pathway enrichment **40**
***In vitro* study** **40**
5.1 Experimental design **41**
5.2 Experimental procedures **41**
5.2.1 QUANTI-Blue™ 41
5.2.2 Flow cytometry 41
5.2.3 Immunohistochemistry 42
5.2.4 Western Blotting 42
5.2.5 ELISA 43
Statistical analysis **43**
WP1. Clinical & molecular study of KC disease **46**
Chapter 1 ..... **47**
Chapter 2 ..... **58**
WP2. Clinical & molecular study of KC at-risk stages **78**

Chapter 3 79
Chapter 4 118
WP3. Human LF as a therapeutic strategy for KC 142
Chapter 5 143
Discussion 163
Tear proteomics in KC disease 163
Tear proteomics in KC risk-stages and biomechanical weakness 166
Proteomic overlap between KC and KC at-risk stages 169
LF in KC disease and its potential as a therapeutic target. 171
Conclusions 175
Bibliography 177
Annexes 195

Resumo

O queratocono (QC) é unha ectasia corneal progresiva e dexenerativa na que se produce un adelgazamento, debilitamento e incurvamento do tecido corneal que da lugar a un deterioro substancial da visión nos pacientes que a padecen. Por definición, trátase dunha patoloxía crónica, usualmente bilateral e asimétrica, cunha evolución que pode variar dende estadios leves a estadios notablemente avanzados. A aparición temperá do QC, afectando principalmente a pacientes novos, conleva non só un forte impacto ao longo da vida do paciente, senón tamén un importante problema socio-sanitario.

No que se refire á etiopatoxénese da enfermidade, na actualidade considérase que as alteracións bioquímicas e moleculares (como a apoptose dos queratocitos estromáis e a perda de fibras de coláxeno, entre outras...) inducen un enfraquecemento e adelgazamento do tecido corneal (volvéndose menos ríxido e menos resistente) que precede e promove a protrusión do mesmo (baixo a influenza da presión intraocular), rematando por adquirir una morfoloxía final abrupta e marcadamente asimétrica. A pesar de que o diagnóstico clínico do QC baséase en ferramentas de imaxe como a topografía ou a tomografía corneal, estas técnicas teñen unha limitada capacidade para detectar a enfermidade subclínica ou a predisposición do tecido ao desenvolvemento da patoloxía. Tratando de facer fronte a este reto emerxeron as ferramentas de exploración das propiedades biomecánicas da córnea, cuxo primeiro obxectivo é a detección de disfuncións na resistencia e rixidez corneais que poidan alertar sobre a predisposición intrínseca do tecido ao posible desenvolvemento do QC.

Considerando que **non existen tratamentos médicos/farmacolóxicos curativos ou preventivos** para o QC, senón que a abordaxe actual tenta mellorar a calidade visual a través de estratexias ópticas, ou ben reforzar a estrutura corneal para evitar a súa progresión cara estadios máis avanzados, parece imprescindible afondar nas bases fisiopatolóxicas da enfermidade que poidan achegarnos a un diagnóstico de precisión e a terapias dirixidas á enfermidade temperá.

En termos etiolóxicos, **a orixe do QC parece responder a unha complexa rede multifactorial cunha base xenética** que determina a predisposición ao seu desenvolvemento, e unha serie de factores mecánico-ambientais que favorecen a súa aparición e progresión. A predisposición xenética é explicada como a coexistencia de múltiples variantes patoxénicas que conforman un xenoma altamente susceptible á aparición da patoloxía. Son diversos achados os que apoian a base xenético-hereditaria do QC, dende a alta prevalencia da enfermidade nos familiares dos pacientes con QC, a alta concordanza

na severidade e no patrón topográfico da enfermidade en xemelgos monocigóticos fronte a dicigóticos, así como as peculiares características das córneas dos familiares que en numerosas ocasións se asemellan a estadios subclínicos ou frustres da enfermidade. Sustentándose nestas bases, a historia familiar de QC é considerada un dos principais factores de risco para a súa aparición, **apuntando aos familiares de primeira orde como a poboación máis susceptible ao desenvolvemento do QC**.

En relación aos factores mecánicos e ambientais, é ben coñecido e descrito que o frotamento ocular vigoroso e recorrente, así como a excesiva exposición á luz UV, entre outros, estimulan a progresión rápida e agresiva da patoloxía. Nos últimos anos leváronse a cabo numerosos esforzos para tratar de comprender o entramado molecular subxacente aos cambios histolóxicos do tecido corneal no QC. Neste sentido, os estudos en diferentes mostras biolóxicas (de sangue, lágrima, e tecido corneal estromal e epitelial) achegaron valiosa información sobre a **participación de certos procesos biolóxicos** na súa fisipatoloxía; como o aumento da inflamación, a contribución da inmunidade innata, o dano oxidativo, así como o aumento da expresión e actividade de proteasas de matriz e por tanto o aumento da degradación tisular.

A pesar de que o QC describíase no pasado como unha enfermidade non inflamatoria, debido á ausencia dos signos cardinais da inflamación (tales como rubor, calor, dor, e tumor), nos últimos anos numerosos estudos sinalaron a presenza de marcadores inflamatorios nas mostras destes pacientes, suxerindo a súa similitude a un **proceso inflamatorio crónico** determinado por un desequilibrio entre as moléculas pro e anti-inflamatorias que promoven a lesión tisular ao longo do tempo e sen autolimitación aparente. Nesta liña, a sobreexpresión de receptores toll-like tipo 2 e 4 observada no epitelio corneal e conxuntival así como en monocitos e neutrófilos de pacientes con QC, tamén promove a hipótese de que a estimulación persistente destes receptores de **inmunidade innata** podería contribuír na activación crónica dos eventos inflamatorios.

O dano oxidativo altamente nocivo para os compoñentes celulares e as estruturas tisulares tamén foi amplamente referido no QC. Neste sentido, proponse a **redución da capacidade antioxidante** das células corneais dos pacientes con QC pola baixa expresión de moléculas esenciais na defensa oxidativa como a superoxido dismutasa. Dito defecto antioxidante xustificaría os altos niveis de especies reactivas atopados nos cultivos *in vitro* de fibroblastos de córneas queratocónicas, determinando un tecido altamente susceptible ao dano oxidativo. Ademais, recoñécese que existe unha retroalimentación activa entre os procesos oxidativos e inflamatorios, de forma que un estado oxidativo persistente tamén promove a prolongación do estado inflamatorio, o que parece encaixar na trama fisiopatolóxica do QC.

A perda de proteoglicanos e fibras de coláxeno, así como a destrución da matriz extracelular, tamén son sinais distintivos da enfermidade. De feito, nas mostras de pacientes con QC observouse o **aumento da expresión e da actividade das proteasas de matriz** xunto ca

infraexpresión dos seus inhibidores, asociándoos á severidade da enfermidade e recoñecéndoos como principais **responsables do adelgazamento tisular**.

A pesar de que a arquitectura fisiopatolóxica do QC estase descifrando progresivamente, aínda quedan moitas cuestións por resolver. A maior parte das **dúbidas** concéntranse **arredor dos cambios temperás que impulsan a cascada de acontecementos observados no QC clínico**, iniciando co enfraquecemento do tecido corneal e determinando a susceptibilidade ao desenvolvemento da enfermidade. Polo tanto, o **obxectivo principal** deste traballo foi **afondar naquelas alteracións proteómicas lagrimais que puideran exercer un papel determinante no deterioro das propiedades biomecánicas corneais, así como na susceptibilidade dunha poboación altamente vulnerable ao desenvolvemento do QC, como é o caso dos fillos destes pacientes.** A identificación de ditos biomarcadores tamén permitiu coñecer os mecanismos e vías biolóxicas afectados, e por tanto, facilitar o desenvolvemento de novas estratexias de detección e diagnóstico temperá.

A análise dos fluídos biolóxicos na procura de marcadores máis específicos e sensibles é unha estratexia amplamente empregada nunha gran variedade de enfermidades. Estudos previos demostraron a existencia de vías de comunicación entre a lágrima, o epitelio, e o estroma corneal, mostrando que os compoñentes lagrimais poden afectar ao fenotipo das células epiteliais e dos queratocitos. Isto converte á **lágrima** nun **fluído de fácil acceso, non invasivo, e cun potencial prometedor no estudo de biomarcadores** indicativos do estado dos tecidos subxacentes así como doutras patoloxías. A evolución das ferramentas -ómicas de análise e cuantificación de mostras permitiu explorar gran cantidade de moléculas empregando cantidades de mostra significativamente reducidas, promovendo técnicas óptimas para o estudo masivo dalgúns biofluídos como a lágrima. Tendo en conta estas vantaxes, decidimos utilizar a **espectrometría de masas combinada con cromatografía líquida** (LC-MS/MS) como **técnica de elección para o análise das mostras de lágrima**.

No contexto da procura de biomarcadores este traballo incluíu dúas fases**:**

A primeira fase enfocouse nos propios **pacientes con QC**, realizando un estudo clínico-molecular do tipo caso-control onde analizamos mostras lagrimais de 25 pacientes con QC e 25 suxeitos control emparellados en idade e sexo. Este **primeiro paquete de traballo** (*capítulos 1 e 2* desta tese de doutoramento - integrados polos artigos "*Tear proteomics in keratoconus: a quantitative SWATH-MS analysis*" e "*Shot-gun proteomics for the identification and profiling of the tear fluid of keratoconus patients*") tiña a finalidade de determinar as redes e conexións entre os biomarcadores que definirían os principais mecanismos moleculares participantes no curso fisiopatolóxico da enfermidade, e que, poderían servir de guía para os estudos da segunda fase centrados nos estadios máis temperás e preclínicos da patoloxía. Con este obxectivo, realizamos estudos de tomografía mediante Pentacam® HR e analizamos mostra de lágrima que foi extraída con tiras de

Schirmer. Para a análise molecular, empregamos a técnica SWATH-MS (do inglés, *Sequential Window Acquisition for all Theoretical Mass Spectra*) para cuantificar proteínas, e o modo de adquisición dependente de datos (DDA-MS) para observar globalmente e de maneira cualitativa as diferenzas xerais entre as proteínas presentes nas mostras dos pacientes con QC e as dos suxeitos control. Os nosos estudos mostraron diferenzas substanciais entre a composición da lágrima dos pacientes con QC e a dos suxeitos control, onde aproximadamente un terzo das proteínas identificadas diferían entre ambos grupos. Alén diso, os resultados da cuantificación revelaron a desregulación de 18 proteínas nas mostras de QC que, conxuntamente coas que tan só estaban presentes nas mostras destes pacientes, asociábanse a procesos de organización de citoesqueleto, estrés oxidativo, alteracións no transporte e homeostase de ións férricos, e a eventos inflamatorios.

Un dos achados máis salientables desta primeira fase **foi a drástica infraexpresión da transferrina** nas mostras de lágrima dos pacientes con QC. Concretamente, esta proteína presentaba unha expresión catro veces inferior á observada nas mostras dos suxeitos control, o cal suxire unha **posible alteración no transporte e homeostase de ferro no fluído lagrimal dos pacientes con QC** por tratarse da principal proteína humana de transporte e unión a ións férricos. Tendo en conta que un dos signos biomicroscópicos máis característicos desta patoloxía é o anel de Fleischer (definido como o depósito de ferritina na membrana basal do epitelio corneal) e que ante o aumento dos niveis de ferro libre (non ligado a ningunha proteína de transporte) este é capaz de filtrarse nos tecidos, o desaxuste no sistema de transporte e metabolismo do ferro na lágrima podería constituír unha explicación lóxica para a súa acumulación e filtración no tecido corneal. Adicionalmente, observouse a desregulación de proteínas de implicación oxidativa (como a peroxiredoxina-1 ou a proteína de choque térmico β-1) e a presenza de clústeres de aldehido deshidroxenasas e peptidil-prolil cis-trans-isomerasas (identificados tan só nas mostras dos pacientes con QC), os cales desempeñan un papel significativo na neutralización e a eliminación de radicais libres e por tanto ofrecen un potente sistema de defensa antioxidante. Ditos achados **parecen responder á demanda dun tecido corneal exposto a altos niveis de estrés oxidativo**, que poderían ser impulsados por diversas fontes como a toxicidade da sobrecarga férrica e a incapacidade antioxidante celular.

O trasfondo inflamatorio do QC foi apoiado pola desregulación de proteínas ligadas activamente a procesos inflamatorios como a anexina A1, anexina A2, α1-glicoproteína ácida, ou a S100A4. **O impacto sobre os procesos estruturais e as comunicacións celulares** suxeriuse tras observar a desregulación da cofilina-1, plastina-3, tubulina-1, latexina, e tamén do inhibidor 1 de disociación de Rho GDP, tratándose de proteínas que participan activamente na ensamblaxe dos filamentos de actina, da organización do citoesqueleto, e que forman parte de importantes vías de mecanotransdución corneal como é o caso da vía Rho.

Considerando os resultados obtidos en conxunción ao reportado en estudos previos, a **inflamación e o estrés oxidativo parecen actuar de forma sinérxica no QC**, podendo desencadear o dano e os procesos de morte celular no epitelio e no estroma corneal.

A segunda fase do traballo (*capítulos 3 e 4* desta tese de doutoramento) centrouse en responder a hipótese central do proxecto, enfocado en **dilucidar os marcadores lagrimais** e os **mecanismos biolóxicos asociados ao deterioro das propiedades biomecánicas corneais e a susceptibilidade dos fillos de pacientes con QC para desenvolver dita patoloxía**. Este segundo estudo caso-control incluíu un total de 80 fillos de pacientes con QC (O-KC) con idades comprendidas entre 8 e 18 anos (cuxo criterio principal de inclusión foi presentar un pai/nai diagnosticado de QC), e 42 suxeitos control emparellados en idade e sexo co grupo anterior, que como criterio fundamental para a participación no estudo non poderían presentar historia familiar de QC ou outro tipo de ectasia corneal así como tampouco características corneais compatibles con algún tipo de ectasia corneal. A parte clínica deste estudo incluíu a avaliación das propiedades biomecánicas e das características tomográficas corneais mediante os dispositivos Corvis® ST e Pentacam® HR. Primeiramente, os ollos do grupo O-KC foron clasificados en base ao Índice Biomecánico de Corvis (CBI), o cal presenta unha alta sensibilidade e especificidade para detectar as alteracións biomecánicas que poderían alertar sobre o risco ao posible desenvolvemento de ectasias corneais. Nesta liña, os ollos deste grupo foron clasificados como ollos con baixo risco ao desenvolvemento de ectasia (O-KC-LR, CBI<0.25), ollos con risco moderado ao desenvolvemento de ectasia (O-KC-MR, CBI 0.25-0.50), e ollos con alto risco ao desenvolvemento de ectasia (O-KC-HR, CBI>0.50). Por outra banda, todos os ollos do grupo control cumpriron o criterio de mostrar un índice CBI indicativo de baixo risco ao desenvolvemento de ectasia (CBI<0.25). Para a realización da análise molecular extraéronse mostras de fluído lagrimal a todos os participantes empregando tiras de Schirmer, que foron analizadas por LC-MS/MS e, unha vez identificados os biomarcadores de interese, estes foron validados coa técnica ELISA.

En canto aos **resultados relativos á parte clínica**, observouse que **un 29% dos ollos do grupo O-KC mostraban moderado ou alto risco ao desenvolvemento de ectasia**, apoiando o reportado previamente noutros estudos onde atoparon que os familiares dos pacientes con QC evidenciaban valores de resistencia e rixidez corneal inferiores aos referidos no grupo control. O estudo das características morfolóxicas tamén resaltou o observado nas variables paquimétricas, onde o espesor central, mínimo, así como as variables relativas á progresión paquimétrica diferenciaban os grupos de moderado e alto risco fronte ao grupo de baixo risco e o control, de forma que, a medida que as propiedades biomecánicas empeoraban, observábase unha diminución dos valores de paquimetría corneal central e mínima, así como maiores diferenzas entre o grosor central e o periférico (alteracións da progresión do espesor corneal). Estes resultados suxeriron que as alteracións no espesor corneal e a progresión paquimétrica poderían estimular ou exacerbar cambios nas propiedades biomecánicas da córnea.

A análise da lágrima por LC-MS/MS revelou a desregulación de 15 proteínas nas mostras dos fillos de pacientes con QC. A maior parte destas proteínas mostraban unha expresión diferencial en todos os grupos de O-KC fronte ao control, incluso en aqueles que foran categorizados como de baixo risco ao desenvolvemento de ectasia e que, polo tanto, non presentaban alteracións biomecánicas de alerta. Outro aspecto a destacar foi que, en xeral, a medida que os índices biomecánicos sinalaban maior risco ao desenvolvemento de ectasia, acentuábase a infra ou sobre expresión de ditas proteínas, suxerindo a súa posible asociación co deterioro e o enfraquecemento corneal.

O **estudo de ontoloxía xenética das proteínas desreguladas nos grupos O-KC** achegou importante información acerca das implicacións biolóxicas de ditos marcadores. Neste sentido, cabe salientar que ditas proteínas relacionábanse con procesos descritos previamente asociados á fisiopatoloxía do QC, tales como procesos de comunicación intercelular e vías de mecanotransdución e resposta a estímulos mecánicos, a estrés oxidativo, e a inflamación:

- **O impacto na comunicación intercelular e as vías de mecanotransdución** manifestouse debido a desregulación da cofilina-1 (CFL1), a subunidade catalítica da calpaína-1 (CAPN1), ezrina (EZN), α-actinina 4 (ACNT4), e a actina citoplasmática-2 (ACTG), sendo todas elas moléculas implicadas activamente en procesos de migración e adhesión celular, entrecruzamento de filamentos de actina, e remodelación do citoesqueleto de actina. Concretamente, a CFL1, a CAPN1 e a EZN son requiridas na regulación da morfoloxía celular, a adhesión celular ao substrato, a despolimerización dos filamentos de actina, e a regulación da dinámica do citoesqueleto a través de diferentes vías de sinalización como a vía das integrinas, da β-catenina, das Rho GTPasas, ou da mTOR. Ao mesmo tempo, a ACNT4 é un axente reticulante de filamentos de actina que tamén participa nas unións estreitas das células epiteliais, e a ACTG é unha proteína constitutiva dos filamentos de actina. Considerando que o QC é unha patoloxía con afectación mecánica a nivel epitelial-estromal, a desregulación de ditas proteínas podería relacionarse co declive biomecánico nestas estruturas.

- A relación cos procesos de **estrés oxidativo** evidenciouse debido a infraexpresión de varias proteínas con roles esenciais na protección fronte o dano oxidativo como a lipocalina-1 (LCN-1), lactoferrina (LF), superóxido dismutasa-1 (SOD1), e a peroxiredoxina-1 (PRDX1). Todos estes marcadores xa foran asociados previamente á fisiopatoloxía do QC. Dita infraexpresión intensificábase nos grupos O-KC con índices biomecánicos indicativos de maior inestabilidade tisular, suxerindo unha capacidade antioxidante mais reducida a medida que a biomecánica corneal se deterioraba.

- Curiosamente, a LF foi unha das proteínas máis infraexpresadas nas mostras dos O-KC, o cal encaixa co reportado en estudos realizados en QC clínico, onde atoparon unha clara redución na expresión deste marcador en lágrima. O potencial da LF como biomarcador

diagnóstico e prognóstico tamén destacou debido aos seus altos valores de sensibilidade e especificidade para a discriminación entre os grupos O-KC e o grupo control, así como tamén para a detección do grupo de alto risco ao desenvolvemento de ectasia. Os principais motivos explicativos do posible impacto da LF no QC susténtanse na súa capacidade antioxidante mediante a regulación dos niveis de ferro libre nos fluídos biolóxicos (uníndose aos ións férricos, e por tanto diminuíndo a cantidade extracelular de ferro non ligado e a súa potencial toxicidade) e na súa natureza inmunomoduladora e antiinflamatoria, de forma que unha baixa expresión desta proteína contribuiría no dano celular derivado dos eventos oxidativos e inflamatorios.

Mais alá do impacto individual de cada unha das proteínas desreguladas, realizamos unha **análise de regresión loxística** onde determinamos as mellores combinacións daqueles biomarcadores que presentaban alta sensibilidade e especificidade na análise ROC para discriminar entre o grupo de control e os grupos O-KC. En total, creáronse **tres paneis de proteínas altamente sensibles e específicos para a detección de cada unha das condicións dos grupos O-KC**. A LF, LCN-1, SOD1, CAPN1, EZN, e APOA2 foron os marcadores seleccionados para conformar o primeiro panel de proteínas que diferenciaba cunha sensibilidade do 87% e especificidade do 66% (AUC 0.819) o grupo control e o grupo de fillos de pacientes con QC que non amosaban alteracións biomecánicas compatibles con ectasia corneal (O-KC_LR). O segundo panel incluíu a LCN-1, SOD1, e EZN como os mellores candidatos para a estimación do risco moderado ao desenvolvemento de ectasia, obtendo unha sensibilidade do 96% e especificidade do 67% (AUC 0.856) para a discriminación entre o grupo de estudo con risco moderado ao desenvolvemento de ectasia (O-KC_MR) e o grupo control. Finalmente, o último panel de proteínas determinou a combinación da LF, LCN-1, PRDX1, SOD1 e EZN como o mellor modelo para a predición da condición de alto risco ao desenvolvemento de ectasia, alcanzando unha sensibilidade do 92% e unha especificidade do 70% (AUC 0.848) para a diferenciación entre o grupo de estudo de alto risco ao desenvolvemento de ectasia (O-KC_HR) e o grupo control.

Considerando que a desregulación destes biomarcadores podía observarse **incluso antes da detección de alteracións no comportamento biomecánico corneal**, os nosos resultados suxiren unha **alteración molecular estrutural que precede ao debilitamento corneal detectado coas ferramentas clínicas de avaliación da biomecánica dispoñibles na actualidade**. Ditos resultados integran o capítulo 3 desta tese de doutoramento, mediante o artigo titulado "*Tear proteomic analysis from offspring of keratoconus patients: new insights into corneal biomechanical weakness & disease risk stages".*

Nesta segunda fase do proxecto de tese tamén se incluíu un **estudo de seguimento** no cal se realizaron novamente probas de biomecánica, tomografía e análise molecular aos fillos dos pacientes con QC. O principal propósito deste estudo de cohortes foi **determinar os cambios temperás na biomecánica e na tomografía corneal relacionados coa posible evolución cara un maior deterioro biomecánico/tomográfico ou incluso cara o**

desenvolvemento clínico do QC tres anos despois da primeira visita. Adicionalmente, tamén se analizaron os niveis de LF en lágrima mediante ELISA coa finalidade de determinar a súa posible asociación co debilitamento corneal e a progresión ao QC clínico.

Os resultados do estudo de seguimento amosaron que un 21% dos ollos pertencentes ao grupo de baixo risco (O-KC_LR) empeoraban a súa puntuación CBI e progresaban a estadios de risco moderado ou alto ao desenvolvemento de ectasia. Así mesmo, o 39% dos ollos que ao inicio do estudo presentaban alteracións moderadas na biomecánica corneal (O-KC_MR) progresaban a estadios de alto risco tres anos despois da visita inicial, e de igual forma tamén o 39% dos ollos que inicialmente xa tiñan un índice CBI indicativo de alto risco (O-KC_HR) evolucionaban tres anos despois a un declive biomecánico maior ou incluso a alteracións tomográficas xa compatibles cun QC clínico.

O deterioro biomecánico asociouse principalmente con alteracións nos valores de amplitude de deformación, tempo e velocidade da aplanación corneal, e con anomalías nos parámetros de progresión paquimétrica. Especificamente, **tódolos casos que cursaron con empeoramento e progresión no índice CBI mostraban alteracións nos parámetros que relacionan o espesor entre o centro e a periferia corneal** (ARTh e PachySlope), suxerindo que os cambios en ditos parámetros poderían constituír os signos detectables máis precoces do deterioro biomecánico.

En relación a análise molecular, **non se observaron diferenzas na expresión de LF entre antes e despois dos seguimentos** para ningún dos grupos con deterioro biomecánico; non obstante, o**s valores sempre continuaban sendo inferiores aos reportados no grupo control**, o que parece relacionar a infraexpresión da LF coa historia familiar positiva de QC pero non co deterioro biomecánico. O capítulo 4 recolle todos os resultados obtidos no estudo de seguimento, e compoñen o artigo titulado "*Clinical and molecular outcomes of the three-year follow-up of the offspring of keratoconus patients".*

Finalmente, baseándonos na evidencia previa da desregulación da LF en mostras de lágrima de pacientes con QC, no observado durante a segunda parte deste proxecto de tese onde a LF se estableceu como unha das proteínas máis infraexpresadas nas mostras dos fillos de pacientes con QC amosando ademais un gran potencial como biomarcador diagnóstico e prognóstico, e tamén considerando a súa capacidade como ligando endóxeno e modulador da actividade dos receptores toll-like (TLR) (previamente descritos como biomarcadores sensibles e específicos da enfermidade de QC)**, o último paquete de traballo** deste proxecto de tese **pretendeu demostrar a capacidade inmunomoduladora da LF sobre TLR2 e por tanto o seu potencial como aproximación terapéutica.**

Con este obxectivo, o capítulo 5 (mediante o artigo "*Inmunomodulatory effect of human lactoferrin on Toll-like receptors 2 expression as therapeutic approach for keratoconus")* centrouse por unha banda na validación da infraexpresión de dita proteína en soro e lágrima

de mostras de pacientes con diagnóstico clínico de QC, empregando a técnica ELISA para a súa cuantificación; e por outra banda na realización dun estudo *in vitro* coa liña celular HEK-Blue™ hTLR2 especificamente deseñada para o estudo de agonistas e antagonistas dos TLR2 co fin de determinar o papel inmunomodulador da LF sobre ditos receptores de inmunidade innata. Cabe destacar que, as mostras empregadas para a análise molecular, así como a base de dados relativa ás características clínicas e de marcadores de inflamación e inmunidade dos pacientes incluídos neste estudo pertencían a nosa liña de *Patoloxía Ocular Corneal (2019/623)* na que se recolle información relativa a pacientes que xa participaron previamente noutros estudos do noso grupo. Como era de esperar, a análise de LF mediante ELISA demostrou que os niveis de dita proteína **diminuían drasticamente tanto nas mostras de soro como de lágrima dos pacientes con QC respecto aos controis**. Ademais, a baixa concentración de LF en soro correlacionábase de maneira robusta cos marcadores de inflamación-inmunidade (como TLR2, IL-1β, IL-6, TNF-α, ou MMP-9) en sangue, e a infraexpresión de LF en lágrima tamén se correlacionaba fortemente cos marcadores de inmunidade na superficie ocular (TLR2 en córnea e conxuntiva) así como cos parámetros topográficos asociados á severidade do QC.

En relación ao estudo *in vitro*, o deseño deste estudo incluíu a determinación dos niveis de expresión de TLR2 trala súa estimulación (empregando Pam2CSK4 e Pam3CSK4), neutralización e inmunomodulación nos cultivos HEK-Blue™ hTLR2. Para a neutralización dos receptores empregouse un anticorpo monoclonal IgA fronte ao TLR2 humano. Para a avaliación da LF como inmunomodulador dos TLR2, os cultivos tratáronse a diferentes concentracións de LF humana seguindo o mesmo protocolo que o establecido para o anticorpo Anti-hTLR2-IgA. A sobreexpresión, neutralización e inmunomodulación de TLR2 determinouse en primeiro lugar medindo a produción de fosfatasa alcalina embrionaria (SEAP) co ensaio QUANTI-Blue™ e, posteriormente, mediante citometría de fluxo, inmunohistoquímica, western blot e ELISA validouse a expresión e funcionalidade de TLR2. **Os resultados amosaron que a incubación con 2mg/mL de LF humana reducía significativamente a expresión de TLR2** e a **cantidade de SEAP e IL-8** liberada ao sobrenadante nos cultivos celulares, **proporcionando unha clara evidencia do papel inmunomodulador da LF sobre a expresión dos receptores TLR2 e apoiando o potencial da LF como estratexia terapéutica.**

Brevemente, neste proxecto de tese demostrouse a utilidade da lágrima como fonte de biomarcadores na patoloxía do QC**.** Específicamente, verificouse a importancia dos procesos de estrés oxidativo, inflamación, e das alteracións no transporte e homeostase do ferro na fisiopatoloxía desta enfermidade. Determináronse biomarcadores sensibles e específicos na detección das alteracións biomecánicas da cornea e a susceptibilidade da descendencia dos pacientes con QC ao posible desenvolvemento da patoloxía. Así como tamén evidenciouse o potencial da LF humana como inmunomodulador dos TLR2, e por tanto como posible estratéxica terapéutica para o QC.

Abbreviations

A1DA	Corneal deformation amplitude at the first applanation
A2DA	Corneal deformation amplitude at the second applanation
A1DLA	Corneal deflection amplitude at the first applanation
A2DLA	Corneal deflection amplitude at the second applanation
A1DLAr	Corneal deflection area at the first applanation
A2DLAr	Corneal deflection area at the second applanation
A1DLL	Corneal deflection length at the first applanation
A2DLL	Corneal deflection length at the second applanation
A1T	Time from the beginning of the air-puff until the first corneal applanation
A2T	Time from the beginning of the air-puff until the first/second applanation
A1V	Velocity of the corneal apex during the first corneal applanation
A2V	Velocity of the corneal apex during the second corneal applanation
ACTG	Actin cytoplasmic 2
ACTN4	α-actinin 4
AE	Anterior corneal elevation
AFU	Arbitrary Fluorescence Units
AGT	Angiotensinogen
AHSG	α2-HS-glycoprotein
AIC	Alkaike's information criterion
ALB	Serum albumin
ALDH	Aldehyde dehydrogenase
ANXA1	Annexin A1
ANXA2	Annexin A2
AP-1	Activating protein-1
APOA1	Apolipoprotein A-I
APOA2	Apolipoprotein A-II
APOBEC3A	DNA dC→>dU-editing enzyme APOBEC-3A
ARHGDIA	ρ GDP-dissociation inhibitor 1
ARTh	Ambrosio Relational Thickness horizontal
ARTmax	Maximum Ambrosio Relational Thickness
ASS1	Argininosuccinate synthase
AUC	Area Under the Curve
BAD	Belin-Ambrosio Enhanced Ectasia Display
BAD-D	Belin-Ambrosio total Deviation value
BFS	Best-fit sphere
bIOP	Biomechanical corrected intraocular pressure
CAP1	Adenylyl cyclase-associated protein 1
CAP2	Adenylyl cyclase-associated protein 2
CAPN1	Calpain-1 catalytic subunit
CBI	Corvis Biomechanical Index
CCT	Central Corneal Thickness
CCT_C	Central Corneal Thickness by Corvis® ST

CCT_P	Central Corneal Thickness by Pentacam® HR
CE	Collision Energy
CFL1	Cofilin-1
CH	Corneal Hysteresis
CI	Confidence Interval
CLEK	Collaborative Longitudinal Evaluation of Keratoconus
cps	Count per second
CRF	Corneal Resistance Factor
CUR	Curtain gas
CXL	Corneal collagen cross-linking
D	Diopters
D-PBS	Dulbecco's Phosphate Buffered Saline
DA	Deformation Amplitude
DA Ratio Max	Maximum ratio of deformation amplitude
DAB	3,30-diaminobenzidine
DAmax	Maximum deformation amplitude
DDA-MS	Data-dependent acquisition modes
DIA-MS	Data-independent acquisition modes
ECM	Extracellular matrix
ELISA	Enzyme-Linked Immunosorbent Assays
EZR	Ezrin
FC	Fold Change
FDR	False Discovery Rate
FITC	Fluorescein isothiocyanate
FOXO	Forkhead box, class O gene
FoxO	Forkhead box, class O proteins
GC	Vitamin D binding protein
GO	Gene Ontology
GS1	Ion source gas 1
GSH/GSSG	Reduced glutathione/oxidized glutathione ratio
GWAS	Genome-Wide Association Studies
GWLS	Genome-Wide Linkage Studies
h	Hour
HC	Highest radius concavity
HCDA	Deformation amplitude at the highest corneal concavity
HCdArclength	Highest concavity delta arc length
HCDLA	Deflection amplitude at maximum deformation
HCDLAr	Deflection area at maximum deformation
HCDLL	Highest concavity deflection length
HCT	Time from the initiation of the air-puff until the highest corneal concavity
HO-2	Heme oxygenase 2
HPSA8	Heat shock cognate 71-kDa protein 8
HPX	Hemopexin
HSPB1	Heat shock protein beta-1
I-S asymmetry	Inferior-Superior dioptric asymmetry
IDIS	Health research institute of Santiago de Compostela
IgA	Immunoglobulin A

IgG	Immunoglobulin G
IGKC	Immunoglobulin kappa chain
IKK	IkappaB kinase
IL	Interleukin
INGO	Instituto Galego de Oftalmoloxía
IOP	Intraocular pressure
IQR	Interquartile range
IR	Integrated radius
IRAK	IL-1 receptor-associated kinase
iRT	Ion Retention Time
ISVF	Ion spray voltage floating
JCR	Journal Citations Reports
JIF	Journal Impact Factor
K1	Keratometry in the flattest meridian
K2	Keratometry in the steeper meridian
KC	Keratoconus
kDa	Kilodalton
Kmax	Maximum dioptric power
KRT	Keratin
KRT5	Keratin type II cytoskeletal 5
LC-MS/MS	Liquid chromatography with tandem mass spectrometry
LCN-1	Lipocalin-1
LF/LTF	Lactoferrin/Lactotransferrin
LFU	Lacrimal Functional Unit
LIMK1	LIM domain kinase 1
LIMK2	LIM domain kinase 2
LRA	Logistic Regression Analysis
LXN	Latexin
LYZ	Lysozyme
m/z	Mass to charge ratio
maxDP	Maximum dioptric power
min	Minutes
MLR	Most Like Ratio
mm	Millimeter
mM	Millimolar
MMP	Matrix metalloproteinase
MS	Mass Spectrometry
ms	Milliseconds
MTP	Minimum Thickness Point
MyD88	Primary myeloid differentiation response gene 88
NADPH	Nicothiamide-Adenine Dinucleotide phosphate
NF-kB	Nuclear factor- kB
ng	Nanogram
O-KC	KC offspring
O-KC-LR	Eyes of offspring of KC patients with low-risk of ectasia development
O-KC-MR	Eyes of offspring of KC patients with moderate-risk of ectasia development
O-KC-HR	Eyes of offspring of KC patients with a high-risk of ectasia development

O-KC-LR_MR O-KC-LR eyes that progressed to a moderate risk stage after 3 years
O-KC-LR_HR O-KC-LR eyes that progressed to a high-risk stage after 3 years
O-KC-MR_HR O-KC-MR eyes that progressed to a high-risk stage after 3 years
O-KC-HR_prog O-KC-HR eyes that presented biomechanical worsening after 3 years
ORA Ocular Response Analyzer
ORM1 α1-acid glycoprotein 1

Pam2CSK4 Synthetic diacylated lipopeptide
Pam3CSK4 Synthetic diacylated lipopeptide
PCA Principal Component Analysis
PD Peak distance at the highest concavity
PDC Corneal central power
PE Posterior corneal elevation
PGD 6-phosphogluconate dehydrogenase decarboxylating
PLGA D,L-lactide-co-glycolic acid
PLS3 Plastin 3
PMD Pellucid Marginal Degeneration
PPIase Peptidyl-prolyl cis-trans isomerases
ppm Parts per million
PRDX Peroxiredoxin
PVDF Polyvinylidene fluoride

RENOIR Corneal Neurodegeneration group
RNS Reactive Nitrogen Species
ROC Receiver operating characteristic curve analysis
ROIs Regions of interest
ROS Reactive Oxygen Species
RT Room Temperature

s Second
S100A11 Protein S100 A11
SD Standard Deviation
SEAP Secreted Embryonic Alkaline Phosphatase
SNPs Single Nucleotide Polymorphisms
SOD Superoxide dismutase
SP-A1 Stiffness parameter at the first applanation
SSI Stress-Strain Index
SWATH-MS Sequential Window Acquisition for All Theoretical Mass Spectra

TAB Transforming growth factor-β- activated kinase 1 binding protein
TAK1 Transforming growth factor-β- activated kinase 1
TBI Tomographic and Biomechanical Index
TBST Tris chloride Buffered Saline with Tween®
TF Transferrin/serotransferrin
TIMP Tissue inhibitor metalloprotease
TLR Toll-like receptor
TNF- α Tumor Necrosis Factor-alpha
TNF- β Tumor Necrosis Factor-beta
TRAF6 Transforming protein tyrosine kinases 6
TTR Transthyretin
TUBA1C Tubulin α1C chain

USC Universidade de Santiago de Compostela

V	Volt
WB	Western Blot
WP	Work Package
$Z3^{\pm 1}$	Vertical coma
ZAG	Zinc-α2-glycoprotein
ZG16B	Zymogen granule protein 18 homolog B
µg	Microgram
µL	Microliter
µm	Microns

Introduction

Justification and hypothesis

Objectives

Methodology

WP1. Clinical & molecular study of KC disease

WP2. Clinical & molecular study of KC at-risk stages

WP3. Human LF as a therapeutic strategy for KC

Discussion

Conclusions

Introduction

Keratoconus

1.1 Definition and main remarks

Keratoconus (KC) is the most common corneal ectasia, in which, as the name suggests, the corneal structure takes on a central or paracentral conical shape arising from weakening, thinning, and protrusion of the corneal tissue.[1] By definition, KC is chronic and degenerative, usually bilateral, and asymmetric, with an unpredictable course that can range from mild to severe stages.[2,3]

Biomechanical failure of the corneal tissue promoted by the molecular and morphological changes in tissue cells during the disease development is currently considered the driver to ectasia onset.[4,5]

Under this process, the steep and sharply asymmetric final corneal shape, resulting from the stromal and epithelial destructuring, induces high irregular astigmatism and increased magnitudes of higher-order aberrations, leading to significant visual impairment.[6]

The early onset of KC, affecting mainly young patients, entails not only a strong impact throughout the patient's life but also a major socio-health problem.[7]

In terms of etiology, KC stems from a complex multifactorial origin involving the interplay of mechanical-environmental factors alongside a genetic predisposition to its development.[8,9] This genetic predisposition has been explained as the coexistence of multiple pathogenic variants that make up a highly susceptible genome to the disease onset,[10] and diverse inheritance patterns seem to explain the high prevalence of the disease in KC first-degree relatives, which are considered the most vulnerable population for KC development.[9,11]

Numerous studies focused on unraveling the biochemical and molecular events intertwining in the pathophysiology of the disease have allowed us to move beyond non-inflammatory attribution to a much more in-depth understanding, acknowledging the role of chronic inflammation and oxidative stress in cell degeneration during corneal ectasias.[12–17] However, despite the mechanisms linked to the clinical disease appear to be increasingly clear, the molecular drivers associated with the earliest stages of the disease as well as the

at-risk stages have barely been determined, highlighting the necessity of deciphering the initial triggering events to enable the optimization of preventive and early monitoring therapies.

1.2 Delving deeper into corneal ectasias

The term "corneal ectasia" includes several conditions recognized by the Global Consensus on Keratoconus and Ectatic Diseases. These include KC, pellucid marginal degeneration (PMD), keratoglobus, and iatrogenic surgery ectasia.[18]

One of the main ways of classifying corneal ectasia involves its origin, which may be triggered naturally or secondary to a structural impact on the corneal tissue following surgery. Ectatic processes that arise after a surgical procedure, generally associated with refractive purposes, are known as iatrogenic ectasia or post-refractive surgery ectasia.[19,20] In this regard, the rise of refractive surgery and the emergence of innovative procedures encouraged research into the causalities of ectasia origin and the detection of mild or at-risk forms.

Besides origin, localization of the maximum thinning area is also effective for corneal ectasia characterization, differentiating between central or paracentral (typical of KC), generalized (distinctive of keratoglobus) or peripheral (the signature of pellucid degeneration) thinning.[21]

Given the histopathological, topographical and pachymetric similarities between all these conditions, it has been proposed that they may represent a phenotypic variation of the same pathogenic mechanism, even with some different clinical hallmarks such as the corneal zone concerned, age of onset, rate of progression or biomicroscopic features.[22] In this context, shared origin or genotypic compatibility could explain the existence of two conditions in the same individual, being relatively usual co-occurrence of two different degenerations, such as PMD in the contralateral eye of the patient with KC, keratoglobus in the contralateral eye of patients with KC or PMD, and even atypical patterns of KC with globular or peripherical forms.[23,24]

KC stands out as the most prevalent corneal ectasia, becoming the most studied type of corneal ectasia and the most convenient model for understanding the molecular insights of these set of pathologies. In this sense, throughout this doctoral thesis we focused on the KC pathophysiology related to its predisposition and onset.

Table 1 summarizes the clinical criteria for the differential diagnosis of corneal ectasias based on nature, morphology, and biomicroscopy.

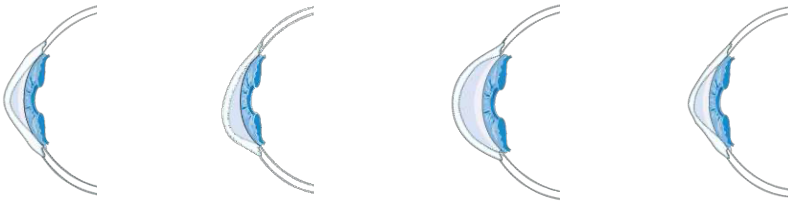
	Features	KC	Pellucid marginal degeneration	Keratoglobus	Iatrogenic ectasia
GENERAL ISSUES	Origin	Natural	Natural	Natural	Iatrogenic
	Onset	Puberty or earlier	20-40 years of age	Usually at birth	6 months after surgery
	Frecuency	Most frequent ectasia	Less frequent	Rare	Infrequent
MORPHOLOGY	Location	Axial	Peripheral	Globular	Axial
	Thinning	Central / Paracentral	Lower band	Widespread	Central / Paracentral
	Steepening	Apex, coincident with thinning area	Superior to thinning area	Widespread	Widespread
	Symmetry	Asymmetric	Asymmetric	Symmetric	Asymmetric
	Laterality	Usually bilateral	Usually bilateral	Bilateral	Usually bilateral
BIOMICROSCOPY	Fleischer ring	Frequent	In some cases	None	In some cases
	Vogt striaes	Frequent	Infrequent	Infrequent	Infrequent
	Corneal scarring	Frequent	After hydrops	Moderate frecuency	Infrequent
					

Table 1. Description of the morphological, biomicroscopic and general characteristics of the different corneal ectasias. . Self-created table using elements with Creative Common license.

1.3 Epidemiology

KC prevalence and incidence estimation differed over the last century, depending largely on the geographical area, and being underestimated in many cases due to the symptomatic diagnosis of the pathology. In this sense, visual impairment appears in moderate to advanced

stages of the disease, leaving the subtle or subclinical forms hidden and undetected in most cases. Advances in more sensitive imaging tools allowed the updating of prevalence data, which is now estimated to be 1:375.[25] Results on sex-specific rates are controversial, and overall, KC is considered to affect both sexes similarly.[3,7,26] Regarding disease onset, it is usually diagnosed in the twenties or even earlier, with an average age of 20 ± 6.4 years.[27] However, the time of diagnosis does not reflect the onset of the pathological process, which would start some time earlier. A negative correlation between age of diagnosis and severity has been reported, and pediatric KC has been described as a more aggressive condition, with a faster progression and often reaching more severe stages than when it develops in late adolescence.[26] In this sense, it has been estimated that 28% of pediatric KC cases are diagnosed in already severe stages.[26,28–30]

1.4 Aetiology

The multifactorial nature of KC involves genetic-molecular factors that determine the risk of its development and mechanical-environmental factors that heavily influence its progression. From a pathophysiological perspective, KC seems to represent the final path of different pathological processes that arise from a sensitive genetic signature and subsequently evolve under the influence of several internal and external risk factors.

1.4.1 Genetics and inheritance

The genetic background of KC has long been suggested given its association with other genetic syndromes,[31–33] the high developmental risk in KC relatives,[9] as well as the higher concordance in the topographic pattern in monozygotic over dizygotic twins.[34,35]

Genetics

Genetic and transcriptomic studies determined multiple candidates and variants associated with KC, proposing an oligogenic causality in which multiple pathogenic variants reside in an individual within a highly susceptible genome.[10] From a narrowly genetic point of view, the *genome-wide association studies* (GWAS) provided a deeper insight into the genetic architecture of KC disease, revealing more than twenty loci linked to KC disease.[36–40] At the same time, GWAS focused on some specific hallmarks of KC, such as central corneal thickness (CCT), corneal hysteresis (CH), and the corneal resistance factor (CRF), provided a comprehensive understanding of the genetic load that affects all these traits and confirmed the overlap with some of the reported variations in KC disease.[40] In this sense, the last GWAS over CCT determined 41 loci associated with CCT and also with KC predisposition, highlighting collagen and extracellular matrix (ECM) remodeling paths as a central regulator of both conditions.[41] Similarly, GWAS about the biomechanical parameters (CH, and CRF) dilucidated the role of *FNDC3B, ZNF469, MPDZ*, and *FOXO1* in biomechanical

decline,[42] which previously were associated with both KC predisposition and CCT variability.

On the other hand, over the years, gene expression studies found numerous genes with differential expression between KC and healthy corneal tissues.[43–46] Most of them were linked to collagen synthesis and organization, cellular adhesion, extracellular matrix (ECM) degradation and remodeling, and oxidative protection, strengthening the relevance of these processes in the pathophysiological basis of the KC disease.[47,48]

Moreover, *genome-wide linkage studies* (GWLS) genotyping families affected by KC also described several genomic loci associated with familial KC, standing out single nucleotide polymorphisms (SNPs) associated with the *LOX, DOCK9, COL5A1, PPIP5K2, MIR184,* and *CAST* genes.[49–52]

Overall, genetic analysis concluded the polygenic nature of this disease, where variations in a complex network of genes would lead to KC traits development.

Inheritance

Whereas KC could appear sporadically with no Mendelian patterns of inheritance to support its origin, having a first-degree relative affected by this condition is considered one of the most relevant risk factors.[53] KC first-degree relatives have shown between 15 to 67 times higher risk of developing the disease than the population with no family history of KC.[9,54] In addition, available data at present indicates that up to 26% of patients with KC report a positive family history of this disease, and the presence of two or more relatives with KC within the family has been associated with increased disease progression and severity.[55,56] The higher concordance in severity and topographic pattern of the disease in monozygotic over dizygotic twins supports the genetic contribution, and consanguineous marriage is identified as a risk factor for offspring.[34,35,57] The reported inheritance pattern of familial KC is usually autosomal dominant and occasionally recessive, with incomplete penetrance and variable phenotype,[11,58] and family-based genetic studies identified specific genes that seem to contribute to the genetic KC predisposition, suggesting a complex mode of genetic inheritance.[59]

Furthermore, observational clinical studies held significant value in the field of familial KC, as observations of common abnormalities in the corneal biomechanics and morphology in KC relatives flagged their possible risk to disease development. In this regard, it has already been reported that even without fully developed KC patterns, KC relatives commonly exhibit steeper and thinner corneas, even with features resembling subclinical KC or KC suspect.[60–62] In the same way, biomechanical weakness resulting from decreased corneal stiffness and strength has also been described in KC relatives.[63,64]

1.4.2 Mechanical and environmental factors

The influence of mechanical and environmental factors on the phenotypic profile of KC and its progression has been widely recognized. The impact of the environmental realm could explain the differences in KC prevalence across different geographical areas, where increased UV exposure has been postulated to be an aggravating factor of corneal oxidative damage, that plays a key role in the disease's pathophysiology.[65]

Chronic mechanical trauma encourages inflammatory processes and biomechanical tissue instability, becoming one of the most dangerous habits for KC progression and severity.[66] This mechanical stress is mainly associated with the habit of eye rubbing, informed by about a half of KC patients.[67]Eye rubbing linked to KC has been well characterized, and described as being energetic, vigorous, and prolonged, often more intense than that caused by atopy or allergy.[68–70] During ocular rubbing, microtrauma on corneal epithelial cells promotes the release of metalloproteases and inflammatory cytokines that contribute to tissue damage.[71] The underlying reasons for severe eye rubbing point to intense eye itching, however, the question of whether ocular itching in ectasias stems from an allergic or atopic cause remains unclear. Previous studies suggest that allergies may affect roughly one-third of KC patients,[69,72] but inconsistencies between studies make difficult establish a definitive consensus on the relationship between allergic conditions and ectasia.

At present, it seems reasonable to consider the hypothesis that eye itching of KC patients is a consequence of the interaction of several conditioning factors: (i) the inflammatory imbalance on the ocular surface in the KC disease, (ii) changes in tear fluid composition, (iii) high sensitivity to external stimuli due to corneal tissue instability, (iv) allergy, eye rubbing, and the unsuitable fitting of contact lenses also contribute to eye itching due to the increase in inflammatory mediators.

1.5 Pathophysiology

While the precise molecular network behind KC pathophysiology remains unclear, over the last few years multiple studies have described some of the pathological events that appear to be associated with the disease onset and progression.[73] The biochemical standpoint suggests the convergence of three mainly pathogenic mechanisms that would lead to the KC morphological changes: oxidative stress, inflammatory and immune dysregulation, and degradation of the extracellular matrix, which synergistically contribute to and promote early cell death and degeneration in the corneal tissue.[12–14,74–78] Additionally, the contribution of hormonal factors in the KC pathophysiology also has been reported.[79]
Figure 1 illustrates the main pathological processes described in the KC disease.

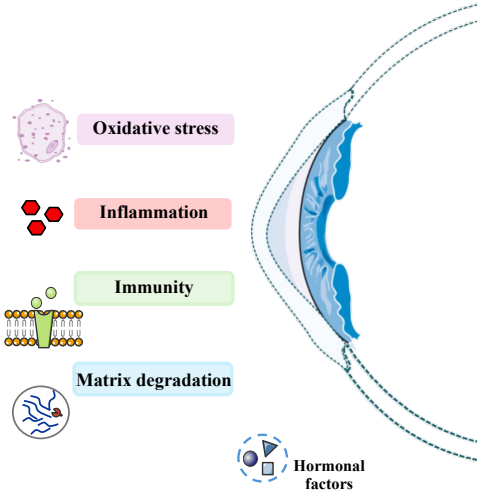


Figure 1. Summary of the main pathological processes involved the KC disease. Self-create image using elements with Creative Common license.

1.5.1 Oxidative stress

Oxidative stress arises from an imbalance between reactive oxygen species (ROS) and cellular antioxidant capacity, where the accumulation of unneutralized ROS leads to cytotoxic deposition of metabolites such as nitric oxide that damage tissues through membrane disruption, cellular DNA damage, membrane lipid peroxidation, inactivation of receptor proteins and enzymes, and finally cellular apoptosis and autophagosome-mediated autophagy.[80] The involvement of oxidative stress in the pathophysiology of KC has been reported many times, proposing a reduced antioxidant capacity of keratoconic corneal epithelial and stromal cells.[75,81] The decreasing antioxidant capacity has been hypothesized through the under-expression of some essential enzymes for oxidative defense, such as superoxide dismutase (SOD).[82] SODs are the primary defense systems for neutralizing free radicals and protecting against oxidative damage in cells,[83] and lower expression of SOD1 was found in the tear fluid, serum, and corneal tissue of patients with KC.[76,84,85] NADPH dehydrogenase, aldehyde dehydrogenase (ALDH), and heme oxygenase 2 (HO-2) expression also was decreased in the corneal epithelial cells of KC patients, supporting a weaker oxidative protection system.[86,87] In the same line, several non-enzymatic antioxidant mechanisms also showed a significant decrease in the KC corneas, including decreased glutathione, reduced glutathione/oxidized glutathione ratio (GSH/GSSG), and lower expression of antioxidant proteins such as transferrin (TF) and lactoferrin (LF).[14,16,84,86,88] Multiple antioxidant genes are dysregulated in KC, and genetic variations in *FOXO* (Forkhead box, class O) have been widely associated with KC disease.[40,89] FoxO proteins represent a family of transcription factors that takes on a critical role in redox regulation and oxidative defense by promoting the transcription of genes encoding key antioxidant proteins such as SODs and peroxiredoxins (PRDXs).[90] *In vitro* studies demonstrated a higher production of ROS and RNS (reactive nitrogen species) by KC fibroblasts,[17] so, all these

findings together seem to explain the redox imbalance and the lower total antioxidant capacity observed in both corneal tissue and tear fluid of KC patients.

1.5.2 Inflammation

Inflammation is a defensive, repair, and functional recovery precursor mechanism triggered upon alterations or damage in tissue homeostasis.[91] In general, it is a non-specific response that occurs mainly in vascularized connective tissues and aims to stop aggression and repair its consequences. Acute inflammation is associated with vasodilatation, alterations in capillary permeability, and accumulation of white blood cells and proteins.[92] This assumption of the inflammatory concept limited the attribution of inflammation in the pathophysiology of KC due to the avascular nature of the cornea and the absence of such cardinal inflammatory signs. However, over the last few years, many studies have pointed to the dysregulation of inflammatory markers in KC, suggesting the contribution of inflammatory pathophysiological events which would more closely resemble a chronic inflammatory process, characterized by the release and activation of molecular mediators that promote tissue injury over time and without apparent self-limitation.[93,94]

Dysregulation of inflammatory factors has been described in tears, serum and saliva fluids, as well as at the tissue level (corneal epithelium and stromal keratocytes) of KC corneas.[95] Specifically, tears and corneal epithelium from KC patients showed up-regulation of proinflammatory cytokines such as interleukins (IL)-1, IL-4, IL-5, IL-6, IL-8, tumor necrosis factor-alpha (TNF-alpha), and numerous matrix metalloproteases (MMP-1, MMP-2, MMP-3, MMP-7, MMP-9), determining a positive correlation between the rise of inflammatory mediators and the disease progression.[12,13,15,96] In the same way, under-expression of MMP inhibitors such as tissue inhibitor metalloprotease 1 (TIMP-1) was also observed in KC corneas.[97]

Furthermore, *in vitro* studies demonstrated that microtrauma induced by eye rubbing on the corneal surface induces the release of inflammatory mediators and increased proteolytic activity in both KC and healthy eyes, supporting the influence of mechanical stress on the increased inflammatory response and KC progression.[71]

1.5.3 Innate immunity

The exposure of the ocular surface to constant environmental aggressions requires a mechanical, anatomical, and immunological defense system that preserves its integrity and proper functionality. For this purpose, the eye is defined as an immuno-privileged organ exhibiting a remarkable capacity for self-regulation during inflammatory processes to prevent damage to its structures. Mechanisms that account for the immune privilege include the physical and molecular barriers, the immunological tolerance of the anterior segment, and the intra-ocular immunosuppressive microenvironment.[98] The tear fluid is the primary

source of immunological effectors in the ocular surface, providing many components with antimicrobial, anti-inflammatory, and immunomodulatory properties. In the same way, the cornea also contributes to the immune privilege due to the lack of lymphatic drainage and vascularization. Our group first reported the involvement of innate immunity among the pathophysiological events underlying KC development by observing the over-expression of toll-like receptors (TLR) 2 and 4 in the corneal and conjunctival epithelial cells, as well as in blood cells of KC patients compared to healthy controls.[77,99,100] Furthermore, TLR2 and TLR4 overexpression has been associated with KC severity, being postulated as a good prognostic biomarkers of the disease (*European patent EP15382060 extended to: Singapore, Japan, Austria and Canada*). The specific value of these biomarkers was also supported by its higher expression in the first-degree relatives of KC patients and also in other corneal ectasias, such as the pellucid marginal degeneration, considered as a phenotypic variation of the same pathogenic mechanism.[100,101]

TLRs are evolutionarily highly conserved type I transmembrane proteins whose activation induces signaling and expression of inflammatory cascades and molecules.[102] The most common signaling path of TLR is mediated by MyD88 (primary myeloid differentiation response gene 88).[103] When MyD88 is stimulated, it interacts with IRAK (IL-1 receptor-associated kinase) type 1 or 4, and IRAK binds to the TRAF6 (transforming protein tyrosine kinases 6) adaptor protein which acts through two pathways: one activating the transcription factor AP-1 (activating protein-1) and the other activating the TAK1/TAB (transforming growth factor-β- activated kinase 1/ transforming growth factor-β- activated kinase 1 binding proteins) complex and enhancing the IKK (IkappaB kinase) activity. During this second activation path, IKK phosphorylates the IkB domain of the NF-kB factor (nuclear factor- kB), leading to its degradation and the translocation of p65 to the nucleus. Finally, the translocation of NF-kB to the nucleus induces the release of pro-inflammatory cytokines and results in the beginning of the inflammatory response secondary to the innate immune response. That´s the basis underlying the relationship between the overexpression of inflammatory mediators and immune effectors in KC disease, where prolonged activation of the immune system could contribute to the chronic inflammatory state reported on the ocular surface of these patients.

Considering that persistent stimulation of innate immune receptors may contribute to chronic activation of inflammatory events, the therapeutic potential of TLRs blocking has also been suggested, specifically for diseases where inflammation promotes and exacerbates the remaining pathological processes. This is supported by the fact that, by acting upstream of the activation of the immune-inflammatory cascade, their inhibition could reduce the release of inflammatory cytokines and would be more effective than acting directly on the specific molecules.[104,105]

In this regard, there are several ways for TRLs blocking.[105] The first option is based on the use of neutralizing antibodies; however, it would only be useful for the cell-surface TLRs

inhibition. To address this limitation, synthetic antagonists can also be used, but their efficacy and side effects are difficult to determine. In the same line, the inhibition of signaling pathways by blocking some of the activation kinases also allows receptor inactivation but may lead to excessive immunosuppression. Finally, the last path for TLR blocking includes some endogenous ligands which can modulate the activation of TLRs, including the fibronectin, heat shock proteins, several unsaturated fatty acids, and LF, representing a promising pathway for the regulation of the activation and functionality of these receptors.[106]

Specifically, LF is an iron-binding glycoprotein belonging to the TF family and which under-expression has been previously associated with KC pathophysiology.[14,16] In structural terms, LF has two homologous globular lobes (N-lobe and C-lobe) with two domains per lobe (N1,N2,C1, and C2). In addition, two LF conformational states have been characterized: the holo-LF (representing the iron-free protein where the two lobes are free of iron) and the apo-LF (as the fully iron-loaded protein, the two lobes are iron bonded).[107] Apart from its ability for iron binding and transport, LF has multiple biological functions that have led to great interest in its potential as a therapeutic target in several conditions.[108,109] Regarding immunity, the immunomodulatory function of the LF has been demonstrated by different paths, such as its interaction with some pathogen-associated molecular patterns involved in the TLR4 signaling cascade, promoting the inhibition of the receptor, and preventing the release of proinflammatory cytokines and the recruitment of immune cells to inflammatory sites.[110] Although interactions between LF and TLR4 have been well described, the influence of this protein on TLR2 (one of the most sensitive and specific biomarkers identified for KC disease) is not well documented.

Figure 2 shows how the mentioned pathological processes could promote epithelial cell damage in KC.

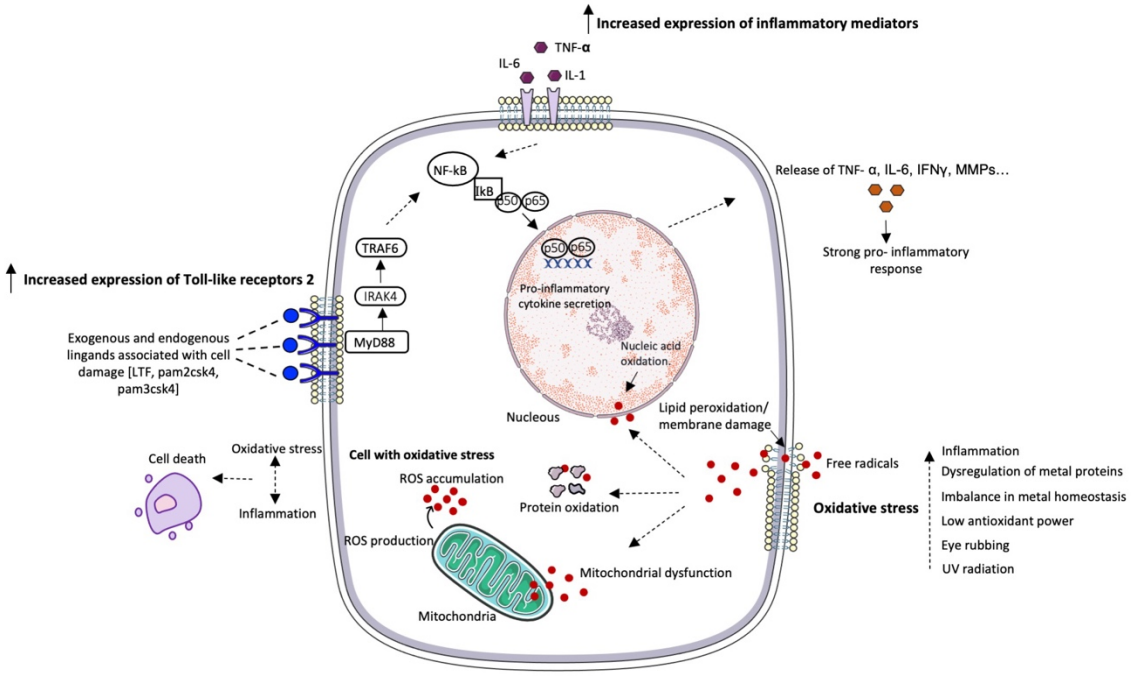


Figure 2. Schematic representation of epithelial cell damage in KC. Self-create image using elements with Creative Common license.

1.5.4 Extracellular matrix degradation

ECM disruption in KC pathogenesis has been described through collagen and proteoglycan loss in the corneal stroma of KC patients. In more detail, a decrease of collagen type I, III, V, VI, and XII has been reported in the stroma of the cornea with KC, along with a reduction of proteins involved in the hydroxylation of collagen propynyl residues (hydroxyproline and prolyl-4-hydroxylase) and of several proteoglycans such as keratan sulfate, lumican, keratocane or decorin.[111,112] Moreover, dysregulation of some genes codifying ECM structural proteins was also observed in the KC samples.[113] All these findings seem to represent the basis behind collagen fiber destructuring and matrix disassembly, compromising the stability of the corneal tissue in KC disease.

Additionally, the dysregulation of the matrix metalloproteinase system has been classically related to corneal thinning. Over-expression of MMP-1 and MMP-9 coupled with downregulation of their endogenous tissue inhibitors (TIMPs) has been proposed as the main mechanism underlying stromal degradation.[12,78,96] MMP-9 expression in KC corneas demonstrates a tenfold increase compared to healthy controls, exhibiting a positive correlation with disease severity.[12,13] Similarly, other degradative enzymes, such as cathepsins, have also been overexpressed in the KC tissue, probably further contributing to the ECM stromal degradation. [114]

1.5.5 Hormonal factors

Knowledge of the estrogen, androgen, and progesterone receptor expression in corneal epithelial cells and keratocytes suggests the possible relationship between hormones and corneal biomechanical properties at different life stages.[115] In this context, the involvement of hormonal factors in the pathophysiology of KC is supported by the usual development of KC during puberty and the biomechanical changes and disease progression observed in pregnancy.[116,117]About biomechanics and pregnancy, estrogen levels that increase significantly during pregnancy have been shown to affect both corneal thickness and biomechanical behavior.[79] Supporting the potential role of the MMP system in KC pathogenesis, previous studies reported an analogous dysregulation during pregnancy. This dysregulation is characterized by increased expression of MMPs and a concomitant downregulation of their endogenous inhibitors (TIMPs), leading to increased proteolytic activity and tissue degradation, compromising biomechanical function, and promoting KC progression.[118] While studies using vascular smooth muscle cells have demonstrated that hormonal factors, such as elevated estrogen, can modulate the expression of MMPs (upregulating MT1-MMP [MMP-2 activator] and MMP-3 in the presence of IL-1β)[119], the precise interplay between hormones and the MMP system within the corneal tissue remains to be elucidated.

1.6 Histology and semiology

Histological changes of the corneal tissue in KC disease have been well characterized and give rise to the main corneal signs that determine the semiology of the pathology.

1.6.1 Histology

Histological alterations in corneal tissue during KC disease are primarily associated with the loss and disorganization of corneal structural components. Corneal tissue consists of six layers, from the outermost to the innermost: epithelium, Bowman's membrane, stroma, Dua layer, Descemet's membrane, and endothelium.

KC affects predominantly the anterior corneal area, showing changes in the epithelial cell morphology with deposition of iron particles (Fleischer ring), evidencing disruptions in the Bowman’s membrane, and implying a strong impact on the corneal stroma, with a loss of collagen lamellae, disorganization and alterations in fiber orientation, and decreased density of keratocytes.[120–122] Corneal thinning during KC disease reflects mainly the alterations at the epithelial and stromal levels **[Figure 3].** Innermost layers usually remain intact, although there may be folds ("striae") in Descemet's membrane that disappear when pressure is applied.

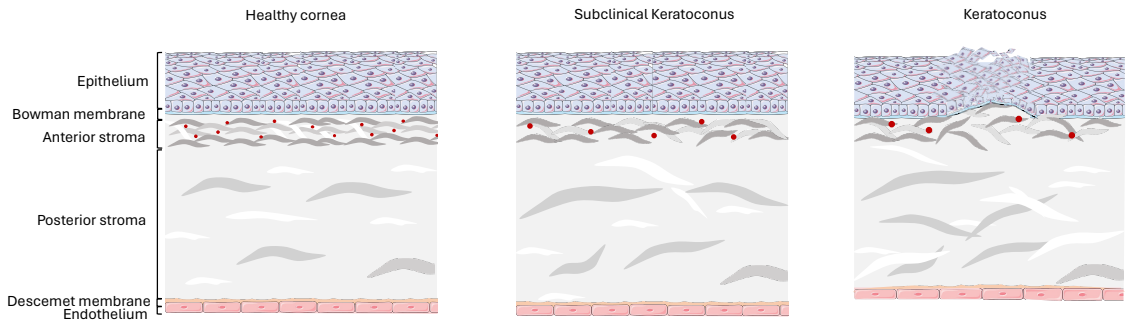


Figure 3. Histological changes of the corneal tissue during KC disease, including morphological changes in epithelial and stromal cells, alterations in the density and cross-linking of collagen lamellae and fibers, disruption of the Bowman's membrane, and thinning of the epithelial and stromal area. Self-create image using elements with Creative Common license.

1.6.2 Semiology

Regarding KC signs, they differ depending on disease severity and become more evident at advanced stages. In many cases, retinoscopy examination alerts to the existence of an undiagnosed KC observing two reflexes oriented in the same direction but moving in opposing directions, called scissors reflex, which indicate the presence of an irregular refractive error. Characteristic signs observed by slit-lamp examination include prominent corneal nerves, Vogt striae's (stress lines, tiny and vertical crossing the corneal depth), Fleischer ring (ferritin deposits in the epithelial basement membrane), and two corneal protrusion derived signs; the Munson's sign (an V-shaped indentation observed in the lower eyelid when the patient is looking downwards), and the Rizzuti's sign (a bright reflection from the nasal area of the limbus when light is directed to the limbus temporal area).[3] Ultimately, at severe stages of the disease, the cornea may lose its transparency with scars or leukomas secondary to hydrops.

Furthermore, in refractive terms, early KC usually presents without visual impairment; however, as the disease progresses, the spherical refractive component and the irregular astigmatism increase, and higher-order aberrations increasingly disrupt the retinal image, making progressive deterioration of visual quality the main symptom of the KC patient.[123] In addition, affected contrast sensitivity and impaired binocular vision also have been reported in KC patients.[124,125]

1.7 Diagnosis and classification

Differential diagnosis of KC is based on different tools such as corneal topography and tomography, which are highly sensitive for the detection of clinical disease as well as for monitoring its progression. In addition, slit-lamp biomicroscopic findings as well as refractive signs and symptoms leading to alterations in optical quality also help to determine an accurate KC diagnosis. However, major limitations of these tools lie in their limited

ability to detect corneal ectasia in its earliest stages when there are no topographical changes or obvious signs in the corneal area.

Considering that the current hypothesis assumes that the molecular and morphological changes that occur in the corneal tissue cells during KC development modify the focal biomechanical properties of the corneal structure, promoting tissue protrusion (under the influence of the intraocular pressure) and leading to tomographic and topographic alterations, exploring the corneal biomechanical response in early clinical screening for KC seems essential.[4,5] For this purpose, different tools have been developed for the assessment of corneal biomechanical behavior and the recognition of milder or at-risk forms of KC.

1.7.1 Corneal biomechanics

Corneal biomechanics has emerged as a rapidly evolving field within ophthalmology due to its potential applicability in several subspecialties.[126] One of its main applications focuses on the detection of corneal tissue weakness that suggests an intrinsic predisposition of the corneal tissue to the development of ectasia when no biomicroscopic or tomographic warning signs are yet evident; however, despite its potential for this purpose, it is an emerging tool that has not yet settled into clinical routine. The emergence of new treatment modalities aimed at slowing disease progression in mild stages, such as corneal collagen cross-linking (CXL), highlighted the need for new tools of early and accurate diagnosis to maximize the yield and efficacy of innovative therapeutic approaches. In this line, corneal biomechanics allows knowledge about the risk, diagnosis, and staging of KC, overcoming the limitations of tomographic methods, and evidencing a paradigm shift for prediction and early detection of corneal ectasias.[127]

In vivo measurement of the corneal biomechanical properties became possible for the first time with the introduction of the Ocular Response Analyzer (ORA; Reichert Ophthalmic Instruments, Buffalo, NY), a non-contact tonometer that emits a collimated air puff to indent a 3 to 6 mm area of the apical cornea and including an electro-optical system that monitors bidirectional corneal motion by reflecting an infrared beam.[128] ORA biomechanical parameters include the CH, which represents the viscoelastic nature of the cornea or its viscous-damping capacity, and the CRF, offering information about the corneal resistance. Although its arrival marked the beginning of the field of clinical biomechanical assessment, the diagnostic utility of CH and CRF for detecting mild ectasia appears to be limited in terms of sensitivity and specificity.[129,130]

More recently, the Corvis® ST device (Oculus, Wezlar, Germany) was developed. Like the ORA, it is a non-contact tonometer but, in this case, including an ultra-high-speed Scheimpflug camera for corneal biomechanics assessment.[131] During the measurement cycle, the cornea undergoes a stress-strain process involving three stages of deformation (first applanation, maximum concavity, and second applanation) until recover its original

shape (**Figure 4**). Corvis® ST records all parameters related to the different corneal deformation processes, comparing them directly with the expected values and integrating highly specific indexes for the detection of the biomechanical anomalies related to the development of corneal ectasia. The main differences between Corvis® ST and ORA relate on one hand to the use of the Scheimpflug camera instead of infrared beam reflection, which allows 140 horizontal 8 millimeter (mm) frames to be acquired in a total duration of 33 milliseconds (ms), giving a much more complete assessment of the corneal deformation process, and, on the other hand, with the fixed maximum air puff pressure determined by the Corvis® ST in each scan, instead of in the ORA where the air puff pressure is highly influenced by the pressure at the first applanation.[132]

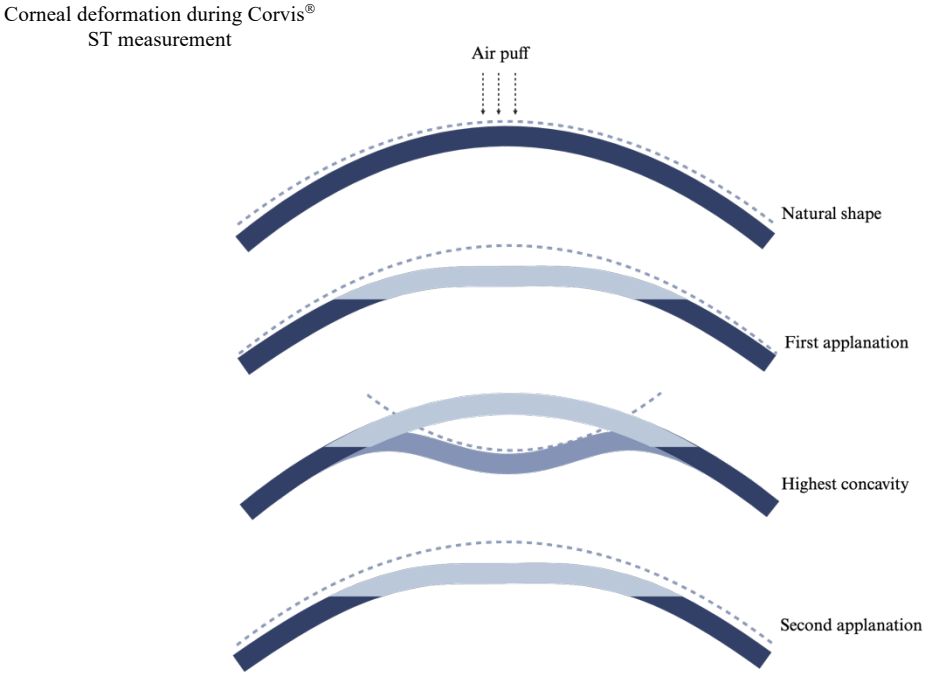


Figure 4. Schematic representation of the corneal biomechanical behavior during Corvis® ST assessment. Self-create image using elements with BioRender software.

This device calculates corneal deformation parameters based on the analysis of the corneal dynamic response, describing as deformation parameters those in which whole eye motion is not compensated, and as deflection parameters those that compensate the displacement of the whole eye. Therefore, the deformation amplitude (DA) indicates the displacement of the corneal apex in the anteroposterior direction, whose maximum value is obtained at the point of highest concavity (HC). The corneal applanation time (A1T/A2T), velocity (A1V/A2V) and length (A1DLL/A2DLL) are recorded from the beginning of the air-puff until the first/second applanation. Likewise, maximum value of the radius of curvature during the concave phase of deformation (Max Inverse Radius) and the integrated radius (IR), which

is the integrated area under the radius of the inversed curvature during the concave phase are also detailed. In this line, larger concave radius values (indicating a flatter corneal curvature) correspond to a higher resistance to deformation and increased corneal stiffness. Conversely, the higher values of IR and Max Inverse Radius underlie the higher concave curvature and thus the lower corneal strength and stiffness.[132]

An additional advantage of Corvis® ST is the ability to detect abnormalities in corneal pachymetric progression based on the horizontal imaging of the cornea. This translates to the ability to assess the profile or rate of increase in corneal thickness from the vertex to the nasal and temporal sides, calculating a specific index as the Ambrosio Relational Thickness horizontal (ARTh) which provides information about the relationship between the thinnest point of the cornea and the rate of pachymetric progression.[133] In the same line, the Pachy Slope parameter also reports corneal thickness changes from the center to the periphery, averagely determined at 2.5 mm from the apex. Detailed characterization of the pachymetric changes along the corneal surface allows an accurate and close view of the morphological abnormalities of the corneal structure than that provided by the static thickness measurement values, enabling the detection of abnormalities in the pachymetric progression of corneas whose central or minimum thickness values could be within the "normal range".[134]

As for the values of corneal stiffness and stress-strain, Corvis® ST provides the SP-A1 value as a marker of corneal stiffness, calculated as the adjusted pressure at the first applanation less the intraocular pressure (IOP) divided by the deflection amplitude at the first applanation.[135,136] SP-A1 has shown significantly lower values in eyes with KC compared to healthy eyes,[137] as well as a negative correlation with densitometry values,[138] so that corneas with higher back-scattering would show lower values of SP-A1 and compromised corneal stiffness. The stress-strain index (SSI) was subsequently created for the estimation of the *in vivo* elastic properties of the cornea. The SSI index was developed from an algorithm based on predictions of corneal behavior using finite element numerical modeling that simulate the effects of IOP, and the puff of air emitted by the device.[139]

Finally, using logistic regression analysis considering corneal deformation and stiffness parameters along with corneal thickness and pachymetric progression, the Corvis Biomechanical Index (CBI) was developed.[135,140] This regression analysis specifically included the following parameters: CCT, bIOP (biomechanically corrected intraocular pressure), deformation amplitude (DA), standard deviation of DA, A1V (velocity of the corneal apex during the first applanation), PD (distance between two corneal peaks at the highest concavity time), HCdArclength (Highest concavity delta arc length), HCDLAr (highest concavity deflection area), DARatioMax1mm/DARatioMax2mm (maximum ratio of deformation amplitude measured at 1 or 2 mm from the center of the cornea), inverse concave radius, HC radius (radius highest concavity), SP-A1 (stiffness parameter at first applanation), and ARTh (Ambrosio Relational Thickness horizontal).[135] CBI index showed a specificity of 100% and sensitivity of 94% for detecting KC eyes with a cutoff value of

0.5 and an area under the curve (AUC) of 0.983.[135] For subclinical KC detection, the efficacy of CBI index was also demonstrated with a sensitivity and specificity of around 80% and an AUC=0.858.[141]

1.7.2 Corneal topography and tomography

Corneal deformation during KC disease has traditionally been detected and monitored using corneal topographic and tomographic tools. Our knowledge of morphologic changes in corneal tissue has been growing with the progress of new technologies, improving accuracy in sensing increasingly subtle changes on the corneal architecture.

Given the diagnostic, staging and progression criteria defined for corneal ectasia, topography (evaluating anterior corneal curvature and wavefront aberrations) and tomography (analyzing anterior and posterior elevation and pachymetry) have been the classic tools used in clinical practice.[9,142]

Placido disc-based corneal topography represents one of the most frequently used tools for the detection of clinical ectasia and the characterization of the curvature and asymmetry of the anterior corneal surface,[143] however, the ability of corneal topography to detect changes preliminary to the onset of corneal ectasia is limited. Typical signs of KC observed through topographic imaging tools include areas of curvature with values greater than 47D, astigmatism with the rule and with infero-superior asymmetry in the mid-peripheral cornea, or oblique astigmatism with any type of corneal asymmetry.[3] The topographic pattern can take different shapes and change with disease progression; however, the asymmetric bow tie, oval or rounded shapes are usually predominant. In terms of aberrometry, changes in corneal shape and curvature induce an increase on the magnitude of high-order aberrations, especially on the levels of primary vertical coma and coma-like, that directly impact the visual quality of KC patients.[144]

Despite the weakness of these devices in detecting ectasia suspect, some features such as increased focal curvature and the existence of corneal asymmetry in the inferior quadrant, inferotemporal or inferonasal with central or paracentral involvement are considered warning signs of the possible development and progression of KC.[145,146]

The need to improve the diagnostic ability of corneal ectasia at earlier or at-risk stages prompted the development of elevation tomography tools, which enable scanning both the anterior and posterior corneal surfaces. In this regard, changes in corneal thickness and posterior elevation usually begin before alterations in frontal corneal curvature, so tomography imaging allows the detection of abnormalities that would be missed with a strict examination of the front cornea.[147–149] During KC progression, the increase in posterior corneal elevation and the reduction in corneal thickness are usual, frequently

matching the point of maximum corneal thinning and steepest curvature, and the location of highest posterior elevation.

Focusing on the advantages of tomography arises the Scheimpflug-based tomography, technology in which curvature maps are derived from elevation maps, providing high corneal coverage with a complete scan of the pachymetric progression along the corneal frame and low sensitivity to the tear film influence. The assessment of the corneal pachymetric distribution and progression becomes one of the main strengths of this technique, as ectatic corneas show an abrupt and rapid thinning from the periphery to the minimum thickness point but may present central or minimum thickness values equal to healthy corneas.

Pentacam® (Oculus, Wezlar, Germany) is the most widely used Scheimpflug-based tomography device in clinical practice. From a technical view, the elevation results obtained with this system are compared with a reference surface that magnifies the differences of the scanned cornea. In most applications, the best-fit sphere (BFS) is the reference surface of choice, so elevation alterations in an ectatic cornea reflect as a raised area to the BFS in the elevation maps. Pentacam® is an optimized device for ectasia screening, including specific screens and algorithms for enhanced ectasia visualization,[150,151] such as the Belin-Ambrosio Enhanced Ectasia Display (BAD), which incorporates the following parameters in a linear regression to identify the potential corneal ectasia with high sensibility and specificity[152]: anterior elevation in the thickness point, posterior elevation in the thickness point, minimum corneal thickness, location area of the minimum corneal thickness, pachymetric progression, relational thickness, and maximum corneal curvature.[151,153]

Furthermore, the development of the Tomographic and Biomechanical Index (TBI) by merging the results provided by the Corvis® ST corneal biomechanical scanner and those derived from Pentacam® tomographic data yielded a new index with 100% sensitivity and specificity for the detection of clinical ectasia.[154] The singularity of this index lies in taking advantage of the benefits of both tools as well as their potential for detecting ectatic abnormalities at their earliest stages. For combining data and optimizing the detection of ectasia-associated corneal abnormalities, some artificial intelligence methods (including logistic regression analysis with forward stepwise inclusion, support vector machine, and random forest) were applied. As a result, with a cut-off value of 0.79, TBI showed 100% of sensitivity and specificity to detect the clinical KC, and with a 0.29 value (90.4% sensitivity and 96% specificity) the fruste KC eyes.[154]

1.7.3 Classification

Classification and staging of KC disease are necessary for the design and optimization of the therapeutic options. The first step is to define subclinical and fruste disease states. In this sense, currently the term subclinical KC is used by scientists and clinicians to refer to

eyes with a regular slit lamp examination but with certain suspicious tomographic features that suggest a possible future development of KC but have not yet emerged as such. On the other hand, KC fruste has a different meaning, defining the topographically and biomicroscopically normal eye of a patient with KC in the contralateral eye.[146]

Although there is no Gold-Standard classification system, several modalities have been proposed, such as the Amsler-Krumeich,[155] the Collaborative Longitudinal Evaluation of Keratoconus (CLEK),[7] and the recently ABCD Belin classifications.[156] Most classifications stage the disease from mild to severe (or grade I to grade IV), based on corneal anterior curvature, corneal thickness, refraction and presence or absence of corneal scarring. As an innovation, the Belin ABCD classification offers a detailed and individual assessment of each of its parameters, including **A.** anterior radius of curvature, measured in the 3mm zone around the thinnest corneal point. **B.** posterior radius of curvature, measured in the 3mm zone around the thinnest corneal point. **C.** Minimum corneal pachymetry value. **D.** Best corrected visual acuity and corneal scarring.[156]

1.8 Treatment

Currently, available therapeutic options for KC do not offer a cure for the underlying disease, focusing on the optical compensation of corneal irregularity, strengthening the corneal tissue to slow disease progression, or ultimately replacing the affected area with healthy tissue.[1]

Optical management of corneal irregularity depends largely on disease severity. Patients with mild KC may compensate for the refractive error with ophthalmic lenses or hydrophilic contact lenses; however, as the disease progresses, the fitting of special contact lenses, such as rigid gas permeable, hybrid, or scleral lenses, is essential for the simulation of a regular corneal surface that allows a sharp retinal image.[157,158] Optical compensation should be attempted in all patients with corneal ectasia, as proper fitting of contact lenses will not aggravate disease progression.[159–161]

Regarding the surgical possibilities, to strengthening the corneal tissue and slow down the progression of KC, CXL technique was developed based on increasing corneal stiffness and strength by creating photochemical and covalent cross-links between the stromal collagen fibers.[162,163] CXL has successfully demonstrated to be an effective tool for slowing the KC progression and may be performed with or without de-epithelialization (epi-off / epi-on), being indicated in mild-moderate cases without severe corneal thinning and incurvation.[164,165]

Intrastromal rings constitute another surgical alternative to reshape the corneal geometry and improve the visual quality. The objective is to reinforce and restore the shape of the cornea improving not only visual acuity but also the fitting of contact lenses. Finally, when

refractive correction is insufficient, contact lens intolerance or fitting challenges significantly compromise wear time, and visual acuity is too impaired, corneal keratoplasty is the latest treatment alternative for KC, intended for severe and irreversible cases, with a long rehabilitation period and limited visual recovery.[166,167]

Besides all these optical and surgical procedures, warnings such as avoiding eye rubbing should be conveyed to the KC patient.[168] The relationship of eye rubbing with allergic events, as well as the association of chronic inflammation with disease severity, makes using topical anti-allergic and anti-inflammatory drugs also recommended to improve the ocular surface microenvironment and the associated symptomatology; however, there is no specific pharmacological treatment for KC disease. To address this gap, the last part of this thesis focused on studying human lactoferrin (LF or LTF) as a possible specific therapeutic strategy for the pathology of KC. Human LF is a glycoprotein whose involvement in KC pathophysiology has been widely studied by our group.[14,107] Besides that, LF's inherent properties as an immunomodulatory, anti-inflammatory, and antioxidant factor could make it an excellent therapeutic agent to cope with the main pathological paths involved in the KC disease. At the same time, its ability to be loaded easily into highly biocompatible and effective nanostructured and controlled release systems for its delivery on the ocular surface also supports its potential as a therapeutic approach.[169–171]

Tear fluid in the diagnosis and prognosis of KC disease.

The ocular surface is an anatomical complex that includes the tear fluid, eyelids, cornea, and conjunctiva. Constant exposure to the environment makes the ocular surface a critical area for injury, where the tear fluid plays a key role in protection, inflammatory suppression, defense, and heal traumatic or surgical injuries, maintaining the integrity of the ocular surface system. In addition to its protective role, previous studies have demonstrated communication pathways among the tear film, the corneal epithelium, and the corneal stroma, showing that the tear components can affect the phenotype of epithelial cells and stromal keratocytes.[172,173] Tear biomolecules are also vulnerable to changes associated with ocular diseases, providing information about the underlying tissues, and becoming an easily and promising source of specific biomarkers.

2.1 Production, release, and delivery of the tear fluid

The tear fluid exhibits a complex composition arising from the contributions of multiple secretory structures. Its production is controlled by the lacrimal functional unit (LFU), which includes the lacrimal glands, meibomian glands, accessory lacrimal glands, sebaceous glands, conjunctival globet cells, corneal and conjunctival epithelial cells,

eyelids, and the interconnecting innervation (starting with the stimulation of the corneal nerve endings and following with the modulation of the lacrimal gland activity).[174] The neural complex underlying tear production and secretion consists of interacting neural networks with sensory pathways (afferent innervation) and signaling pathways (efferent innervation) by the different members of the LFU. The sensory pathway originates in the densely innervated cornea, and the signals travel along the ophthalmic branch of the trigeminal nerve (V) to the cerebral pons. Here, synapses occur between these sensory pathways and the parasympathetic neurons of the facial nerve (VII). These parasympathetic neurons project towards a cluster of nerve cells called the pterygopalatine ganglion, which acts as a relay station, receiving signals from the facial nerve and sending outgoing signals (efferent pathways) to the lacrimal glands and globet conjunctival epithelial cells for tear production.[175] Therefore, the well-functioning LFU is essential in maintaining tear homeostasis, so abnormalities in corneal architecture and innervation could throw off the balance of the tear fluid homeostasis and composition.

2.2 Composition

In general terms, the tear fluid contains a specific blend of mucins, proteins, lipids, electrolytes, water, metabolites, vitamins, and a small percentage of other components (such a small organic molecules, cellular debris, nucleotides…); which interact intimately and define the main three layers of the tear film. In addition, blood plasma ultrafiltrate also enriches the tear fluid composition.[176]

The mucin layer contains a highly hydrated aqueous complex with mucin glycoproteins providing hydration and wettability to the hydrophobic surface epithelial cell membranes.[177] These mucins are secreted and released by the superficial epithelial cells of the cornea and conjunctiva and by the conjunctival globet cells.[178,179] Regarding protein composition, advances in proteomic profiling and discovery tools increased our knowledge of the protein constituents of tear fluid. More than 1500 proteins have been identified in tear fluid samples, including antioxidant, anti-inflammatory, antimicrobial, immunological, growth, and supportive factors, essential for nutrition, moisturization, and protection of the epithelial tissues.[180,181] Among tear proteins, some of them are predominantly expressed, such as LF, lipocalin-1 (LCN-1), lysozyme C (LYZ), or albumin.[181] The nature of these proteins come from different sources and may be secreted by the lacrimal gland or be serum proteins present in the tear film due to the permeability of the blood vessels. Changes in tear proteins expression have been associated with several ocular or even systemic diseases, leading to an increase in research focused on identifying specific tear protein biomarkers that could be useful for sensitive and accurate diagnosis of a wide range of pathologies.[182–186] Finally, lipid composition of the tear fluid consists of a mixture of lipids secreted mainly by the meibomian glands, building up a lipid bilayer consisting of an inner layer of polar lipids in contact with the aqueous layer and a surface layer of non-polar lipids. The main role of the

lipidic components is creating a smooth optical surface, reducing the surface tension of the tear film, and slowing tear evaporation.[187,188] Even though the tear fluid is usually represented as a bounded layer structure, this model provides a basic framework of the real complexity of tears, which comprise a dynamic and cohesive system functioning as a unified whole.

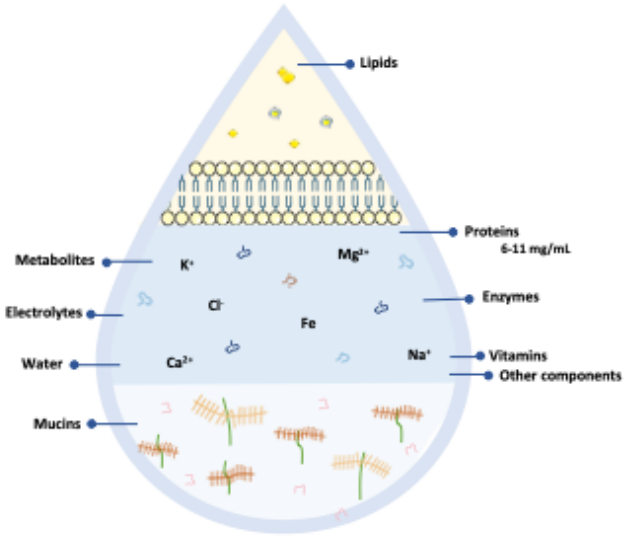


Figure 4. Overview of tear composition. Self-created image using elements with Creative Common license.

2.3 Tear fluid as a biomarker source in KC disease

From the knowledge of the tear fluid potential to provide new insights into the understanding of ocular physiology and in detecting and monitoring ocular pathologies, numerous studies have focused on searching for specific tear biomarkers for KC disease.[12,13,15,189,190] To this end, different tear components have been analyzed to determine their possible involvement in the KC disease. Reviewing the existing literature, previous studies reported differences in tear lipidic composition, metabolomics, and proteomics in patients with KC compared to healthy subjects. Regarding the alterations in the lipidic composition, currently available data indicates that KC patients show a high prevalence of meibomian gland dysfunction, positively associated with the disease severity.[191] Additionally, reduced tear film lipid layer was also observed in these patients together with a decrease in the partial blink rate,[192] which could influence the greater tear instability reported in KC.[193]

Metabolomic studies showed the dysregulation of several metabolites in the KC patient`s tears, revealing a lower antioxidant capacity and alterations in the oxidation state by reduced glutathione-glutathione disulfide ratio (GSH-to-GSSG), low levels of the glutathione metabolite, and also by the up-regulation of the lactate-pyruvate ratio in the KC samples. Additionally, dysregulation of metabolites affecting glycolysis and gluconeogenesis processes (such as 3-phosphoglycerate and 1,3 diphosphate glycerate), as well as citric acid

cycle (with increased isocitrate, aconitate, malate, and acetyl phosphate levels) and urea cycle (with higher ornithine and aspartate expression levels) were also found in the tear fluid of KC patients.[194] In the same line, changes in some organic acids expression in the KC patient`s tears after CXL were also observed (such as increasing N-acetyl-L-aspartic acid and decreasing 3-OH butyric acid and lactic acid/malic acid ratio), proposing alterations in energy and glucose metabolism during corneal reticulation.[195]

Proteins are the major effectors of the body, participating in all physiological processes such as transport, structure, metabolism, immunity, or cellular signaling. The promising role of proteins as molecular targets for both disease diagnosis and treatment has driven the rapidly growing in protein identification and quantification tools. In this line, the screening of the tear proteomic profile coupled with studies targeting on specific proteins have described a large part of the pathophysiological processes involved in KC disease, designing the molecular signature of this pathology, and deepening our understanding on its etiology.

2.3.1 The KC tear proteome

Of all components of tear fluid, proteins have been the target molecules in most KC studies. In this regard, one of the most relevant findings in the tear samples of KC patients was the increase expression of inflammatory markers such as IL-6, TNF-alpha, and MMP-9, moving away from the non-inflammatory definition of this pathology and suggesting the existence of chronic inflammation during its pathogenesis.[12,13,15,96,196] In addition, further research identified changes in other proteins with anti-inflammatory and immune functions, such as LF, zinc-α2-glycoprotein (ZAG), and immunoglobulin kappa chain (IGKC), pointing toward the possible role of innate immunity in the KC pathophysiology.[14] Following these preliminary approaches, a wide variety of studies have validated and complemented these findings, so that, to date, overexpression of multiple proinflammatory molecules has been observed in the tear fluid of patients with KC, including IL-1, IL-1β, IL-6, IL-8, IL-17, Interferon-γ, TNF-alpha, and TNF-beta.[12–15,189,197–199] In the same line, levels of some anti-inflammatory proteins such as LF, IL-10, IL-13, lipophilin A and C were decreased in the KC tear samples, revealing an imbalance between de pro and anti-inflammatory proteins and underlining the existence of a chronic inflammatory environment that promotes cell damage during KC disease. [14,16,189,200,201]

In the same way, analysis of tear fluid has further elucidated the potential role of oxidative stress in the KC pathophysiology. The ocular surface, being directly exposed to the environment, is particularly susceptible to oxidative stress, so it contains a high percentage of specific molecules that try to combat and maintain the levels of tissue-damaging reactive species. The imbalance of redox homeostasis in KC tears has been observed in several studies by the dysregulation of some proteins vital for oxidative balance such as SOD and others that may contribute by different paths to the increase of oxidative levels such as LF. [194,202]

Lastly, tear fluid has also become a reliable source of biomarkers indicative of cell damage and breakdown. In this regard, higher expression of MMP-9 in KC tear samples has been blamed as a critical biomarker responsible for pathological and excessive tissue degradation in KC disease.[13,15,96,203] Besides MMP-9, other matrix metalloproteases have shown higher expression in tears of KC patients, such as MMP-1, MMP-2, MMP-3, MMP-7, and MMP-13, and, conversely, endogenous inhibitors of MMPs, such as TIMP1 were observed under-expressed in comparison to the healthy controls.[15,204]

2.3.2 New tools and recent advances for proteomic profiling

While it is true that many tear biomarkers with a promising role in KC development have been identified, the complex sequence and interplay of the pathological events remain unclear. Most of the studies carried out to date used different techniques designed for the identification and quantification of specific proteins or protein panels; however, in most of the cases, isolated biomarkers still lack sufficient specificity and sensitivity to become useful in clinical practice, and the complexity of some diseases requires a deeper comprehension of the underlying pathophysiological context. To this end, the leap to omics tools enables not only the massive discovery of possible specific biomarkers, but also provides insights into the interaction networks between potential biomarkers and their signaling paths.

Over the last few years, proteomic approaches have increased their potential applications and become a powerful hypothesis generator.[205] Mass spectrometry (MS) emerged as the dominant method for proteomic studies, supported by its ability to detect and quantify changes in complex protein biofluids, as well as enabling the exploration of a large part of the protein profile. In this regard, MS uses different modes of data acquisition for protein identification and quantification, may be data-dependent acquisition modes (DDA-MS), where the most abundant precursor ions (those with the highest intensity at each chromatographic peak) are selected for fragmentation, analysis, and quantification by the tandem MS instruments, or data-independent acquisition modes (DIA-MS), which fragments and analyzes all peptides in the sample in each cycle, avoiding any bias caused by the pre-selection of specific precursor ions.[206] Among DIA-MS modes, sequential window acquisition for all theoretical mass spectra (SWATH-MS) represents an innovative approach that combines the data extracted from DIA-MS files but using higher resolution mass analysis to obtain precise protein quantification. This method is based on two processes: firstly, with the building of the MS-spectral library (by DDA-MS acquisition mode) which contains all the peptide information such as retention time, precursor *m/z*, and MS/MS spectra, and secondly, the samples are individually run in a DDA-MS acquisition mode for protein quantification. Due to its high sensitivity and quantification ability, SWATH-MS is considered an optimal technology for biomarker discovery.[207]

The proteome is a dynamic system in which protein-protein interactions are key in modulating the cellular phenotype and in regulating biological systems. In this line, the ongoing development and evolution of data analysis and interpretation tools have allowed the exploration and the accurate characterization of the interplay between potential protein biomarkers; describing the molecular mechanisms and biological pathways that could be involved in disease pathophysiology, and creating a comprehensive map of molecular alterations that provides valuable information for possible new diagnostic and therapeutic strategies.

Considering that the connection between the KC pathological events is not fully understood, proteomic studies offer an excellent alternative to identify and design combinations of biomarkers that improve the diagnostic and prognostic ability. Furthermore, the small biological sample required for the analysis and the big data provided make it an optimal tool for some biofluids, such as the tear fluid.[206,208,209] Based on the advantages of the LC-MS/MS, this project focused on that technology for biomarker network discovery. Specifically, we used a DDA workflow for protein identification and profiling and the Sequential Window Acquisition of All Theoretical Mass Spectra (SWATH-MS) method for protein quantification.

Introduction

Justification and hypothesis

Objectives

Methodology

WP1. Clinical & molecular study of KC disease

WP2. Clinical & molecular study of KC at-risk stages

WP3. Human LF as a therapeutic strategy for KC

Discussion

Conclusions

Justification and hypothesis

Keratoconus disease is characterized by biomechanical instability of the corneal tissue that preludes the tomographic and aberrometric changes that lead to visual loss. Several biomarkers with a promising role in the development of KC have been identified; however, the underlying complex sequence and interplay of the pathological events influencing biomechanical weakness remain unclear.

The higher prevalence in first-degree relatives of patients with KC and the association of disease severity and aggressive progression with the presence of two or more relatives with KC within the family make the KC family history the leading risk factor for disease development.

Evidence of communication pathways between the tear fluid, the epithelium, and the corneal stroma revealed the potential role of this fluid as a biomarker source in KC disease.

In this way, the hypothesis of this project postulates that the offspring of KC patients will present alterations in the tear proteomic expression that determine the susceptibility signature of the disease development. Likewise, tear proteomics mapping will bring a deep knowledge of the molecular drivers underlying alterations in corneal biomechanical properties in the at-risk stages of KC, providing new insights into the molecular mechanisms involved in the earliest disease and offering potential new therapeutic targets.

Introduction

Justification and hypothesis

Objectives

Methodology

WP1. Clinical & molecular study of KC disease

WP2. Clinical & molecular study of KC at-risk stages

WP3. Human LF as a therapeutic strategy for KC

Discussion

Conclusions

Objectives

The **main objective** of this study is to elucidate the molecular drivers underlying KC susceptibility in the offspring of KC patients, as well as to decode the biological mechanisms influencing corneal biomechanical weakness.

To this end, three work packages (WP) were established outlining the following specific objectives:

WP1. Clinical & molecular study of KC disease. To provide new insights into tear proteomic biomarkers and pathophysiological pathways of KC disease using liquid chromatography with tandem mass spectrometry (LC-MS/MS).

1.1 To analyze quantitatively the tear proteome of KC patients identifying the network of potential biomarkers of KC disease as well as their biological involvement in this pathology.
Addressed in Chapter 1: Tear proteomics in keratoconus: a SWATH-MS analysis.

1.2 To characterize qualitatively the global tear proteomic profile of KC patients obtaining an extensively view of the KC pathophysiology.
Addressed in Chapter 2: Shotgun proteomics for the identification and profiling of the tear proteome of keratoconus patients.

WP2. Clinical & molecular study of KC at-risk stages. To shed light on the molecular drivers and their main pathways accounting for KC risk, corneal biomechanical instability, and disease progression in the offspring of KC patients.

2.1 To analyze tear proteome of young KC offspring and determine the molecular drivers and mechanisms associated with corneal biomechanical weakness in KC susceptibility stages.
Addressed in Chapter 3: Tear proteomic analysis from offspring of keratoconus patients: new insights into corneal biomechanical weakness & disease risk stages.

2.2 To assess the corneal biomechanical and tomographical properties, and the expression of tear LF associated with biomechanical instability in young KC offspring during a three-year follow-up.
Addressed in Chapter 4: Clinical and molecular outcomes of three-years follow-up of offspring of keratoconus patients.

WP3. Human LF as a therapeutic strategy for KC. To determine the LF involvement in KC disease: (i) relationship with the disease's immune–inflammatory status [TLR2 expression], and (ii) immunomodulatory capacity as a therapeutic approach.

3.1 To measure the serum and tear LF levels in KC patients and their correlation with the KC immune-inflammatory microenvironment and severity.
Addressed in Chapter 5: Immunomodulatory effect of human lactoferrin on toll-like receptors 2 expression as therapeutic approach for keratoconus.

3.2 To determine the immunomodulatory capacity of LF on TLR2 expression using stimulated HEK-blue^{TM} human TLR2 (hTLR2) cell culture.
Addressed in Chapter 5: Immunomodulatory effect of human lactoferrin on toll-like receptors 2 expression as therapeutic approach for keratoconus.

Introduction

Justification and hypothesis

Objectives

Methodology

WP1. Clinical & molecular study of KC disease

WP2. Clinical & molecular study of KC at-risk stages

WP3. Human LF as a therapeutic strategy for KC

Discussion

Conclusions

Methodology

Clinical studies

3.1 Study design and participants

All clinical studies included in this doctoral thesis were performed following the principles of the Declaration of Helsinki of the World Medical Association. The Ethics Committee for Clinical Research of Santiago-Lugo authorized the ophthalmological clinical protocols and the biological sample extractions (registration codes: 2019/623 & 2020/089) (**Annexes 1-2**). All participants involved in these studies were recruited at the Instituto Galego de Oftalmoloxía (INGO), Santiago de Compostela, Spain. Each participant was informed and asked to sign a consent form outlining the study objectives, ophthalmologic procedures, biological sample collection, and potential undesirable events associated with sample extraction. The same researchers performed all the tests. All observational studies comply the STROBE checklist (**Annex 3**). **Table 3** summarizes the main design features of the five clinical studies included in this thesis project (each chapter is a scientific article).

	Chapter	Study selection	Sample size	Clinical procedures	Biological extraction	Molecular analysis
WP1	**Chapter 1** Tear proteomics in keratoconus disease: a SWATH-MS analysis.	Case-control study	25 KC patients 25 Control subjects	-Anamnesis -Ocular health exploration -Tomography	Tear fluid	• LC-MS/MS - DDA - SWATH-MS
WP1	**Chapter 2** Shotgun proteomics for the identification and profiling of the tear proteome of keratoconus patients.	Case-control study	25 KC patients 25 Control subjects	-Anamnesis -Ocular health exploration -Tomography	Tear fluid	• LC-MS/MS - DDA • ELISA
WP2	**Chapter 3** Tear proteomic analysis from offspring of keratoconus patients: new insights into corneal biomechanical weakness & disease risk stages.	Case-control study	80 KC offspring 42 Control subjects	-Anamnesis -Ocular health exploration -Biomechanical imaging -Tomography	Tear fluid	• LC-MS/MS - DDA - SWATH-MS • ELISA
WP2	**Chapter 4** Clinical and molecular outcomes of three-years follow-up of offspring of keratoconus patients.	Cohort study	80 KC offspring	-Anamnesis -Ocular health exploration -Biomechanical imaging -Tomography	Tear fluid	• ELISA
WP3	**Chapter 5** Immunomodulatory effect of human lactoferrin on toll-like receptors 2 expression as therapeutic approach for keratoconus.	Case-control study *In vitro* study	90 KC patients 60 Control subjects HEK- Blue™ hTLR2 cell culture	-Anamnesis -Ocular health exploration -Tomography -	Tear fluid Blood -	• ELISA • Flow cytometry • Immunohistochemistry • Western Blot • ELISA

Table 3. Design and main characteristics of the five studies included in this thesis. Self-created table.

For the studies including KC patients [**Chapters 1, 2, 5**], the main inclusion criterion for the study group was the KC diagnosis supported by biomicroscopy exploration and tomography imaging, following the diagnosis standards outlined in the literature.[210] Conversely, healthy control participants had to be matched in sex and age with the previous group and have normal tomographic and biomicroscopic features, without any corneal characteristics or irregular astigmatism suggesting a subclinical state of the disease and also without a family history of KC or other corneal ectasias.

Additionally, for the two studies involving young offspring of KC patients [**Chapter 3 and 4**], the main inclusion criteria for the study group (KC offspring, O-KC) were to be between eight and eighteen years old and having a parent diagnosed with clinical KC, supported by slit-lamp examination and corneal topography and tomography exams. Control participants should be sex-, and age-matched with the O-KC group, not have any family member diagnosed with subclinical or clinical corneal ectasia (neither first-degree relatives nor any other relatives) and having normal clinical parameters without alterations in the biomechanical and tomographical evaluation.

Common inclusion criteria for all studies included (1) Schirmer ≥15 mm in 5 min; (2) conjunctival hyperemia < 2 (Nathan Efron scale)[211] ; (3) at least 1 week without contact lenses and/or eye drops. Corneal trauma or disease, surgeries in the anterior segment, active ocular or systemic inflammation, treatment with anti-inflammatory drugs, as well as renal, hepatic, or hematological diseases were exclusion criteria for all groups. All participants reported European ancestry. The recruitment of study participants started in 2020 and extended until 2023.

For each study, the sample size was calculated using EPIDAT 3.1 software, considering as a calculation variable the concentration of different tear biomarkers obtained in previous studies and using the independent group mean comparison test, accepting the highest possible confidence and power.

3.2 Clinical measurements and protocols

3.2.1 Anamnesis

At the beginning of each study, anamnesis collected data about sex, age, presence of allergic, general, or ocular disease, family history of corneal ectasia, or other relevant conditions. Allergic diseases included atopic conditions such as rhinitis, asthma, or dermatitis, seasonal or chronic allergies, as well as food and drug allergies. Ongoing treatments, use of contact lenses, specific type of contact lenses, as well as presence or not of frequent itching and/or eye rubbing were also documented. Specifically for KC patients, the age at disease diagnosis was included.

3.2.2 Ocular health

Ocular health evaluation was based on an in-depth biomicroscopic exploration to identify any signs on the ocular surface related to KC disease (such as corneal nerves, Fleischer ring, Vogt striae's, leucoma…) or other corneo-conjunctival alterations (neovascularization, epitheliopathy, hyperemia...). In addition, far visual acuity was measured with Snellen optotypes at six meters, recording the obtained results with and without the best optical correction. The device used for these explorations was the Topcon IS-600 refraction unit (serial no. 1227386) with a Topcon SL-2 biomicroscope.

3.2.3 Corneal biomechanics

Scanning of the corneal biomechanical behavior was performed using the Corvis® ST (Oculus, Wetzlar, Germany) device, a non-contact tonometer which uses an ultra-high-speed Scheimpflug camera optimized to assess the dynamic response of the corneal tissue to an air-puff. Corvis® ST records the biomechanical data relative to the three corneal stages of deformation (first applanation, maximum concavity, and second applanation), and describes as deformation parameters those in which whole eye motion is not compensated, and as deflection parameters those that compensate the displacement of the eye.

Three measurements were made three times per eye, and the average of the obtained values was calculated. **Table 3** summarizes the biomechanical data recorded by Corvis® ST.

Corvis® ST parameters	Definition
bIOP	Biomechanical corrected intraocular pressure (mmHg).
A1T/A2T	Time from the beginning of the air-puff until the first/second applanation (ms).
A1V/A2V	Velocity of the corneal apex during the first/second applanation (m/s).
HCT	Time from the initiation of the air-puff until the highest corneal concavity (ms).
A1DA/A2DA	Deformation amplitude at the first/second applanation (mm).
DAmax	Maximum deformation amplitude (mm).
HCDA	Deformation amplitude at the highest corneal concavity (mm)
A1DLL/ A2DLL	Deflection length at the first/second applanation (mm).
HCDLL	Highest concavity deflection length (mm).
A1DLA/ A2DLA	Deflection amplitude at the fist/second applanation (mm).
HCDLA	Deflection amplitude at maximum deformation (mm).
A1DLAr/ A2DLAr	Deflection area at the first/second applanation (mm^2).
HCDLAr	Deflection area at maximum deformation (mm^2).
HCdArclength	Highest concavity delta arc length (mm).
PD	Peak distance, distance between two corneal peaks at the highest concavity (mm).
DARatioMax (1 mm) DARatioMax (2 mm)	Maximum ratio of deformation amplitude measured at 1 or 2 mm from the center of the cornea (mm).
IR	Integrated radius (mm^{-1}).
Max Inverse Radius	Maximum value of the radius of curvature during the concave phase of the deformation (mm^{-1}).
HC radius	Radius of corneal curvature during the highest concavity (mm).
CCT	Central corneal thickness (µm).
ARTh	Ambrosio Relational Thickness horizontal.
Pachy Slope	Changes of corneal thickness from the corneal center to the periphery, averagely determined at 2.5mm from the apex (µm).
SP-A1	Stiffness parameter at the first applanation.
CBI	Corvis Biomechanical Index.
SSI	Stress-Strain Index.

Table 3. Description of the Corvis® ST biomechanical data. Self-created table.

3.2.4 Corneal tomography

Corneal tomography was assessed by Pentacam® HR (Oculus, Wetzlar, Germany), and the following tomographic parameters were analyzed: corneal central power (PDC), keratometry in the flattest meridian (K1), keratometry in the steeper meridian (K2), maximum dioptric power (Kmax), inferior-superior dioptric asymmetry (I-S asymmetry), maximum Ambrosio Relational Thickness (ARTmax), central corneal thickness (CCT), minimum thickness point (MTP), anterior and posterior surfaces elevation (AE and PE), total deviation value (BAD-D) and the Tomographic and Biomechanical Index (TBI).

Molecular analysis

4.1 Sample extraction

4.1.1 Tear fluid

Tear collection was performed using Schirmer strips (Tear Strips, Contacare Ophthalmics & Diagnostics, Gujarat, India). Strips were placed over the lower eyelid, roughly 3 mm from the lateral edge, and were removed when the sample reached 15mm on the Schirmer scale (9µL), remaining in contact with the ocular surface for less than 5 minutes (min). Tear samples were extracted under suitable environmental conditions and without previous administration of drugs, artificial tears, or vital dyes; gloves were used to avoid contamination of the samples. Immediately after collection, the strips were frozen and stored at −80°C until their analysis. All studies used the same protocol for tear extraction.

4.1.2 Blood

Blood samples were extracted by venipuncture and collected in EDTA-anticoagulated tubes. Before freezing at -80ºC, blood samples were processed for serum extraction.

4.2 Sample preparation

4.2.1 Tear samples processing

Schirmer's strips were thawed cold for 30 min to prevent protein degradation. For protein extraction, Schirmer strips were cut and incubated 1 hour (h) at RT in 100 µL solution of 100 mM ammonium bicarbonate. Samples were centrifuged for 20min at 13000*x g,* and the supernatant was transferred to a new Eppendorf tube. Then, 600 µL of acetone was added to the Eppendorf containing the supernatant and incubated at -20ºC overnight. Subsequently, samples were centrifuged for 20min at 13000x *g* and the supernatant was removed. To evaporate the acetone, the pellet was dried at room temperature (RT) for 1h, and after 100 µL of miliQ water was added. Lastly, an RC-DC kit (Bio-Rad Laboratories,

Hercules, CA, USA) was used to measure the amount of protein. Tear samples were used for LC-MS/MS analysis, as well as for ELISA protein quantification.

4.2.2 Blood samples processing

Blood samples were used to determine serum LF concentrations. For obtaining the serum samples, blood was centrifuged for 15 min at 3000x *g* and the serum was transferred to a new tube.

4.3 Sample analysis

4.3.1 Mass spectrometry analysis by TripleTOF 6600 LC-MS/MS system

Tear fluid samples were used firstly for the LC-MS/MS analysis to determinate the dysregulated proteins and potential tear biomarkers. The proteomic analysis was performed in collaboration with the proteomics platform of the Health Research Institute of Santiago de Compostela, according to their protocols for tear sample studies. Methodology used for LC-MS/MS is generally described in this section, but is also specified in each chapter, including the tryptic digestion, the DDA protein identification method and the SWATH-MS mode for protein quantification.

Tryptic digestion

For trypsin digestion, 100µg of protein from tear fluid of each sample was loaded on a 10% SDS-PAGE gel. The run was interrupted when the front penetrated 3mm into the resolving gel.[212,213] The protein band was visualized with Sypro-Ruby fluorescent staining (Lonza, Porriño, Pontevedra, Spain), excised, and processed for in-gel tryptic digestion following the standard protocol of Shevchenko et al,[214] with minor modifications. 10 mM dithiothreitol (Sigma-Aldrich, St. Louis, MO, USA) in 50 mM ammonium bicarbonate (Sigma-Aldrich, St. Louis, MO, USA) was used for gel pieces reduction and 55 mM iodoacetamide (Sigma-Aldrich, St. Louis, MO, USA) in 50 mM ammonium bicarbonate for alkylation. Next, pieces were washed with 50 mM ammonium bicarbonate in 50% methanol (HPLC grade, Scharlau, Barcelona, Spain), dehydrated by adding acetonitrile (HPLC grade, Scharlau, Barcelona, Spain), and dried in a SpeedVac. At last, modified porcine trypsin (Promega, Madison, WI, USA) was added at a concentration of 20 ng/µL in 20 mM ammonium bicarbonate and incubated overnight at 37 ºC. Peptides were extracted by three 20-min incubations in 40 µL of 60% acetonitrile in 0.5% HCOOH and stored at -20°C.

Data-dependent acquisition (DDA)

Data acquisition

For the data-dependent acquisition and protein identification, peptides were resuspended in 100µL of mobile phase A (2% acetonitrile, 0.1%, formic acid), by sonication for 10 min to obtain 1µg/µL peptide solution. The gradient was created using a micro-liquid chromatography system (Eksigent Technologies nanoLC 400, Sciex, Framingham, MA, USA) coupled to a high-speed Triple TOF 6600 mass spectrometer (Sciex, Framingham, MA, USA) with a microflow source. Peptides (4 µg of each sample) were separated using reverse-phase chromatography, using a ChromXP C18CL analytical column (150 µL ×0.3mm, 120Å, s-3 µL) (Sciex, Framingham, MA, USA). The trap column was a YMC-TRIART C18 (YMC Technologies, Teknokroma) with a 3 mm particle size and 120 Å pore size, switched online with the analytical column. The loading pump delivered a solution of 0.1% formic acid in water at 10 µL/min. The micro-pump generated a flow rate of 5 µl/min and was operated under gradient elution conditions. For that, 0.1% formic acid in water was used as mobile phase A, and 0.1% formic acid in acetonitrile as mobile phase B. Peptides were separated using a 90-min gradient ranging from 2% to 90% mobile phase B.

Data acquisition was performed in a TripleTOF 6600 System (Sciex, Framingham, MA, USA) using a Data Dependent workflow (DDA). A Micro source (Sciex) was used for the interface between microLC and MS, with an application of 2600 V voltage. Source and interface conditions were the following: ion spray voltage floating (ISVF) 5500 V, curtain gas (CUR) 25, collision energy (CE) 10 and ion source gas 1 (GS1) 25. The instrument was operated with Analyst TF 1.7.1 software (Sciex, USA). Switching criteria were set to ions greater than mass-to-charge ratio (m/z) 350 and smaller than m/z 1400 with a charge state of 2–5, mass tolerance 250 ppm, and an abundance threshold of more than 200 counts (cps). Former target ions were excluded for 15 second (s). The instrument was automatically calibrated every 4h using external calibrant tryptic peptides from PepCalMix.

Data analysis

ProteinPilot™ (version 5.0.1; Sciex; Framingham, MA, USA) was used for data file processing, using a specific Human UniProt database. The search was performed specifying iodoacetamide as an alkylation of the cysteines as a fixed modification. False Discovery Rate (FDR) was calculated by a non-linear fitting method displaying identified proteins with an FDR rate between 1 and 10%.

Relative quantification by Sequential Window Acquisition for All Theoretical Mass Spectra (SWATH-MS)

Spectral library creation

To build the MS/MS spectral libraries, peptide solutions were analyzed by a DDA method using micro-LC-MS/MS as described before. Pools were made using 3 µL of each sample to obtain a general representation of the peptides and proteins present in all samples. 4 µL

of each pool was separated into a micro-LC system Ekspert nLC425 (Eksigen, Dublin, CA, USA) as described before but using a 40-min gradient. The SWATH acquisition mode consisted of a 250 ms survey (MS scan) MS1 from 400 to 1250 m/z followed by an (MS/MS analysis) MS2 analysis scan from 100 to 1500 m/z (25 ms acquisition time) of the top 100 precursor ions from the survey scan, for a total cycle time of 2.8 s. Fragmented precursors were then added to a dynamic exclusion list for 15 s; any singly charged ions were excluded from the (MS/MS analysis) MS2 analysis.
Peptide and protein identifications were performed using Protein Pilot software (version 5.0.1, Sciex) with a Human-specific UniProt database, specifying iodoacetamide as an alkylation of the cysteines as a fixed modification. The false discovery rate (FDR) was set to 1 for both peptides and proteins. The MS/MS spectra, the ion data, and the retention time of the identified peptides and proteins were used to generate the spectral library for SWATH peak extraction using the add-in for PeakView Software (version 2.2, Sciex) MS/MS^{ALL} with SWATH Acquisition MicroApp (version 2.0, Sciex). Peptides with a confidence score above 99% (as obtained from the Protein Pilot database search) were included in the spectral library.

SWATH-MS quantification

Regarding relative quantification by SWATH-MS acquisition, 4µL of each sample was analyzed in a data-independent acquisition method (DIA). The method is based on repeating a cycle consisting of the acquisition of 100 sequential overlapping precursor isolation windows of variable width (1 m/z overlap), covering the mass range from 400 to 1250 m/z with a previous TOF MS1 scan (400 to 1500 m/z, 50 ms acquisition time) for each cycle. The total cycle time was 6.3s.

Data analysis

Data extraction of chromatographic fragment ion profiles from the SWATH method was performed with PeakView software (version 2.2; Sciex, Framingham, MA, USA) using the SWATH AcquisitionMicroApp (version 2.0; Sciex, Framingham, MA, USA), which processed the data using the spectral library created from the DDA data. Five-min windows and 30 ppm widths were used to extract the ion chromatograms; SWATH quantization was attempted for all proteins in the ion library that were identified by ProteinPilot^{TM} with an FDR below 1%. The retention times from the peptides that were selected for each protein were realigned in each run according to the iRT peptides present in the samples and eluted along the whole-time axis. The extracted ion chromatograms were then generated for each selected fragment ion; the peak areas for the protein were obtained by summing the peak areas from 10 peptides (MS1 scan) and 7 corresponding fragment ions (MS2 scan) from each peptide. PeakView computed an FDR and a score for each assigned peptide according to the chromatographic and spectra components; only peptides with an FDR below 1 % were used for protein quantization. Protein quantization was calculated by adding the peak areas of the corresponding peptides.

Integrated peak areas were exported directly to MarkerView software (Sciex, Framingham, MA, USA) for relative quantitative analysis. The export generated three files containing quantitative information about individual ions, the summed intensity of different ions for a particular peptide, and the summed intensity of different peptides for a particular protein. MarkerView uses processing algorithms that accurately find chromatographic and spectral peaks directly from raw SWATH data. Data alignment via MarkerView compensates for small variations in mass and retention time values, ensuring that identical compounds from different samples are accurately compared to each other. A most-like ratio (MLR) normalization was performed after statistical analysis to control for possible uneven sample loss across the different samples during the sample preparation process.[215,216] Multivariate statistical analysis through principal component analysis (PCA) was performed to compare sample data. The mean MS peak area of each protein was obtained from the SWATH-MS replicates of each condition.

4.3.2 ELISA

Validation of the main LC-MS/MS candidate tear biomarkers and determination of tear and serum LF concentrations were performed using Enzyme-Linked Immunosorbent Assays (ELISA). All assays were carried out following the manufacturer's protocols. Samples were diluted for optimal protein quantification according to the relative concentration of each biomarker in tears or serum. Sample dilution and ELISA kit specifications are available in each study chapter.

4.4 Gene Ontology analysis: Protein interaction networks and pathway enrichment.

In silico tools were used to determine the protein-protein interaction networks and to perform the gene ontology (GO) enrichment analysis for functional characterization.
Via STRING software (Functional Protein Association Network, free access at https://string-db.org) protein interaction maps were created. For protein coverage visualization, Venn diagrams were created using the Bioinformatics & Evolutionary Genomics tool (free access at http://bioinformatics.psb.ugent.be/webtools/Venn/). For GO analysis and functional enrichment, several open-access software, such as Funrich 3.1.3, Panther Classification System (free access at https://pantherdb.org), or ShinyGo 0.80 (free access at http://bioinformatics.sdstate.edu/go/), were used to explore the main biological pathways, molecular functions, and cellular components related to dysregulated proteins. UniProt codes were required for the search and identification of each protein.

In vitro study

In vitro study was performed using the HEK-Blue™ hTLR2 (Cat.#hkb-htlr2, InvivoGen, Toulouse, France) cell line, specifically designed to assess the TLR stimulation,

neutralization, and immunomodulation. This cell line is obtained by co-transfection of *hTLR2* and secreted embryonic alkaline phosphatase (*SEAP*) reporter genes into human embryonic kidney 293 (HEK293) cells. The *SEAP* reporter gene is placed under the control of the IFN- minimal promoter, fused to NF-kB and AP-1-binding sites; so, when a TLR2 ligand activates NF-kB and AP-1, the production of SEAP is induced. As negative control, HEK-Blue™ Null1 (the parental cell line of HEK-Blue™ hTLR2) was used. HEK-Blue™ Null1 (Cat.#hkb-null1, InvivoGen, Toulouse, France) was obtained by transfection of *SEAP* reporter gene into HEK293 cells, without *hTLR2*-reported gene.

For *in vitro* experiments, both cell lines were seeded, cultured, grown, and propagated according to the manufacturer's instructions. Each experiment of the *in vitro* study comprised at least three replicates for each measurement.

5.1 Experimental design

TLR2 overexpression was obtained by incubating HEK-Blue™ cell cultures for 18 h with two synthetic lipopeptides TLR2 agonists, Pam2CSK4 (10 ng/mL, InvivoGen, Toulouse, France) or Pam3CSK4 (100 ng/mL, InvivoGen, Toulouse, France). For TLR2 expression neutralization, an IgA monoclonal antibody to human TLR2 (Anti-hTLR2-IgA, 10g/mL, InvivoGen, Toulouse, France) was used. Neutralizing protocol was performed following the manufacturer's instructions. To assess the immunomodulatory activity of LF over TLR2 expression, HEK-Blue™ cell cultures were pre-incubated with different concentrations (0.01–2 mg/mL) of human LF (L1294, Sigma, St. Louise, MO, USA). Detailed neutralizing protocol and LF dose for the *in vitro* studies are available in **Chapter 5**.

The overexpression, neutralization, and immunomodulation of TLR2 were determined at first by measuring SEAP production with QUANTI-Blue™ assay, followed by flow cytometry, immunohistochemistry, Western Blot and ELISA to confirm TLR2 expression and functionality.

5.2 Experimental procedures

5.2.1 QUANTI-Blue™

QUANTI-Blue™ (rep-qbs, InvivoGen, Toulouse, France) colorimetric enzyme assay was performed to detect SEAP in cell supernatant. In this line, the supernatant of unstimulated, stimulated, neutralized, and immunomodulated HEK-Blue™ cell cultures were collected for SEAP quantification using a spectrophotometer (Synergy 2, BioTek, USA) at a 655 nm wavelength, according to the provided instructions.

5.2.2 Flow cytometry

TRL2 expression was verified also by flow cytometry using an FACSAria iiu flow cytometer (BD Biosciences, Franklin Lakes, NJ, USA) with FACSDiva software (BD Biosciences, Franklin Lakes, NJ, USA). The protocol for flow cytometry analysis included the trypsinization (trypsin-EDTA, Gibco, Gaithersburg, MD, USA) of the unstimulated, stimulated, neutralized, and immunomodulated HEK-Blue™ cell cultures. To obtain the cell pellet, cells were removed from the 24-well plates in which they were seeded and centrifuged 5 min at 200x *g*. After that, the cell pellet was resuspended in D-PBS (ATCC, Virginia, USA) and incubated for 20 min with FITC anti-TLR2-conjugated monoclonal antibodies (5 µL, Immunostep, Salamanca, Spain). Samples were washed with D-PBS and centrifuged before the analysis to avoid that the background from the antibody may interfere with the study. Unlabeled and thus non-fluorescent cells, as well as HEK-BlueTM Null1 cells, were used as both negative controls. TLR2 expression was reported as arbitrary fluorescence units (AFU).

5.2.3 Immunohistochemistry

For the immunohistochemistry analysis, slides were incubated at RT in: (1) mouse monoclonal antibody to TLR2 (ab9100) (Abcam, Cambridge, UK) at 1:100 for 30 min; (2) EnVision®+ Dual Link System-HRP (dextran polymer conjugated with horseradish peroxidase and affinity-isolated goat anti-mouse and goat anti-rabbit immunoglobulins) (Dako-Agilent, K4065) for 20 min; (3) DAB+ substrate-chromogen solution (1 mL of substrate buffer solution containing hydrogen peroxide and 20 µL of 3,30-diaminobenzidine tetrahydrochloride chromogen solution) for 10 min; and (4) EnVision FLEX hematoxylin for 15 min. An AutostainerLink 48immunostainer (Dako-Agilent, Santa Clara, CA, USA) was used to perform immunohistochemistry. Intensity of TLR2 staining was quantified using ImageJ (Rasband, WS, USA) by measuring the inverted DAB signal and calculating the average with at least thirteen cells for each image.

5.2.4 Western Blotting

Western blotting (WB) was also performed for TLR2 relative quantification. For sample preparation, the unstimulated, stimulated, neutralized, and immunomodulated HEK-blue™ cell cultures were trypsinized, removed from the 12-well plates in which they were seeded, and centrifuged. After centrifugation, the cell pellets were resuspended in RIPA lysis buffer (ThermoScientific, Waltham, MA, USA) with protease inhibitor (Roche, Suiza) and shacked for15 min on ice. After that, the lysates were collected and centrifuged at 21000x *g* for 30 min at 4 ºC, and the supernatants were collected and stored at -80ºC until the analysis. Total amount of protein was measured with a micro-BCA protein assay kit (Thermo Scientific, Waltham, MA, USA) following the manufacturer's instructions. Samples were aliquoted with 15 µg of total protein combined with 4x loading buffer and denatured in a 95ºC metal bath during 10 min. Samples were loaded and run on SDS-PAGE 10% protein gel using a fixed 140 V voltage. Then, proteins were electro-transferred to a Polyvinylidene fluoride (PVDF) membrane (Amersham™ Hybond 0.45,

USA) with a Trans-Blot semi-dry system (Bio-Rad, Hercules, CA, USA) and a limited voltage of 25V and 180mA for 1h and 40 min. Following protein transfer, post-blot membranes were blocked with 3% bovine serum albumin (BSA, Sigma, St. Louise, MO, USA) (3% BSA diluted in Tris chloride Buffered Saline with Tween® 20 (TBST)) for 45 min, and incubated overnight at RT in agitation with 1:500 rabbit polyclonal Anti-TLR2 (A11225, ABclonal, Woburn, MA, USA) and with 1:2000 rabbit polyclonal Anti-β-actin control protein (Abcam, UK), both diluted in 3% BSA-TBST. Subsequently, membranes were washed three times in TBST and incubated again for 1h at RT in agitation with 1:5000 HRP-conjugated goat anti-rabbit IgG secondary antibody (Dako, Denmark) diluted in 3% BSA-TBST. Lastly, membranes were washed in TBST and revealed with Pierce™ ECLWestern Blotting Substrate (Thermo Fisher, Lexington, MA, USA). The band was detected using the ChemiDoc™ MP imaging system (Bio-Rad, Hercules, CA, USA) and the results were analyzed by ImageJ (Rasband, WS, USA) determining the mean grey value of protein bands delimited in the regions of interest (ROIs). The molecular weight is 89 kDa for TLR2 and 42 kDa for β-actin. Relative expression of TLR2 to β-actin was calculated for each sample, followed by group-wise normalization to the control.

5.2.5 ELISA

Functionality of TLR2 was also confirmed by the measurement of IL-8 in the supernatant of unstimulated, stimulated, neutralized, and immunomodulated HEK-Blue™ cell cultures. IL-8 concentration was quantified by ELISA (EK0413, Boster, Pleasanton, CA, USA) following the manufacturer's protocol.

Statistical analysis

SPSS 29.0 (IBM, USA) for Mac and GraphPad Prism 8.0 (San Diego, CA, USA) were used for statistical analysis. Quantitative variables were described using the mean and standard deviation (± SD) for normal distribution, and the median and interquartile range [IQR] for non-normal distribution. The normality of the variables was confirmed using the most appropriate and recommended test for each study. Bivariate comparisons were performed using the chi-square test for categorical variables, and parametric (t-student) or non-parametric (u-Mann-Whitney) tests for continuous variables according to their normality. Variables were represented by pie charts, error bars, box, or column plots respectively.

For multiple comparisons, one-way ANOVA (for normal variables) or Kruskal-Wallis (for non- normal ones) tests were used. Bivariate correlations were analyzed using Pearson`s or Spearman's coefficients depending on the variable's normality and were represented by scatter plots. Receiver operating characteristic (ROC) curve analysis was performed to determine the potential role of dysregulated proteins as KC biomarkers and its sensitivity and specificity. Logistic analysis regression model (LRA) was performed

using a backward elimination method and the Akaike's information criterion (AIC) as a global selection criterion to identify the optimal subset of predictors to model the probability of the different biomechanical conditions. $p<0.05$ was considered statistically significant in all tests.

Introduction

Justification and hypothesis

Objectives

Methodology

WP1. Clinical & molecular study of KC disease

WP2. Clinical & molecular study of KC at-risk stages

WP3. Human LF as a therapeutic strategy for KC

Discussion

Conclusions

WP1. Clinical & molecular study of KC disease

The two articles [**Chapters 1** and **2**] included in the first work package of this thesis focus on the search for tear proteomic biomarker networks that define the molecular mechanisms interconnected during KC pathophysiology. For this purpose, the tear fluid of 25 KC patients and 25 control subjects' sex- and age-matched was analyzed by LC-MS/MS. In **Chapter 1**, we used the SWATH-MS data-independent acquisition method to perform a global protein quantification and to identify the dysregulated tear proteins and their functional association with KC disease. In a complementary way, **Chapter 2** followed a qualitative approach using an LC-MS/MS data-dependent workflow to obtain an extensive view of the KC tear proteome, attempting to overcome events that might be missed by quantitative limitations and enlarging our understanding of the disease's pathophysiology.

Chapter 1

Tear proteomics in keratoconus disease: a SWATH-MS analysis

Maite López-López[1,2]*, Uxía Regueiro[1,2]*, Susana B. Bravo[3], María del Pilar Chantada-Vázquez[3], Rubén Varela-Fernández[2,4], Paulo Ávila-Gómez[2], Pablo Hervella[2#], Isabel Lema[1,2,5#].

[1] Department of Surgery and Medical-Surgical Specialties. Faculty of Optics and Optometry, Universidade de Santiago de Compostela (USC), Santiago de Compostela, Spain.
[2] Clinical Neurosciences Research Laboratory, Health Research Institute of Santiago de Compostela (IDIS), Santiago de Compostela, Spain.
[3] Proteomic Unit, Health Research Institute of Santiago de Compostela (IDIS), Santiago de Compostela, Spain.
[4] Department of Pharmacology, Pharmacy and Pharmaceutical Technology. Universidade de Santiago de Compostela (USC). Campus Vida. Santiago de Compostela, Spain.
[5] Instituto Galego de Oftalmoloxía (INGO), Hospital Provincial de Conxo, Santiago de Compostela, Spain.

* These authors have equally contributed to this work as First Authors.
[#] These authors have equally contributed to this work as Corresponding Authors.

Published in *Investigative Ophthalmology & Vision Science (IOVS).* 2021;62(10):30.

Journal Citations Reports (JCR) Metrics: 2021
Journal Impact Factor (JIF): 4.925
JIF Quartile: Q1
Journal Position: 10/62 *Ophthalmology*
JCR abbreviation: INVEST OPHTH VIS SCI
ISSN: 0146-0404

Author contribution. López-López M contributed to the conceptualization, design, formal analysis and investigation, writing and original draft preparation of this manuscript.

Open Access license details are provided in **Annex 4**.

Cornea

Tear Proteomics in Keratoconus: A Quantitative SWATH-MS Analysis

Maite López-López,[1,2] Uxía Regueiro,[1,2] Susana B. Bravo,[3] María del Pilar Chantada-Vázquez,[3] Rubén Varela-Fernández,[2,4] Paulo Ávila-Gómez,[2] Pablo Hervella,[2] and Isabel Lema[1,2,5]

[1]Department of Surgery and Medical-Surgical Specialties. Faculty of Optics and Optometry, Universidade de Santiago de Compostela, Santiago de Compostela, Spain
[2]Clinical Neurosciences Research Laboratory, Health Research Institute of Santiago de Compostela (IDIS), Santiago de Compostela, Spain
[3]Proteomic Unit, Health Research Institute of Santiago de Compostela (IDIS), Santiago de Compostela, Spain
[4]Department of Pharmacology, Pharmacy and Pharmaceutical Technology. Universidade de Santiago de Compostela (USC), Campus Vida, Santiago de Compostela, Spain
[5]Instituto Galego de Oftalmoloxía (INGO), Hospital Provincial de Conxo, Santiago de Compostela, Spain

Correspondence: Isabel Lema, Instituto Galego de Oftalmoloxía, Hospital Provincial de Conxo, Compostela 15706—Santiago de Compostela (Spain); mariaisabel.lema@usc.es.
Pablo Hervella, Clinical Neurosciences Research Laboratory, Health Research Institute of Santiago de Compostela, 15706—Santiago de Compostela (Spain); pablo.hervella.lorenzo@sergas.es.

MLL and UR have equally contributed to this work.

Received: May 5, 2021
Accepted: August 2, 2021
Published: August 25, 2021

Citation: López-López M, Regueiro U, Bravo SB, et al. Tear proteomics in keratoconus: A quantitative SWATH-MS analysis. *Invest Ophthalmol Vis Sci.* 2021;62(10):30. https://doi.org/10.1167/iovs.62.10.30

Purpose. To elucidate dysregulated proteins in keratoconus (KC) to provide a better understanding of the molecular mechanisms that lead to the development of the disease using sequential window acquisition of all theoretical mass spectra (SWATH-MS) as a protein quantification tool of the tear proteomic profile.

Methods. Prospective cross-sectional study that includes 25 keratoconic eyes and 25 healthy eyes. All participants underwent a clinical, tomographic, and aberrometric exam. Tear sample was collected using Schirmer strips and analyzed by liquid chromatography with tandem mass spectrometry. SWATH-MS was used as a quantification tool of the tear proteomic profile. The expression of the quantified proteins was compared between groups, and the biological and molecular functions of the dysregulated proteins as well as their functional relationships were studied by in silico analysis.

Results. A total of 203 proteins were quantified in tear samples of patients with KC and control participants, of which 18 showed differential expression between groups ($P < 0.05$). An increase in the expression of 7 proteins and a decrease in the expression of 11 proteins were observed. Protein–protein interactions and gene ontology analysis showed the involvement of these dysregulated proteins in structural, inflammatory-immune, iron homeostasis, oxidative stress, and extracellular matrix proteolysis processes.

Conclusions. Tear protein quantification has revealed the dysregulation of proteins involved in biological processes previously associated with KC. Among them, iron homeostasis should be highlighted as a relevant pathway in the KC pathophysiology, and it should be taken into account in the development of therapeutic targets to cope with tissue damage derived from iron accumulation and toxicity.

Keywords: keratoconus, tear fluid, proteomics, mass spectrometry, SWATH-MS

Keratoconus (KC) is a chronic, progressive, and degenerative disease characterized by alterations at the corneostructural level such as thinning, protrusion, and increased curvature of the corneal tissue.[1]

Generally, KC is an asymmetric condition whose structural changes lead to the appearance of refractive errors, especially irregular astigmatisms, which represent a significant loss of vision and, consequently, a great impact on quality of life.[2] Although KC usually appears in isolation, roughly a quarter of diagnosed patients report a positive family history of this disease, which suggests the influence of heredity in its etiopathogenesis.[3,4]

Keratoconus was considered a noninflammatory disease, but recent studies have shown the alteration in the expression of molecules involved in inflammatory processes, as well as in oxidative stress, extracellular matrix proteolysis, and cellular apoptosis,[5–10] evidencing the participation of all of these biological mechanisms in the KC pathophysiology.

In the keratoconic corneal tissue, a link between oxidative stress and cell damage of stromal keratocytes was found, demonstrated by the increase of free radicals and other reactive species,[11] as well as the decrease in the activity of antioxidant enzymes and other protective molecules against free radicals,[12] which finally result in an increasing thinning of the corneal stroma with the progression of the disease.

In addition, the imbalance between pro- and anti-inflammatory proteins and the increase in matrix metalloproteinase activity reported in KC samples are also associated with the biochemical development of the disease, promoting a decrease in corneal tissue integrity.[13]

Tear fluid is a biological component that covers, protects, and nourishes the ocular surface, especially the corneal

Copyright 2021 The Authors

This work is licensed under a Creative Commons Attribution-NonCommercial-NoDerivatives 4.0 International License.

Downloaded from iovs.arvojournals.org on 05/16/2022

Investigative Ophthalmology & Visual Science

epithelium. Previous studies have described the exchange of growth factors and other molecules between the tear film, the epithelium, and the corneal stroma, showing that the tear components can affect the phenotype of epithelial cells and stromal keratocytes.[14,15] Thus, tears become an easily accessible biological fluid with direct information from the corneal tissues, allowing the assessment of the underlying tissues and playing a key role in the detection of molecular changes that may interfere with the development of KC.

Previous studies have suggested that changes in the expression of certain proteins in tears may be indicative of an increase of proteolytic activity and the existence of complex chronic inflammatory processes in the pathophysiology of the disease.[16,17] However, most of the studies carried out to date have been focused on the analysis of specific proteins[18,19] with the limitation that isolated biomarkers still lack sufficient specificity and sensibility to be applied in clinical practice.[20] To the best of our knowledge, this is the first study that uses the sequential window acquisition of all theoretical mass spectra (SWATH-MS) as a protein quantification tool of tear samples from patients with KC compared to control participants. SWATH-MS is a data independent acquisition method for simultaneous protein identification and quantification that allows a complete and permanent recording of all fragment ions of the detectable peptide present in a biological sample.

Therefore, the aim of this work is to perform a global quantification of the proteomic profile of the tear fluid, in order to identify differentially expressed proteins in tears of patients with KC, as well as their functional and biological relationships, that could be potential biomarkers of the disease. Moreover, the biological relationships among proteins with differential expression studied by in silico analysis would provide a better understanding of the molecular mechanisms that lead to the development of the disease.

Methods

The present study was carried out following the principles of the Declaration of Helsinki of the World Medical Association. The Ethics Committee for Clinical Research of Galicia approved the ophthalmologic protocol and the biological sample extraction to which all study participants were subjected (2019/623). All participants underwent an ophthalmologic examination that included a common clinical, topographic, aberrometric, and tomographic evaluation. Tear fluid was collected using Schirmer strips. All participants were expressly cited for the purposes of this study and properly informed prior to signing informed consent. All examinations were performed by the same two researchers. The ophthalmologic examination consisted of anamnesis and clinical evaluation, in which the collected data included age, sex, patient´s history of eye disease, patient´s medical history (allergy, eye rubbing, eye itching), positive family history of corneal ectasia, and biomicroscopic exam. Atopic conditions such as asthma, rhinitis, or atopic dermatitis were included as allergic diseases. The ophthalmologic examination also consisted of topographic, aberrometric, and tomographic evaluation, in which dioptric central power, flattest corneal meridian, steeper meridian, maximum dioptric power, inferior-superior dioptric asymmetry, Ambrosio relational thickness, D-index (Belin-Ambrosio deviation index), vertical anterior coma for 3 mm of diameter, minimum thickness point, and posterior elevation were the parameters included in this evaluation. All variables were measured using the PENTACAM tomographer (version 1.6r2031b; Oculus, Wetzlar, Germany).

Study Participants

We have designed a prospective and cross-sectional study in which 25 patients with KC and 25 control participants were enrolled. Patients with KC and control participants were recruited at the Instituto Galego de Oftalmoloxía, Santiago de Compostela, Spain. The main inclusion criteria were the KC diagnosis, supported by slit-lamp examination with the following clinical signs depending on the stage: prominent corneal nerves, Vogt's striae, Fleischer ring, and Munson sign, backed up by topography, aberrometry, and tomography evaluation. All the patients with KC did not present an evolving corneal ectasia, and their age was higher than the usual maximum age of progression of the disease. Inclusion criteria for the control group included normal clinical parameters without alterations in the tomographic evaluation or irregular astigmatisms that could suggest a subclinical state of the disease. Any control participants with family history of KC were also excluded.

The common inclusion criteria for both groups were Schirmer $\geq$15 mm in 5 minutes, conjunctival hyperemia $<$2 (Nathan Efron scale),[21] and at least 1 week with no contact lenses and no instillation of artificial tears or other eye drops. The common exclusion criteria for both groups included previous surgical intervention in the previous segment, corneal trauma or disease, existence of active ocular or systemic inflammation, current treatment with local or systemic anti-inflammatory drugs, infections in the days preceding sample collection, and pregnancy. Renal, hepatic, or hematologic diseases as well as solid tumors were also exclusion criteria for both groups.

Tear Collection, Analysis, and Quantification

Tear Collection. Tear samples were obtained by placing a Schirmer strip over the lower eyelid, approximately 3 mm from the lateral edge, without previous instillation of drugs, vital dyes, or other eye drops. For the collection of tears, the study participants closed their eyes until collecting the same amount of sample, delimited by the scale present on the Schirmer strips. One strip was used for each participant, and the total amount of tear collected corresponded to 15 mm on the strip´s scale. The samples were frozen and stored at −80°C immediately after collection. All samples were collected between January and February to avoid the influence of allergies in the tear analysis.

Tear Analysis. Tear proteins were extracted by cutting and incubating the Schirmer strips in 100 µL of 100 mM ammonium bicarbonate at room temperature for 1 hour. Samples were centrifuged for 20 minutes at 13,000 × *g*, and the supernatant was transferred to a new tube. Then the protein was precipitated by the MeOH/$CHCl_3$ method, and the amount of protein was measured using a RC-DC kit (Bio-Rad, Hercules, CA, USA).[22]

In relation to tryptic digestion for mass spectrometry, 100 µg protein was concentrated on a 10% SDS-PAGE gel. The gel was allowed to run until the front entered 3 mm of the separator gel.[23,24] The protein band was visualized with Sypro-Ruby fluorescent staining (Lonza, Porriño, Pontevedra, Spain), excised, and subjected to tryptic digestion following the standard protocol of Shevchenko et al.,[25] with minor modifications.

Investigative Ophthalmology & Visual Science

Downloaded from iovs.arvojournals.org on 05/16/2022

SWATH-MS Quantification. Once the proteins were digested, two pools (control and KC) were created using 3 µL of each individual sample. The peptide mixtures (from sample pools) were analyzed using a data-dependent acquisition (DDA) method with micro–liquid chromatography with tandem mass spectrometry (LC-MS/MS) technology to build the MS/MS spectral libraries, as previously described.[26–28] Protein and peptide identification was carried out using the Protein Pilot software (version 5.0.1; Sciex; Framingham, MA, USA) with a Human Uniprot database specifying iodoacetamide as alkylation of the cysteines. The false discovery rate was adjusted to 1% for both proteins and peptides. The MS/MS spectra, the ion data, and the retention time of the identified peptides and proteins were used to generate the spectral library. The spectral library was used to create the spectral window acquisition used in the SWATH-MS method. Then the samples (4 µL) were individually analyzed using three technical replicated by sample to ensure the mass spectometer accuray. The method is based on repeating a cycle that consists of the acquisition of a certain number of scans or time of flight mass spectometry (TOF MS/M) windows. The width of the variable windows was optimized for each set of samples according to the ionic density found in the previous DDA (files used in the library) by means of the SWATH variable window calculator (Sciex, Framingham, MA, USA) spreadsheet.

The data extraction of fragmented ion chromatographic profiles using the SWATH method was performed with the PeakView software (version 2.2; Sciex, Framingham, MA, USA) by the SWATH AcquistionMicroApp (version 2.0; Sciex, Framingham, MA, USA).

Proteins with more than 10 peptides and seven transitions (fragments) were selected based on signal intensity to generate the integrated area peaks for the quantification. Any shared or modified peptides were excluded. Integrated area peaks were exported to the MarkerView software (Sciex, Framingham, MA, USA) for relative quantitative analysis. MarkerView uses processing algorithms that accurately find chromatographic and spectral peaks direct from the raw SWATH data. Data alignment by MarkerView compensates for minor variations in both mass and retention time values, ensuring that identical compounds in different samples are accurately compared with one another. A most like ratio normalization was performed to control for possible uneven sample loss across the different samples during the sample preparation process. Unsupervised multivariate statistical analysis using principal component analysis was performed to compare the data among the samples.[29,30] The average MS peak area of each protein was derived from the biological replicates of the SWATH-MS of each sample, followed by a Student's *t*-test analysis using the MarkerView software for comparison among the samples based on the averaged area sums of all the transitions derived for each protein. The *t*-test was used to indicate how well each variable distinguishes the two groups, reported as a *P* value. The set of differentially expressed proteins ($P < 0.05$) with a 1.13-fold increase or 0.88-fold decrease was selected for each library.

Functional Enrichment and Interaction Network Analysis

In this study, a functional enrichment and interaction network analysis of the dysregulated proteins in the tear proteome between KC and control participants was performed. STRING: Functional protein association network (free access at https://string-db.org)[31] and FunRich: Functional Enrichment analysis tool[32] (open-access software version 3.1.3) were used to develop interaction maps and analyze biological processes and molecular functions. First, differently expressed proteins between KC and control tear samples were filtered by fold change (FC, whenever this was higher or lower than 1) and *P* value (<0.05). Subsequently, the list of the Uniprot codes of the proteins that met both requirements was analyzed using the STRING and FunRich databases.[33]

Statistical Analysis

Statistical analysis was made using SPSS 20.0 software for Windows (IBM, New York, NY, USA). A Kolmogorov–Smirnov test was used to determine the variable distribution. Descriptive statistical analyses were expressed as percentages for categorical variables, mean ± SD values were used for continuous quantitative variables with normal distribution, and discontinuous variables were expressed as median [quartile]. The bivariate comparison of groups was made with the χ^2 test (categorical variables), Student's *t*-test (normal continuous variables), and Mann–Whitney *U* test (no normal continuous variables). Graphic expressions of the comparisons between normal continuous variables were made using error bars, and continuous variables with nonnormal distribution were represented by box plots. Volcano plot was performed using the GraphPad Prism software (GraphPad Software, San Diego, CA, USA), and the resulting graph was generated by plotting the $\log_2$ FC for the identified proteins against their corresponding adjusted $\log_{10}$ *P* value. FC indicates upregulated proteins if FC >1 or downregulated proteins if FC <1. A $P < 0.05$ value was considered statistically significant in all tests.

Results

Clinical Features

In this study, the tear fluid from 25 eyes of 25 patients with KC (60% male; mean age, 44.88 ± 5.01 years) and 25 eyes of 25 control participants (60% male; mean age, 43.96 ± 6.94 years) were analyzed. Both groups were matched in age and sex, so no differences were found for those variables. No significant differences were found regarding the presence of allergic conditions ($P = 0.247$); however, the measurement of visual acuity was significantly lower ($P < 0.01$) in the KC group, while eye rubbing ($P < 0.05$) and ocular itching ($P < 0.05$) were significantly higher in the KC group. In relation to the biomicroscopic examination, within the study group, 48% had visible corneal nerves, 36% Fleischer rings, and 12% Voght striae. Among patients with KC, 12% of the eyes had grade I, 44% grade II, 36% grade III, and 8% grade IV, according to the Amsler–Krumeich classification.[34] As expected, the topographic, aberrometric, and tomographic variables evidenced significant differences between groups. Table 1 shows the clinical and topographic, aberrometric, and tomographic characteristics of the KC and control groups.

Proteomic Analysis

The collected tear samples were analyzed by LC-MS/MS mass spectrometry, and a quantitative analysis was carried out to identify the proteins with differential expression in the tear fluid between groups.

Investigative Ophthalmology & Visual Science

Downloaded from iovs.arvojournals.org on 05/16/2022

Table 1. Clinical, Topographic, Aberrometric, and Tomographic Characteristics of KC and Control Groups

Characteristic	Control	KC	*P* Value
Allergic disease (%)	28	44	0.247
Itching (%)	4	72	<0.0001
Rubbing (%)	4	64	<0.0001
DCP (D)	43.30 ± 1.44	51.36 ± 6.72	<0.0001
K1 (D)	42.70 ± 1.39	47.14 ± 5.31	<0.0001
K2 (D)	43.73 ± 1.48	50.47 ± 5.28	<0.0001
maxDP (D)	44.40 ± 1.25	55.56 ± 7.10	<0.0001
I-S asymmetry (D)	−0.08 ± 0.60	5.14 ± 3.54	<0.0001
ART	416 ± 60	144 ± 62	<0.0001
D	1.07 ± 0.52	10.35 ± 6.98	<0.0001
$Z_3^{\pm 1}$ (µm)	1.52 ± 0.71	9.82 ± 4.15	<0.001
MTP (µm)	534 ± 22	445 ± 67	<0.0001
PE (µm)	9.20 ± 3.73	67.96 ± 31.33	<0.0001

Sample size: KC = 25 participants, 25 eyes; controls = 25 participants, 25 eyes.

ART, Ambrosio relational thickness; D, Belin-Ambrosio deviation index; DCP, dioptric central power; I-S asymmetry, inferior-superior dioptric asymmetry; K1, flattest corneal meridian; K2, steeper corneal meridian; maxDP, maximum dioptric power; MTP, minimum thickness point; PE, posterior elevation; $Z_3^{\pm 1}$, vertical coma.

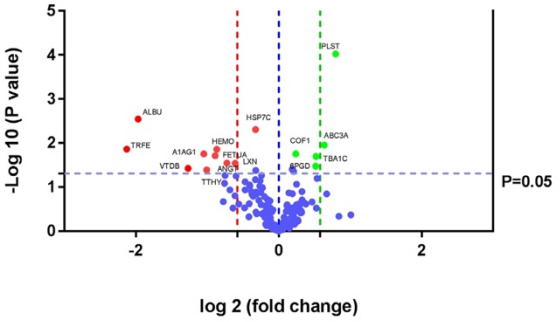


Figure 1. Volcano plot of tear quantitative proteomics data. Volcano plot shows the significantly differentially abundant proteins in tears by quantitative proteomics analysis. Proteins are ranked in a volcano plot according to their statistical *P* value (y-axis) as $-\log_{10}$ and their relative abundance ratio ($\log_2$ FC) between KC and control samples (x-axis). Off-centered spots are those that vary the most between both groups. The cutoffs for significant changes are FC of 1.13 and $P < 0.05$. *Red spots* show the downregulated proteins in KC, *green spots* show the upregulated proteins in KC, and *blue spots* show the nondysregulated proteins between both groups. A1AG1, α1-acid glycoprotein 1; ABEC3A, DNA dC→dU-editing enzyme APOBEC-3A; ALBU, serum albumin; ANGT, angiotensinogen; COF1, cofilin 1; FETUA, α2-HS-glycoprotein; HEMO, hemopexin; HSP7C, heat shock cognate 71-kDa protein; LXN, latexin; PLST, plastin 3; TBA1C, tubulin α1C chain; TRFE, serotransferrin; TTHY, transthyretin; VTDB, vitamin D binding protein; 6PGD, 6-phosphogluconate dehydrogenase decarboxylating.

A total of 203 proteins were quantified in the tear preparations of KC and control groups using the SWATH-MS quantification method (available in Supplementary Table S1). Among the identified proteins, 18 showed significant differential expression between both groups. Table 2 shows the proteins with differential expression between KC and control samples, ordered from the most overexpressed (FC > 1.13) to the least expressed (FC < 0.88) in KC tears.

Among the 18 proteins with differential expression, 7 showed upregulation and 11 downregulation in KC tears.

A volcano plot (Fig. 1) was used to represent the global quantification of the tear proteins between healthy participants and patients with KC as well as the dysregulated proteins between groups.

Regarding the seven upregulated proteins in KC samples, we observed an increase in the expression of plastin 3 (FC = 1.736); DNA dC→dU-editing enzyme APOBEC-3A1 (FC = 1.555); tubulin α1C chain (FC = 1.435); 6-phosphogluconate dehydrogenase, decarboxylating (FC = 1.430); cofilin 1 (FC = 1.180); annexin A2 (FC = 1.155); and annexin A1 (FC = 1.139). The remaining 11 proteins were found downregulated in KC samples. This group included serotransferrin (FC = 0.228), serum albumin (FC = 0.255), vitamin D binding protein (FC = 0.414), α1-acid glycoprotein 1 (FC = 0.483), transthyretin (FC = 0.496), α2-HS-glycoprotein (FC = 0.540), hemopexin (FC = 0.547),

Table 2. Proteins With Differential Expression Between KC and Control Group Using SWATH-MS

Protein	Uniprot Code	Protein Abbreviation	*P* Value	FC
Plastin 3	sp|P13797|PLST_HUMAN	PLS3, PLST	<0.0001	1.736
DNA dC→dU-editing enzyme APOBEC-3A	sp|P31941|ABC3A_HUMAN	ABC3A, APOBEC3A	0.011	1.555
Tubulin α1C chain	sp|Q9BQE3|TBA1C_HUMAN	TBA1C, TUBA1C	0.020	1.435
6-Phosphogluconate dehydrogenase, decarboxylating	sp|P52209|6PGD_HUMAN	6PGD, PGD	0.033	1.430
Cofilin 1	sp|P23528|COF1_HUMAN	CFL1, COF1	0.017	1.180
Annexin A2	sp|P07355|ANXA2_HUMAN	ANXA 2	0.044	1.155
Annexin A1	sp|P04083|ANXA1_HUMAN	ANXA 1	0.039	1.139
ρ GDP-dissociation inhibitor 1	sp|P52565|GDIR1_HUMAN	ARHGDIA	0.042	0.799
Heat shock cognate 71-kDa protein	sp|P11142|HSP7C_HUMAN	HSP7C, HPSA8	0.004	0.797
Latexin	sp|Q9BS40|LXN_HUMAN	LXN	0.029	0.655
Angiotensinogen	sp|P01019|ANGT_HUMAN	ANGT, AGT	0.028	0.604
Hemopexin	sp|P02790|HEMO_HUMAN	HEMO, HPX	0.014	0.547
α2-HS-glycoprotein	sp|P02765|FETUA_HUMAN	AHSG, FETUA	0.019	0.540
Transthyretin	sp|P02766|TTHY_HUMAN	TTHY, TTR	0.040	0.496
α1-Acid glycoprotein 1	sp|P02763|A1AG1_HUMAN	A1AG1, ORM1	0.018	0.483
Vitamin D binding protein	sp|P02774|VTDB_HUMAN	VTDB, GC	0.038	0.414
Serum albumin	sp|P02768|ALBU_HUMAN	ALB, ALBU	0.003	0.255
Serotransferrin	sp|P02787|TRFE_HUMAN	TRFE, TF	0.014	0.228

FC shown in upregulated proteins if FC > 1 or in downregulated proteins if FC < 1. Sample size: KC = 25 participants, 25 eyes; controls = 25 participants, 25 eyes.

Downloaded from iovs.arvojournals.org on 05/16/2022

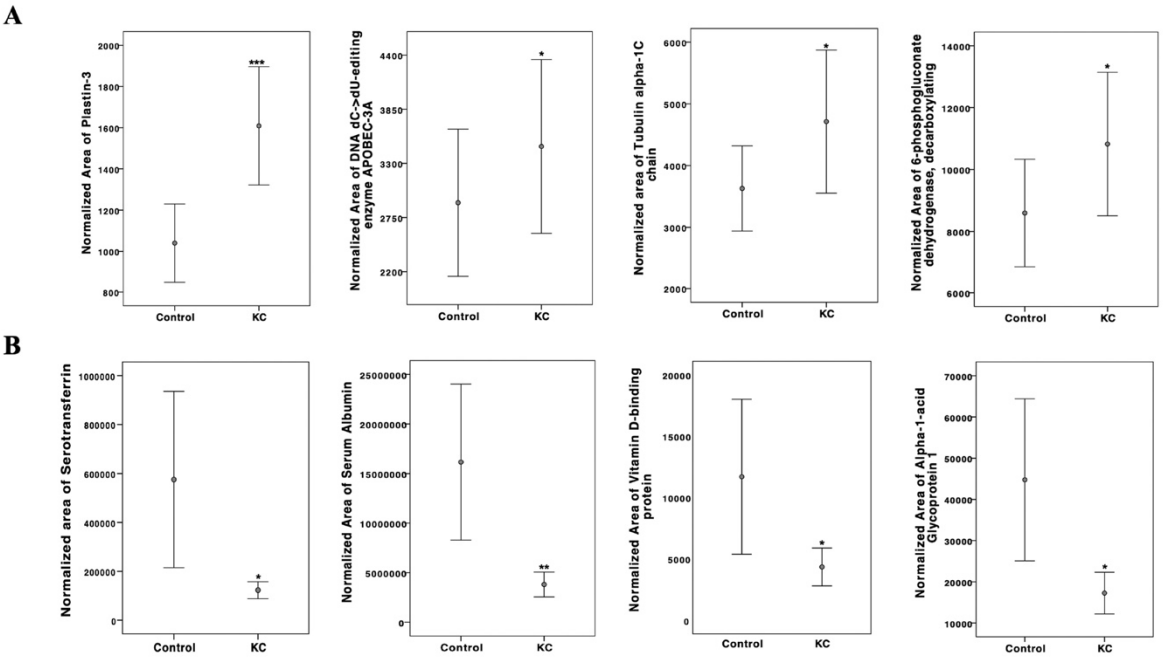


FIGURE 2. (**A**) Representation of the mean ± SD normalized area of the four most overexpressed proteins in the tears of patients with KC. (**B**) Representation of the mean ± SD normalized area of the four most underexpressed proteins in the tears of patients with KC. The normalized area was obtained from the SWATH method for each individual sample. The mean ± SD of the normalized area for each group was represented by error bars for having a normal distribution in the Kolmogorov–Smirnov test. Statistical differences with regard to controls: $^{*}P < 0.05$, $^{**}P < 0.01$, $^{***}P < 0.001$ (P values in Table 2). Sample size: control = 25 eyes; KC = 25 eyes.

angiotensinogen (FC = 0.604), latexin (FC = 0.655), heat shock cognate 71-kDa protein (FC = 0.797), and ρ GDP-dissociation inhibitor 1 (FC = 0.799), cited from most to least underexpressed. Figure 2 shows the four most overexpressed and the four more underexpressed proteins in KC tears in comparison to the control group.

Biological Pathways and Molecular Functions of Dysregulated Proteins in KC Tears

To achieve a better understanding of the biological importance of differential proteins as well as their possible implications in the pathophysiology of the KC, we observed their molecular functions and biological implications performing in silico analysis with STRING, a protein–protein interaction network tool. In this way, a map of the interaction of proteins and their main biological functions was obtained. Figure 3 shows the most representative biological processes involving the overexpressed proteins. These processes included IL-12–mediated signaling pathway, positive regulation of vesicle fusion, regulation of wound healing, actin cytoskeleton organization, and supramolecular fiber organization.

In relation to the 11 downregulated proteins, a decrease in the expression of proteins involved in transport processes, iron transport and homeostasis, extracellular organization, negative regulation of endopeptidase activity, and acute phase and inflammatory response was observed. All these processes are represented in Figure 4.

Complementary, we carried out a search for biological processes and functions of the differentially expressed proteins using the FunRich tool. According to the previous analysis, the results revealed the involvement of overexpressed proteins in the regulation of apoptotic processes, response to hydrogen peroxides, and innate immune response, as well as the participation of downexpressed proteins in iron homeostasis and transport, vitamin D metabolic process, vitamin transport, and inflammatory processes. Figure 5 summarizes the main biological processes and molecular functions of the differentially expressed proteins in tears from patients with KC.

DISCUSSION

In this study, we have focused on the complete analysis of the tear proteome to elucidate proteins with differential expression in KC disease and to study their possible functional relationships.

MS in association with LC has become a commonly used method to study disease markers in different types of samples such as tissues or biological fluids.[35] In this work, we used the LC-MS technique for analyzing proteins associated with KC in tear samples and SWATH-MS as a quantification method. LC combined with MS has been previously used for tear analysis of patients with KC, although with different protein quantification methods.[36,37]

Among the total proteins quantified, 18 showed a differential expression between groups. These proteins were fundamentally related to structural, inflammatory, and oxidative stress and iron transport and homeostasis processes.

In relation to structural processes, three of the most overexpressed proteins in the tears of patients with KC were associated with the organization and composition of the

Investigative Ophthalmology & Visual Science

Downloaded from iovs.arvojournals.org on 05/16/2022

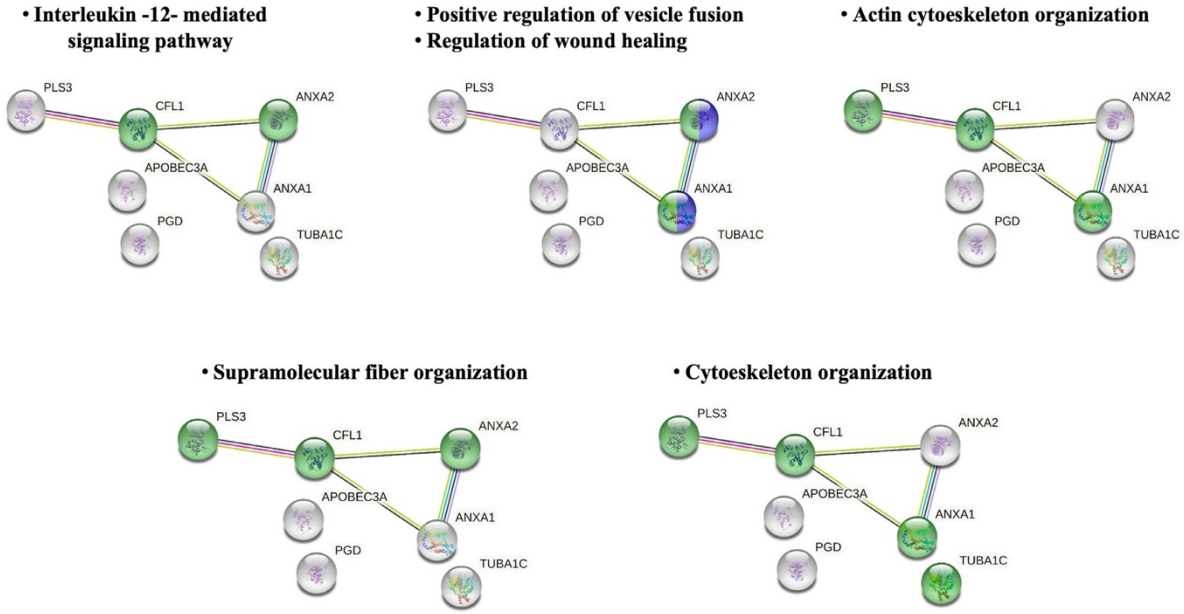


Figure 3. Main biological processes of proteins upregulated in KC samples. Protein–protein interactions were made using the STRING interaction network. Proteins upregulated are represented as a cluster. The *colored* proteins in the clusters are involved in the indicated biological process. Classification of proteins was based on Gene Ontology (GO) biological processes. All the biological processes that are referred to present a false discovery rate (FDR) less than 0.05. ANXA1, annexin A1; ANXA2, annexin A2; APOBEC3A, DNA dC→>dU-editing enzyme APOBEC-3A; CFL1, cofilin 1; PLS3, plastin 3; PGD, 6-phosphogluconate dehydrogenase decarboxylating; TUBA1C, tubulin α1C chain.

cytoskeleton. Plastin 3, an actin clustering protein with an important role in the organization of the cytoskeleton,[38] was the most overexpressed protein in the tears of patients with KC. In the same way, we observed an increase in cofilin 1, an actin binding protein involved in the regulation of actin filament length and organization of the cytoskeleton,[39] and in tubulin α1-C, a protein from the tubulin family that constitutes one of the main components of microtubules. Our results are in line with previous studies that have reported an overexpression of proteins of the tubulin family in epithelial samples of keratoconic corneas[40] and suggest that the accumulation of structural proteins (in tears or in corneal tissues) could be due to an increase in their synthesis to cope with the thinning of the corneal tissue induced by the increase in degradative proteins.[40]

The influence of innate immunity as well as inflammatory processes on KC pathophysiology has already been described in numerous studies. Specifically, previous studies observed an increase in proinflammatory proteins such as IL-6 and TNF-α[19] in tear samples, suggesting the involvement of chronic inflammatory events in KC pathogenesis. A recent study from our group confirmed the overexpression of Toll-like receptors 2 and 4 in corneal and conjunctival epithelial samples of patients with KC, in agreement with the implication of innate immunity in the disease progression.[7,41] In this case, our results showed differences in the expression of some proteins such as annexin 1 (upregulated), α1-acid glycoprotein 1, and α2-HS-glycoprotein (downregulated) in the tears of patients with KC, which are involved in the regulation of the inflammatory and immune response. Previous studies in aqueous humor samples also observed a decrease in α1-acid glycoprotein 1 levels compared to control samples,[42] evidencing an imbalance between pro- and anti-inflammatory proteins in the tissues and the biological fluids of patients with KC. Vitamin D binding protein was the third most underexpressed protein in the tear samples of KC eyes. This is the main vitamin D transport protein in the body, and it is essential for maintaining circulating vitamin D levels and preventing its deficiency. This protein has a wide variety of functions, and at the tear level, it has shown anti-inflammatory properties, playing an important role in the protection of the ocular surface. Previous studies reported a deficit in vitamin D levels in the blood samples of patients with KC, as well as a negative correlation between vitamin D levels and the progression of the disease.[43–45] Under normal conditions, vitamin D levels are higher in tears than in blood[46]; therefore, the reported deficit in blood may be in good agreement with the deficit we have observed in tears.

Serotransferrin was the highest underexpressed protein compared with the control group. Serotransferrin is an essential glycoprotein for iron transport that binds to free iron ions that are toxic and potentially damaging for tissues.[47] Indeed, free iron ions (unbounded to serotransferrin or other iron-transport proteins) may accumulates in tissues, leading to an increase of oxidative stress and reactive species, which promotes cellular damage and tissue injury.[48,49] The decrease in serotransferrin levels was also reported in the corneal stroma of patients with KC, and previous studies associated certain polymorphisms of the transferrin gene with the risk of the appearance of KC.[50] Similar to serotransferrin, some studies have already reported the underexpression of lactoferrin in tears of these patients.[6,18] Lactoferrin is also a protein of the transferrin family that, in addition to iron transport, has antimicrobial, anti-inflammatory, antioxidant, and immunomodulatory

Downloaded from iovs.arvojournals.org on 05/16/2022

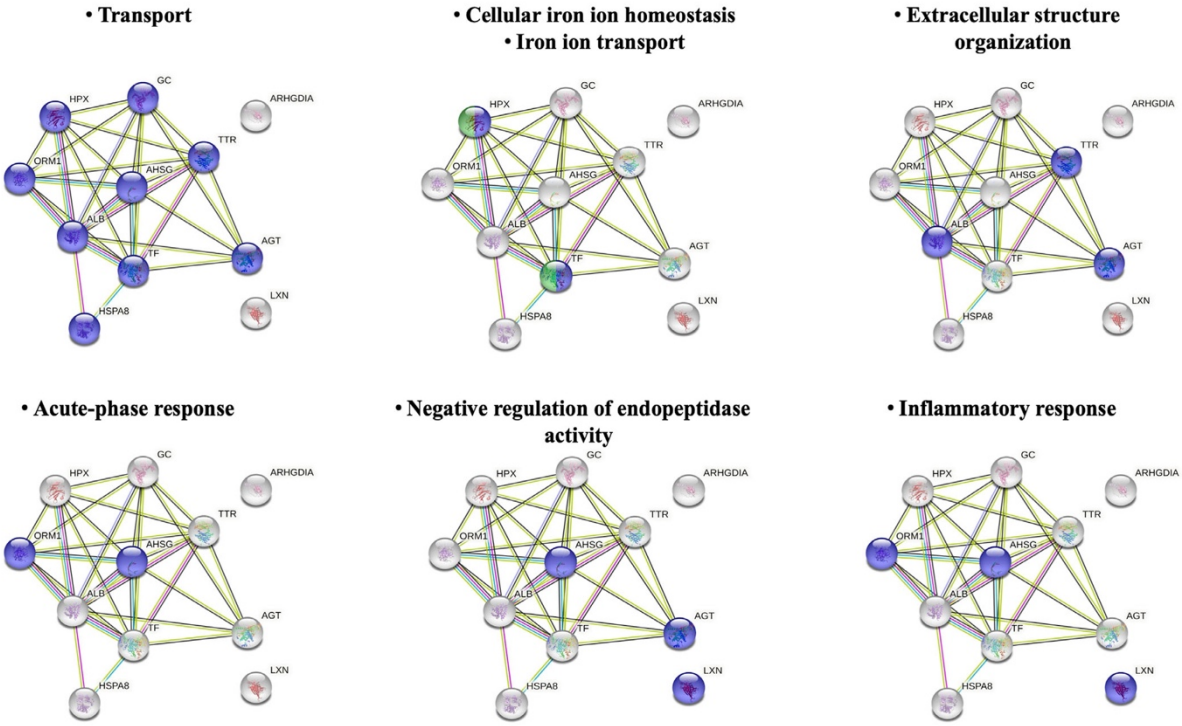


Figure 4. Main biological processes of proteins downregulated in KC samples. Protein–protein interactions were made using the STRING interaction network. Proteins downregulated are represented as a cluster. The *colored* proteins in the clusters are involved in the indicated biological process. Classification of proteins was based on GO biological processes. All the biological processes that are referred to present an FDR less than 0.05. AGT, angiotensinogen; AHSG, α2-HS-glycoprotein; ALB, serum albumin; ARHGDIA, ρ GDP-dissociation inhibitor 1; GC, vitamin D binding protein; HPSA8, heat shock cognate 71-kDa protein; HPX, hemopexin; LXN, latexin; ORM1, α1-acid glycoprotein 1; TF, serotransferrin; TTR, transthyretin.

functions in its apo (iron-free) form.[51] The importance of lactoferrin underexpression in tears of patients with KC has been previously associated with its anti-inflammatory and immunomodulatory properties; however, it is possible that its underexpression contributes to increased oxidative stress due to its function as an iron transporter.

Extracellular iron is usually found in normal tear composition, transported among tissues by proteins such as lactoferrin or transferrin.[49] Taking into account that one of the main histologic characteristics of keratoconic corneas is the iron deposition in the epithelial basement membrane (Fleischer ring), a decrease in the expression of iron-binding proteins in tears could contribute to its filtration and accumulation in the corneal epithelial tissue, whose toxicity would lead to an oxidative microenvironment and cell damage or death cell processes such as ferroptosis.[52] Ferroptosis is an iron-dependent cell death process that has been discovered in recent years and is often accompanied by iron accumulation and lipid peroxidation. Recent research has demonstrated that this type of cell death process plays an important role in the appearance and progression of numerous diseases, such as Parkinson and other neurologic diseases[53,54]; therefore, the study of their biological effects has become a key point for the development of new therapeutic strategies. In the case of KC, the alteration of iron transporting proteins, its accumulation in the epithelial tissue, the increase of reactive species, and the decrease in the expression of proteins with antioxidant activity may indicate the possible implication of this mechanism in the death of stromal keratocytes and in the epithelial degeneration.[12,55–57]

Regarding the increase of oxidative stress levels, in this study, we have found a decrease in serum albumin, hemopexin, and heat shock cognate 71 kDa. Recently, albumin has been associated with antioxidant and antiapoptotic mechanisms as well as vascular integrity. Elevated levels of albumin in tears are used as a marker of active inflammation and ocular damage,[58] but in KC pathology, the decrease in tear albumin levels could affect its antioxidant and antiapoptotic properties, aggravating the processes of cell death and oxidative stress characteristic of the pathophysiology of the disease.[59]

Hemopexin and heat shock cognate 71 kDa are proteins that present antioxidant activity and are part of the response to oxidative stress.[60] Considering that the cornea is potentially susceptible to increased levels of oxidative stress due to constant exposure to ultraviolet light, our results suggest that the antioxidant defense mechanisms and neutralization of reactive species in tears may not be sufficient and contribute to increased oxidative stress in tissues.

Balasubramanian et al.[61] described the dysregulation of five proteins (cathepsin, cystatin S, cystatin SN, α-fibrinogen, and PIGR) in the tears of patients with KC, mainly related to wound healing and proteolysis. Also, regarding cell

Investigative Ophthalmology & Visual Science

Downloaded from iovs.arvojournals.org on 05/16/2022

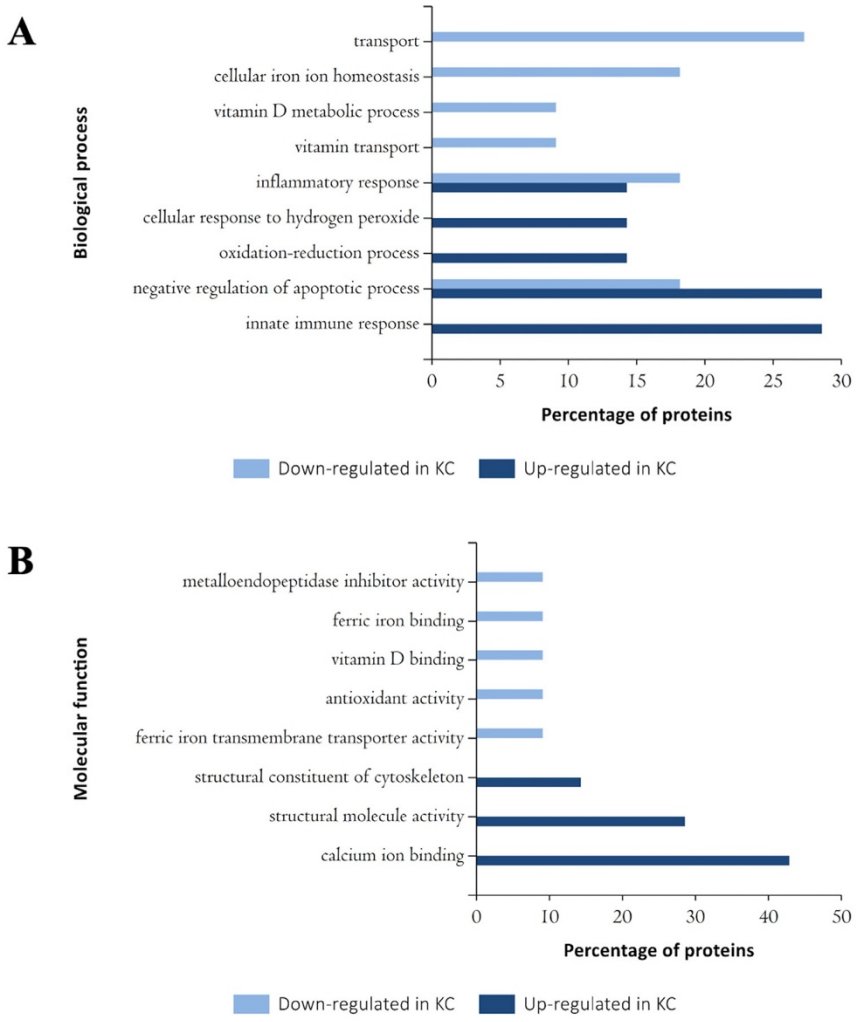


Figure 5. (**A**) Biological processes mainly related to the differentially expressed proteins. (**B**) Molecular functions mainly related to the differentially expressed proteins. GO enrichment of dysregulated proteins used the FunRich functional tool. The histograms represent the main categories for each GO term in which differentially expressed proteins were involved ($P < 0.05$). The y-axis shows the biological processes, and the x-axis shows the percentage of proteins involved in this process compared with the total proteins in the database.

damage, we observed a decrease in the expression of latexin, angiotensinogen, and α2-HS-glycoprotein, which belong to the family of protease inhibitor proteins and could compromise the integrity of the corneal tissue due to an increase in the activity of proteases.

Although this study used a novel MS method (SWATH-MS) for analyzing the proteomic profile of tear samples in KC, it has some limitations. The SWATH method is a specific, reproducible, and sensitive approach that allows relative or absolute quantification of proteins. However, the number of proteins identified/quantified is mostly limited by the composition of the spectral library, which was created using a pool of proteins for each condition. In the SWATH technique, seven transitions are quantified for each peptide. Therefore, 10 peptides per protein must be identified to extract the peak areas needed for quantification. Consequently, library proteins in which fewer than 10 peptides are identified will not be quantified by the SWATH method.

Moreover, in this study, the biological functions and relationships between the dysregulated proteins have only been analyzed in silico, so in vitro assays should be developed to confirm the protein–protein interactions as well as validate our results as potential biomarker for the KC disease.

In relation to the sample size, the present study was conducted on a small sample, which did not allow for stratification of the eyes according to the degree of the disease, and in addition, a number of employed KC eyes showed moderated degrees of the disease, but a smaller number of patients had slight or severe degrees.

These weaknesses should be considered in future studies for elucidating the molecular and biological processes

Investigative Ophthalmology & Visual Science

Downloaded from iovs.arvojournals.org on 05/16/2022

that lead to the progression of the disease as well as those alterations related to the different stages of the disease.

Overall, our results in tear fluid have shown the implication of several biological processes in the KC pathophysiology, such as oxidative stress, matrix degradation, cellular death, and immune or inflammatory responses, pathways that have also been referred to in the corneal tissues.[9,55,62,63] Therefore, tear fluid becomes a good alternative for the study of the KC pathophysiology, being able to reflect the molecular mechanisms that determine the pathologic conditions of the disease. However, despite the fact that the biological pathways involved appear to be clear, the triggering factor or factors remain potentially unknown.

In conclusion, our findings strengthen the theory by describing keratoconus as a pathology of multifactorial origin involving genetic, environmental, and biomolecular factors. The biological processes that are involved in its pathophysiology are partially understood (inflammatory, immune, oxidative stress, and cell death), and the decrease in proteins that participate in transport and iron homeostasis that we observed at the tear level could make evident another fundamental pathway in the pathogenesis of the disease. These findings may be key to the development of therapeutic strategies to cope with the tissue damage that derives from iron accumulation and toxicity. A better understanding of the cytotoxic mechanisms triggered by the accumulation of iron in corneal tissues is necessary, as well as a comprehensive research related to the alteration of this event in the preclinical stages of the disease.

Acknowledgments

This project has been awarded with a grant from the Spanish Ministry of Science and Innovation, project PI18/00159, funded by Insituto de Salud Carlos III and co-funded by European Union (ERDF/ESF, "A way to make Europe"/"Investing in your future"). ML-L recognizes the support from a Xunta de Galicia (Galician Innovation Agency GAIN: IN607A2018/3) fellowship. UR is recipient of a research contract funded by the Spanish Research Network on Cerebrovascular Diseases INVICTUS PLUS (RD16/0019/0001). Similarly, RV-F acknowledges the financial support of the FIDIS (Health Research Institute of Santiago de Compostela Foundation). The funders had no role in the study design, data collection and analysis, decision to publish, or preparation of the manuscript.

Disclosure: **M. López-López**, None; **U. Regueiro**, None; **S.B. Bravo**, None; **M. del Pilar Chantada-Vázquez**, None; **R. Varela-Fernández**, None; **P. Ávila-Gómez**, None; **P. Hervella**, None; **I. Lema**, None

References

1. Belin MW, Asota IM, Ambrosio R, Khachikian SS. What's in a name: keratoconus, pellucid marginal degeneration, and related thinning disorders. *Am J Ophthalmol*. 2011;152(2):157–162.
2. Wagner H, Barr JT, Zadnik K. Collaborative Longitudinal Evaluation of Keratoconus (CLEK) study: methods and findings to date. *Contact Lens Anterior Eye*. 2007;30(4):223–232.
3. Assiri AA, Yousuf BI, Quantock AJ, Murphy PJ. Incidence and severity of keratoconus in Asir province, Saudi Arabia. *Br J Ophthalmol*. 2005;89(11):1403–1406.
4. Naderan M, Rajabi MT, Zarrinbakhsh P, Naderan M, Bakhshi A. Association between family history and keratoconus severity. *Curr Eye Res*. 2016;41(11):1414–1418.
5. McMonnies CW. Inflammation and keratoconus. *Optom Vis Sci*. 2015;92(2):35–41.
6. Lema I, Brea D, Rodríguez-González R, Díez-Feijoo E, Sobrino T. Proteomic analysis of the tear film in patients with keratoconus. *Mol Vis*. 2010;16:2055–2061.
7. Malfeito M, Regueiro U, Pérez-Mato M, Campos F, Sobrino T, Lema I. Innate immunity biomarkers for early detection of keratoconus. *Ocul Immunol Inflamm*. 2019;27(6):942–948.
8. Toprak I, Kucukatay V, Yildirim C, Kilic-Toprak E, Kilic-Erkek O. Increased systemic oxidative stress in patients with keratoconus. *Eye (Lond)*. 2014;28(3):285–289.
9. Regueiro U, Pérez-Mato M, Hervella P, Campos F, Sobrino T, Lema I. Toll-like receptors as diagnostic targets in pellucid marginal degeneration. *Exp Eye Res*. 2020;200:108211.
10. Wojcik K, Kaminska A, Blasiak J, Szaflik J, Szaflik JP. Oxidative stress in the pathogenesis of keratoconus and Fuchs endothelial corneal dystrophy. *Int J Mol Sci*. 2013;14(9):19294–19308.
11. Chwa M, Atilano SR, Reddy V, Jordan N, Kim DW, Kenney MC. Increased stress-induced generation of reactive oxygen species and apoptosis in human keratoconus fibroblasts. *Invest Ophthalmol Vis Sci*. 2006;47(5):1902–1910.
12. Olofsson EM, Marklund SL, Pedrosa-Domellöf F, Behndig A. Interleukin-1alpha downregulates extracellular-superoxide dismutase in human corneal keratoconus stromal cells. *Mol Vis*. 2007;13:1285–1290.
13. Lema I, Duran J. Inflammatory molecules in the tears of patients with keratoconus. *Ophthalmology*. 2005;112(4):654–659.
14. Li Q, Weng J, Mohan RR, et al. Hepatocyte growth factor and hepatocyte growth factor receptor in the lacrimal gland, tears, and cornea. *Invest Ophthalmol Vis Sci*. 1996;37(5):727–739.
15. Vesaluoma M, Teppo AM, Grönhagen-Riska C, Tervo T. Release of TGF-β1 and VEGF in tears following photorefractive keratectomy. *Curr Eye Res*. 1997;16(1):19–25.
16. Balasubramanian SA, Mohan S, Pye DC, Willcox MD. Proteases, proteolysis and inflammatory molecules in the tears of people with keratoconus. *Acta Ophthalmol*. 2012;90(4):303–309.
17. Sorkhabi R, Ghorbanihaghjo A, Taheri N, Ahoor MH. Tear film inflammatory mediators in patients with keratoconus. *Int Ophthalmol*. 2015;35(4):467–472.
18. Balasubramanian SA, Pye DC, Willcox MD. Levels of lactoferrin, secretory IgA and serum albumin in the tear film of people with keratoconus. *Exp Eye Res*. 2012;96(1):132–137.
19. Lema I, Sobrino T, Duran JA, Brea D, Diez-Feijoo E. Subclinical keratoconus and inflammatory molecules from tears. *Br J Ophthalmol*. 2009;93(6):820–824.
20. Azkargorta M, Soria J, Acera A, Iloro I, Elortza F. Human tear proteomics and peptidomics in ophthalmology: toward the translation of proteomic biomarkers into clinical practice. *J Proteomics*. 2017;150:359–367.
21. Efron N. Grading scales for contact lens complications. *Ophthalmic Physiol Opt*. 1998;18(2):182–186.
22. Chantada-Vázquez MDP, García Vence M, Serna A, Núñez C, Bravo SB. SWATH-MS protocols in human diseases. *Methods Mol Biol*. 2021; 2259:105–141.
23. Bonzon-Kulichenko E, Pérez-Hernández D, Núñez E, et al. A robust method for quantitative high-throughput analysis of proteomes by 18O labeling. *Mol Cell Proteomics*. 2011;10(1):M110.003335.
24. Pérez-Hernández D, Gutiérrez-Vázquez C, Jorge I, et al. The intracellular interactome of tetraspanin-enriched microdomains reveals their function as sorting machineries toward exosomes. *J Biol Chem*. 2013;288(17):11649–11661.
25. Shevchenko A, Wilm M, Vorm O, Mann M. Mass spectrometric sequencing of proteins from silver-stained polyacrylamide gels. *Anal Chem*. 1996;68(5):850–858.

Investigative Ophthalmology & Visual Science

Downloaded from iovs.arvojournals.org on 05/16/2022

26. Chantada-Vázquez MDP, López AC, García-Vence M, Acea-Nebril B, Bravo SB, Núñez C. Protein corona gold nanoparticles fingerprinting reveals a profile of blood coagulation proteins in the serum of her2-overexpressing breast cancer patients. *Int J Mol Sci*. 2020;21(22):1–18.
27. Peñas-Martínez J, Barrachina MN, Cuenca-Zamora EJ, et al. Qualitative and quantitative comparison of plasma exosomes from neonates and adults. *Int J Mol Sci*. 2021;22(4):1926.
28. Camino T, Lago-Baameiro N, Bravo SB, et al. Human obese white adipose tissue sheds depot-specific extracellular vesicles and reveals candidate biomarkers for monitoring obesity and its comorbidities [published online January 17, 2021]. *Transl Res*.
29. Redestig H, Fukushima A, Stenlund H, et al. Compensation for systematic cross-contribution improves normalization of mass spectrometry–based metabolomics data. *Anal Chem*. 2009;81(19):7974–7980.
30. Lambert JP, Ivosev G, Couzens AL, et al. Mapping differential interactomes by affinity purification coupled with data-independent mass spectrometry acquisition. *Nat Methods*. 2013;10(12):1239–1245.
31. Szklarczyk D, Morris JH, Cook H, et al. The STRING database in 2017: quality-controlled protein-protein association networks, made broadly accessible. *Nucleic Acids Res*. 2017;45(D1):D362–D368.
32. Pathan M, Keerthikumar S, Ang CS, et al. FunRich: an open access standalone functional enrichment and interaction network analysis tool. *Proteomics*. 2015;15(15):2597–2601.
33. Huang DW, Sherman BT, Lempicki RA. Bioinformatics enrichment tools: paths toward the comprehensive functional analysis of large gene lists. *Nucleic Acids Res*. 2009;37(1):1–13.
34. Krumeich JH, Daniel J, Knalle A. Live-epikeratophakia for keratoconus. *J Cataract Refract Surg*. 1998;24(4):456–463.
35. Shilov I V, Seymourt SL, Patel AA, et al. The paragon algorithm, a next generation search engine that uses sequence temperature values sequence temperature values and feature probabilities to identify peptides from tandem mass spectra. *Mol Cell Proteomics*. 2007;6(9):1638–1655.
36. Pannebaker C, Chandler HL, Nichols JJ. Tear proteomics in keratoconus. *Mol Vis*. 2010;16:1949–1957.
37. Acera A, Vecino E, Rodríguez-Agirretxe I, Aloria K, Arizmendi JM, et al. Changes in tear protein profile in keratoconus disease. *Eye*. 2011;25(9):1225–1233
38. Lin CS, Park T, Chen ZP, Leavitt J. Human plastin genes: comparative gene structure, chromosome location, and differential expression in normal and neoplastic cells. *J Biol Chem*. 1993;268(4):2781–2792.
39. Ostrowska Z, Moraczewska J. Cofilin—a protein controlling dynamics of actin filaments. *Postepy Hig Med Dosw (Online)*. 2017;71:339–351.
40. Joseph R, Srivastava OP, Pfister RR. Differential epithelial and stromal protein profiles in keratoconus and normal human corneas. *Exp Eye Res*. 2011;92(4):282–298.
41. Regueiro U, López-López M, Hervella P, Sobrino T, Lema I. Corneal and conjunctival alteration of innate immune expression in first-degree relatives of keratoconus patients. Graefe's *Arch Clin Exp Ophthalmol*. 2021;259(2):459–467.
42. Soria J, Villarrubia A, Merayo-Lloves J, et al. Label- free LC-MS/MS quantitative analysis of aqueous humor from keratoconic and normal eyes. *Mol Vis*. 2015;21:451–460.
43. Akkaya S, Ulusoy DM. Serum vitamin D levels in patients with keratoconus. *Ocul Immunol Inflamm*. 2020;28(3):348–353.
44. Zarei-Ghanavati S, Yahaghi B, Hassanzadeh S, Mobarhan MG, Hakimi HR, Eghbali P. Serum 25-hydroxyvitamin D, selenium, zinc and copper in patients with keratoconus. *J Curr Ophthalmol*. 2020;32(1):26–31.
45. Aslan MG, Fındık H, Okutucu M, et al. Serum 25-hydroxy vitamin D, vitamin B12, and folic acid levels in progressive and nonprogressive keratoconus. *Cornea*. 2021;40(3):334–341.
46. Sethu S, Shetty R, Deshpande K, et al. Correlation between tear fluid and serum vitamin D levels. *Eye Vis*. 2016;3(1):22.
47. Gomme PT, McCann KB. Transferrin: structure, function and potential therapeutic actions. *Drug Discov Today*. 2005;10(4):267–273.
48. Lieu PT, Heiskala M, Peterson PA, Yang Y. The roles of iron in health and disease. *Mol Aspects Med*. 2001;22(1–2):1–87.
49. Papanikolaou G, Pantopoulos K. Iron metabolism and toxicity. *Toxicol Appl Pharmacol*. 2005;202(2):199–211.
50. Wójcik KA, Synowiec E, Jiménez-García MP, et al. Polymorphism of the transferrin gene in eye diseases: keratoconus and Fuchs endothelial corneal dystrophy. *Biomed Res Int*. 2013;2013:247438.
51. González-Chávez SA, Arévalo-Gallegos S, Rascón-Cruz Q. Lactoferrin: structure, function and applications. *Int J Antimicrob Agents*. 2009;33(4):301.e1–301.e8.
52. Loh A, Hadziahmetovic M, Dunaief JL. Iron homeostasis and eye disease. *Biochim Biophys Acta*. 2009;1790(7):637–649.
53. Do Van B, Gouel F, Jonneaux A, et al. Ferroptosis, a newly characterized form of cell death in Parkinson's disease that is regulated by PKC. *Neurobiol Dis*. 2016;94:169–178.
54. Hambright WS, Fonseca RS, Chen L, Na R, Ran Q. Ablation of ferroptosis regulator glutathione peroxidase 4 in forebrain neurons promotes cognitive impairment and neurodegeneration. *Redox Biol*. 2017;12:8–17.
55. Arnal E, Peris-Martínez C, Menezo JL, Johnsen-Soriano S, Romero FJ. Oxidative stress in keratoconus? *Invest Opthalmol Vis Sci*. 2011;52(12):8592–8597.
56. Chwa M, Atilano SR, Hertzog D, Zheng H, Langberg J, et al. Hypersensitive response to oxidative stress in keratoconus corneal fibroblasts. *Invest Ophthalmol Vis Sci*. 2008;49(10):4361–4369.
57. Navel V, Malecaze J, Pereira B, et al. Oxidative and antioxidative stress markers in keratoconus: a systematic review and meta-analysis [published online December 23, 2020]. *Acta Ophthalmol*.
58. Versura P, Nanni P, Bavelloni A, et al. Tear proteomics in evaporative dry eye disease. *Eye*. 2010;24(8):1396–1402.
59. Rozga J, Piatek T, Małkowski P. Human albumin: old, new, and emerging applications. *Ann Transplant*. 2013;18(1):205–217.
60. Tolosano E, Altruda F. Hemopexin: structure, function, and regulation. *DNA Cell Biol*. 2002;21(4):297–306.
61. Balasubramanian SA, Wasinger VC, Pye DC, Willcox MD. Preliminary identification of differentially expressed tear proteins in keratoconus. *Mol Vis*. 2013;19:2124–2134.
62. Pahuja N, Kumar NR, Shroff R, et al. Differential molecular expression of extracellular matrix and inflammatory genes at the corneal cone apex drives focal weakening in keratoconus. *Invest Ophthalmol Vis Sci*. 2016;57(13):5372–5382.
63. Collier SA, Madigan MC, Penfold PL. Expression of membrane-type 1 matrix metalloproteinase (MT1-MMP) and MMP-2 in normal and keratoconus corneas. *Curr Eye Res*. 2000;21(2):662–668.

Downloaded from iovs.arvojournals.org on 05/16/2022

Chapter 2

Shotgun proteomics for the identification and profiling of the tear proteome of keratoconus patients

Maite López-López[1,2]*, Uxía Regueiro[1,2]*, Susana B. Bravo[3], María del Pilar Chantada-Vázquez[3], Carmen Pena[3], Elío Díez-Feijoo[1,2,5], Pablo Hervella[4#], Isabel Lema[1,2,5#].

[1] Corneal Neurodegeneration Group (RENOIR). Clinical Neurosciences Research Laboratory (LINC), Health Research Institute of Santiago de Compostela (IDIS), Santiago de Compostela, Spain.
[2] Department of Surgery and Medical-Surgical Specialties. Faculty of Optics and Optometry, University of Santiago de Compostela, Santiago de Compostela, Spain.
[3] Proteomic Unit, Health Research Institute of Santiago de Compostela (IDIS), Santiago de Compostela, Spain.
[4] Neuroimaging and Biotechnology Group (NOBEL). Clinical Neurosciences Research Laboratory (LINC), Health Research Institute of Santiago de Compostela (IDIS), Santiago de Compostela, Spain.
[5] Instituto Galego de Oftalmoloxía (INGO), Hospital Provincial de Conxo, Santiago de Compostela, Spain.

* These authors have equally contributed to this work as First Authors.
[#] These authors have equally contributed to this work as Corresponding Authors.

Published in *Investigative Ophthalmology & Visual Science (IOVS).* 2022;63(5):12.

Journal Citations Reports (JCR) Metrics: 2022
Journal Impact Factor (JIF): 4.400
JIF Quartile: Q1
Journal Position: 7/62 *Ophthalmology*
JCR abbreviation: INVEST OPHTH VIS SCI
ISSN: 0146-0404

Author contribution. López-López M contributed to the conceptualization, design, formal analysis and investigation, writing and original draft preparation of this manuscript.

Open Access license details are provided in **Annex 4**.

Cornea

Shotgun Proteomics for the Identification and Profiling of the Tear Proteome of Keratoconus Patients

Maite López-López,[1,2] Uxía Regueiro,[1,2] Susana Belén Bravo,[3] María del Pilar Chantada-Vázquez,[3] Carmen Pena,[3] Elío Díez-Feijoo,[1,2,5] Pablo Hervella,[4] and Isabel Lema[1,2,5]

[1]Corneal Neurodegeneration Group (RENOIR), Clinical Neurosciences Research Laboratory (LINC), Health Research Institute of Santiago de Compostela (IDIS), Santiago de Compostela, Spain
[2]Department of Surgery and Medical-Surgical Specialties, Faculty of Optics and Optometry, University of Santiago de Compostela, Santiago de Compostela, Spain
[3]Proteomic Unit, Health Research Institute of Santiago de Compostela (IDIS), Santiago de Compostela, Spain
[4]Neuroimaging and Biotechnology Group (NOBEL), Clinical Neurosciences Research Laboratory (LINC), Health Research Institute of Santiago de Compostela (IDIS), Santiago de Compostela, Spain
[5]Galician Institute of Ophthalmology (INGO), Conxo Provincial Hospital, Santiago de Compostela, Spain

Correspondence: Isabel Lema, Corneal Degeneration Group (RENOIR), Clinical Neurosciences Research Laboratory (LINC), Health Research Institute of Santiago de Compostela (IDIS), Hospital Clínico Universitario, Travesía da Choupana S/N, 15706, Santiago de Compostela, Spain;
mariaisabel.lema@usc.es.
Pablo Hervella, Neuroimaging and Biotechnology Group (NOBEL), Clinical Neurosciences Research Laboratory (LINC), Health Research Institute of Santiago de Compostela (IDIS), Hospital Clínico Universitario, Travesía da Choupana S/N, 15706, Santiago de Compostela, Spain;
pablo.hervella.lorenzo@sergas.es.

MLL and UR have equally contributed to this work.

Received: December 29, 2021
Accepted: April 22, 2022
Published: May 12, 2022

Citation: López-López M, Regueiro U, Bravo SB, et al. Shotgun proteomics for the identification and profiling of the tear proteome of keratoconus patients. *Invest Ophthalmol Vis Sci.* 2022;63(5):12. https://doi.org/10.1167/iovs.63.5.12

Purpose. The qualitative approach followed in this study aims to obtain an extensive view of the keratoconus (KC) tear proteome, which could highlight proteins previously undetected and enlarge our knowledge of the disease's pathophysiology.

Methods. Twenty-five patients diagnosed with KC and 25 control subjects were studied in a prospective, cross-sectional study. KC screening examinations, including clinical and tomographic examinations, were performed on all participants. Tear samples were collected using Schirmer strips and analyzed by liquid chromatography-tandem mass spectrometry in a data-dependent workflow. A spectral count was used as a semi-quantification tool. The tear proteomes of both groups were identified and profiled, and the functional interactions and biological characterization of differential proteins were analyzed using in silico tools.

Results. We identified a total of 232 proteins, of whom 133 were expressed in both groups' samples; 41 were observed only in control samples and 58 were identified just in tears of patients with KC. A semiquantitative analysis showed the dysregulation of 17 proteins in the KC samples. An in silico analysis linked proteins only expressed in KC samples to oxidative stress, skin development, and apoptosis. The dysregulation of proteins involved in iron transport, inflammation, oxidative stress, and protease inhibition was observed in the semiquantitative results.

Conclusions. A shotgun analysis showed that the tear proteome of patients with KC differed from controls by more than one-third of the total proteins identified, highlighting the relationship of the proteins only expressed in KC tears with processes of cell death, oxidative damage, and inflammation. The underexpression of proteins involved in iron pathways might support the iron imbalance as a contributing factor to cellular damage and death in KC disease.

Keywords: keratoconus, mass spectrometry, proteomics, shotgun, tear fluid

Keratoconus (KC) is a chronic and degenerative condition marked by pathological weakening, thinning, and protrusion of the corneal tissue.[1] KC leads to visual impairment because of irregular astigmatism and high-order aberrations, resulting from thinning and an increased curvature of the cornea. KC may occur either in isolation, in combination with other clinical diseases, or as a complement of another syndrome.[2] In most cases, it is a bilateral and asymmetric disorder that begins in adolescence and progress up to 30 to 40 years of age. Currently, KC is described as a multifactorial disease in which mechanical–environmental factors coexist with a genetic predisposition to its development.[3,4]

In recent years, many studies have been carried out to determine the biochemical and biomolecular changes that may impact the KC onset and progression.[5–8] In this regard, an analysis of the tears and corneal tissue from patients with KC has revealed overexpression of inflammatory cytokines such as IL-1, IL-1ß, IL-6, IL-17, TNF-α, and TNF-ß.[9–11] In addition, previous studies from our group have shown the involvement of innate immunity in the pathophysiology

Copyright 2022 The Authors

This work is licensed under a Creative Commons Attribution-NonCommercial-NoDerivatives 4.0 International License.

Downloaded from iovs.arvojournals.org on 05/16/2022

Investigative Ophthalmology & Visual Science

of KC, observing an increase in the expression of Toll-like receptors 2 and 4 in corneal and conjunctival epithelial cells, as well as in blood monocytes and neutrophils.[5,12,13] Oxidative stress also seems to play a crucial role in the pathophysiology of KC, as evidenced by numerous studies that have reported higher levels of damaging free radicals and lower levels of antioxidant molecules in the KC samples.[14–16] The extracellular matrix degradation and the apoptosis of corneal stromal and epithelial cells are triggered by both an increase in metalloproteinases levels and a decrease in the levels of their inhibitors,[17–20] which may be aggravated by the intense and frequent eye rubbing characteristic of patients with KC. Based on these characteristics, biological pathways such as inflammation, the innate immune response, oxidative stress, matrix proteolysis, and apoptosis have been brought to the spotlight in the pathophysiology of KC.

Biomolecules expressed in tears are vulnerable to changes associated with ocular diseases, providing information about the corneal tissue's conditions.[21] Tear fluid has become an easily accessible biological fluid that could play a key role in the detection of molecular changes that may be involved in the development of KC.

Recently, our group carried out a quantification approach of the tear proteome of patients with KC and control participants, using for the first time the sequential window acquisition for all theoretical mass spectra to identify the main dysregulated proteins in the tears of patients with KC.[22] In this way, results from the quantitative study revealed that dysregulated proteins were involved in the central processes of the KC pathophysiology, such as inflammation, oxidative stress, matrix proteolysis, and iron homeostasis.[22] However, the qualitative approach followed in this study aims to complement our previous results, trying to overcome the main handicap of quantitative studies (in which it is necessary to recognize a critical number of peptides to achieve protein quantification), and to obtain an even more extensive view of the tear proteomic profile of the patients with KC. Based on these factors, we performed a shotgun analysis to massively identify the tear proteome of patients with KC, which could highlight proteins undetected in the quantitative analysis and enlarge our knowledge of the disease's pathophysiology.

Methods

The current study was carried out following the standards of the Declaration of Helsinki of the World Medical Association (as revised in Brazil 2013). The Ethics Committee for Clinical Research of Galicia (2019/623) approved the clinical, topographic, and tomographic protocol, including the biological sample extraction for all subjects. Each participant gave written informed consent after a thorough description of the methods and tests. All tests were performed by the same researchers. Regarding the data collected, variables included age, gender, patient's ocular history, patient medical history (allergy and other conditions such as eye itching and eye rubbing), and family history of corneal ectasia. Atopic conditions such as asthma, rhinitis, and atopic dermatitis were included as allergic diseases. Regarding the ophthalmological examination, topographic, and tomographic examinations were performed, including maximum dioptric power, flattest corneal meridian, steeper meridian, inferior–superior dioptric asymmetry, minimum thickness point, and posterior elevation. All variables were measured using PENTACAM (Oculus, Wetzlar, Germany).

Study Subjects

This prospective and cross-sectional study included 50 subjects divided into two groups: 25 patients diagnosed with KC (study group) and 25 control participants (control group). The inclusion criteria for the study group was the diagnosis of KC, supported by slit-lamp examination and corneal topography and tomography examinations. Conjunctival hyperemia of less than 2 (Nathan Efron scale),[23] Schirmer test of more than 15 mm in 5 minutes, and at least 5 days without contact lenses, artificial tears, or eye drops were the common inclusion criteria for all groups. The common exclusion criteria for both groups included corneal trauma or disease, previous surgical intervention in the anterior segment, active ocular or systemic inflammation, current treatment with local or systemic anti-inflammatory drugs, and/or pregnancy. Renal, hepatic, or hematologic diseases, as well as solid tumors, were also exclusion criteria for both groups. Control subjects with a family history of corneal ectasia were excluded. This study involved the same participants who were enrolled in our previous sequential window acquisition for all theoretical mass spectra analysis.[22]

Tear Sample Extraction and Analysis

Tear samples were collected using Schirmer Strips. Strips were removed when the sample reached the 15 mm on the Schirmer scale (9 µL). Samples were extracted without previous instillation of drugs, artificial tears, or vital dyes, and immediately after collection they were frozen and stored at −80°C until their analysis.

Sample Preparation

Proteins were extracted by cutting and incubating Schirmer strips for 1 hour (h) at room temperature in a 100-µL solution of 100 mM ammonium bicarbonate. Samples were centrifuged for 20 minutes at 13,000x*g*, and the supernatant was transferred to a new tube. Subsequently, 600 µL of acetone were added to the new Eppendorf with the supernatant and incubate at –20°C overnight. After this time, samples were centrifuged 20 min at 13,000x*g* and the supernatant was removed. The pellet was dried at room temperature for 1 h to evaporate the acetone and 100 µL of miliQ was added. Finally, the amount of protein was measured using a RC-DC kit (BioRad, Hercules, CA).[24] These samples were used both for tryptic digestion and micro-liquid chromatography with tandem mass spectrometry (LC-MS/MS) analysis as well as for the quantification by ELISA.

Tryptic Digestion

Trypsin digestion was performed as described previously by our group.[22] Briefly, 100 µg of protein was concentrated on a 10% SDS-PAGE gel. The gel was allowed to run until the front entered 3 mm of the separator gel.[25,26] The protein band was visualized with Sypro-Ruby fluorescent staining (Lonza, Porriño, Pontevedra, Spain), excised and subjected to tryptic digestion following the standard protocol of Shevchenko et al.,[27] with minor modifications. The peptides were extracted and stored at –20°C until their use.

Protein Identification by Shotgun (LC-MS/MS)

Digested peptides were resuspended in 20 µL of mobile phase A (2% acetonitrile, 0.1%, formic acid), by sonication for

Downloaded from iovs.arvojournals.org on 05/16/2022

10 minutes to obtain 1 µg/µL peptide solution. We injected 4 µg (4 µL) of each sample and separated by reverse phase chromatography using a ChromXP C18CL column (150 µL × 0.3 mm, 120ª, s-3 µL) (Sciex, Framingham, MA).

Data acquisition was performed on a Triple-TOF 6600 system (Sciex) using a data-dependent workflow with micro-LC-MS/MS technology. After MS/MS acquisition, the files were processed with ProteinPilot 5.0.1 software (Sciex) using the Paragon algorithm for database searching and Progroup for data clustering. Searches were performed using a human-specific Uniprot database (Swiss-Prot), trypsin as enzyme of digestion, and cysteine alkylation as fixed modification. The search was performed allowing a fragment ion mass tolerance of 0.100 Da and a parent ion tolerance of 0,050 Da. The false discovery rate was obtained by a nonlinear adjustment that considers correctly identified proteins with a false discovery rate of less than 1%.

Semiquantitative Analysis by Spectral Count

The Scaffold program was used for semiquantification by spectral counting (version Scaffold_5.0.1, Proteome Software Inc., Portland, OR). The total samples of both groups (control and KC) were subgrouped for quantification.

MS/MS-based peptide and protein identifications performed in ProteinPilot software were validated by Scaffold. Peptide identifications were accepted if they could be established at greater than 95.0% probability by the Percolator posterior error probability calculation.[28] Protein identifications with a probability of greater than 99.0% and at least two identified peptides were accepted. Protein probabilities were assigned by the Protein Prophet algorithm.[29] Proteins that contained similar peptides and could not be differentiated based on MS/MS analysis alone were grouped to satisfy the principles of parsimony. Proteins sharing significant peptide evidence were grouped into clusters. The Fisher's exact test and the Benjamini–Hochberg multiple correction test were used for quantification and fold change determination.

ELISA Quantification

ELISA on human tears were performed using commercial kits from FineTests for the following four proteins: albumin (ELISA kit catalog number EH2613), transferrin (ELISA kit catalog number EH0385), peroxiredoxin-1 (ELISA kit catalog number EH2166), and mammaglobin-B (ELISA kit catalog number EH4335). All assays were carried out following the manufacturer's protocols and were optimized and used with the following dilution factors: 1:50 for peroxiredoxin-1 and transferrin, 1:100 for albumin, and 1:200 for mammaglobin-B. All samples were assayed in duplicate, and the mean values were reported as nanograms per milliliter. Curve Expert 1.4 was used for curve and data analysis and box plots were performed using GraphPad Prism 8.0 (San Diego, CA) software.

Interaction Networks and Gene Ontology Enrichment Analysis

Protein–protein interactions and gene ontology (GO) enrichment analysis were performed to determine the interactions and functional characteristics of the identified proteins.

To create protein interaction maps, we used STRING (Functional Protein Association Network, free access at https://string-db.org) program, and to analyze biological processes and molecular functions we use the following tools: function enrichment interaction analysis (FunRich) and the Panther Classification System. We use Uniprot codes for the identification and functional characterization of each protein.

Statistical Analysis

SPSS 20.0 for Mac (IBM, Armonk, NY) and GraphPad Prism 8.0 were used for statistical analysis. The Kolmogorov–Smirnov test was used to confirm the normality of the quantitative variables. For categorical variables, the results were represented as percentages, and for continuous quantitative variables with a normal distribution, the mean ± standard deviation was used. Error bars were used to represent comparisons between normal continuous variables and box plots were used to represent continuous variables with non-normal distributions. The χ^2 test (for categorical variables), Student t test contrasts (for normal continuous variables), and the Mann–Whitney U test (for non-normal continuous variables) were used to compare groups bivariately. The Fisher exact test and Benjamini–Hochberg multiple correction test were used for quantification and FC determination in the spectral counting semiquantitative analysis. FC indicates upregulated proteins if the FC was more than 1 or downregulated proteins if the FC was less than 1. A P value of less than 0.05 was considered statistically significant in all tests.

Results

Clinical Features

In this study, we included 25 healthy eyes from 25 control subjects (60% male; mean age, 43.96 ± 6.94 years) and 25 eyes from 25 patients with KC (60% male; mean age, 44.88 ± 5.01 years). No differences were found regarding age and sex because both groups were previously matched according to these conditions. Allergic disorders showed no statistical differences between groups (P = .247). Patients with KC reported a higher rate of eye itching (72%) and, as a result, a higher rate of eye rubbing (64%) than the control subjects (4% for each condition) (P < .0001). Predictably, we found differences between the groups for all topographic and tomographic parameters. The clinical features as well as the topographic and tomographic parameters of each study group are displayed in Table 1.

Table 1. Clinical and Topographic–Tomographic Characteristics of Each Study Group

	Control	*KC*	*P* Value
Allergic disease (%)	28	44	0.247
Itching (%)	4	72	**<0.0001**
Rubbing (%)	4	64	**<0.0001**
K1 (D)	42.70 ± 1.39	47.14 ± 5.31	**<0.0001**
K2 (D)	43.73 ± 1.48	50.47 ± 5.28	**<0.0001**
maxDP (D)	44.40 ± 1.25	55.56 ± 7.10	**<0.0001**
MTP (µm)	534.00 ± 21.69	445.00 ± 66.65	**<0.0001**
PE	9.20 ± 3.73	67.96 ± 31.33	**<0.0001**

K1, flattest corneal meridian; K2, steeper corneal meridian; maxDP, maximum dioptric power; MTP, minimum thickness point; PE, posterior elevation.

Size sample: KC = 25 subjects, 25 eyes; controls = 25 subjects, 25 eyes.

Downloaded from iovs.arvojournals.org on 05/16/2022

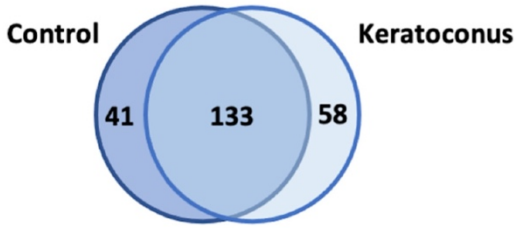


Figure 1. Venn diagram shows the number of unique and overlapping proteins identified in the qualitative proteomic analysis of the tear samples of patients with KC and control subjects.

Data-dependent Workflow Shotgun Analysis of the Tear Proteome

Using micro-LC-MS/MS technology in data-dependent workflow mode, we performed a shotgun analysis to identify the complete profile of proteins expressed in the tear samples of patients with KC and control participants. We identified 232 proteins with a false discovery rate of less than 1%. Of the total identified proteins, 133 were expressed in both groups' samples, 41 were observed only in the control samples, and 58 were identified just in the tears of patients with KC. The list of the 232 proteins identified (expressed in both groups and only found in KC or control samples) is available in supplementary data (Supplementary Table S1), including the main functional protein classification. A Venn diagram (Fig. 1) presents the distribution of proteins identified in both tear profiles.

Protein–Protein Interaction Network and Functional Pathway Enrichment Analysis

The proteomic tear profile of the control group and the KC group was analyzed and categorized. To clarify the differences in protein composition between the two protein profiles, we performed a global categorization of all the proteins found in the shotgun analysis according to the protein class ontology. Moreover, proteins only expressed in the tears of the controls (absent in KC) or only expressed in the KC profile were analyzed separately to detail the differences between the two profiles. For this purpose, we used the PANTHER tool (free access at http://pantherdb.org), inserting the Uniprot code of each protein of interest and selecting the type of GO enrichment analysis categorization.

The proteomic profile of both groups showed a large percentage of immunomodulatory and defense proteins. Moreover, proteins with metabolic, cell signaling, cellular adhesion, binding, transport, transfer or carrier, adaptor, transcriptional regulator, or cytoskeletal activity were also detected (Fig. 2.A_1 and 2.B_1). Figures 2.A_2 and 2.B_2 depicts the main categories in which proteins only expressed in controls or in the KC group were involved. In this regard, tear samples from patients with KC showed a higher percentage of structural, metabolic, and chaperone proteins, expressing transcriptional proteins that were not present in the control group.

In line with the previous GO analysis according to the protein type, we carried out an analysis of the functional interactions over proteins only expressed in the tears of patients with KC, which could evidence critical biological processes in the pathophysiological development of the disease. We used the STRING Interaction Network to explore the protein–protein interactions (Fig. 3).

Keratins (KRT), peptidyl-prolyl cis-trans isomerases (PPIases), and aldehyde-dehydrogenases (ALDH) formed three different clusters in the interaction network analysis. The KRT cluster included 13 cuticular and cytoskeletal keratins, the PPIases cluster was made up of 5 proteins from the PPIase family, and the last cluster consisted of 10 ALDH family members. Supplementary Table S1 presents the complete names and Uniprot codes for each of the proteins.

In silico functional and biological characterization using STRING and FunRich tools determined that proteins only expressed in the KC samples were mainly related with processes such as skin–epidermis development, epithelial cell differentiation, aldehyde cell metabolic processes, and oxidation–reduction processes. The graphs show the differences between the main biological processes (Fig. 4A) and molecular functions (Fig. 4B) related to the proteins of KC and control tear proteome. Oxidative stress, hydrogen peroxide catabolic processes, oxidation–reduction processes, aging, and epidermis development were the most enriched process related to the KC proteome.

In the same way, a molecular function analysis reflected an increase in the KC proteomic profile of proteins related to structural and oxidative stress-related activities (such as antioxidant, peroxiredoxin, and aldehyde dehydrogenase activity) and, conversely, a decrease in zinc- and iron-binding proteins as well as in protease inhibitors.

Semiquantitative Analysis by Spectral Count and ELISA Validations

After the qualitative analysis, we performed a semiquantification to determine proteins with differential expression between groups using the Scaffold Proteome Software. In this way, the dysregulation of 17 proteins in the KC samples was observed in the semiquantification. Of these proteins, 13 showed an overexpression in KC tears, whereas the remaining four were underexpressed. Table 2 lists the proteins with different expressions between the groups.

In the GO analysis targeting differentially expressed proteins, upregulated proteins were related to skin development and cell proliferation processes (KRT type 1 cytoskeletal 9, KRT type II cytoskeletal 1), inflammatory response (S100-A4 protein, Zymogen granule protein 18 homolog B [ZG16B], and lysozyme C), and defense to oxidative stress (peroxiredoxin-1). Instead, downregulated proteins were associated with iron binding and transport, zinc and cooper binding, antioxidant activity, and protease binding and inhibition. Figures 5A and 5B present the main biological functions and processes involving differentially expressed (upregulated or downregulated) proteins.

Four of the most dysregulated proteins were quantified by ELISA analysis as a validation of the semiquantification results shown elsewhere in this article. In this regard, the concentrations of serotransferrin (TF) and albumin (downregulated in KC samples in the semiquantification) and mammaglobin-B and peroxiredoxin-1 (upregulated in KC samples) were measured. Figure 6 presents the ELISA quantification of these proteins in the KC and control groups.

Investigative Ophthalmology & Visual Science

Downloaded from iovs.arvojournals.org on 05/16/2022

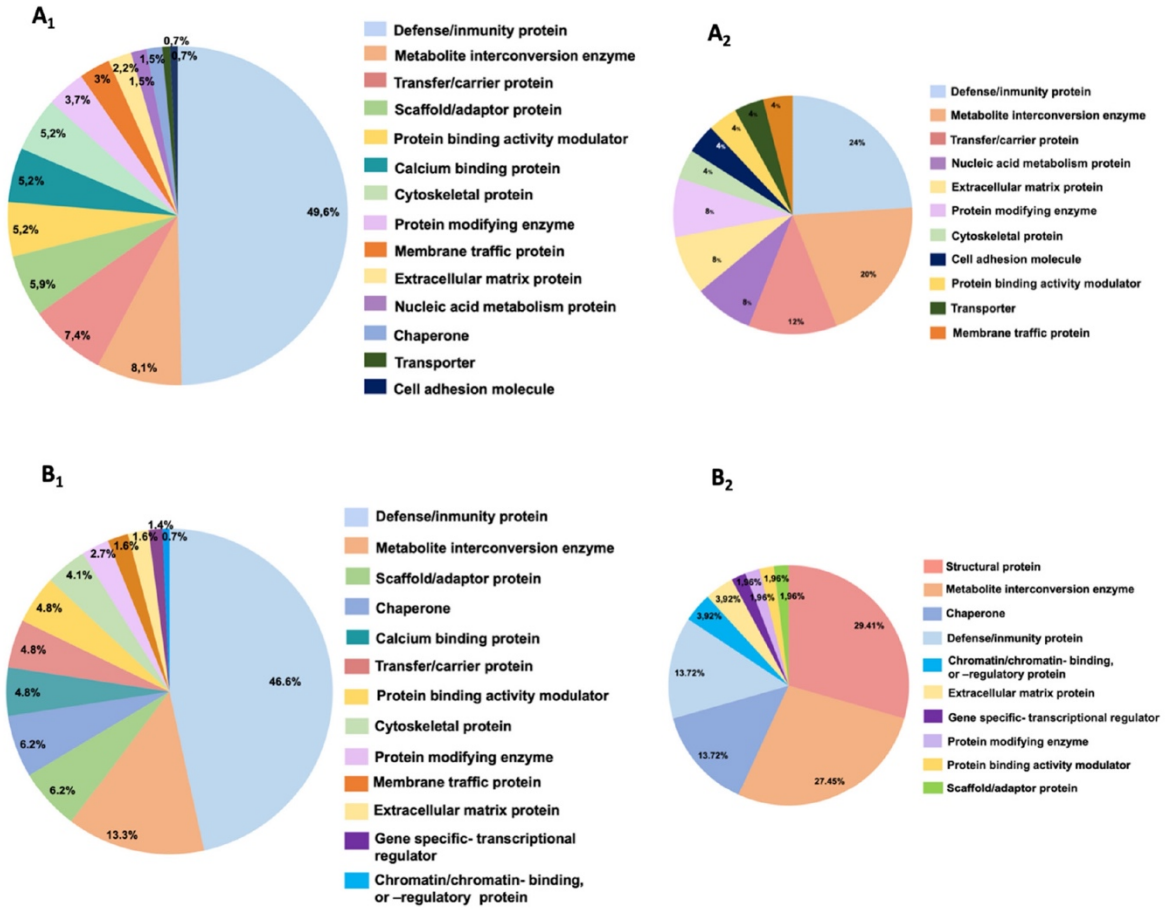


Figure 2. Charts integrated into this figure represent the types of proteins that make up the tear profile of the control ($\mathbf{A_1}$ and $\mathbf{A_2}$) and participants with KC ($\mathbf{B_1}$ and $\mathbf{B_2}$). ($\mathbf{A_1}$) Different types of proteins that composed the control tear profile. ($\mathbf{A_2}$) The categories in which the 41 proteins exclusively found in control participants' tears were involved. ($\mathbf{B_1}$) The types of proteins that composed the proteomic profile of the tear of patients with KC. ($\mathbf{B_2}$) The main categories for the proteins only expressed in the KC tear samples.

Discussion

Shotgun proteomics approaches have achieved great popularity and acceptance in recent years for offering additional insight into the molecular pathways involved in the pathophysiology of many diseases. Quantitative analyses provide valuable information about specific targets; however, qualitative approaches are essential in the search for a global characterization that does not leave behind events overlooked by quantitative limitations. In this way, we performed a shotgun proteomic approach to obtain an even more extensive view of the tear proteomic profile of the patients with KC, as well as to observe the differences regarding the proteomic profile of control subjects. We also performed a semiquantification analysis by spectral count to determine the differentially expressed proteins between groups, and several of the most dysregulated proteomic candidates were validated by ELISA.

In silico tools were used to study the interaction networks and to characterize the biological and functional profile of the proteins. A GO analysis of the tear protein composition of both groups revealed that a large percentage of the identified proteins had immunomodulatory and defense properties, mainly related to the pivotal role of the tear fluid against external pathogens and damage.[30] Metabolic, cell signaling, cellular adhesion, transport, or transfer or carrier were other of the most enriched molecular functions.

The tear composition of patients with KC showed remarkable differences concerning the control group, differing from the control tear proteome in more than one-third of the total proteins identified. An interaction network analysis between proteins expressed only in KC tear samples identified three protein clusters with specific functions. First, we identified a cluster composed of 13 cuticular and cytoskeletal keratins. KRT constitute the main component of the outermost layer of the epidermis and are also expressed in the corneal epithelium cells, but they are not present in tears under normal conditions. Previous studies reported the presence of keratins in the tear samples of patients with KC, relating this finding as a possible consequence of the eyelid filtration owing to ocular rubbing, a frequent habit of the patients with KC.[31] Nevertheless, six keratins that we have identified in the tears of patients with KC are expressed in the corneal epithelium (KRT Hb6, KRT14-KRT17, and KRT19),[32]

Downloaded from iovs.arvojournals.org on 05/16/2022

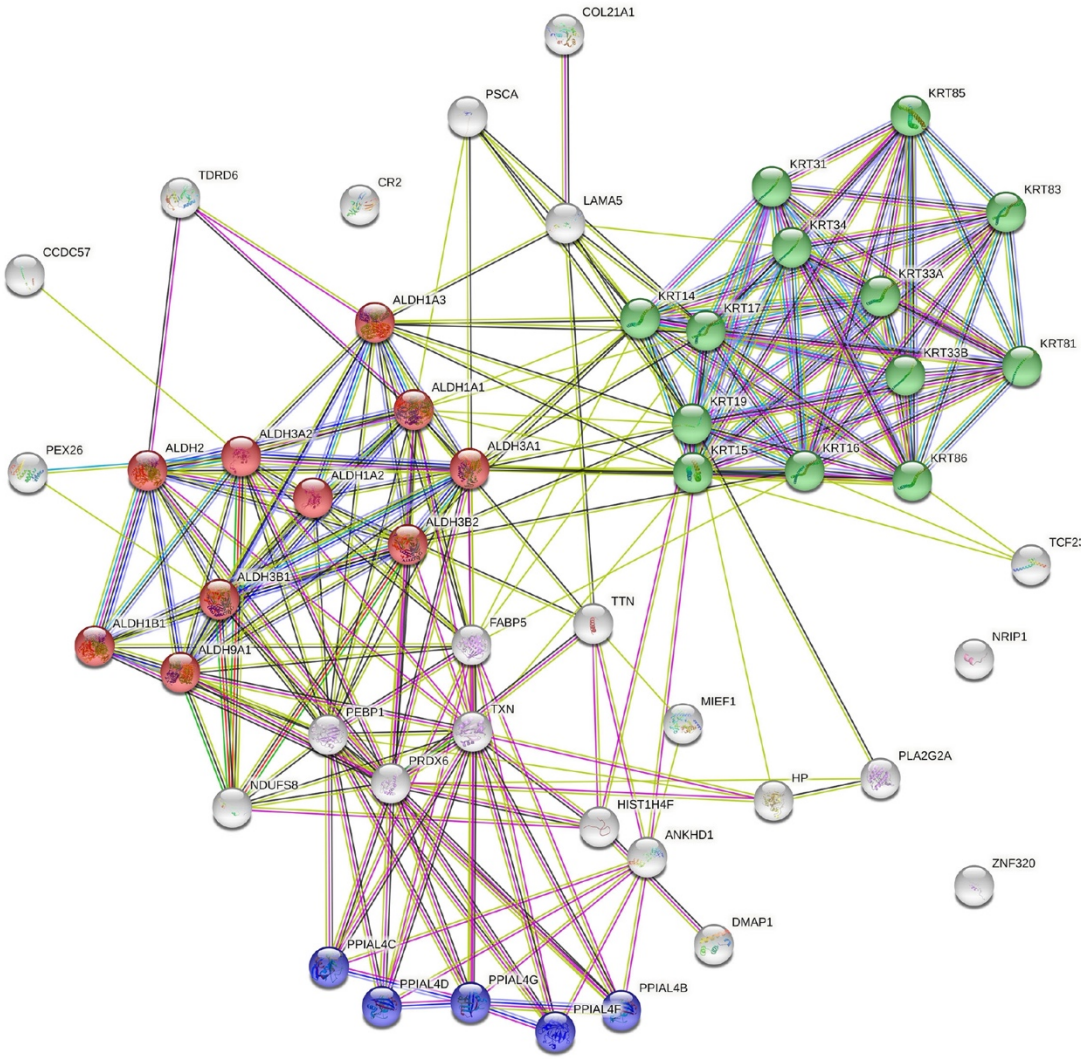


Figure 3. STRING Interaction Network of proteins only identified in KC tears. Three clusters were observed in the interaction network, formed mainly by three types of proteins, so that the green balloons point to the group of cuticular and cytoskeleton keratins, blue balloons to the PPIases, and red balloons refer to the proteins of the aldehyde dehydrogenase family.

suggesting that its presence in the tear fluid may be associated with epithelial cell death and epithelial desquamation, that altogether result in the overall thinning of the cornea seen in KC pathophysiology.

Five members of the PPIases were assembled in the second cluster. PPIases are a protein folding enzymes that catalyzes the cis–trans isomerization of proline imidic peptide bonds in oligopeptides.[33] Besides that, these proteins have and important role in the cellular response to UV radiation as well as in the regulation of UV-induced apoptosis.[34] The involvement of PPIases in the pathogenesis of KC is broadly unknown, but, considering that the cornea is subjected to high levels of UV radiation, PPIases properties as regulators of UV-induced apoptosis could be related to the degeneration and death of the corneal epithelium and stroma cells, as a result of the redox imbalance in the KC cornea.

Finally, an enrichment of processes such as aldehyde oxidation-reduction and response to reactive oxygen species was observed, which was predominantly related to the expression of 10 proteins from the ALDHs in KC tear samples. Owing to their critical role in neutralizing and removing aldehyde radicals, ALDHs are extensively expressed in the corneal tissue, providing important protection against oxidative stress.[35–37] Research about the ALDHs in tears is scarce and there is no previous information about its dysregulation in the tear samples of patients with KC. However, the increased expression of ALDH proteins has been observed in the tear fluid of patients with other ocular surface diseases, such as the dry eye.[38,39]

Despite the lack of data on KC tear samples, the upregulation of ALDH3A1 has also been reported in the KC corneal stroma.[40] Therefore, our results in tear samples are in agreement with these studies and suggest that ALDH expression

Downloaded from iovs.arvojournals.org on 05/16/2022

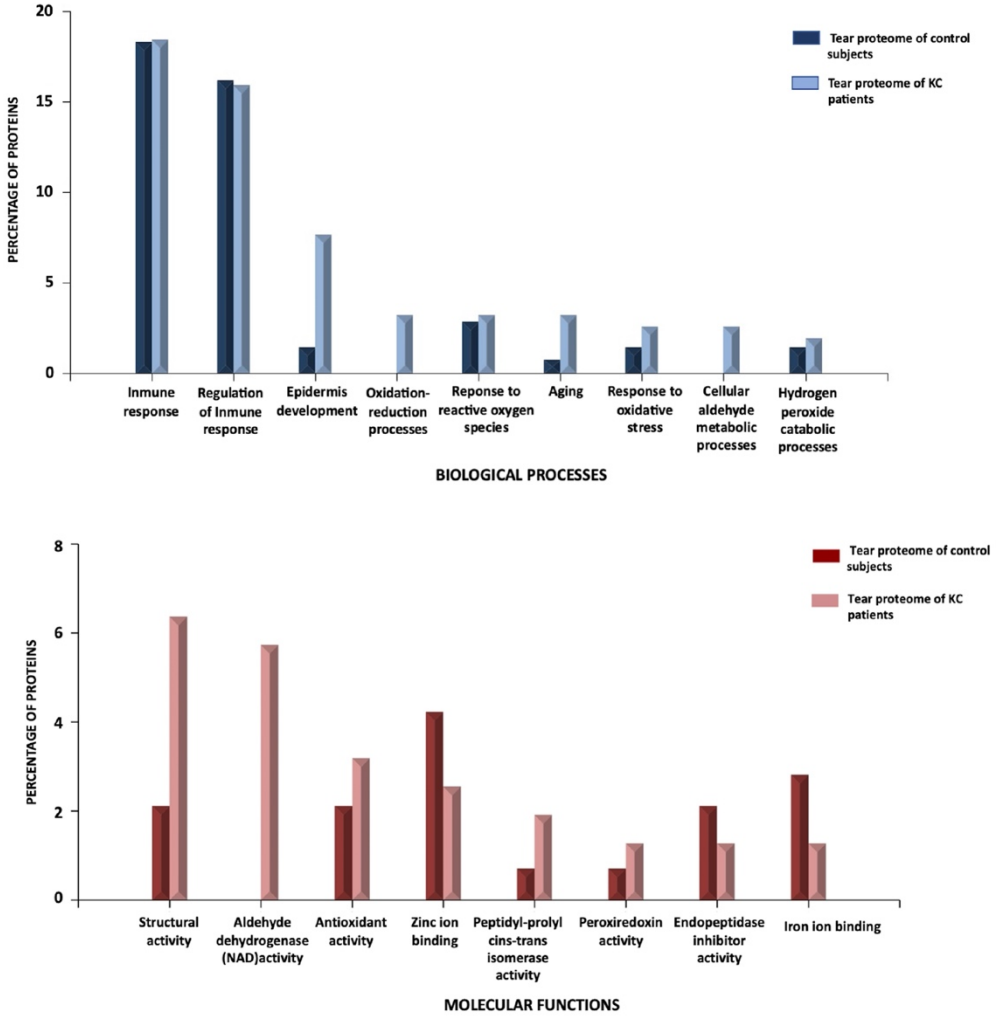


Figure 4. GO enrichment of tear proteomic profile of KC and control subjects, using the FunRich tool. (**A**) The differences in the main biological processes related to the tear proteome of patients with KC and control subjects, and (**B**) the differences in the main molecular functions associated with them. The histograms represent the main categories for each GO term in which proteins were involved ($P < 0.05$). The x axis shows the biological processes and molecular functions, and the y axis shows the percentage of proteins involved in this process compared with the total proteins in the database.

Table 2. Proteins With Different Expression Between KC and Control Samples

Protein Name	Protein Code	*P* Value	FC
Peroxiredoxin-1	Q06830	0.0007	5.8 ↑
ZG16B	Q96DA0	0.024	4.3 ↑
KRT, type I cytoskeletal 9	P35527	0.0066	2.4 ↑
Mammaglobin- B	O75556	0.00063	2.1 ↑
Heat shock protein β- 1	P04792	0.0053	2.0 ↑
Protein S100- A4	P26447	0.026	2.0 ↑
Polymeric immunoglobulin receptor	P01833	0.0027	1.6 ↑
Secretoglobin family 1D member	O95968	0.027	1.5 ↑
Cluster of cystatin-S	P01036	0.039	1.5 ↑
KRT, type II cytoskeletal 1	P04269	0.034	1.4 ↑
Extracellular glycoprotein lacritin	Q9GZZ8	<0.0005	1.4 ↑
Lipocalin-1	P31025	0.0048	1.3 ↑
Lysozyme C	P61626	0.043	1.3 ↑
TF	P02768	<0.0005	0.5 ↓
Serotransferrin	P02787	<0.0001	0.4 ↓
Immunoglobulin constant mu	P01871	0.040	0.2 ↓
Alpha 1-antitrypsin	P01009	0.0042	0.2 ↓

FC shown upregulated proteins if FC > 1 or downregulated proteins if FC < 1.

Size sample: KC = 25 subjects, 25 eyes; controls = 25 subjects, 25 eyes.

may be related to the tear's redox imbalance and the greater demand for oxidative protection in patients with KC' tears and tissues.

In relation to the oxidative stress cycle involving PPIases and ALDHs, semiquantification analysis also revealed the dysregulation of some stress-related proteins. For instance, we observed a five-fold increase of peroxiredoxin-1 expression in KC samples compared with the control samples, which was subsequently validated by ELISA. Peroxiredoxin-1 belongs to the family of ubiquitinated peroxiredoxins and plays a crucial role in cell proliferation as well as in catalyzing peroxide reduction; in this sense, its overexpression has been described as a key factor in the protection against oxidative stress.[41] Changes in the expression of these proteins have been previously observed in some systemic and ocular surface conditions like psoriasis, pterygium and dry eye,[42–44] all of them, on a different etiological basis, characterized by lesions and alterations at the skin or epithelial level. In the case of KC, the overexpression

Investigative Ophthalmology & Visual Science

Downloaded from iovs.arvojournals.org on 05/16/2022

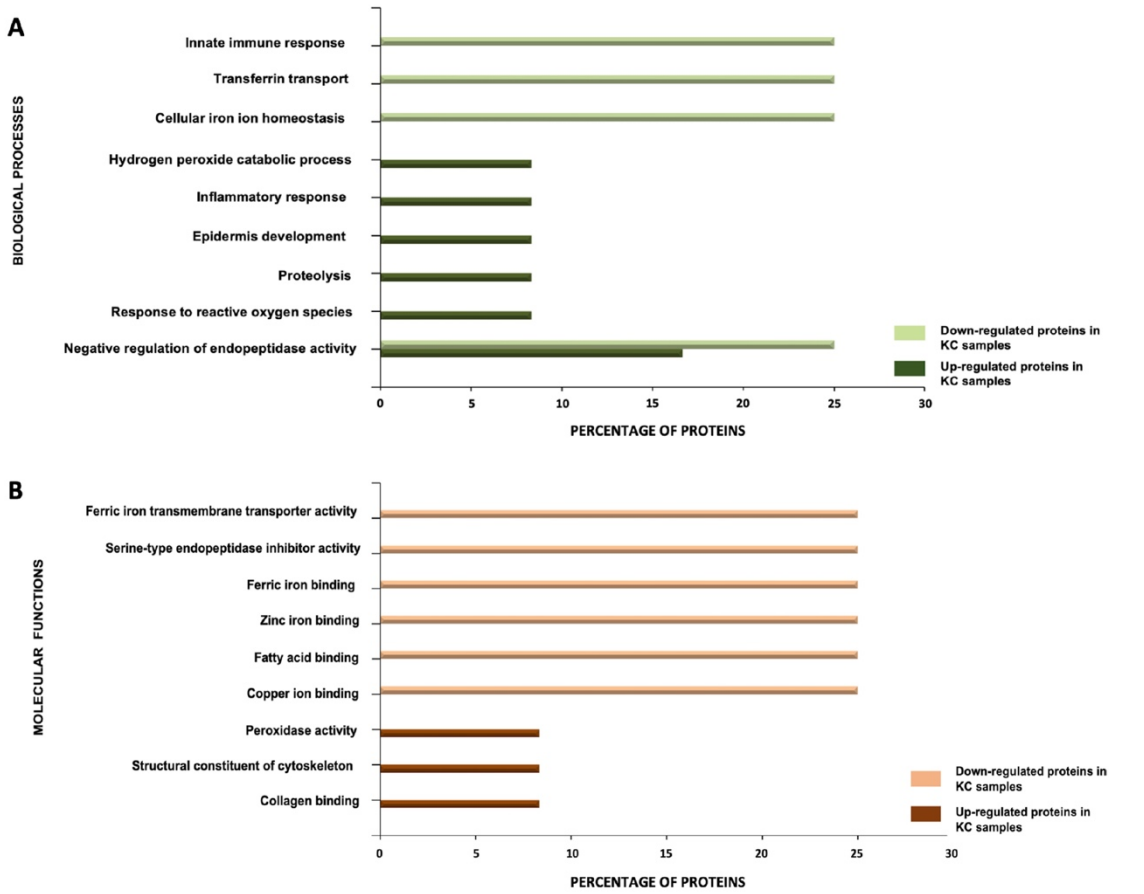


Figure 5. (**A**) Main biological processes associated with dysregulated (upregulated and downregulated) proteins in samples from patients with KC. The graph was made using the Functional Enrichment Analysis tool (FunRich). (**B**) Main molecular functions associated with dysregulated (upregulated and downregulated) proteins in samples from patients with KC. The graph was made using the Functional Enrichment Analysis tool (FunRich). Percentages reflect our study proteins involved in the different biological processes and molecular functions, in relation to the total proteins in the database.

of this protein could be related to its pathophysiology in several ways; first, with increased levels of oxidative stress and consequently with increased antioxidant demand, and, in a complementary pathway to corneal epithelial desquamation and corneal tissue injury. In the same way, heat shock protein beta-1 (HSPB1) was also overexpressed in the KC samples. Enrichment of the HSPs has been described previously in the corneal and tear samples of patients with KC.[45] In particular, HSPB1 comes to the HSP family, which is expressed in a variety of cells and tissues under normal conditions.[46] HSPB1 is inducibly increased in stressful conditions, such as pH shift, heat shock, or hypoxia, to cope with and prevent cell death triggered by different pathways. In addition, HSPB1 has been considered an important regulator of the ferroptosis, a possible pathway of cell death in the pathophysiology of KC.[22,47]

One of the main sources of redox imbalance and increase in reactive species could be the disruption of iron transport and homeostasis in the tear samples of patients with KC. As such, our results, validated by ELISA, evidenced a decreased expression of iron related proteins such as TF and albumin. TF is a glycoprotein with specific functions in the control of iron homeostasis and the prevention of the harmful effects of free unbound iron.[48] Free unbound iron is potentially toxic owing to its ability to produce reactive species by different reactions. Moreover, free iron ions have high susceptibility to accumulate in the tissues by pathways not fully described, contributing to cell damage and tissue injury.[49]

The internalization, storage, and export of cellular iron is controlled in a coordinated manner by very strict mechanisms contributing to the proper maintenance of intracellular iron levels. Therefore, an imbalance in some of the components involved in iron homeostasis (such as lactotransferrin (LTF), TF, and TF receptor, among others) triggers potentially detrimental effects. In addition, a downregulation in TF expression has been reported in inflammatory and iron overload conditions.[49] Our results in tear samples are in agreement with previous studies, in which TF levels are decreased in the corneal stroma of patients with KC; in addition, some TF gene polymorphisms have been linked to the risk of developing KC.[50] Similarly, albumin is an antioxidant protein that can bind weakly to iron ions at high concentrations, contributing to a decrease in the levels of oxidative stress caused by free iron.[51,52] Previous studies

Downloaded from iovs.arvojournals.org on 05/16/2022

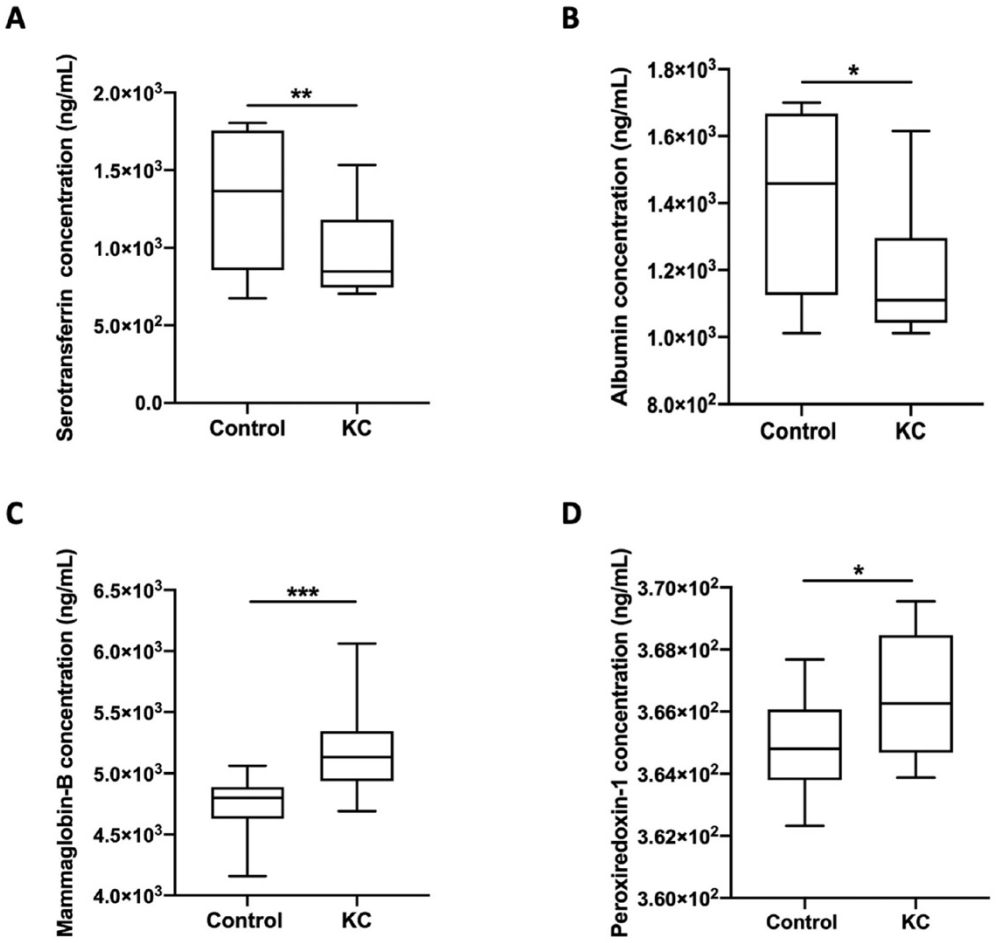


FIGURE 6. Box plot representation of the (**A**) TF, (**B**) albumin, (**C**) mammaglobin-B, and (**D**) peroxiredoxin-1 concentrations (ng/mL) in the tear samples of control and KC participants, measured by ELISA. $^{*}P < 0.05$, $^{**}P < 0.01$, $^{***}P < 0.001$.

have suggested that the depletion of different proteins such as lactoferrin and albumin disrupts iron homeostasis during KC pathophysiology.[22,53,54] In this context, decreased transferrin and albumin expression could indicate a detrimental and chronic oxidative state in corneal tissues, caused by the underexpression of proteins necessary for iron transport and homeostasis.

Ongoing oxidative stress drives the activation of chronic inflammatory pathways that are involved in a wide range of degenerative diseases.[55–57] In this regard, the upregulation of proteins with inflammatory implication as S100-A4 protein, ZG16B, or lysozyme C was observed in the KC tear samples.

S100 proteins have been suggested as molecular targets in ocular surface inflammatory diseases.[58] These proteins are commonly known as alarm- or damage-associated patterns and are frequently exported to the extracellular space to fight oxidative damage and increased stress levels. Apoptosis, inflammation, angiogenesis, and cell differentiation are just a few of the biological processes in which S100-A4 is involved. It plays a fundamental role in the activation of proinflammatory pathways, promoting the release of cytokines, growth factors, and other inflammatory molecules.[59] Specifically, S100-A4 can promote the expression of matrix metalloproteinases,[60] whose overexpression has been observed in KC tissues and tears, linking to the progressive weakening of the corneal tissue. Our results in tears are consistent with previous studies, which showed that elevated levels of S100-A4 in the corneal epithelium of patients with KC, confirming the pathophysiology's inflammatory processes.[61]

In contrast with the S100s, the functions of ZG16B and mammaglobin-B in tears are potentially unknown. A role in maintaining the inflammatory state in cancerous tissues has been postulated for ZG16B,[62] and mammaglobin-B has been proposed as a prognostic biomarker of uterine endometrial cancer.[63] At the tear level, the overexpression of ZG16B has been found in patients with dry eye,[39] and previous studies have suggested the possible involvement of mammaglobin-B in the lipid tear film structure. Moreover, the dysregulation of mammaglobin-B was previously described in the KC tear samples.[64] However, further studies are needed to determine the possible implications of these proteins in the tear fluid and thus in the KC pathophysiology.

Lysozyme C, an essential antimicrobial and inflammatory regulator in the tear fluid, was also upregulated in KC. The

Downloaded from iovs.arvojournals.org on 05/16/2022

dysregulation of this protein was previously observed in tear samples from patients with low-grade KC, suggesting that this protein may play a key role from the early stages of the disease, but its specific function has not yet been clarified.[65]

In addition to proteins involved in the tight circle of oxidative stress and inflammation, the downregulation of alpha 1-antitrypsin and the upregulation of lipocalin 1 were also observed. Thus, the antiproteolytic properties of the first one and the close relationship with lipid peroxidation of the second one could also compromise corneal tissue integrity.

Although this is an innovative study with new findings that shed some light on the biological mechanism on the KC physiopathology, there are also several limitations. We recognize that the small sample size did not for allow the subcategorization of patients according to the severity of KC, so our research was unable to detect the proteins altered at different stages of the disease. As a result, further studies are needed to detail the intertwining events as the disease progresses.

In conclusion, this shotgun analysis revealed that the KC tear proteome differed from the control tear proteome in more than one-third of the total proteins identified. These differences have highlighted the importance of oxidative damage, inflammation, and cell death processes in the KC tear samples. In this sense, the alteration of iron homeostasis and its link with oxidative stress and inflammation could be postulated as contributing factors to the cellular damage characteristic of the disease. Moreover, the discovery of the biological pathways and molecular mechanisms that describe and characterize the pathophysiology of KC brings us closer to an in vitro model, a promising step toward developing diagnostic and therapeutic targets.

Acknowledgments

Funded by a grant from the Spanish Ministry of Economy and Competitiveness (Instituto de Salud Carlos III: PI18/00159); Xunta de Galicia (Consellería de Economía e Industria: IN607A2018/3), and the European Union Program ERFD. M. López-López recognizes the support from Spanish Research Network on Cerebrovascular Diseases INVICTUS PLUS (RD16/0019/0001). Similarly, U. Regueiro acknowledges a Xunta de Galicia (Galician Innovation Agency GAIN: IN606B-2021/001) postdoctoral fellowship. The funders had no role in the study design, data collection and analysis, decision to publish, or preparation of the manuscript.

Disclosure: **M. López-López,** None; **U. Regueiro,** None; **S.B. Bravo,** None; **M.d.P Chantada-Vázquez,** None; **C. Pena,** None; **E. Díez-Feijoo,** None; **P. Hervella,** None; **I. Lema,** None

References

1. Belin MW, Asota IM, Ambrosio R, Khachikian SS. What's in a name: keratoconus, pellucid marginal degeneration, and related thinning disorders. *Am J Ophthalmol*. 2011;152(2):157–162.
2. Maumenee IH. The cornea in connective tissue diseases. *Ophthalmology*. 1978;85(10):1014–1017.
3. Mas Tur V, MacGregor C, Jayaswal R, O'Brart D, Maycock N. A review of keratoconus: diagnosis, pathophysiology, and genetics. *Surv Ophthalmol*. 2017;62:770–783.
4. Ferrari G, Rama P. The keratoconus enigma: a review with emphasis on pathogenesis. *Ocul Surf*. 2020;18(3):363–373.
5. Lema I, Duran J. Inflammatory molecules in the tears of patients with keratoconus. *Ophthalmology*. 2005;112(4):654–659.
6. Balasubramanian SA, Mohan S, Pye DC, Willcox MD. Proteases, proteolysis and inflammatory molecules in the tears of people with keratoconus. *Acta Ophthalmol*. 2012;90(4):303–309.
7. Wojcik K, Kaminska A, Blasiak J, Szaflik J, Szaflik JP. Oxidative stress in the pathogenesis of keratoconus and Fuchs endothelial corneal dystrophy. *Int J Mol Sci*. 2013;14(9):19294–19308.
8. Sorkhabi R, Ghorbanihaghjo A, Taheri N, Ahoor MH. Tear film inflammatory mediators in patients with keratoconus. *Int Ophthalmol*. 2015;35(4):467–472.
9. Yam GH-F, Fuest M, Zhou L, et al. Differential epithelial and stromal protein profiles in cone and non-cone regions of keratoconus corneas. *Sci Rep*. 2019;9(1):2965.
10. Regueiro U, López-López M, Hervella P, Sobrino T, Lema I. Corneal and conjunctival alteration of innate immune expression in first-degree relatives of keratoconus patients. *Graefes Arch Clin Exp Ophthalmol*. 2021;259(2):459–467.
11. Lema I, Sobrino T, Duran JA, Brea D, Diez-Feijoo E. Subclinical keratoconus and inflammatory molecules from tears. *Br J Ophthalmol*. 2009;93(6):820–824.
12. Sobrino T, Regueiro U, Malfeito M, et al. Higher expression of Toll-like receptors 2 and 4 in blood cells of keratoconus patients. *Sci Rep*. 2017;7(1):12975.
13. Regueiro U, Pérez-Mato M, Hervella P, Campos F, Sobrino T, Lema I. Toll-like receptors as diagnostic targets in pellucid marginal degeneration. *Exp Eye Res*. 2020;200:108211.
14. Chwa M, Atilano SR, Reddy V, Jordan N, Kim DW, Kenney MC. Increased stress-induced generation of reactive oxygen species and apoptosis in human keratoconus fibroblasts. *Invest Ophthalmol Vis Sci*. 2006;47(5):1902–1910.
15. Behndig A, Karlsson K, Johansson BO, Brännström T, Marklund SL. Superoxide dismutase isoenzymes in the normal and diseased human cornea. *Invest Ophthalmol Vis Sci*. 2001;42(10):2293–2296.
16. Toprak I, Kucukatay V, Yildirim C, Kilic-Toprak E, Kilic-Erkek O. Increased systemic oxidative stress in patients with keratoconus. *Eye (Lond)*. 2014;28(3):285–289.
17. Balasubramanian SA, Pye DC, Willcox MD. Are proteinases the reason for keratoconus? *Curr Eye Res*. 2010;35(3):185–191.
18. Zhou L, Sawaguchi S, Twining SS, Sugar J, Feder RS, Yue BY. Expression of degradative enzymes and protease inhibitors in corneas with keratoconus. *Invest Ophthalmol Vis Sci*. 1998;39(7):1117–1124.
19. Di Martino E, Ali M, Inglehearn CF. Matrix metalloproteinases in keratoconus – too much of a good thing? *Exp Eye Res*. 2019;182:137–143.
20. Shetty R, Ghosh A, Lim RR, et al. Elevated expression of matrix metalloproteinase-9 and inflammatory cytokines in keratoconus patients is inhibited by cyclosporine A. *Invest Ophthalmol Vis Sci*. 2015;56(2):738–750.
21. Vesaluoma M, Teppo AM, Grönhagen-Riska C, Tervo T. Release of TGF-β1 and VEGF in tears following photorefractive keratectomy. *Curr Eye Res*. 1997;16(1):19–25.
22. López-López M, Regueiro U, Bravo SB, et al. Tear proteomics in keratoconus: a quantitative SWATH-MS analysis. *Invest Ophthalmol Vis Sci*. 2021;62(10):30.
23. Efron N. Grading scales for contact lens complications. *Ophthalmic Physiol Opt*. 1998;18(2):182–186.
24. del Chantada-Vázquez MP, García Vence M, Serna A, Núñez C, Bravo SB. SWATH-MS protocols in human diseases. In: *Methods in Molecular Biology. Vol 2259*. Totowa, NJ: Humana Press Inc; 2021:105–141.
25. Bonzon-Kulichenko E, Pérez-Hernández D, Núñez E, et al. A robust method for quantitative high-throughput analysis of proteomes by 18O labeling. *Mol Cell Proteomics*. 2011;10(1):M110.003335.
26. Perez-Hernandez D, Gutiérrez-Vázquez C, Jorge I, et al. The intracellular interactome of tetraspanin-enriched

Investigative Ophthalmology & Visual Science

Downloaded from iovs.arvojournals.org on 05/16/2022

microdomains reveals their function as sorting machineries toward exosomes. *J Biol Chem*. 2013;288(17):11649–11661.

27. Shevchenko A, Wilm M, Vorm O, Mann M. Mass spectrometric sequencing of proteins from silver-stained polyacrylamide gels. *Anal Chem*. 1996;68(5):850–858.
28. Käll L, Storey JD, Noble WS. Non-parametric estimation of posterior error probabilities associated with peptides identified by tandem mass spectrometry. *Bioinformatics*. 2008;24(16):i42–i48.
29. Nesvizhskii AI, Keller A, Kolker E, Aebersold R. A statistical model for identifying proteins by tandem mass spectrometry. *Anal Chem*. 2003;75(17):4646–4658.
30. Pflugfelder SC, Stern ME. Biological functions of tear film. *Exp Eye Res*. 2020;197:108115.
31. Balasubramanian SA, Wasinger VC, Pye DC, Willcox MD. Preliminary identification of differentially expressed tear proteins in keratoconus. *Mol Vis*. 2013;19:2124–2134.
32. Dyrlund TF, Poulsen ET, Scavenius C, et al. Human cornea proteome: identification and quantitation of the proteins of the three main layers including epithelium, stroma, and endothelium. *J Proteome Res*. 2012;11(8):4231–4239.
33. Schiene-Fischer C. Multidomain peptidyl prolyl cis/trans isomerases. *Biochim Biophys Acta Gen Subj*. 2015;1850(10):2005–2016.
34. McClements L, Annett S, Yakkundi A, Robson T. The role of peptidyl prolyl isomerases in aging and vascular diseases. *Curr Mol Pharmacol*. 2015;9(2):165–179.
35. Voulgaridou GP, Tsochantaridis I, Tolkas C, et al. Aldehyde dehydrogenase 3A1 confers oxidative stress resistance accompanied by altered DNA damage response in human corneal epithelial cells. *Free Radic Biol Med*. 2020;150:66–74.
36. Pappa A, Estey T, Manzer R, Brown D, Vasiliou V. Human aldehyde dehydrogenase 3A1 (ALDH3A1): biochemical characterization and immunohistochemical localization in the cornea. *Biochem J*. 2003;376:615–623.
37. Stagos D, Chen Y, Cantore M, Jester JV, Vasiliou V. Corneal aldehyde dehydrogenases: multiple functions and novel nuclear localization. *Brain Res Bull*. 2010;81(2-3):211–218.
38. Li B, Sheng M, Li J, et al. Tear proteomic analysis of Sjögren syndrome patients with dry eye syndrome by two-dimensional-nano-liquid chromatography coupled with tandem mass spectrometry. *Sci Rep*. 2014;4:5772.
39. Perumal N, Funke S, Pfeiffer N, Grus FH. Proteomics analysis of human tears from aqueous-deficient and evaporative dry eye patients. *Sci Rep*. 2016;6(1):1–12.
40. Joseph R, Srivastava OP, Pfister RR. Differential epithelial and stromal protein profiles in keratoconus and normal human corneas. *Exp Eye Res*. 2011;92(4):282–298.
41. Lovatt M, Adnan K, Kocaba V, Dirisamer M, Peh GSL, Mehta JS. Peroxiredoxin-1 regulates lipid peroxidation in corneal endothelial cells. *Redox Biol*. 2020;30:101417.
42. Bautista-de Lucio VM, López-Espinosa NL, Robles-Contreras A, et al. Overexpression of peroxiredoxin 2 in pterygium. A proteomic approach. *Exp Eye Res*. 2013;110:70–75.
43. Ryu J, Park SG, Park BC, Choe M, Lee KS, Cho JW. Proteomic analysis of psoriatic skin tissue for identification of differentially expressed proteins: up-regulation of GSTP1, SFN and PRDX2 in psoriatic skin. *Int J Mol Med*. 2011;28(5):785–792.
44. Soria J, Acera A, Durán JA, et al. The analysis of human conjunctival epithelium proteome in ocular surface diseases using impression cytology and 2D-DIGE. *Exp Eye Res*. 2018;167:31–43.
45. Zhou L, Yue BY, Twining SS, Sugar J, Feder RS. Expression of wound healing and stress-related proteins in keratoconus corneas. *Curr Eye Res*. 1996;15(11):1124–1131.
46. Georgopoulos C, Welch WJ. Role of the major heat shock proteins as molecular chaperones. *Annu Rev Cell Biol*. 1993;9:601–634.
47. Sun X, Ou Z, Xie M, et al. HSPB1 as a novel regulator of ferroptotic cancer cell death. *Oncogene*. 2015;34(45):5617–5625.
48. Gomme PT, McCann KB, Bertolini J. Transferrin: structure, function and potential therapeutic actions. *Drug Discov Today*. 2005;10(4):267–273.
49. Bartnikas TB. Known and potential roles of transferrin in iron biology. *Biometals*. 2012;25(4):677.
50. Wójcik KA, Synowiec E, Jiménez-García MP, et al. Polymorphism of the transferrin gene in eye diseases: keratoconus and Fuchs endothelial corneal dystrophy. *Biomed Res Int*. 2013;2013:247438.
51. Halliwell B. Albumin—an important extracellular antioxidant? *Biochem Pharmacol*. 1988;37(4):569–571.
52. Roche M, Rondeau P, Singh NR, Tarnus E, Bourdon E. The antioxidant properties of serum albumin. *FEBS Lett*. 2008;582(13):1783–1787.
53. Lema I, Brea D, Rodríguez-González R, Díez-Feijoo E, Sobrino T. Proteomic analysis of the tear film in patients with keratoconus. *Mol Vis*. 2010;16:2055–2061.
54. Balasubramanian SA, Pye DC, Willcox MD. Levels of lactoferrin, secretory IgA and serum albumin in the tear film of people with keratoconus. *Exp Eye Res*. 2012;96(1):132–137.
55. Salzano S, Checconi P, Hanschmann EM, et al. Linkage of inflammation and oxidative stress via release of glutathionylated peroxiredoxin-2, which acts as a danger signal. *Proc Natl Acad Sci USA*. 2014;111(33):12157–12162.
56. Reuter S, Gupta SC, Chaturvedi MM, Aggarwal BB. Oxidative stress, inflammation, and cancer: how are they linked? *Free Radic Biol Med*. 2010;49(11):1603–1616.
57. Hussain T, Tan B, Yin Y, Blachier F, Tossou MCB, Rahu N. Oxidative stress and inflammation: what polyphenols can do for us? *Oxid Med Cell Longev*. 2016;2016:7432797.
58. Tong L, Lan W, Lim RR, Chaurasia SS. S100A proteins as molecular targets in the ocular surface inflammatory diseases. *Ocul Surf*. 2014;12(1):23–31.
59. Ambartsumian N, Klingelhöfer J, Grigorian M. The multifaceted S100A4 protein in cancer and inflammation. *Methods Mol Biol*. 2019;1929:339–365.
60. Elenjord R, Ljones H, Sundkvist E, Loennechen T, Winberg JO. Dysregulation of matrix metalloproteinases and their tissue inhibitors by S100A4. *Connect Tissue Res*. 2008;49(3):185–188.
61. Nielsen K, Vorum H, Fagerholm P, et al. Proteome profiling of corneal epithelium and identification of marker proteins for keratoconus, a pilot study. *Exp Eye Res*. 2006;82(2):201–209.
62. Lu H, Shi C, Liu X, et al. Identification of ZG16B as a prognostic biomarker in breast cancer. *Open Med (Wars)*. 2020;16(1):1–13.
63. Li J, Xu W, Zhu Y. Mammaglobin B may be a prognostic biomarker of uterine corpus endometrial cancer. *Oncol Lett*. 2020;20(5):255.
64. Pannebaker C, Chandler HL, Nichols JJ. Tear proteomics in keratoconus. *Mol Vis*. 2010;16:1949–1957.
65. Yenihayat F, Altıntaş Ö, Kasap M, Akpınar G, Güzel N, Çelik OS. Comparative proteome analysis of the tear samples in patients with low-grade keratoconus. *Int Ophthalmol*. 2018;38(5):1895–1905.

Downloaded from iovs.arvojournals.org on 05/16/2022

Supplementary material & data

Chapter 2

Classification	UniProt Code	Protein Name
	Q9BWW8	Apolipoprotein L6
	P02647	Apolipoprotein A-I
Binding activity	P05090	Apolipoprotein D
	P01877	Inmunoglobulin heavy constant alpha 2
	P01860	Inmunoglobulin heavy constant gamma 3
	P0DOY2	Inmunoglobulin lambda constant 2
	A0A0C4DH41	Inmunoglobulin heavy variable 4-61
	A0A0B4J1X5	Inmunoglobulin heavy variable 3-74
	P01871	Inmunoglobulin heavy contstant mu
	A0A0B4J1V6	Inmunoglobulin heavy variable 3-73
	P06703	Protein S100-A6
	P01876	Inmunoglobulin heavy contstant alpha 1
	Q02548	Paired box protein Pax-5
	Q14D04	Ventricular zone-expressed PH domain-containing protein homolog 1
	P01009	Alpha 1-antitrypsin
	P31949	Protein S100-A11
	P04883	Anexin A1
	A0A0B4JIV0	Inmunoglobulin heavy variable 3-15
	Q02410	Amyloid-beta A4 precursor protein
	P01825	Inmunoglobulin heavy variable 4-59
	Q8IVF4	Dynein heavy chain 10, axonemal
	Q9NQT5	Exosome complex component RRP40
	A0A0B4J1U7	Inmunoglobulin heavy variable 6-1
	B9A064	Inmunoglobulin lambda-like polypeptide 5
	P21817	Ryanodine receptor 1
	P0DP07	Inmunoglobulin heavy variable 4-31
	Q9H6T0	Epithelial splicing regulatory protein 2
	Q8IW93	Rho guanine nucleotide exchange factor 19
	P0DOY3	Inmunoglobulin lambda constant 3
	Q99698	Lysosomal-trafficking regulator
	Q9VJV9	Probable ATP-dependent RNA helicase DDX41
	P01834	Inmunoglobulin kappa constant
	P02774	Vitamin D-binding protein
	Q9Y536	Peptidyl-prolyl cis-trans isomerase A-like 4A
	P0DN37	Peptidyl-prolyl cis-trans isomerase A-like 4G
	P0DN26	Peptidyl-prolyl cis-trans isomerase A-like 4F
	F5H284	Peptidyl-prolyl cis-trans isomerase A-like 4D
	A0A0B4J2A2	Peptidyl-prolyl cis-trans isomerase A-like 4C
	A0A075B759	Peptidyl-prolyl cis-trans isomerase A-like 4E
	P26447	Protein S100- A4
	P00738	Haptoglobin
	O75556	Mammaglobin-B
	P02768	Albumin
	Q01469	Fatty acid-binding protein, epidermal
	Q7Z412	Peroxisome assembly protein 26
	P20023	Complement receptor type 2
	Q96DA0	Zymogen granule protein 18 homolog B

O60522	Tudor domain-containing protein 6
P62805	Histone H4
P48552	Nuclear receptor-interacting protein 1
P20061	Transcobalamin-1
P41002	Cyclin-F
P80188	Neutrophil gelatinase- associated lipocalin
P01824	Inmunoglobulin heavy variable 4-39
P01780	Inmunoglobulin heavy variable 3-7
P17931	Galectin-3
Q08AD1	Calmodulin-regulated spectrin-associated protein 2
P0DP08	Inmunoglobulin heavy variable 4-38-2
A0A0B4J1Y9	Inmunoglobulin heavy variable 3-72
P0DP06	Inmunoglobulin heavy variable 4-30-4
P01857	Inmunoglobulin heavy constant gamma 1
P29353	SHC-transforming protein 1
P01742	Inmunoglobulin heavy variable 1-69
Q9UIQ6	Leucyl-cystinyl aminopeptidase
Q13620	Cullin-4B
P02765	Alpha-2-HS-glycoprotein
P06331	Inmunoglobulin heavy variable 4-34
Q0IIN9	Putative uncharacterized protein ZNF252P-AS1
O43653	Prostate stem cell antigen
A2RUB1	Meiosis-specific coiled-coil domain-containing protein MEIOC
Q9H6Q4	Cytosolic iron-sulfur assembly component 3
Q99811	Paired mesoderm homeobox protein 2
P54821	Paired mesoderm homeobox protein 1
Q08380	Galectin-3-binding protein
Q13421	Mesothelin
Q9BSU1	Phagosome assembly factor 1
Q8WZ42	Titin
P04433	Immunoglobulin kappa variable 3-11
A0A0A0MRZ8	Immunoglobulin kappa variable 3D-11
Q9NQG6	Mitochondrial dynamics protein MID51
P01706	Immunoglobulin lambda variable 2-11
P01709	Immunoglobulin lambda variable 2-8
P01721	Immunoglobulin lambda variable 6-57
P01703	Immunoglobulin lambda variable 1-40
P01699	Immunoglobulin lambda variable 1-44
A0A075B6J9	Immunoglobulin lambda variable 2-18
P30086	Phosphatidylethanolamine-binding protein 1
Q32P28	Prolyl 3-hydroxylase 1
Q02410	Amyloid-beta A4 precursor protein-binding family A member 1
A0A0B4J1X5	Immunoglobulin heavy variable 3-74
A0A075B6I0	Immunoglobulin lambda variable 8-61
P01742	Immunoglobulin heavy variable 1-69
P01780	Immunoglobulin heavy variable 3-7
P02766	Transthyretin
P01034	Cystatin-C

Q8IVF4	Dynein axonemal heavy chain 10
P01619	Inmunoglobulin Kappa variable 3-20
P31025	Lipocalin-1
Q9UGM3	Deleted in malignant brain tumors 1 protein
P61769	Beta-2-microglobulin
P06702	Protein S100-A9
P01591	Immunoglobulin J chain
P05109	Protein S100-A8
P01615	Inmunoglobulin Kappa variable 2D-28
P01614	Inmunoglobulin Kappa variable 2D-40
A0A087WW87	Inmunoglobulin Kappa variable 2-40
A0A075B6P5	Inmunoglobulin Kappa variable 2-28
A0A0A0MRZ7	Inmunoglobulin Kappa variable 2D-26
A0A075B6S2	Inmunoglobulin Kappa variable 2D-29
A0A075B6S6	Inmunoglobulin Kappa variable 2D-30
P62937	Peptidyl-prolyl cis-trans isomerase A
P06312	Inmunoglobulin kappa variable 4-1
P01624	Inmunoglobulin kappa variable 3-15
A0A0C4DH55	Inmunoglobulin kappa variable 3D-7
P59666	Neutrophil defensin 3
P59665	Neutrophil defensin 1
P04211	Inmunoglobulin lambda variable 7-43
A0A075B6I9	Inmunoglobulin lambda variable 7-46
P01700	Inmunoglobulin lambda variable 1-47
Q04917	14-3-3 protein eta
P61981	14-3-3 protein gamma
P63104	14-3-3 protein zeta/delta
P62258	14-3-3 protein epsilon
P31947	14-3-3 protein sigma
P31946	14-3-3 protein beta/alpha
P27348	14-3-3 protein theta
P06310	Inmunoglobulin Kappa variable 2-30
A0A0B4J1Y9	Inmunoglobulin heavy variable 3-72
Q13296	Mammaglobin-A
Q9Y6N7	Roundabout homolog 1
A2NJV5	Inmunoglobulin kappa variable 2-29
A0A0C4DH68	Inmunoglobulin kappa variable 2-24
P0DP09	Inmunoglobulin kappa variable 1-13
P04432	Inmunoglobulin kappa variable 1D-39
P04430	Inmunoglobulin kappa variable 1-16
P01611	Inmunoglobulin kappa variable 1D-12
P01602	Inmunoglobulin kappa variable 1-5
P01601	Inmunoglobulin kappa variable 1D-16
P01599	Inmunoglobulin kappa variable 1-17
P01597	Inmunoglobulin kappa variable 1-39
A0A0C4DH73	Inmunoglobulin kappa variable 1-12
A0A0C4DH72	Inmunoglobulin kappa variable 1-6
A0A0C4DH69	Inmunoglobulin kappa variable 1-9
A0A0C4DH67	Inmunoglobulin kappa variable 1-8
A0A0B4J2D9	Inmunoglobulin kappa variable 1D-13

	A0A075B6S5	Inmunoglobulin kappa variable 1-27
	A0A075B6S4	Inmunoglobulin kappa variable 1D-17
	A0A0C4DH24	Inmunoglobulin kappa variable 6-21
	A0A0A0MT36	Inmunoglobulin kappa variable 6D-21
	Q8NDX1	PH and SEC7 domain-containing protein 4
	Q8NBS9	Thioredoxin domain-containing protein 5
	Q8IYW2	Cilia- and flagella-associated protein 26
	Q9UJV9	Probable ATP-dependent RNA helicase DDX41
	Q8N4P6	Leucine-rich repeat-containing protein 71
	Q99459	Cell division cycle 5-like protein
	Q86WR0	Coiled-coil domain-containing protein 25
Catalytic activity	P6174	Triosephosphate isomerase
	Q06830	Peroxiredoxin-1
	P01009	Alpha 1- antitrypsin
	P04083	Annexin A1
	Q5T241	Tau-tubulin kinase 1
	P12273	Prolactin-inducible protein
	Q8IVF4	Dynein heavy chain 10, axonemal
	P06733	Alpha-enolase
	Q9VJV9	Probable ATP- dependent RNA helicase DDX41
	Q99935	Opiorphin prepropeptide
	P41002	Cyclin-F
	P03973	Antileukoproteinase
	P30044	Peroxiredoxin-5, mitochondrial
	P09211	Glutathione S- transferase P
	P17540	Creatine kinase S- type, mitochondrial
	Q13825	REVERSED Methylglutaconyl- coA hydratase, mitochondrial
	P61626	Lysozyme C
	P12532	Creatine kinase U, type, mitochondrial
	Q13620	Cullin-4B
	P02765	Alpha-2-HS-glycoprotein
	P05091	Aldehyde dehydrogenase, mitochondrial
	P00352	Retinal dehydrogenase 1
	P47895	Aldehyde dehydrogenase family 1 member A3
	P30837	Aldehyde dehydrogenase X, mitochondrial
	O94788	Retinal dehydrogenase 2
	P51648	Aldehyde dehydrogenase family 3 member A2
	P49189	4-trimethylaminobutyraldehyde dehydrogenase
	P48448	Aldehyde dehydrogenase family 3 member B2
	P43353	Aldehyde dehydrogenase family 3 member B1
	P30838	Aldehyde dehydrogenase, dimeric NADP-preferring
	P10599	Thioredoxin
	O00217	NADH dehydrogenase [ubiquinone] iron-sulfur protein 8, mitochondrial
	P49189	4-trimethylaminobutyraldehyde dehydrogenase
	P14555	Phospholipase A2, membrane associated
	Q8N118	Cytochrome P450 4X1
	P60174	Triosephosphatase isomerase
	P51648	Fatty aldehyde dehydrogenase

	P30041	Peroxiredoxin-6
Enzyme regulator activiy	P04083	Annexin A1
	Q8IW93	Rho guanine nucleotide Exchange factor 19
	Q99935	Opiorphin preprepeptide
	P41002	Cyclin-F
	P03973	Antileukoproteinase
	P02765	Alpha-2-HS-glycoprotein
	Q9GZZ8	Extracellular glycoprotein lacritin
	Q9NPF5	DNA methyltransferase 1-associated protein 1
	Q7RTU1	Transcription factor 23
	P04792	Heat Shock Protein beta-1
	Q66K66	Transmembrane protein 198
	Q2TAC2	Coiled-coil domain-containing protein 57
	A2RRD8	Zinc finger protein 320
	Q6ZWK6	Transmembrane protease serine 11F
	Q9BS26	Endoplasmic reticulum resident protein 44
	P01833	Polymeric immunoglobulin receptor
	P01036	Cystatin-S
	Q16378	Proline-rich protein 4
	O95968	Secretoglobin family 1D member 1
	Q6S8J3	POTE ankyrin domain family member E
	P0CG38	POTE ankyrin domain family member I
	A5A3E0	POTE ankyrin domain family member F
	P01037	Cystatin-SN
	Q8N7U6	EF-hand domain-containing family member B
	Q15345	Leucine-rich repeat-containing protein 41
Transporter activity	P02787	Serotransferrin
	Q96JE7	Protein transport protein Sec16B
	P02788	Lactotransferrin
	P25311	Zinc-alpha-2- glycoprotein
	P19652	Alpha-1-acid glycoprotein 2
	P02763	Alpha-1-acid glycoprotein 1
Structural activity	P13646	Keratin, type I cytoskeletal 13
	P04264	Keratin, type II cytoskeletal 1
	P13645	Keratin, type I cytoskeletal 10
	P35908	Keratin, type II cytoskeletal 2 epidermal
	P35527	Keratin,type I cytoskeletal 9
	Q14533	Keratin, type II cuticular Hb1
	P78385	Keratin, type II cuticular Hb3
	O43790	Keratin, type II cuticular Hb6
	O76011	Keratin, type I cuticular Ha4
	Q14525	Keratin, type I cuticular Ha3-II
	O76009	Keratin, type I cuticular Ha3-I
	P08779	Keratin, type I cytoskeletal 16
	P02533	Keratin, type I cytoskeletal 14
	Q04695	Keratin, type I cytoskeletal 17
	P19012	Keratin, type I cytoskeletal 15
	P08727	Keratin, type I cytoskeletal 19
	Q15323	Keratin, type I cuticular Ha1

P78386	Keratin, type II cuticular Hb5
O15230	Laminin subunit alpha-5
Q96P44	Collagen alpha-1(XXI) chain
Q6W4X9	Mucin-6
P68133	Actin, alpha skeletal muscle
P68032	Actin, alpha cardiac muscle 1
P63261	Actin, cytoplasmic 2
P62736	Actin, aortic smooth muscle
P60709	Actin, cytoplasmic 1
P63267	Actin, gamma-enteric smooth muscle

This table shows the total number of proteins identified in the tear samples. In red appear those proteins only identified in the samples keratoconus patients and in blue those that were only observed in the tears of the controls.
Size Sample: KC= 25 subjects, 25 eyes; Controls= 25 subjects, 25 eyes.

Introduction

Justification and hypothesis

Objectives

Methodology

WP1. Clinical & molecular study of KC disease

WP2. Clinical & molecular study of KC at-risk stages

WP3. Human LF as a therapeutic strategy for KC

Discussion

Conclusions

WP2. Clinical & molecular study of KC at-risk stages

The inheritance background of the KC disease has long been recognized, and a positive family history of KC, particularly within first-degree relatives, emerges as the most significant risk factor for disease development. On this basis, **Chapters 3** and **4** aim to answer the central hypothesis of the project, focused on elucidating the tear biomarkers and biological mechanisms underlying the susceptibility to KC development in a sensitive cohort of young offspring of KC patients. Firstly, in **Chapter 3**, the tear fluid of 80 KC offspring and 42 control subjects was analyzed using LC-MS/MS, trying to get closer to the molecular drivers underlying the KC susceptibility and potentially explaining the corneal biomechanical weakening observed in early KC development. On the other hand, a cohort study approach was adopted in **Chapter 4**, including a three-year follow-up of the offspring of KC patients to assess the evolution of the biomechanical, tomographical, and molecular markers associated with the disease development and progression.

Chapter 3

Tear proteomic analysis from offspring of keratoconus patients: new insights into corneal biomechanical weakness & disease risk stages

Maite López-López[1,2*], Uxía Regueiro[1,2*#], Susana B. Bravo[3], Carmen Pena[3], Yaiza Pastoriza[1,2], Mercedes Conde-Amboage[4,5], Pablo Hervella[6], Isabel Lema[1,2,7#].

[1] Corneal Neurodegeneration Group (RENOIR). Clinical Neurosciences Research Laboratory (LINC), Health Research Institute of Santiago de Compostela (IDIS), Santiago de Compostela, Spain.
[2] Department of Surgery and Medical-Surgical Specialties. Faculty of Optics and Optometry, University of Santiago de Compostela, Santiago de Compostela, Spain.
[3] Proteomic Unit, Health Research Institute of Santiago de Compostela (IDIS), Santiago de Compostela, Spain.
[4] Department of Statistics, Mathematical Analysis and Optimization. Universidade de Santiago de Compostela (USC). Spain.
[5] CITMAga, 15782 Santiago de Compostela, Spain.
[6] Neuroimaging and Biotechnology Group (NOBEL). Clinical Neurosciences Research Laboratory (LINC), Health Research Institute of Santiago de Compostela (IDIS), Santiago de Compostela, Spain.
[7] Instituto Galego de Oftalmoloxía (INGO), Complexo Hospitalario Universitario de Santiago (CHUS), Santiago de Compostela, Spain.

* These authors have equally contributed to this work as First Authors.
# These authors have equally contributed to this work as Corresponding Authors.

Under-review in: *American Journal of Ophthalmology* [Submission code: AJO-24-1970]

Journal Citations Reports (JCR) Metrics: 2023
Journal Impact Factor (JIF): 4.1
JIF Quartile: Q1
Journal Position: 12/ 95 *Ophthalmology*
JCR abbreviation: Am J Ophthalmol
ISSN: 0002-9394

Author contribution. López-López M contributed to the conceptualization, design, formal analysis and investigation, writing and original draft preparation of this manuscript.

Abstract

Purpose: To analyze the tear proteome of keratoconus offspring (O-KC) and assess the molecular drivers underlying corneal biomechanical weakening at KC-risk stages.

Design: Cross-sectional study.

Participants: 80 O-KC young participants and 42 controls without KC family history.

Methods: O-KC eyes were classified as low, moderate, and high-risk of KC development (O-KC-LR, O-KC-MR, O-KC-HR) based on the corneal biomechanical behavior. Tear fluid was extracted using Schirmer strips, and the proteomic profile was mapped using LC-MS/MS. Bioinformatic tools were used to determine the dysregulated protein's biological implications. Sensitivity-specificity of each biomarker for differentiating between controls and O-KC groups was determined. Logistic regression analysis (LRA) identified the optimal subset of predictors for modelling the probability of each biomechanical condition.

Results: 29% O-KC eyes showed moderate/high alterations in corneal biomechanical behavior. 15 proteins were dysregulated in the tear samples of O-KC groups compared to controls ($p<0.05$). Dysregulated proteins were associated with oxidative stress, cell-adhesion, cytoskeleton organization, and mechanotransduction paths such as RhoA, mTOR, or E-cadherin/N-cadherin signaling. LRA determined three protein panels with high sensitivity-specificity for discriminating between the control and O-KC groups with different biomechanical risk.

Conclusions: This study revealed new promising biomarkers for early detection of KC-risk. Oxidative stress and cell structural alterations appear to begin long before the onset of clinical signs and even before biomechanical alterations can be detected with current clinical tools. Understanding how an initial imbalance of oxidative stress affects cellular mechanobiology is critical in developing new therapeutic strategies for early KC treatment.

Background

Keratoconus (KC) is a chronic and degenerative corneal ectasia that leads to severe visual impairment because of irregular astigmatism and high-order aberrations arising from weakening, thinning, and protrusion of the corneal tissue.[1] KC affects all ethnicities and both sexes, begins in adolescence (or even earlier), and progresses up to 30-40 years of age, causing a strong impact throughout the patient's life.[2] KC evolves quickly in its early stages and becomes especially aggressive in its development in children, lengthening the period of disease progression and often reaching considerably more severe stages than when it develops in late adolescence.[3-5] Approximately 28% of children with KC present an already advanced state of the disease at the time of diagnosis,[6] so an early diagnosis and a careful follow-up are crucial to providing adequate management of the disease, as, in advanced stages, KC remains one of the most frequent causes of corneal keratoplasty with limited visual recovery.[7]

Advances in new methods for imaging and assessing corneal biomechanics have provided new insights into the alterations at this level in the KC cornea. In this sense, currently, it is considered that the molecular and morphological changes that occur in the corneal tissue cells during KC development modify the focal biomechanical properties of the corneal structure, promoting tissue protrusion (under the influence of the intraocular pressure) and leading to tomographic and topographic alterations.[8,9] This mismatch of corneal biomechanical properties before corneal tissue protrusion has underlined the importance of studying the biomechanical response in early clinical screening for KC, evidencing a paradigm shift for prediction and early diagnosis of corneal ectasias. In this way, the increase of corneal biomechanics examination in recent years, as well as the existence of studies with large cohorts of participants, has allowed the development of indexes that discriminate with high sensitivity and specificity the biomechanical alterations that could lead to the onset of corneal ectasias, as is the case of the Corvis Biomechanical Index (CBI, Corvis® ST).[8]

Although the etiology of KC is still not entirely clear, previous studies have concluded that genetic predisposition and mechanical-environmental factors play an essential role in its development.[10]

The genetic background of KC has long been suggested based on the higher concordance of the disease in monozygotic over dizygotic twins,[11,12] as well as on its association with other genetic syndromes such as Down's syndrome,[13,14] Ehlers-Danlos syndrome,[15] or Leber's congenital amaurosis.[16,17] Besides that, family history of KC is consistently identified as the leading risk factor for the disease development, supported by the fact that up to 26% of KC patients have a family history of this disease,[18] and by the higher prevalence (15 to 67 times higher risk of disease development) in the first-degree KC relatives compared to the general population.[19] Recent studies showed that this prevalence

could be even higher in first-degree pediatric relatives, and disease progression could be more severe when two or more relatives with KC coexist within the family.[20,21] For these reasons, first-degree pediatric relatives of KC patients are considered the most vulnerable population for disease development.

In the search for KC biomarkers that help to understand the pathophysiological mechanisms involved in its onset and progression, tear fluid has become an attractive and accessible source that could be useful in identifying the molecular targets responsible for KC development.[22-26] Tear biomolecules are susceptible to alterations caused by ocular diseases, providing valuable information about the corneal tissue conditions and playing a key role in detecting biochemical changes that may lead the disease development.

Currently, the diagnosis of KC is based on clinical and imaging tools that provide evidence of the signs of manifest disease but without the ability to predict the predisposition for KC onset and progression. Based on the vulnerability of first-degree pediatric KC relatives to develop the disease, as well as the potential of tear fluid as a biomarker source, the purpose of this study is to analyze quantitatively and qualitatively the tear proteome of young KC offspring using micro–liquid chromatography coupled to tandem mass spectrometry, trying to get closer to the molecular drivers underlying the alterations in corneal biomechanical properties at at-risk stages of KC and to provide new insights into the molecular mechanisms involved in the earlier stages of the disease.

Methods

Study design and participants

Study design

The present study was performed following the principles of the Declaration of Helsinki of the World Medical Association. The Ethics Committee for Clinical Research of Galicia (2019/623) authorized the ophthalmologic clinical protocol and the extraction of biological samples. In terms of study design, this was a cross-sectional study, involving a total of 42 eyes from 42 control subjects without a family history of KC and 160 eyes from 80 young offspring of KC patients. All participants underwent an ophthalmological exam with tear fluid extraction. Each participant was informed and asked to sign a consent form outlining the study objectives, ophthalmologic procedures, biological sample collection, and potential undesirable events associated with biological sample extraction.

The same researchers performed all the tests. The ophthalmologic protocol included anamnesis, biomechanical and tomographic corneal imaging studies, as well as ocular health examination. Tear fluid was collected using Schirmer strips.

Full anamnesis collected data about age, sex, ocular history, medical history (allergies, asthma, rhinitis, atopic dermatitis, or any condition relevant to the present study), and

family history of corneal ectasia or other ocular conditions. A biomechanical scan was performed to determine the corneal dynamic behavior in response to an air-puff pulse. Corvis® ST (Oculus, Wetzlar, Germany) was used for the biomechanical assessment. Detailed information on all the Corvis® ST parameters studied is available in **Supplementary Methods S1**. Tomographic imaging was carried out using Pentacam® HR (Oculus, Wetzlar, Germany). The Pentacam® HR parameters evaluated are listed in **Supplementary Methods S1**.

Ocular health examination was based on an in-depth biomicroscopic assessment to identify any signs on the ocular surface related to KC disease or other ocular conditions.

Study subjects

This study involved 122 subjects divided into two groups: 42 control participants without a family history of KC (control group) and 80 young offspring of patients diagnosed with KC (O-KC, study group). All participants were recruited at the Instituto Galego de Oftalmoloxía (INGO) in Santiago de Compostela, Spain. As for ethnicity, all participants in this study reported European ancestry. Inclusion criteria for the study group included having a parent diagnosed with clinical KC, supported by slit-lamp examination and corneal topography and tomography exams. Participants belonging to this group could have corneal features consistent with normal corneal architecture, subclinical state of KC, or clinical manifestation of the disease. Moreover, the eyes of the offspring of KC patients were classified according to the CBI biomechanical index,[8] resulting in a total of 3 study subgroups: 1. Eyes of offspring of KC patients with low-risk of ectasia development [CBI<0.25] (O-KC-LR group), 2. Eyes of offspring of KC patients with moderate risk of ectasia development [CBI 0.25-0.50] (O-KC-MR group), and 3. Eyes of offspring of KC patients with a high risk of ectasia development [CBI >0.50] (O-KC-HR group).

About the control group, the main inclusion criteria were not having any family member diagnosed with subclinical or clinical KC (neither first-degree relatives nor any other relatives), having normal clinical parameters without alterations in the tomographic evaluation, not presenting irregular astigmatism that could suggest a subclinical state of the disease, as well as showing a CBI-index in the biomechanical exam lower than 0.25 (indicative of a low risk of ectasia development).

Common inclusion requirements for all groups were conjunctival hyperemia <2 (Nathan Efron scale[27]), Schirmer test >15mm in 5 minutes (min), and at least 5 days without contact lenses, artificial tears, or eye drops. Previous surgical intervention in the anterior segment, active ocular or systemic inflammation, current treatment with local or systemic anti-inflammatory drugs, and/or other corneal or systemic diseases (renal, hepatic, hematologic diseases, or solid tumors) were the exclusion criteria for both groups.

Sample extraction and processing

Sample extraction

The tear samples were extracted by placing a Schirmer strip (Tear Strips, Contacare Ophthalmics & Diagnostics, Gujarat, India) over the lower eyelid about 3mm from the lateral edge. One strip was used for each eye and was removed when the sample reached 15mm on the Schirmer scale (9µL), remaining in contact with the ocular surface for less than 5 min. Tear samples were extracted under suitable environmental conditions and without previous administration of drugs, artificial tears, or vital dyes. Immediately after collection, the strips were frozen and stored at −80°C until their analysis.

Sample preparation

Firstly, Schirmer's strips were thawed for 30min at room temperature (RT). For protein extraction, Schirmer strips were cut and incubated for 1 hour (h) at RT in a 100µL solution of 100 mM ammonium bicarbonate. Samples were centrifuged for 20 min at 13000 x g, and the supernatant was placed in a new Eppendorf tube. 600µL of acetone was added to the new Eppendorf with the supernatant and incubated at -20ºC overnight. Subsequently, samples were centrifuged for 20 min at 13000 x g and the supernatant was removed. To evaporate the acetone, the pellet was dried at RT for 1h, and then 100µL of miliQ water was added. Finally, an RC-DC kit (Bio-Rad Laboratories, Hercules, CA, USA) was used to measure the amount of protein.[28]

Mass spectrometry analysis by TripleTOF 6600 LC-MS/MS system

Tryptic digestion

As for trypsin digestion, 100µg of protein from the tear fluid of 202 samples (42 controls and 160 O-KC) was loaded on a 10% SDS-PAGE gel. The run was interrupted when the front penetrated 3mm into the resolving gel.[29,30] The protein band was visualized, with Sypro-Ruby fluorescent staining (Lonza, Porriño, Pontevedra, Spain), excised, and processed for in-gel tryptic digestion as previously described by our group.[25,26] For more details, see **Supplementary Methods S2.**

Data-dependent Acquisition (DDA) & Protein quantification by SWATH-MS (Sequential Window Acquisition for All Theoretical Mass Spectra)

Both proteomic analysis qualitative (DDA) and quantitative (SWATH-MS) were performed as described previously by our group.[25,26] Detailed protocols are available in Supplementary Methods S2. Mass spectrometry proteomics data have been deposited to the ProteomeXchange Consortium via the PRIDE partner repository with the dataset identifier PXD049296.

Protein interaction networks and Gene Ontology analysis

Bioinformatic tools were used to determine the protein-protein interaction networks and to perform the Gene Ontology enrichment analysis (GO). Via STRING program (free access at https://string-db.org) we created the protein interaction maps. FunRich (Function Enrichment Interaction Analysis) and Shiny GO 0.80 (free access at http://bioinformatics.sdstate.edu/go/) software were used to explore the main biological pathways, molecular functions, and cellular components related to dysregulated proteins. Venn diagram was created with the Bioinformatics &Evolutionary Genomics tool (free access at http://bioinformatics.psb.ugent.be/webtools/Venn/). We use UniProt codes for the search and identification of each protein.

ELISA validation

Lactoferrin (LF), cofilin-1 (CFL1), and calpain-1 catalytic subunit (CAPN1) expression were measured in human tears using commercial kits of Enzyme-Linked Immunosorbent Assays (ELISA) from FineTests® [LF (ELISA kit catalog number EH0396); CFL1 (ELISA kit catalog number EH1788); CAPN1 (ELISA kit catalog number EH2761)]. All assays were carried out following the manufacturer's protocols and were optimized and used with the following dilution factors: 1:100000 for LF, 1:50 for CFL1, and 1:5 for CAPN1. Tear samples were assayed in duplicate, and mean expression values were reported as ng/mL. Curve Expert 1.4 and Microsoft Excel were used for curve and data analysis, and graphs were performed using GraphPad Prism 8.0 (San Diego, CA, USA).

Construction of the regression model

Proteins with the highest discriminatory power for the detection of corneal biomechanical changes and KC-risk were analyzed using logistic regression (LRA) to develop the simplest predictive models for each condition. For model fitting and coefficient estimation, we applied a backward method using the Akaike's information criterion (AIC) as a global selection criterion. Considering the following logit formula, those proteins that achieved LRA statistical significance were selected and gathered to define the different protein panels.

$$\pi(x_1, x_{2\ldots}, x_n) = \frac{e^{x'\beta}}{1+e^{x'\beta}}$$

$$^{*}x'\beta = \beta_0 + \beta_1 x_1 + \beta_2 x_2 \ldots + \beta_n x_n$$

* Being n the number of parameters with the best area under the curve (AUC) values determined in the ROC analysis.

Statistical analysis

GraphPad Prism 8.0 (San Diego, CA, USA) and R 4.3.3 software was used for statistical analysis. Categorical variables were represented as percentages. Continuous quantitative variables with a normal distribution were expressed with the mean [± standard deviation (SD)], and variables with a non-normal distribution were presented as median [interquartile range]. D'Agostino test was performed to confirm the normality of the

quantitative variables. Bivariate comparisons were performed using the chi-square test (for categorical variables), and parametric (t-student) or non-parametric (u-Mann-Whitney/ Kruskal-Wallis) test for continuous variables according to their normality. $p \leq 0.05$ value was considered statistically significant in all tests. Fold Change (FC) was calculated as the ratio of the difference between the protein expression (expressed as normalized area) in each group analyzed. FC indicates upregulation if FC >1 or downregulation if FC <1. Dysregulated proteins were analyzed by LRA, fitted using a backward elimination method and AIC as a global selection criterion to identify the optimal subset of predictors to model the probability of the different biomechanical conditions. Receiver operating characteristic (ROC) curve analysis was performed using the pROC R package to determine the potential role of combining dysregulated proteins as biomarkers for discriminating alterations in corneal biomechanical properties and detecting the risk associated with having a parent diagnosed with KC. Cut-off values were selected looking for a good balance between sensitivity and specificity.

Results

Assessment of tear proteomics based on biomechanical screening

In this study, we included 42 healthy eyes from 42 control subjects (61.1% male; mean age, 13.15 ± 4.87 years) and 160 eyes from 80 offspring of KC patients (O-KC, 55.4% male; mean age, 12.31 ± 3.30 years). To focus on the potential biomechanical alterations of the corneal tissue in the study group, the O-KC eyes were classified into three groups of risk for ectasia development according to the CBI index. Based on this, a total of 42 eyes were included in the control group, 114 eyes in the O-KC-LR group [CBI<0.25], 28 eyes in the O-KC-MR group [CBI 0.25-0.50], and 18 eyes in the O-KC-HR group [CBI>0.50]. **Table 1** shows the analysis of demographic (age, sex) and main clinical data associated to KC (presence of allergic disease, ocular itching and eye rubbing) between controls and O-KC groups.

Table 1. Analysis of demographics and main clinical variables of controls and O-KC groups

Variable	Control	O-KC-LR	$p^{\#1}$	O-KC-MR	$p^{\#2}$	O-KC-HR	$p^{\#3}$	$p^{\dagger}$	$p^{\ddagger}$	$p^{\S}$
Age [years]	13±4.8	10±3	0.106	13±2.5	0.248	16±3.7	0.070	**0.010**	**0.002**	0.348
Sex [% male]	61.0	54.2	0.656	53.3	0.757	66.7	1.000	1.000	0.707	0.678
Allergic disease [%]	14.7	18.2	0.774	30.0	0.159	30.0	0.355	0.212	0.417	1.000
Ocular itching [%]	14.5	24.5	0.165	24.0	0.350	18.8	0.703	0.958	0.759	1.000
Eye rubbing [%]	12.9	24.5	0.107	20.0	0.687	18.8	0.687	0.795	0.759	1.000

Sample size: Control (control group, n= 42 eyes, 42 control subjects), **O-KC-LR** (eyes of offspring of KC patients with low risk of ectasia development, n=114 eyes, 59 offspring of KC patients), **O-KC-MR** (eyes of offspring of KC patients with moderate risk of ectasia development, n=28 eyes, 19 offspring of KC patients), **O-KC-HR** (eyes of offspring of KC patients with a high risk of ectasia development, n=18 eyes, 10 offspring of KC patients). **[#1] O-KC-LR compared to control [#2] O-KC-MR compared to control [#3] O-KC-HR compared to control [†] O-KC-LR compared to O-KC-MR [‡] O-KC-LR compared to O-KC-HR [§] O-KC MR compared to O-KC-HR**

No differences were observed for sex, history of allergic disease, eye itching or ocular rubbing between groups. When comparing the age factor between the O-KC groups, moderate-high risk groups had higher ages than the low-risk group.

About biomechanical metrics, **Table 2** shows the comparisons of the Corvis® ST parameters among control eyes, O-KC-LR eyes, O-KC-MR eyes, and O-KC-HR eyes. As expected, the main statistical differences were observed in the O-KC-MR and O-KC-HR groups compared to the remaining ones, concerning the stiffness data (SP-A1), the viscoelastic properties [DARatio max (1mm), DARatio max (2mm), and IR)], as well as the parameters linked to corneal pachymetry and pachymetric progression (CCT_C, ARTh and Pachy Slope).

Table 2. Analysis of Corvis® ST biomechanical parameters in control and O-KC groups.

Parameters	Control	O-KC-LR	p#1	O-KC-MR	p#2	O-KC-HR	p#3	p†	p‡	p§
bIOP [mmHg]	15.60±2.04	16.24±1.88	0.096	15.84±2.20	0.933	15.15±1.90	0.223	0.364	0.053	0.290
A1T [ms]	7.37±0.29	7.44±0.25	1.000	7.24±0.24	0.504	7.18±0.22	0.189	**0.005**	**0.003**	1.000
A1V [m/s]	0.14±0.01	0.14±0.01	1.000	0.15±0.02	1.000	0.16±0.02	0.652	0.711	**0.049**	1.000
A2T [ms]	22.15±0.40	22.01±0.32	0.813	22.20±0.47	1.000	22.14±0.30	1.000	0.205	1.000	1.000
A2V [m/s]	-0.27±0.03	-0.25±0.06	0.992	-0.27±0.03	1.000	-0.28±0.03	1.000	1.000	0.470	1.000
HCT [ms]	17.29±0.67	17.29±0.52	1.000	17.44±'.52	1.000	17.25±0.54	1.000	1.000	1.000	1.000
DAmax [mm]	1.12±0.10	1.06±0.09	**0.048**	1.12±0.10	1.000	1.15±0.09	1.000	**0.041**	**0.006**	1.000
HCDA [mm]	0.91±0.10	0.86±0.09	0.169	0.91±0.09	1.000	0.97±0.10	0.334	0.064	**0.001**	0.643
A1DLL [mm]	2.38±0.11	2.36±0.16	1.000	2.32±0.12	0.251	2.32±1.14	1.000	0.504	1.000	1.000
A2DLL [mm]	3.33±0.65	3.21±0.67	1.000	3.01±0.86	1.000	2.85±0.83	0.350	1.000	0.659	1.000
HCDLL [mm]	6.68±0.50	6.43±0.40	0.054	6.57±0.27	1.000	6.61±0.43	1.000	1.000	1.000	1.000
PD [mm]	5.06±0.27	4.92±0.27	0.155	5.09±0.19	1.000	5.11±0.26	1.000	**0.035**	0.059	1.000
DARatio max [1mm]	1.52±0.05	1.52±0.05	0.685	1.55±0.04	**0.039**	1.58±0.05	**0.000**	**0.004**	**0.000**	0.073
DARatio max [2mm]	4.04±0.36	4.06±0.32	0.885	4.36±0.30	**0.013**	4.76±0.52	**0.000**	**0.002**	**0.000**	**0.004**
IR [mm^{-1}]	7.87±1.06	7.79±0.87	0.657	8.43±0.82	0.294	9.37±1.27	**0.000**	**0.022**	**0.000**	**0.018**
MaxInverseRadius [mm^{-1}]	0.165±0.02	0.162±0.06	0.783	0.173±0.01	0.515	0.188±0.02	0.133	0.285	0.052	0.348
CCT_C [µm]	550±27	549±33	1.000	519±24	**0.001**	509±30	**0.001**	**0.001**	**0.001**	1.000
ARTh	691±194	685±161	0.860	529±137	**0.002**	418±108	**0.000**	**0.000**	**0.000**	0.276
Pachy Slope [µm]	34±10	34±8	0.963	38±7	0.791	44±12	**0.000**	0.355	**0.000**	0.152
SP-A1	99±14	100±12	0.578	87±13	**0.007**	81±13	**0.000**	**0.000**	**0.000**	1.000
CBI	0.12±0.09	0.17±0.14	1.000	0.50±0.10	**0.001**	0.75±0.22	**0.001**	**0.001**	**0.001**	**0.001**
SSI	0.91±0.14	0.99±0.15	0.205	0.96±0.14	1.000	0.83±0.15	0.671	1.000	**0.000**	0.062

Sample size: Control (control group, n= 42 eyes), **O-KC-LR** (eyes of offspring of KC patients with low risk of ectasia development, n=114 eyes), **O-KC-MR** (eyes of offspring of KC patients with moderate risk of ectasia development, n=28 eyes), **O-KC-HR** (eyes of offspring of KC patients with a high risk of ectasia development, n=18 eyes).

Parameters: bIOP [biomechanical corrected intraocular pressure], **A1T/A2T** [first/second applanation time], **A1V/A2V** [first/second applanation velocity], **HCT** [time to the highest concavity], **DAmax** [deformation amplitude], **HCDA** [deflection amplitude at highest corneal concavity], **A1DLL/A2DLL** [first/second applanation deflection length], **HCDLL** [highest concavity deflection length], **PD** [peak distance at the highest concavity], **DAratio max 1mm** [maximum deformation amplitude ratio at 1mm], **DAratio max 2mm** [deformation amplitude ratio max 2mm], **IR** [integrated radius], **Max Inverse Radius** [maximum inverse radius], **CCT_C** [central corneal thickness by Corvis], **ARTh** [Ambrósio Relational Thickness horizontal], **Pachy Slope** [changes of corneal thickness from the corneal center to the periphery], **SP-A1** [stiffness parameter at the first applanation], **CBI** [Corvis Biomechanical Index], and **SSI** [Stress-Strain Index].

#1 O-KC-LR compared to control #2 O-KC-MR compared to control #3 O-KC-HR compared to control † O-KC-LR compared to O-KC-MR ‡ O-KC-LR compared to O-KC-HR § O-KC MR compared to O-KC-HR.

More precisely, in comparison to the control and O-KC-LR groups, both O-KC-MR and O-KC-HR showed a decrease in the SP-A1 parameter (indicating a decrease in the stiffness of the corneal tissue), a decrease in the central pachymetry and pachymetric progression (evidencing lower corneal thickness and alterations in corneal thickness progression), and an increase in the values of the DARatio max (at 1 and 2mm) and IR (pointing out an increase in the central corneal deformation amplitude) (*p values are given in **Table 2**).

After measuring the corneal biomechanical properties, a tomographic examination was performed to determine the morphology of the corneal tissue in the different groups. Predictably, O-KC-HR showed significant differences in all the parameters studied, including corneal curvature, asymmetry, pachymetry, anterior and posterior elevation, and KC-risk indexes (p=0.001) in comparison to the control and O-KC-LR groups. The O-KC-MR group only showed significant differences in the parameters related to pachymetry and pachymetric progression (CCT_P, MTP, and ARTmax) and KC indexes (BAD-D, TBI), in comparison to the control group (p=0.001, p=0.001, p=0.015, and, p=0.040, p=0.001; respectively) and in comparison to the O-KC-LR group (p=0.001, p=0.001, p=0.003, and p=0.028, p=0.001; respectively); evidencing a decrease in the corneal thickness and higher values for the KC tomographical detection indexes. When comparing the O-KC-MR and O-KC-HR groups, there were no differences in terms of pachymetry, whereas all other parameters evaluated, including corneal curvature, asymmetry, anterior and posterior corneal elevation, and KC indexes, were significantly higher in the O-KC-HR group (p=0.001). **Table 3** presents the tomographic data and the comparisons between groups

Table 3. Analysis of Pentacam® HR tomographic parameters in control and O-KC groups.

Parameters	Control	O-KC-LR	$p^{\#1}$	O-KC-MR	$p^{\#2}$	O-KC-HR	$p^{\#3}$	$p^{\dagger}$	$p^{\ddagger}$	$p^{\S}$
PDC [D]	42.78±1.27	43.28±1.22	0.187	43.01±1.28	0.645	45.97±5.52	**0.001**	0.537	**0.001**	**0.001**
K1 [D]	42.23±1.27	42.70±1.24	0.089	42.34±1.25	0.768	44.13±2.75	**0.001**	0.252	**0.001**	**0.001**
K2 [D]	43.34±1.24	43.57±1.52	0.444	43.39±1.32	0.909	46.00±3.46	**0.001**	0.591	**0.001**	**0.001**
Kmax [D]	43.89±1.36	44.12±1.26	0.522	43.99±1.50	0.802	48.79±6.76	**0.001**	0.790	**0.001**	**0.001**
I-S asymm [D]	-0.25±0.60	-0.05±0.57	0.274	0.07±0.87	0.193	1.42±2.69	**0.001**	0.562	**0.001**	**0.001**
ARTmax [µm]	459±69	455±91	0.916	401±68	**0.015**	287±79	**0.001**	**0.003**	**0.001**	**0.001**
CCT_P [µm]	546±26	549±33	0.637	519±25	**0.001**	510±30	**0.001**	**0.001**	**0.001**	0.301
MTP [µm]	542±24	546±32	0.550	516±24	**0.001**	504±30	**0.001**	**0.001**	**0.001**	0.191
AE [µm]	3.00[2.00]	3.00[2.00]	0.685	3.00[3.00]	0.791	4.50[7.00]	**0.001**	0.965	**0.001**	**0.001**
PE [µm]	6.00[6.25]	6.50[8.00]	0.461	7.00[11.00]	0.659	11.00[29.75]	**0.001**	0.898	**0.001**	**0.001**
BAD-D	0.75[0.56]	0.75[0.84]	0.800	1.31[0.90]	**0.040**	1.94[1.96]	**0.001**	**0.028**	**0.001**	**0.001**
TBI	0.00[0.12]	0.08[0.18]	0.169	0.20[0.47]	**0.001**	0.65[0.85]	**0.001**	**0.001**	**0.001**	**0.001**

Sample size: Control (control group, n= 42 eyes), **O-KC-LR** (eyes of offspring of KC patients with low risk of ectasia development, n=114 eyes), **O-KC-MR** (eyes of offspring of KC patients with moderate risk of ectasia development, n=28 eyes), **O-KC-HR** (eyes of offspring of KC patients with a high risk of ectasia development, n=18 eyes).

Parameters: PDC [corneal central power], **K1** [keratometry in the flattest meridian], **K2** [keratometry in the steeper meridian], **Kmax** [maximum dioptric power], **I-S asymm** [inferior-superior dioptric asymmetry], **ARTmax** [maximum Ambrósio Relational Thickness], **CCT_P** [central corneal thickness by Pentacam], **MTP** [minimum thickness point], **AE/PE** [anterior and posterior surfaces elevation], **BAD-D** [total deviation value], and **TBI** [Tomographic and Biomechanical Index].

[#1] O-KC-LR compared to control [#2] O-KC-MR compared to control [#3] O-KC-HR compared to control [†] O-KC-LR compared to O-KC-MR [‡] O-KC-LR compared to O-KC-HR [§] O-KC MR compared to O-KC-HR

Regarding the proteomic study, the SWATH-MS results were analyzed keeping the O-KC group classification based on the biomechanical response of the corneal tissue and including the control group. The purposes were to identify proteins with differential expression between the control and O-KC groups, as well as target proteins associated with corneal biomechanical alterations. In this way, we observed the dysregulation of 15 proteins in the tear fluid of O-KC groups, including the under expression of Lipocalin-1 (LCN-1), Lactoferrin (LF), Argininosuccinate synthase (ASS1), Cofilin-1 (CFL1), Calpain-1 catalytic subunit (CAPN1), Superoxide Dismutase [Cu-Zn] (SOD1), Ezrin (EZR), Peroxiredoxin-1 (PRDX1), Hemopexin (HPX), α-actinin 4 (ACTN4), and Actin cytoplasmic 2 (ACTG); and the overexpression of Keratin type II cytoskeletal 5 (KRT5),

Apolipoprotein A-I (APOA1), Protein S100 A11 (S100A11), and Apolipoprotein A-II (APOA2). Comparative expression of the above-mentioned dysregulated proteins is shown in **Table 4,** described as the ratio between the average normalized area of quantification for each protein per group. The FC expressed indicates the under- or over-expression of each protein in the study groups versus the control.

Table 4. Comparative analysis of the proteins with differential expression between the control and each study group.

Dysregulated proteins	O-KC-LR vs control FC (p-value)	O-KC MR vs control FC (p-value)	O-KC HR vs control FC (p-value)	p†	p‡	p§
LCN-1	0.363 **(p<0.0001)**	0.198 **(p<0.0001)**	0.139 **(p=0.0004)**	**0.008**	0.075	0.506
LF	0.532 **(p<0.0001)**	0.475 **(p=0.004)**	0.458 **(p<0.0001)**	0.793	0.197	0.599
ASS1	0.691 **(p=0.004)**	0.621 **(p=0.013)**	0.834 (p=0.378)	0.816	0.075	0.189
CFL1	0.711 **(p=0.0004)**	0.626 **(p<0.0001)**	0.759 **(p=0.027)**	0.217	0.700	0.112
CAPN1	0.723 **(p=0.004)**	0.773 **(p=0.006)**	0.618 **(p=0.010)**	0.392	0.204	0.891
SOD1	0.782 **(p=0.025)**	0.475 **(p=0.0009)**	0.388 **(p=0.001)**	**0.050**	**0.021**	0.461
EZN	0.787 **(p=0.040)**	0.519 **(p=0.0017)**	0.584 **(p=0.043)**	**0.015**	0.227	0.464
PRDX1	0.840 (p=0.124)	0.609 **(p=0.0007)**	0.546 **(p=0.0014)**	**0.020**	**0.036**	0.867
HPX	0.867 (p=0.089)	0.733 **(p=0.006)**	0.691 **(p=0.0006)**	0.116	**0.016**	0.473
ACTN4	0.930 (p=0.322)	0.723 **(p=0.030)**	0.881 (p=0.250)	0.189	0.606	0.575
ACTG	0.989 (p=0.551)	0.786 **(p=0.039)**	0.862 (p=0.287)	**0.030**	0.235	0.440
KRT5	0.999 (p=0.553)	1.017 (p=0.844)	1.480 **(p=0.0008)**	0.775	**0.001**	**0.011**
APOA1	1.255 **(p=0.047)**	1.496 **(p=0.028)**	1.421 (p=0.076)	0.170	0.105	0.758
S100A11	1.764 **(p=0.007)**	1.803 **(p=0.010)**	1.719 **(p=0.050)**	0,533	0.902	0.801
APOA2	2.551 **(p=0.0001)**	2.106 **(p<0.0001)**	2.583 **(p=0.002)**	0.116	0.663	0.441

Sample size: Control (control group, n= 42 eyes), **O-KC-LR** (eyes of offspring of KC patients with low risk of ectasia development, n=114 eyes), **O-KC-MR** (eyes of offspring of KC patients with moderate risk of ectasia development, n=28 eyes), **O-KC-HR** (eyes of offspring of KC patients with a high risk of ectasia development, n=18 eyes).

Proteins: **LCN-1** (Lipocalin-1), **LF** (Lactoferrin), **ASS1** (Argininosuccinate synthase), **CFL1** (Cofilin-1), **CAPN1** (Calpain-1 catalytic subunit), **SOD1** (Superoxide Dismutase), **EZR** (Ezrin), **PRDX1** (Peroxiredoxin-1), **HPX** (Hemopexin), **ACTN4** (α-actinin 4), **ACTG** (Actin, cytoplasmic 2), **KRT5** (Keratin, type II cytoskeletal 5), **APOA1** (Apolipoprotein A-I), **S100A11** (Protein S100 A11), **APOA2** (Apolipoprotein A-II).

† **O-KC-LR compared to O-KC-MR** ‡ **O-KC-LR compared to O-KC-HR** § **O-KC MR compared to O-KC-HR.**

FC indicates upregulation if FC >1 or downregulation if FC <1.

Most of these proteins showed differential expression in all groups of O-KC compared to the control, even in those cases without detectable alterations in corneal biomechanical properties (O-KC-LR). In general, as biomechanical indexes revealed an increased risk of developing corneal ectasia, the expression of these proteins maintained a trend toward its under/overexpression. **Figure 1** shows the representation of the median [interquartile range] of the MLR-normalized SWATH-MS area of each dysregulated protein.

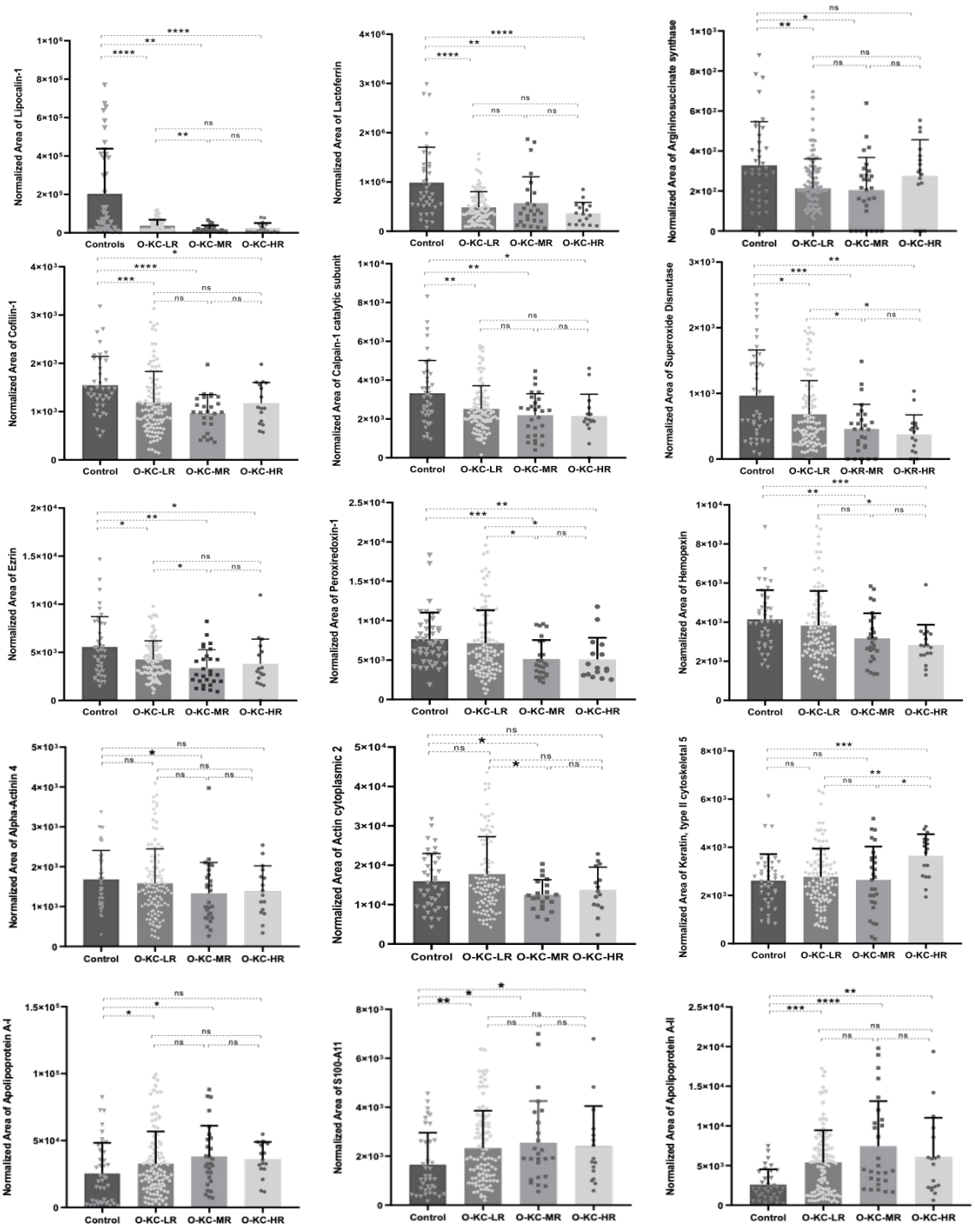


Figure 1. Representation of the median [interquartile range] MLR-normalized SWATH-MS area of the 15 dysregulated proteins in the tear samples of O-KC groups. The normalized area was obtained from the SWATH method for each sample.
Sample size: Control (control group, n= 42 eyes), **O-KC-LR** (eyes of offspring of KC patients with low risk of ectasia development, n=114 eyes), **O-KC-MR** (eyes of offspring of KC patients with moderate risk of ectasia development, n=28 eyes), **O-KC-HR** (eyes of offspring of KC patients with a high risk of ectasia development, n=18 eyes).
*$p < 0.05$, **$p < 0.01$, ***$p < 0.001$, ****p<0.0001, ns: non-significant.

LCN-1, LF, and SOD1 were the most under-expressed proteins in O-KC samples, showing their lower expression in the moderate and high risk of ectasia development groups. ASS1 was under-expressed in the O-KC-LR and O-KC-MR groups compared to controls; however, no differences in its expression were observed among the O-KC groups. Subsequently, CFL1, CAPN1, EZN, PRDX1, and HPX had lower expression in all O-KC groups compared to controls; and, while the differences between O-KC-LR, O-KC-MR, and O-KC-HR groups were not as marked, there was a general trend towards its lower expression as the risk of KC increased. ACTN4 and ACTG, two proteins belonging to the actin family, showed their minimum expression in O-KC-MR; moreover, although significant differences, the median value of these proteins in the O-KC-HR group was still lower than the control and O-KC-LR values.

Regarding overexpressed proteins, statistical analysis revealed that KRT5 substantially increased its expression in the O-KC-HR group, remaining stable (similar to control levels) in the low-risk and moderate-risk groups. APOA1 was up-regulated in all O-KC groups, but the increase was statistically significant only for the low-risk (O-KC-LR) and moderate-risk (O-KC-MR) groups compared to controls. Finally, S100A11 and APOA2 were the two proteins with the highest expression in the O-KC groups compared to controls, and this significant overexpression was stable in all the groups independently of the differences in the biomechanical response.

In order to assess whether the age differences observed between the O-KC groups could influence over dysregulated proteins, potential correlations between these parameters were evaluated. As a result, no relationship was observed between any deregulated protein and the age factor ($p>0.05$ in all study correlations).

Relative to the functional implications of dysregulated proteins, **Figure 2** shows the main biological pathways, molecular functions, and cellular components related to the down and up-regulated proteins in O-KC groups. Down-regulation of several proteins essential for oxidative protection (LCN-1, LF, SOD1), as well as for cell morphology and migration, cell-cell adhesion, F-actin crosslinking, and actin cytoskeletal organization (CFL1, CAPN1, EZN, ACTN4, and ACTG), underlined the possible impact on paths such as ROS degradation, CDC42 signaling events, focal adhesion kinase signaling events, E-cadherin and N-cadherin signaling paths, and RhoA or mTOR pathways [**Figure 2, A_1**]. In this way, a high percentage of these proteins were related to structural activities at the cytoskeleton level [**Figure 2, A_2**]; and the cellular component analysis showed their membership to focal adhesions, cell-substrate junctions, anchoring junctions, and the actin cytoskeleton [**Figure 2, A_3**].

Regarding overexpressed proteins, up-regulation of APOA1 and APOA2 emphasized the enrichment of lipidic processes such as lipoprotein metabolism or lipid digestion, mobilization, and transport. In the same way, the main anatomical entities of the up-regulated proteins were related to lipidic and lipoprotein particles and complexes.

Additionally, the overexpression of S100A11 was associated with the enhancement of structural processes such as integrin-linked kinase signaling. **Figures 2 B_1**, **B_2** and **B_3** depict the biological paths, molecular functions, and cellular components associated with overexpressed proteins.

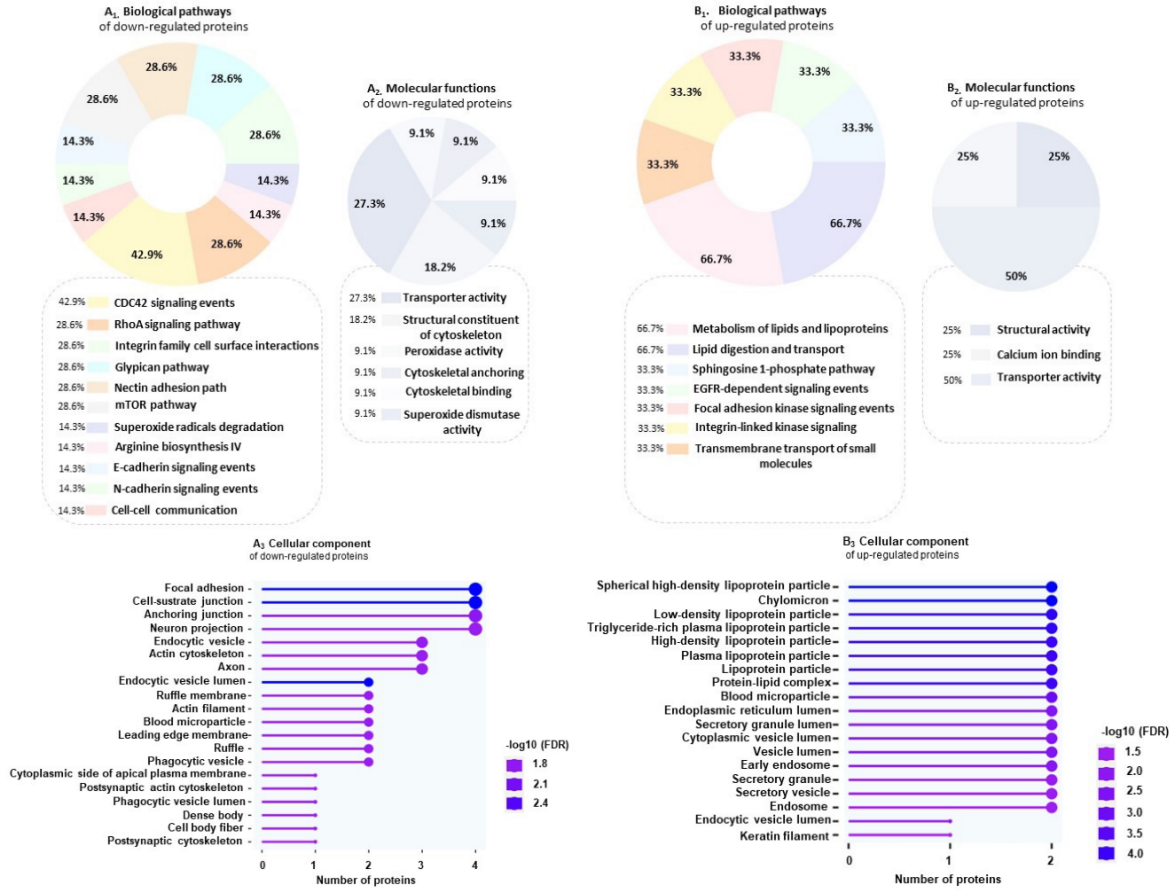


Figure 2. Main biological pathways, molecular functions, and cellular components related to the down-regulated (**A_1, A_2, A_3**) and up-regulated (**B_1, B_2, B_3**) proteins in the O-KC groups. GO enrichment of dysregulated proteins was made using the FunRich functional tool. Charts represent the main biological pathways and molecular functions in which differentially expressed proteins were involved ($p < 0.05$). The percentage of the **A_1, A_2** and **B_1, B_2** refers to the number of dysregulated proteins involved in this process compared with the total proteins in the database.

Data-dependent workflow analysis of the complete tear proteome of control and O-KC groups.

Following a DDA mode, we analyzed the tear proteome of the control and O-KC groups to have a global view of the complete tear proteomic profile of each group. This approach enabled the identification of proteins specifically expressed in each one of the different groups.

With an FDR of less than 10%, 574 proteins were identified in controls, 628 in O-KC-LR, 523 in O-KC-MR, and 396 in O-KC-HR. **Figure 3** includes a Venn diagram (**A**) representing the distribution of unique and overlapping proteins identified in the qualitative analysis of the tear samples of control and O-KC eyes. As a result, out of the total number of proteins identified, 41 were exclusively found in the control group, 49

were only identified in the O-KC-LR group, 20 were uniquely expressed in the O-KC-MR group, and 12 were only in the O-KC-HR group. To determine the potential relevance of these proteins in KC risk and their impact on corneal biomechanical alteration, the biological pathways and molecular functions of the proteins linked to each O-KC group were analyzed by the FunRich software [**Figure 3 (B**)].

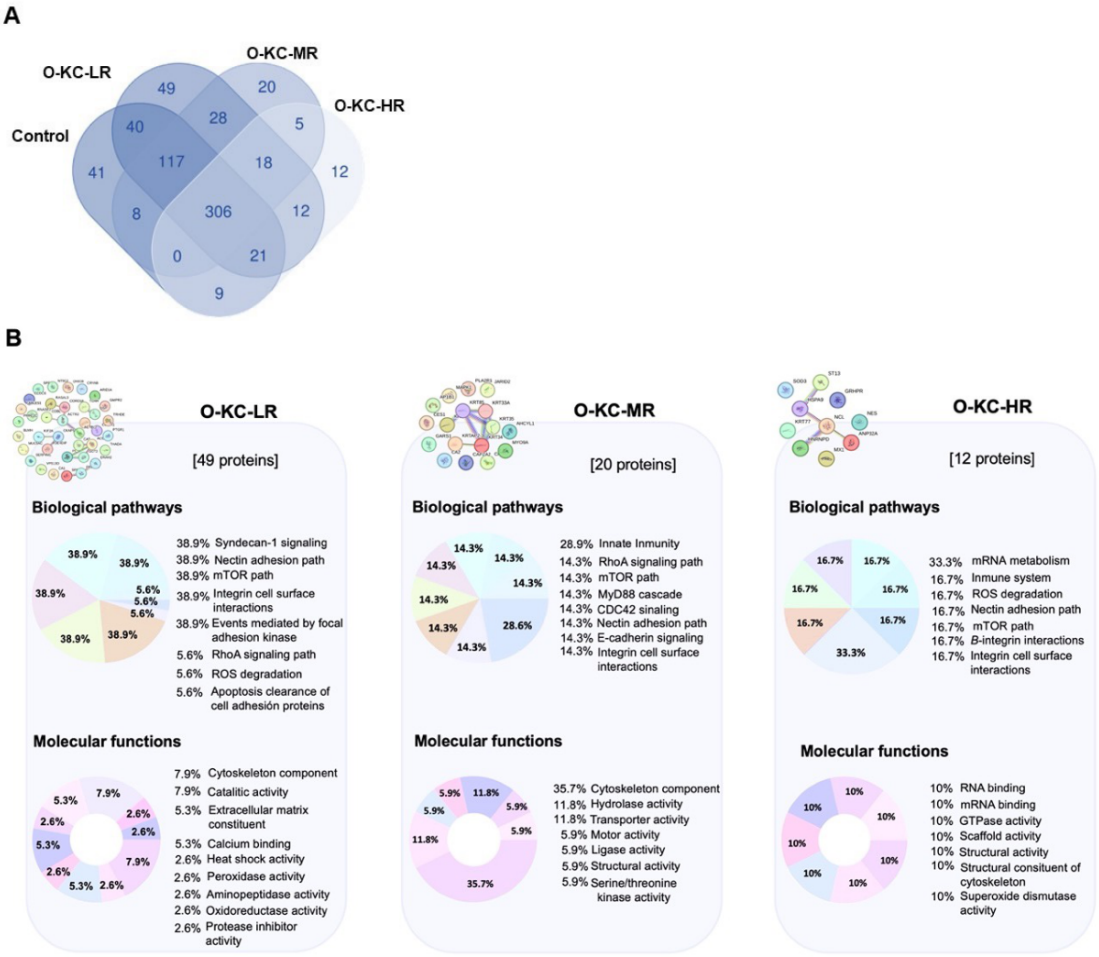


Figure 3. (A) Venn diagram represents the distribution of the unique and overlapping proteins identified in the qualitative analysis of the tear samples of control and O-KC eyes. **(B)** Analysis of the biological pathways and molecular functions associated with the proteins uniquely identified in the O-KC-LR, O-KC-MR, and O-KC-HR groups. The percentages of the charts refer to the number of proteins involved in this process compared with the total proteins in the database.

GO analysis targeted at the proteins exclusively identified in each O-KC group revealed the enrichment of pathways with analogous or complementary purposes in all groups. Most of them were related to cell adhesion events through several molecules such as Nectin, E-cadherin, or B-integrin. Similarly, other paths associated with cytoskeletal remodeling, different phases of the cell cycle, and cell aging (cell growth, differentiation, division, migration, or cell death) were also enriched, such as RhoA and mTOR pathways or the CDC42 signaling events.

Moreover, a large percentage of proteins involved in immunity cascades, such as the MyD88 cascade, was found only expressed in the O-KC-MR and O-KC-HR groups. Regarding the molecular functions, structural activity proteins represented the highest percentage in all O-KC groups.

ELISA validation

Three proteins were selected for further validation by ELISA based on the results obtained in the LC-MS/MS analysis, as well as the potential molecular involvement of these proteins. ELISA assays confirmed the previously observed findings, revealing LF under expression in all O-KC groups, lower CFL1 expression in the O-KC-LR and O-KC-HR groups, and reduced CAPN1 levels in all groups of offspring of KC patients. **Figure 4** depicts the ELISA quantification of the three proteins for each study group.

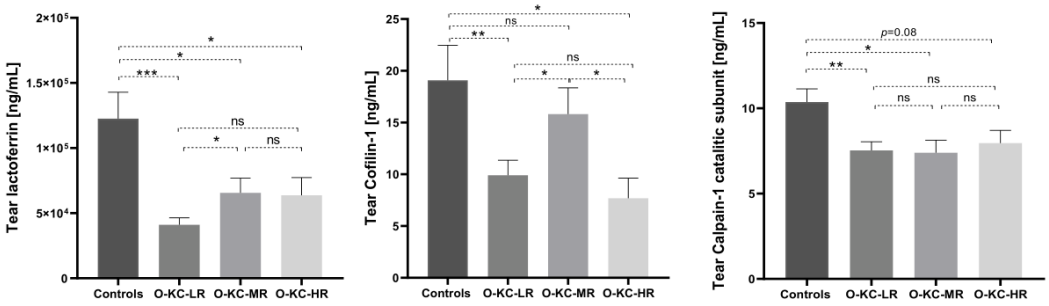


Figure 4. Representation of LF, CFL1, and CAPN1 expression (mean ± SD, ng/mL) in the tear samples of control, O-KC-LR, O-KC-MR, and O-KC-HR eyes, quantified by ELISA. *$p < 0.05$, **$p < 0.01$, ***$p < 0.001$, ns: non-significant.

Diagnostic potential of the dysregulated proteins by ROC analysis and LRA modeling

Receiver operating curve analysis (ROC) of each dysregulated protein in tear samples of O-KC was conducted to predict their ability to discriminate alterations in the corneal biomechanical properties, as well as the risk associated with having a parent with KC. According to the ROC analysis results, LCN-1, LF, SOD1, CFL1, CAPN1, EZN, PRDX1, and APOA2 were the most useful markers to distinguish between controls and O-KC groups. Among them, the highest sensitivity and specificity were found for LCN-1, LF, SOD1, CFL1, CAPN1, and APOA2. The ROC analysis of each protein is given in the **Supplementary Results S3.**

To determine the best protein panels that significantly influenced each biomechanical conditions, the proteins with the best AUC values in the ROC analysis (LCN-1, LF, SOD1, CFL1, CAPN1, EZN, PRDX1, and APOA2) were analyzed by LRA. In this way, for the O-KC-LR estimation model, LF, LCN-1, SOD1, CAPN1, EZN, and APOA2 were the proteins selected to build the following logit formula: $x'\hat{\beta} = 3.485 + (-1.478e^{-6}\ xLF) + (-$

$1.233e^{-5}$ xLCN1) + ($-1.412e^{-3}$ xSOD1) + ($4.339e^{-4}$ xCAPN1) + ($-2.839e^{-4}$ xEZN) + ($1.514e^{-4}$ xAPOA2).

Once the regression model was determined, we studied the ability of this protein panel to differentiate between the control and the O-KC-LR group by a ROC analysis, considering the predictions associated with the logistic model as the discriminant variable. In this sense, we obtained an AUC of 0.819 confidence interval (CI) 95% (0.7257 to 0.9126) with an 87% of sensitivity and 66% of specificity (cut-off value 0.662) for the LCN-1, LF, SOD1, CAPN1, EZN and APOA2 protein panel to discriminate between controls and the O-KC eyes with low risk of ectasia development **[Figure 5.a]**.

For the O-KC-MR prediction model, the selected protein panel included the LCN-1, SOD1, and EZN as the most suitable proteins for the estimation of the moderate-risk of ectasia development. Considering this protein panel, the logit formula was described as follows: $x'\hat{\beta}$= 2.496 + ($-2.650e^{-5}$ xLCN1) + ($-2.071e^{-3}$ xSOD1) + ($-1.267e^{-4}$ xEZN). The ROC analysis supported the potential of this protein panel in discriminating between the control and O-KC-MR, showing an AUC of 0.856 CI 95% (0.7626 to 0.9497) with an 96% of sensitivity and 67% of specificity (cut-off value 0.236) **[Figure 5.b]**.

Finally, LF, LCN-1, PRDX1, SOD1, and EZN were the protein panel selected to establish the prediction model for O-KC-HR condition, described as follows: $x'\hat{\beta}$ = 6.127 + ($-6.178e^{-6}$ xLF) + ($-2.494e^{-5}$ xLCN1) + ($-2.096e^{-3}$ xPRDX1) + ($-2.422e^{-4}$ xSOD1) + ($-2.238e^{-4}$ xEZN). Once again, the ROC analysis confirmed the power of the protein panel to differentiate between the control and the O-KC-HR, with an AUC of 0.848 and 92% sensitivity and 70% specificity (cut-off value 0.100) **[Figure 5.c]**.

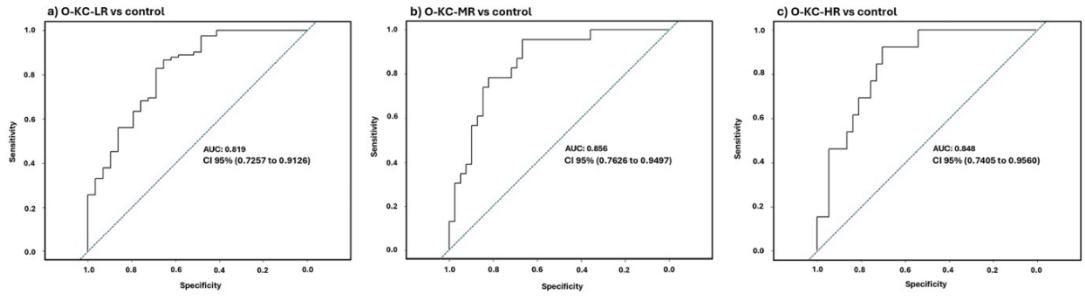


Figure 5. Receiver operating characteristic curve (ROC) analysis of the three protein panels. **A)** ROC curve of the regression model including LCN-1, LF, SOD1, CAPN1, EZN and APOA2 proteins for the O-KC-LR condition. **B)** ROC curve of the regression model including the protein panel of LCN-1, SOD1, and EZN for the O-KC-MR condition. **C)** ROC curve of the regression model including LF, LCN-1, PRDX1, SOD1, and EZN for the O-KC-HR condition.

Table 5 summarizes the specific AUC, CI, sensitivity, specificity, and cut-off values of the proteins integrating each panel.

Table 5. Breakdown of the ROC analysis of each protein panel.

		AUC	CI	Sensitivity	Specificity	Cut-off
	LF	0.742	0.640-0.840	66%	76%	$<5.24x10^5$
	LCN-1	0.707	0.600-0.813	69%	64%	$<4.87x10^4$
Panel 1	**SOD1**	0.619	0.514-0.724	58%	61%	$<5.83x10^2$
O-KC-LR vs control	**CAPN1**	0.651	0.549-0.754	66%	61%	$<2.63x10^3$
	EZN	0.609	0.500-0.717	60%	60%	$<4.51x10^3$
	APOA2	0.701	0.625-0.796	66%	66%	$>2.72x10^3$
Panel 2	**LCN-1**	0.800	0.690-0.900	75%	68%	$<3.03x10^4$
O-KC-MR vs control	**SOD1**	0.715	0.594-0.836	70%	66%	$<5.64x10^2$
	EZN	0.720	0.600-0.841	61%	71%	$<3.39x10^3$
	LF	0.824	0.710-0.930	82%	75%	$<5.41x10^5$
	LCN-1	0.789	0.670-0.900	71%	68%	$<3.20x10^4$
Panel 3	**PRDX1**	0.766	0.612-0.920	75%	71%	$<5.82x10^3$
O-KC-HR vs control	**SOD1**	0.774	0.650-0.890	71%	71%	$<4.87x10^2$
	EZN	0.670	0.516-0.823	65%	71%	$<3.45x10^3$

Proteins: **LCN-1** (Lipocalin-1), **LF** (Lactoferrin), **CAPN1** (Calpain-1 catalytic subunit), **SOD1** (Superoxide Dismutase), **EZR** (Ezrin), **PRDX1** (Peroxiredoxin-1), **APOA2** (Apolipoprotein A-II).

Discussion

Although family history is recognized as a significant risk factor for KC development,[31] studies focused on molecular changes associated with KC in this population are limited, exploring mainly the clinical and morphological characteristics of the corneas of these subjects. In this regard, previous studies have reported that KC relatives commonly exhibit steeper and thinner corneas, even with features resembling subclinical KC.[32-34] In the same way, biomechanical weakness resulting from decreased corneal stiffness and strength has also been described in KC relatives.[35] From a molecular perspective, the brief background on proteomic studies revealed that first-degree relatives of KC showed increased expression of inflammatory molecules (IL-1ß and IL-4) and innate immune receptors (TLR 2) in tears and corneal/conjunctival epithelial cells.[36,37] As well, KC familial genetic studies reported variants in some genes proposing a likely oligogenic causality in which multiple pathogenic variants reside in an individual within a high-susceptibility genome.[38]

The growing interest in studying corneal biomechanical properties to identify early tissue instability in corneal ectasias has received significant attention in clinical research settings;[39,40] however, no studies to date have set out to explore the possible protein drivers of these mechanical alterations. In this sense, this study aimed to determine the proteomic alterations in tear fluid associated with both alterations in corneal biomechanical properties and the risk of KC development related to the presence of a parent diagnosed with the disease. For this purpose, we performed a biomechanical and tomographical assessment in combination with a quantitative and qualitative study of the proteomic profile of the tear fluid of offspring of KC patients and control subjects, using LC-MS/MS for protein identification and quantification.

The first step of this study involved assessing the biomechanical properties of the corneal tissue of the O-KC eyes, to identify any molecular alterations that might be linked to or exacerbated by these biomechanical changes. In this way, among all eyes included in the KC offspring group, 18% showed moderate alterations in the corneal dynamics, indicating a moderate risk of ectasia development [O-KC-MR group], and 11% showed high alterations in the biomechanical exam, pointing out a high-risk of ectasia development [O-KC-HR]. These results align with previous studies which suggested that first-degree relatives of KC patients could exhibit lower hysteresis and corneal resistance compared to the broader population.[35,41]

Subsequently, the morphology of the corneal tissue was studied using tomographic imaging. The most remarkable aspect of the tomographic evaluation was the role of pachymetry metrics. Specifically, central and minimum corneal thickness and the pachymetric progression indexes (ARTmax/ARTh) effectively differentiated the moderate and high-risk groups from the remaining ones. Pachymetric defects are well documented in corneal ectasias, with progressive thinning of the ectasic area with severity.[1] Previous studies have reported that KC corneas, even when matched for thickness with healthy corneas (with corneal thinnest point <500 μm), exhibit significantly weaker biomechanical properties than healthy corneas of equivalent thinning.[42] Moreover, Scheimpflug technology provides detailed information about the spatial thickness distribution across the entire cornea, enabling precise assessment of corneal thickness and pachymetric progression indexes.[43,44] In this line, abnormal pachymetric distribution within the central cornea has been reported in KC patients' contralateral eyes biomechanically and tomographically healthy.[45] These findings are consistent with our results, suggesting that slight and silent variations in corneal thickness and pachymetric progression could stimulate/exacerbate alterations in corneal mechanical behavior.

Although there remains great uncertainty about the specific molecular mechanisms underlying the KC pathophysiology, studies carried out in different types of biological samples from KC patients (such as corneal tissue and tear fluid) highlighted that the increased levels of metalloproteases and the reduced expression of their inhibitors,[22,46,47] the increased markers of oxidative stress and the decreased antioxidant capacity of the corneal cells,[48-52] as well as the dysregulation of proinflammatory/anti-inflammatory interleukins, and immunity molecules,[53-56] could promote early cell death and degeneration in the corneal tissue.

In a global overview, our study revealed the dysregulation of 15 proteins in the tear samples of KC offspring, some of them previously associated with the KC pathophysiology events, such as oxidative stress, inflammation, cell adhesion, cell-cell interaction, cell division and migration, and apoptosis. In the same way, results provided by the qualitative approach showed that the proteins exclusively identified in each O-KC group were also associated with the enrichment of oxidative, apoptosis and structural processes.

The link with oxidative stress conditions was evidenced by the downregulation of several proteins such as Lipocalin-1 (LCN-1), Lactoferrin (LF), Superoxide Dismutase [Cu-Zn] (SOD1), and Peroxiredoxin-1 (PRDX1), which have essential roles in the protection against free radicals. Lipocalin-1 was the most downregulated protein in the O-KC samples. Given the multifunctionality of this protein, its affinity for toxic ligands and its capacity as a scavenger of them constitute its primary function to directly combat oxidative stress.[57] Dysregulation of LCN-1 was previously observed in tear samples of KC patients; however, these studies have reported elevated levels of LCN-1 in KC tear samples compared to healthy controls.[58,59] In this sense, the target population may account for the variability in the findings. This study is focused on the offspring of KC patients, with or without biomechanical alterations, so, our results suggest that LCN-1 deficiency may be linked to earlier disease stages or an increased susceptibility to KC development, contributing to an ineffective protection against harmful species. Subsequently, lactoferrin was the following high under-expressed protein in the study groups. Lower expression of LF in KC tear samples has been previously reported,[23,60,61] seeming to be related to the disease progression.[61] The connecting loops linking LF under expression to the KC pathophysiology rely on its capability to regulate free iron levels in body fluids (by binding Fe^{3+} ions in the extracellular space) and to modulate and reduce the inflammatory and immunity responses.[61-63] Our results showed that LF expression decreased as biomechanical properties indicated further weakening of the corneal tissue. In addition, LF had the highest sensitivity and specificity to discriminate between the controls and the O-KC biomechanically and tomographically healthy (O-KC-LR), and also the best AUC values for detecting the eyes with a high risk of ectasia development (O-KC-HR), suggesting a high potential of LF to be a sensitive and specific biomarker for the detection of at-risk stages of KC disease. Finally, SOD1 and PRDX1 levels also decreased in the O-KC groups compared to the control, lowering their expression with the impairment of corneal biomechanical response. Superoxide dismutases (SODs) are the primary defense systems for neutralizing free radicals and protecting against oxidative damage in cells.[64] There are several diseases associated with SODs dysregulation, and focusing on KC, tear and serum samples of KC patients have shown a sharp decrease in the expression of SOD1.[50,65-67] Because of the protective effect of this family of proteins in cells and tissues, the widespread argument suggests that down-regulation of SOD1 could lead to an antioxidant defense failure in a tissue constantly exposed to high levels of UV radiation and highly vulnerable to oxidative damage. In the same way, peroxiredoxins (PRDXs) represent an important family of antioxidant enzymes with dominant functions in regulating and removing peroxide levels within cells.[68] Like SODs, PRDXs under-expression has been associated with the perturbation of tissue oxidative homeostasis and the activation of apoptotic pathways.[69] At the same time, genetic variations in *FOXO* (Forkhead box, class O) have been widely associated with KC disease,[70,71] as well as with corneal resistance factor and, therefore, with corneal biomechanical behavior.[72] Specifically, the foxO family of transcription factors takes on a critical role in redox regulation and oxidative defense by promoting the transcription of genes encoding antioxidant proteins such as SODs and PRDXs.[73] Therefore, the involvement and relevance of oxidative stress seem unquestionable, not only in the

clinical evolution of KC but also associated with the risk of its development and the biomechanical imbalance.

In terms of mechanobiology and structural integrity, epithelial degeneration during KC disease has been reported by histopathological and *in vivo* confocal microscopy studies, finding alterations in superficial epithelial cell differentiation, abnormalities in basal epithelial density, and a loss of its smoothness and regularity.[74,75] Similarly, abnormalities in stromal architecture are well documented, characterized by a decrease in keratocyte density and collagen fibers, resulting in a severe thinning of this layer.[19,76] The epithelium-stromal interaction is critical, and epithelial damage has been shown to induce cell death in surrounding stromal keratocytes.[77] In this view, some studies suggest that continued damage between the corneal epithelium and stroma may constitute an ongoing circle in the progressive thinning of corneal tissue during KC disease.[78] Corneal thickness is one of the most heritable traits, with a strong genetic component and several associated genomic loci that account for its variability (such as *ZNF469, FOXO1, SMAD3, LOX, COL5A1, MPDZ, FBN2, and SPRY2*), being mainly related to collagen cross-linking, keratocyte growth and migration, epithelial proliferation and differentiation, and extracellular matrix organization.[79] In this regard, we observed the dysregulation of five proteins (CFL1, CAPN1, EZN, ACNT4, and ACTG) that are involved in cell morphology and migration, cell-cell adhesion, cell-substrate binding, F-actin crosslinking, and cytoskeleton remodeling.[80-83] Assuming that KC is associated with biomechanical instability at the epithelial-stromal level, dysregulation of these proteins may contribute to the onset of mechanical decline. CFL1, CAPN1, and EZN are required for the regulation of cell morphology, cell-substrate adhesion, cell-matrix networking, actin depolymerization, and cytoskeleton dynamics via integrin cell surface interactions, β-catenin signaling, and RhoA or mTOR signaling pathways.[84,85] RhoA, Wnt, TGFβ, or Hippo signaling are highly conserved pathways involved in mechanotransduction in the corneal tissue; likewise, integrins and β-catenin play a vital role in focal adhesions and cytoskeletal adherences, so any impact affecting these pathways or components could weaken the cell-cell communication system.[86] CFL1 and CAPN1 dysregulation were previously observed in the stromal fibroblasts and epithelial cells of KC corneas, and changes in the expression of these proteins have been recognized as possible underlying factors of stromal thinning and structural failure.[78,87] In addition, the down-regulation of ACTN4, an F-actin crosslinking protein involved in the tight junctions of epithelial cells,[88] and of ACTG, a member of the actin filaments, was also detected. Reduced expression of the β-actin encoding gene in human corneas with KC suggests that stromal keratocyte depletion may contribute to reduced β-actin expression, leading to destabilization of the cytoskeleton, and eventually stromal thinning and weakening.[89,90] Although our results showed no differences between all groups for ACTN4 and ACTG expression, the trend of both proteins suggested their lower expression as the biomechanical behavior of the corneal structure weakened.

In connection with the pathological events affecting extracellular matrix (ECM) during KC disease, we observed that SSA1 expression was significantly reduced in the O-KC-

LR and O-KC-MR groups in comparison to the controls. KC fibroblasts have shown a deficiency in arginine and spermidine concentrations,[91,92] and even the benefits of supplementation with arginine have been postulated as a potential therapy for KC through its capacity to promote collagen type I production and increasing ECM deposition.[91] As responsible for the biosynthesis of arginine in most body tissues, down-regulation of ASS1 could be associated with the arginine deficiency in KC disease. Considering that the dysregulation of most structural proteins was observed even before detecting clinical alterations in the corneal biomechanical behaviour of O-KC participants, our results seem consistent with a structural disturbance that may even precede the corneal weakening that can be detected with the current clinical biomechanical tools.

Beyond the individual biological impact over KC pathophysiology of the dysregulated proteins, LRA modeling determined the best biomarker combinations to discriminate between the control and the three O-KC groups, creating three specific protein panels with high sensitivity and specificity that could be useful for the future development of new and early diagnosis strategies.

Although this is an innovative study marking the first attempt to identify the proteomic alterations linked to the risk of developing KC and those underlying the biomechanical decline associated with this disease, we have identified some limitations. The first one acknowledges that the subcategorization of the O-KC led to an uneven distribution of participants across the study groups. To address this limitation, future studies should include more participants in groups with smaller sample sizes. Secondly, this study did not include a follow-up of the O-KC participants, so it seems desirable to design future prospective cohort studies to assess the evolution of these markers in those subjects who may develop clinical disease, a task we are currently working on.

In summary, the proteomic approach of this study emphasizes the relevance of some target proteins previously recognized to have a significant role in clinical KC, indicating their involvement in the disease's early and at-risk stages. In this sense, the high sensitivity and specificity of LCN1, LF, SOD1, EZN, and CAPN1 for detecting biomechanical alterations of corneal tissue make them promising biomarkers in the early detection of KC. Oxidative stress and cell structural alterations appear to begin long before the onset of clinical signs and even before alterations in the corneal biomechanics that can be detected with the current tools. A thorough insight into the interplay between oxidative and structural events influencing cellular mechanobiology is required to develop effective therapeutic strategies for early KC management.

Acknowledgments

The authors would like to sincerely thank all the participants involved in this study, as well as OCULUS Iberia S.L. for their collaboration in providing the biomechanics and tomography devices required for this work.

Author contributions

Conceptualization, M.L.L., U.R., and I.L.; methodology, M.L.L., U.R., S.B., and C.P.; formal analysis and investigation, M.L.L., M.C.A.; resources, U.R., S.B., P.H., and I.L.; writing- original draft preparation, M.L.L.; writing- review and editing, M.L.L., U.R., Y.P., P.H., and I.L.; supervision, U.R., and I.L.; funding acquisition, M.L.L., U.R., P.H., and I.L. All authors have read and agreed to the published version of the manuscript.

Funding sources

This project has been funded by the Instituto de Salud Carlos III (ISCIII) co-financed by the European Union (UE) (PI23/00323), and the Xunta de Galicia (Consellería de Economía e Industria: IN607A2022/03). M.L.L. acknowledges the financial support from a predoctoral fellowship of Universidade de Santiago de Compostela and Banco Santander. Similarly, U.R. recognizes the support from Xunta de Galicia (Galician Innovation Agency GAIN: IN606C-2024/003) postdoctoral fellowship. The funders had no role in the study design, data collection and analysis, decision to publish, or preparation of the manuscript.

References

1. Belin MW, Asota IM, Ambrosio R, Khachikian SS. What's in a name: keratoconus, pellucid marginal degeneration, and related thinning disorders. Am J Ophthalmol. 2011;152(2):157-162.

2. Wagner H, Barr JT, Zadnik K. Collaborative Longitudinal Evaluation of Keratoconus (CLEK) study: methods and findings to date. Cont Lens Anterior Eye. 2007;30(4):223-232.

3. Ertan A, Muftuoglu O. Keratoconus clinical findings according to different age and gender groups. Cornea. 2008;27(10):1109-1113.

4. Li X, Yang H, Rabinowitz YS. Longitudinal study of keratoconus progression. Exp Eye Res. 2007;85(4):502-507.

5. Léoni-Mesplié S, Mortemousque B, Touboul D, et al. Scalability and severity of keratoconus in children. Am J Ophthalmol. 2012;154(1):56-62.e1

6. Gordon-Shaag A, Millodot M, Kaiserman I, et al. Risk factors for keratoconus in Israel: a case-control study. Ophthalmic Physiol Opt. 2015;35(6):673-681.

7. Keel S, Lingham G, Misra N, et al. Toward Universal Eye Health Coverage-Key Outcomes of the World Health Organization Package of Eye Care Interventions: A Systematic Review. JAMA Ophthalmol. 2022;140(12):1229-1238.

8. Vinciguerra R, Ambrósio R, Elsheikh A, et al. Detection of Keratoconus With a New Biomechanical Index. J Refract Surg. 2016;32(12):803-810.

9. Scarcelli G, Besner S, Pineda R, Yun SH. Biomechanical characterization of keratoconus corneas ex vivo with Brillouin microscopy. Invest Ophthalmol Vis Sc*i*. 2014;55(7):4490-4495.

10. Bykhovskaya Y, Rabinowitz YS. Update on the genetics of keratoconus. Exp Eye Res. 2021;202:108398.

11. Tuft SJ, Hassan H, George S, Frazer DG, Willoughby CE, Liskova P. Keratoconus in 18 pairs of twins. Acta Ophthalmol. 2012;90(6):482-486.

12. Weed KH, MacEwen CJ, McGhee CNJ. The variable expression of keratoconus within monozygotic twins: Dundee University Scottish Keratoconus Study (DUSKS). Contact Lens Anterior Eye. 2006;29(3):123-126.

13. Mathan JJ, Gokul A, Simkin SK, Meyer JJ, Patel D V., McGhee CNJ. Topographic screening reveals keratoconus to be extremely common in Down syndrome. Clin Exp Ophthalmol. 2020;48(9):1160-1167.

14. Vincent AL, Weiser BA, Cupryn M, Stein RM, Abdolell M, Levin A V. Computerized corneal topography in a paediatric population with Down syndrome. Clin Exp Ophthalmol. 2005;33(1):47-52.

15. Robertson I. Keratoconus and the Ehlers-Danlos syndrome: a new aspect of keratoconus. Med J Aust. 1975;1(18):571-573.

16. Elder MJ. Leber congenital amaurosis and its association with keratoconus and keratoglobus. J Pediatr Ophthalmol Strabismus. 1994;31(1):38-40.

17. Hameed A, Khaliq S, Ismail M, Anwar K, Ebenezer ND, et al. A novel locus for Leber congenital amaurosis (LCA4) with anterior keratoconus mapping to chromosome 17p13. Invest Ophthalmol Vis Sci. 2000;41(3):629-633.

18. Olivo-Payne A, Abdala-Figuerola A, Hernandez-Bogantes E, Pedro-Aguilar L, Chan E, Godefrooij D. Optimal management of pediatric keratoconus: challenges and solutions. Clin Ophthalmol. 2019;13:1183-1191.

19. Santodomingo-Rubido J, Carracedo G, Suzaki A, Villa-Collar C, Vincent SJ, Wolffsohn JS. Keratoconus: An updated review. Cont Lens Anterior Eye. 2022;45(3):101559.

20. Awwad ST, Yehia M, Mehanna CJ, et al. Tomographic and Refractive Characteristics of Pediatric First-Degree Relatives of Keratoconus Patients. Am J Ophthalmol. 2019;207:71-76.

21. Naderan M, Rajabi MT, Zarrinbakhsh P, Naderan M, Bakhshi A. Association between Family History and Keratoconus Severity. Curr Eye Res. 2016;41(11):1414-1418.

22. Lema I, Duran J. Inflammatory molecules in the tears of patients with keratoconus. Ophthalmology. 2005;112(4):654-659.

23. Lema I, Brea D, Rodríguez-González R, Díez-Feijoo E, Sobrino T. Proteomic analysis of the tear film in patients with keratoconus. Mol Vis. 2010;16:2055-2061.

24. Balasubramanian SA, Wasinger VC, Pye DC, Willcox MD. Preliminary identification of differentially expressed tear proteins in keratoconus. Mol Vis. 2013;19:2124-2134.

25. López-López M, Regueiro U, Bravo S, et al. Tear proteomics in keratoconus: A quantitative SWATH-MS analysis. Invest Ophthalmol Vis Sci. 2021;62(10):30.

26. López-López M, Regueiro U, Bravo SB, et al. Shotgun Proteomics for the Identification and Profiling of the Tear Proteome of Keratoconus Patients. Invest Ophthalmol Vis Sci. 2022;63(5):12.

27. Efron N. Grading scales for contact lens complications. Ophthalmic Physiol Opt. 1998;18(2):182-186.

28. Chantada-Vázquez MDP, García Vence M, Serna A, Núñez C, Bravo SB. SWATH-MS Protocols in Human Diseases. Methods Mol Biol. 2021;2259:105-141.

29. Bonzon-Kulichenko E, Pérez-Hernández D, Núñez E, et al. A robust method for quantitative high-throughput analysis of proteomes by 18O labeling. Mol Cell Proteomics. 2011;10(1):M110.003335.

30. Perez-Hernandez D, Gutiérrez-Vázquez C, Jorge I, et al. The intracellular interactome of tetraspanin-enriched microdomains reveals their function as sorting machinery toward exosomes. J Biol Chem. 2013;288(17):11649-11661.

31. Lapeyre G, Fournie P, Vernet R, et al. Keratoconus Prevalence in Families: A French Study. Cornea. 2020;39(12):1473-1479.

32. Karimian F, Aramesh S, Rabei HM, Javadi MA, Rafati N. Topographic evaluation of relatives of patients with keratoconus. Cornea. 2008;27(8):874-878.

33. Kaya V, Utine CA, Altunsoy M, Oral D, Yilmaz OF. Evaluation of corneal topography with Orbscan II in first-degree relatives of patients with keratoconus. Cornea. 2008;27(5):531-534.

34. Shneor E, Frucht-Pery J, Granit E, Gordon-Shaag A. The prevalence of corneal abnormalities in first-degree relatives of patients with keratoconus: a prospective case-control study. Ophthalmic Physiol Opt. 2020;40(4):442.

35. Kara N, Altinkaynak H, Baz O, Goker Y. Biomechanical evaluation of cornea in topographically normal relatives of patients with keratoconus. Cornea. 2013;32(3):262-266.

36. Ionescu IC, Corbu CG, Tanase C, et al. Overexpression of Tear Inflammatory Cytokines as Additional Findings in Keratoconus Patients and Their First Degree Family Members. Mediators Inflamm. 2018;2018:4285268.

37. Regueiro U, López-López M, Hervella P, Sobrino T, Lema I. Corneal and conjunctival alteration of innate immune expression in first-degree relatives of keratoconus patients. Graefes Arch Clin Exp Ophthalmol. 2021;259(2):459-467

38. Shinde V, Sobreira N, Wohler ES, et al. Pathogenic alleles in microtubule, secretory granule and extracellular matrix-related genes in familial keratoconus. *Hum Mol Genet*. 2021;30(8).

39. Tian L, Zhang D, Guo L, et al. Comparisons of corneal biomechanical and tomographic parameters among thin normal cornea, forme fruste keratoconus, and mild keratoconus. Eye Vis (Lond). 2021;8(1):44.

40. Wang YM, Chan TCY, Yu M, Jhanji V. Comparison of corneal dynamic and tomographic analysis in normal, forme fruste keratoconic, and keratoconic eyes. J Refract Surg. 2017;33(9):632-638.

41. Ionescu IC, Corbu CG, Nicula C, et al. The importance of corneal biomechanics in assessing first degree family members of keratoconus patients. Rom J Ophthalmol. 2018;62(2):149-154.

42. Sedaghat MR, Momeni-Moghaddam H, Ehsaei A, Vinciguerra R, Zamani O, Robabi H. Comparison of corneal biomechanical properties in healthy thin corneas with matched keratoconus eyes. J Cataract Refract Surg. 2023;49(3):234-238.

43. Ambrósio R, Alonso RS, Luz A, Coca Velarde LG. Corneal-thickness spatial profile and corneal-volume distribution: tomographic indices to detect keratoconus. J Cataract Refract Surg. 2006;32(11):1851-1859.

44. Ambrósio R, Caiado ALC, Guerra FP, et al. Novel pachymetric parameters based on corneal tomography for diagnosing keratoconus. J Refract Surg. 2011;27(10):753-758.

45. Song P, Yang K, Li P, et al. Assessment of Corneal Pachymetry Distribution and Morphologic Changes in Subclinical Keratoconus with Normal Biomechanics. Biomed Res Int. 2019;2019.

46. Lema I, Sobrino T, Duran JA, Brea D, Diez-Feijoo E. Subclinical keratoconus and inflammatory molecules from tears. Br J Ophthalmol. 2009;93(6):820-824.

47. di Martino E, Ali M, Inglehearn CF. Matrix metalloproteinases in keratoconus - Too much of a good thing?. Exp Eye Res. 2019;182:137-143.

48. Shetty R, Sharma A, Pahuja N, et al. Oxidative stress induces dysregulated autophagy in corneal epithelium of keratoconus patients. PLoS One. 2017;12(9):1-20.

49. Chwa M, Atilano SR, Hertzog D, et al. Hypersensitive response to oxidative stress in keratoconus corneal fibroblasts. Invest Ophthalmol Vis Sci. 2008;49(10):4361-4369.

50. Atilano S, Lee D, Fukuhara P, et al. Corneal Oxidative Damage in Keratoconus Cells due to Decreased Oxidant Elimination from Modified Expression Levels of SOD Enzymes, PRDX6, SCARA3, CPSF3, and FOXM1. J Ophthalmic Vis Res. 2019;14(1):62-70.

51. Navel V, Malecaze J, Pereira B, et al. Oxidative and antioxidative stress markers in keratoconus: a systematic review and meta-analysis. Acta Ophthalmol. 2021;99(6):e777-e794.

52. Shinde V, Hu N, Mahale A, et al. RNA sequencing of corneas from two keratoconus patient groups identifies potential biomarkers and decreased NRF2-antioxidant responses. Sci Rep. 2020;10(1):9907.

53. Balasubramanian SA, Mohan S, Pye DC, Willcox MD. Proteases, proteolysis, and inflammatory molecules in the tears of people with keratoconus. Acta Ophthalmol. 2012;90(4):e303-e309.

54. Malfeito M, Regueiro U, Pérez-Mato M, Campos F, Sobrino T, Lema I. Innate Immunity Biomarkers for Early Detection of Keratoconus. Ocul Immunol Inflamm. 2019;27(6):942-948.

55. Lema I, Durán JA, Ruiz C, Díez-Feijoo E, Acera A, Merayo J. Inflammatory response to contact lenses in patients with keratoconus compared with myopic subjects. Cornea. 2008;27(7):758-763.

56. Jun AS, Cope L, Speck C, et al. Subnormal cytokine profile in the tear fluid of keratoconus patients. PLoS One. 2011;6(1):e16437.

57. Lechner M, Wojnar P, Redl B. Human tear lipocalin acts as an oxidative-stress-induced scavenger of potentially harmful lipid peroxidation products in a cell culture system. Biochem J. 2001;356(Pt 1):129-135.

58. Pannebaker C, Chandler HL, Nichols JJ. Tear proteomics in keratoconus. Mol Vis. 2010;16:1949-1957.

59. Acera A, Vecino E, Rodríguez-Agirretxe I, et al. Changes in tear protein profile in keratoconus disease. Eye. 2011;25(9):1225-1233.

60. Balasubramanian SA, Pye DC, Willcox MD. Levels of lactoferrin, secretory IgA and serum albumin in the tear film of people with keratoconus. Exp Eye Res. 2012;96(1):132-137.

61. Regueiro U, López-López M, Varela-Fernández R, Sobrino T, Diez-Feijoo E, Lema I. Immunomodulatory Effect of Human Lactoferrin on Toll-like Receptors 2 Expression as Therapeutic Approach for Keratoconus. Int J Mol Sci. 2022;23(20):12350.

62. Rosa L, Cutone A, Lepanto MS, Paesano R, Valenti P. Lactoferrin: A Natural Glycoprotein Involved in Iron and Inflammatory Homeostasis. Int J Mol Sci. 2017;18(9):1985.

63. Regueiro U, López-López M, Varela-Fernández R, Otero-Espinar FJ, Lema I. Biomedical Applications of Lactoferrin on the Ocular Surface. Pharmaceutics. 2023;15(3):865.

64. Nozik-Grayck E, Suliman HB, Piantadosi CA. Extracellular superoxide dismutase. Int J Biochem Cell Biol. 2005;37(12):2466-2471.

65. Tekin S, Seven E. Assessment of serum catalase, reduced glutathione, and superoxide dismutase activities and malondialdehyde levels in keratoconus patients. Eye (Lond). 2022;36(10):2062-2066.

66. Balmus IM, Alexa AI, Ciuntu RE, et al. Oxidative stress markers dynamics in keratoconus patients' tears before and after corneal collagen crosslinking procedure. Exp Eye Res. 2020;190:107897.

67. Udar N, Atilano SR, Brown DJ, et al. SOD1: A Candidate Gene for Keratoconus. Invest Ophthalmol Vis Sci. 2006;47(8):3345-3351.

68. Perkins A, Nelson KJ, Parsonage D, Poole LB, Karplus PA. Peroxiredoxins: Guardians Against Oxidative Stress and Modulators of Peroxide Signaling. Trends Biochem Sci. 2015;40(8):435.

69. Wojcik K, Kaminska A, Blasiak J, Szaflik J, Szaflik JP. Oxidative stress in the pathogenesis of Keratoconus and Fuchs endothelial corneal dystrophy. Int J Mol Sci. 2013;14(9):19294-19308.

70. Liskova P, Dudakova L, Krepelova A, Klema J, Hysi PG. Replication of SNP associations with keratoconus in a Czech cohort. PLoS One. 2017;12(2):e0172365.

71. Lu Y, Vitart V, Burdon KP, et al. Genome-wide association analyses identify multiple loci associated with central corneal thickness and keratoconus. Nat Genet. 2013;45(2):155-163.

72. Khawaja AP, Rojas Lopez KE, Hardcastle AJ, et al. Genetic Variants Associated with Corneal Biomechanical Properties and Potentially Conferring Susceptibility to Keratoconus in a Genome-Wide Association Study. JAMA Ophthalmol. 2019;137(9):1005-1012.

73. Klotz LO, Sánchez-Ramos C, Prieto-Arroyo I, Urbánek P, Steinbrenner H, Monsalve M. Redox regulation of FoxO transcription factors. Redox Biol. 2015;6.

74. Jongebloed WL, Worst JF. The keratoconus epithelium studied by SEM. Doc Ophthalmol. 1987;67(1-2):171-181.

75. Efron N, Hollingsworth JG. New perspectives on keratoconus as revealed by corneal confocal microscopy. Clin Exp Optom. 2008;91(1):34-55.

76. Sykakis E, Carley F, Irion L, Denton J, Hillarby MC. An in-depth analysis of histopathological characteristics found in keratoconus. Pathology. 2012;44(3):234-239.

77. Wilson SE, He YG, Weng J, et al. Epithelial injury induces keratocyte apoptosis: hypothesized role for the interleukin-1 system in the modulation of corneal tissue organization and wound healing. Exp Eye Res. 1996;62(4):325-327.

78. Lee JE, Oum BS, Choi HY, Lee SU, Lee JS. Evaluation of differentially expressed genes identified in keratoconus. Mol Vis. 2009;15:2480-2487.

79. Choquet H, Melles RB, Yin J, et al. A multiethnic genome-wide analysis of 44,039 individuals identifies 41 new loci associated with central corneal thickness. Commun Biol. 2020;3(1).

80. Bernstein BW, Bamburg JR. ADF/Cofilin: A Functional Node in Cell Biology. Trends Cell Biol. 2010;20(4):187.

81. Wells A, Huttenlocher A, Lauffenburger DA. Calpain proteases in cell adhesion and motility. Int Rev Cytol. 2005;245:1-16.

82. Hoskin V, Szeto A, Ghaffari A, Greer PA, CÃtéc GP, Elliott BE. Ezrin regulates focal adhesion and invadopodia dynamics by altering calpain activity to promote breast cancer cell invasion. Mol Biol Cell. 2015;26(19):3464-3479.

83. Shao H, Wang JH, Pollak MR, Wells A. α-actinin-4 is essential for maintaining the spreading, motility and contractility of fibroblasts. PLoS One. 2010;5(11):e13921.

84. Kulkarni S, Saido TC, Suzuki K, Fox JEB. Calpain mediates integrin-induced signaling at a point upstream of Rho family members. J Biol Chem. 1999;274(30):21265-21275.

85. Hiscox S, Jiang WG. Ezrin regulates cell-cell and cell-matrix adhesion, a possible role with E-cadherin/beta-catenin. J Cell Sci. 1999;112 Pt 18(18):3081-3090.

86. Thomasy SM, Leonard BC, Greiner MA, Skeie JM, Raghunathan VK. Squishy matters - Corneal mechanobiology in health and disease. Prog Retin Eye Res. 2024;99:101234.

87. Joseph R, Srivastava OP, Pfister RR. Differential epithelial and stromal protein profiles in keratoconus and normal human corneas. Exp Eye Res. 2011;92(4):282-298.

88. Otey CA, Carpen O. Alpha-actinin revisited: a fresh look at an old player. Cell Motil Cytoskeleton. 2004;58(2):104-111.

89. Macé M, Galiacy SD, Erraud A, et al. Comparative transcriptome and network biology analyses demonstrate antiproliferative and hyperapoptotic phenotypes in human keratoconus corneas. Invest Ophthalmol Vis Sci. 2011;52(9):6181-6191.

90. Khaled ML, Helwa I, Drewry M, Seremwe M, Estes A, Liu Y. Molecular and histopathological changes associated with keratoconus. Biomed Res Int. 2017;2017:7803029.

91. McKay TB, Priyadarsini S, Rowsey T, Karamichos D. Arginine Supplementation Promotes Extracellular Matrix and Metabolic Changes in Keratoconus. Cells. 2021;10(8):2076.

92. Stachon T, Kolev K, Flaskó Z, Seitz B, Langenbucher A, Szentmáry N. Arginase activity, urea, and hydroxyproline concentration are reduced in keratoconus keratocytes. Graefes Arch Clin Exp Ophthalmol. 2017;255(1):91-97.

Supplementary material & data

Chapter 3

Supplementary Methods S1

Biomechanical evaluation by Corvis® ST (Oculus, Wetzlar, Germany)

Parameters studied:

Time until the first/second applanation (A1T/A2T), velocity of the corneal apex during the first/second applanation (A1V/A2V), time to the highest concavity (HCT), maximum deformation amplitude (DAmax), deflection amplitude at the moment of the highest corneal concavity (HCDA), deflection length at the first/second applanation (A1DLL/A2DLL), highest concavity deflection length (HCDLL), peak distance at the highest concavity (PD), ratio between the deformation amplitude at the apex and at 1mm (DAratio max 1mm), ratio between the deformation amplitude at the apex and at 2mm (DAratio max 2mm), integrated radius (IR), maximum value of the radius of curvature during the concave phase of the deformation (Max Inverse Radius), central corneal thickness by Corvis (CCT_C), Ambrósio Relational Thickness horizontal (ARTh), changes of corneal thickness from the corneal center to the periphery, averagely determined at 2.5mm from the apex (Pachy Slope), stiffness parameter at the first applanation (SP-A1), Corvis Biomechanical Index (CBI), and Stress-Strain Index (SSI).

Tomographic evaluation by Pentacam® HR (Oculus, Wetzlar, Germany)

Parameters studied:

Corneal central power (PDC), keratometry in the flattest meridian (K1), keratometry in the steeper meridian (K2), maximum dioptric power (Kmax), inferior-superior dioptric asymmetry (I-S asymmetry), maximum Ambrósio Relational Thickness (ARTmax), central corneal thickness by Pentacam (CCT_P), minimum thickness point (MTP), anterior and posterior surfaces elevation (AE and PE), total deviation value (BAD-D) and the Tomographic and Biomechanical Index (TBI).

Supplementary Methods S2

Protein tryptic digestion

As for trypsin digestion, 100µg of protein from tear fluid of 202 samples (42 controls and 160 O-KC) was loaded on a 10% SDS-PAGE gel. The run was interrupted when the front penetrated 3mm into the resolving gel.[1,2] The protein band was visualized, with Sypro-Ruby fluorescent staining (Lonza, Porriño, Pontevedra, Spain), excised, and processed for in-gel tryptic digestion

following the standard protocol of Shevchenko et al[3], with minor modifications. 10 mM dithiothreitol (Sigma-Aldrich, St. Louis, MO, USA) in 50 mM ammonium bicarbonate (Sigma-Aldrich, St. Louis, MO, USA) was used for gel pieces reduction and 55 mM iodoacetamide (Sigma-Aldrich, St. Louis, MO, USA) in 50 mM ammonium bicarbonate for alkylation. Next, pieces were washed with 50 mM ammonium bicarbonate in 50% methanol (HPLC grade, Scharlau, Barcelona, Spain), dehydrated by adding acetonitrile (HPLC grade, Scharlau, Barcelona, Spain), and dried in a SpeedVac. At last, modified porcine trypsin (Promega, Madison, WI, USA) was added at a concentration of 20 ng/µL in 20 mM ammonium bicarbonate and incubated overnight at 37 ºC. Peptides were extracted by three 20-minute incubations in 40 µL of 60% acetonitrile in 0.5% HCOOH and stored at -20°C.

Mass spectrometric analysis

Data-dependent Acquisition (DDA)

Digested peptides were resuspended in 100µL of mobile phase A (2% acetonitrile, 0.1%, formic acid), by sonication for 10 min to obtain 1µg/µL peptide solution. The gradient was created using a micro-liquid chromatography system (Eksigent Technologies nanoLC 400, Sciex, Framingham, MA, USA) coupled to a high-speed Triple TOF 6600 mass spectrometer (Sciex, Framingham, MA, USA) with a microflow source. Peptides (4 µg of each sample) were separated using reverse-phase chromatography, using a ChromXP C18CL analytical column (150 µL ×0.3mm, 120Å, s-3 µL) (Sciex, Framingham, MA, USA). The trap column was a YMC-TRIART C18 (YMC Technologies, Teknokroma) with a 3 mm particle size and 120 Å pore size, switched online with the analytical column. The loading pump delivered a solution of 0.1% formic acid in water at 10 µl/min. The micro-pump generated a flow rate of 5 µl/min and was operated under gradient elution conditions. For that, 0.1% formic acid in water was used as mobile phase A, and 0.1% formic acid in acetonitrile as mobile phase B. Peptides were separated using a 90-minute gradient ranging from 2% to 90% mobile phase B.

Data acquisition was performed in a TripleTOF 6600 System (Sciex, Framingham, MA, USA) using a Data Dependent workflow (DDA). A Micro source (Sciex) was used for the interface between microLC and MS, with an application of 2600 V voltage. Source

and interface conditions were the following: ion spray voltage floating (ISVF) 5500 V, curtain gas (CUR) 25, collision energy (CE) 10 and ion source gas 1 (GS1) 25. The instrument was operated with Analyst TF 1.7.1 software (Sciex, USA). Switching criteria were set to ions greater than mass-to-charge ratio (m/z) 350 and smaller than m/z 1400 with a charge state of 2–5, mass tolerance 250 ppm, and an abundance threshold of more than 200 counts (cps). Former target ions were excluded for 15 s. The instrument was automatically calibrated every 4 hours using external calibrant tryptic peptides from PepCalMix.

Data analysis

After MS/MS analysis, ProteinPilot™ (version 5.0.1; Sciex; Framingham, MA, USA) was used for data file processing, using a specific Human UniProt database. The search was performed specifying iodoacetamide as an alkylation of the cysteines as a fixed modification. False Discovery Rate (FDR) was calculated by a non-linear fitting method displaying identified proteins with an FDR rate between 1 and 10%.

Protein quantification by SWATH-MS (Sequential Window Acquisition for All Theoretical Mass Spectra)

Spectral library creation

To build the MS/MS spectral libraries, peptide solutions were analyzed by a DDA method using micro-LC-MS/MS as described before. Two pools (control and O-KC) were made using 3 µL of each sample to obtain a general representation of the peptides and proteins present in all samples. 4 µL of each pool (control and O-KC) was separated into a micro-LC system Ekspert nLC425 (Eksigen, Dublin, CA, USA) as described before but using a 40-minute gradient. The SWATH acquisition mode consisted of a 250 ms survey (MS scan) MS1 from 400 to 1250 m/z followed by an (MS/MS analysis) MS2 analysis scan from 100 to 1500 m/z (25 ms acquisition time) of the top 100 precursor ions from the survey scan, for a total cycle time of 2.8 s. Fragmented precursors were then added to a dynamic exclusion list for 15 s; any singly charged ions were excluded from the (MS/MS analysis) MS2 analysis.

Peptide and protein identifications were performed using Protein Pilot software (version 5.0.1, Sciex) using a Human-specific Uniprot database, specifying iodoacetamide as an alkylation of the cysteines as a fixed modification. The false discovery rate (FDR) was set to 1 for both peptides and proteins. The MS/MS spectra, the ion data, and the retention time of the identified peptides and proteins were used to generate the spectral library for SWATH peak extraction using the add-in for PeakView Software (version 2.2, Sciex) MS/MS^{ALL} with SWATH Acquisition MicroApp (version 2.0, Sciex). Peptides with a confidence score above 99% (as obtained from the Protein Pilot database search) were included in the spectral library.

SWATH-MS relative quantification

Regarding relative quantification by SWATH-MS acquisition, 4µL of each sample was analyzed in a data-independent acquisition method (IDA). The method is based on repeating a cycle consisting of the acquisition of 100 sequential overlapping precursor isolation windows of variable width (1 m/z overlap), covering the mass range from 400

to 1250 m/z with a previous TOF MS1 scan (400 to 1500 m/z, 50 ms acquisition time) for each cycle. The total cycle time was 6.3s.

Data analysis

Data extraction of chromatographic fragment ion profiles from the SWATH method was performed with PeakView software (version 2.2; Sciex, Framingham, MA, USA) using the SWATH AcquisitionMicroApp (version 2.0; Sciex, Framingham, MA, USA), which processed the data using the spectral library created from the DDA data. Five-minute windows and 30 ppm widths were used to extract the ion chromatograms; SWATH quantization was attempted for all proteins in the ion library that were identified by ProteinPilot with an FDR below 1%. The retention times from the peptides that were selected for each protein were realigned in each run according to the iRT peptides present in the samples and eluted along the whole-time axis. The extracted ion chromatograms were then generated for each selected fragment ion; the peak areas for the protein were obtained by summing the peak areas from 10 peptides (MS1 scan) and 7 corresponding fragment ions (MS2 scan) from each peptide. PeakView computed an FDR and a score for each assigned peptide according to the chromatographic and spectra components; only peptides with an FDR below 1 % were used for protein quantization. Protein quantization was calculated by adding the peak areas of the corresponding peptides.

Integrated peak areas were exported directly to MarkerView software (Sciex, Framingham, MA, USA) for relative quantitative analysis. The export generated three files containing quantitative information about individual ions, the summed intensity of different ions for a particular peptide, and the summed intensity of different peptides for a particular protein. MarkerView uses processing algorithms that accurately find chromatographic and spectral peaks directly from raw SWATH data. Data alignment via MarkerView compensates for small variations in mass and retention time values, ensuring that identical compounds from different samples are accurately compared to each other. A most-like ratio (MLR) normalization was performed after statistical analysis to control for possible uneven sample loss across the different samples during the sample preparation process.[4,5]

Multivariate statistical analysis through principal component analysis (PCA) was performed to compare sample data. The mean MS peak area of each protein was obtained from the SWATH-MS replicates of each condition.

SWATH-MS has emerged as a translational and effective tool in different fields, being successfully applied by our group in a large variety of human samples and studies. [6–10]

REFERENCES

1. Bonzon-Kulichenko E, Pérez-Hernández D, Núñez E, et al. A robust method for quantitative high-throughput analysis of proteomes by 18O labeling. *Mol Cell Proteomics*. 2011;10(1).

2. Perez-Hernandez D, Gutiérrez-Vázquez C, Jorge I, et al. The intracellular interactome of tetraspanin-enriched microdomains reveals their function as sorting machineries toward exosomes. *J Biol Chem*. 2013;288(17):11649-

11661.

3. Shevchenko A, Wilm M, Vorm O, Mann M. Mass spectrometric sequencing of proteins from silver-stained polyacrylamide gels. *Anal Chem.* 1996;68(5):850-858.

4. Redestig H, Fukushima A, Stenlund H, et al. Compensation for systematic cross-contribution improves normalization of mass spectrometry based metabolomics data. *Anal Chem*. 2009;81(19):7974-7980.

5. Lambert JP, Ivosev G, Couzens AL, et al. Mapping differential interactomes by affinity purification coupled with data-independent mass spectrometry acquisition. *Nat Methods.* 2013;10(12):1239-1245.

6. López-López M, Regueiro U, Bravo S, et al. Tear proteomics in keratoconus: A quantitative SWATH-MS analysis. *Invest Ophthalmol Vis Sci*. 2021;62(10).

7. Pereira-Veiga T, Bravo S, Gómez-Tato A, et al. Red Blood Cells Protein Profile Is Modified in Breast Cancer Patients. *Mol Cell Proteomics*. 2022;21(12).

8. Álvarez J V., Bravo SB, Chantada-vázquez MP, et al. Plasma Proteomic Analysis in Morquio A Disease. *Int J Mol Sci*. 2021;22(11).

9. Álvarez VJ, Bravo SB, Chantada-Vazquez MP, et al. Characterization of New Proteomic Biomarker Candidates in Mucopolysaccharidosis Type IVA. *Int J Mol Sci.* 2020;22(1):1-22.

10. Gómez-Cid L, López-Donaire ML, Velasco D, et al. Cardiac Extracellular Matrix Hydrogel Enriched with Polyethylene Glycol Presents Improved Gelation Time and Increased On-Target Site Retention of Extracellular Vesicles. *Int J Mol Sci*. 2021;22(17).

Supplementary Results S3

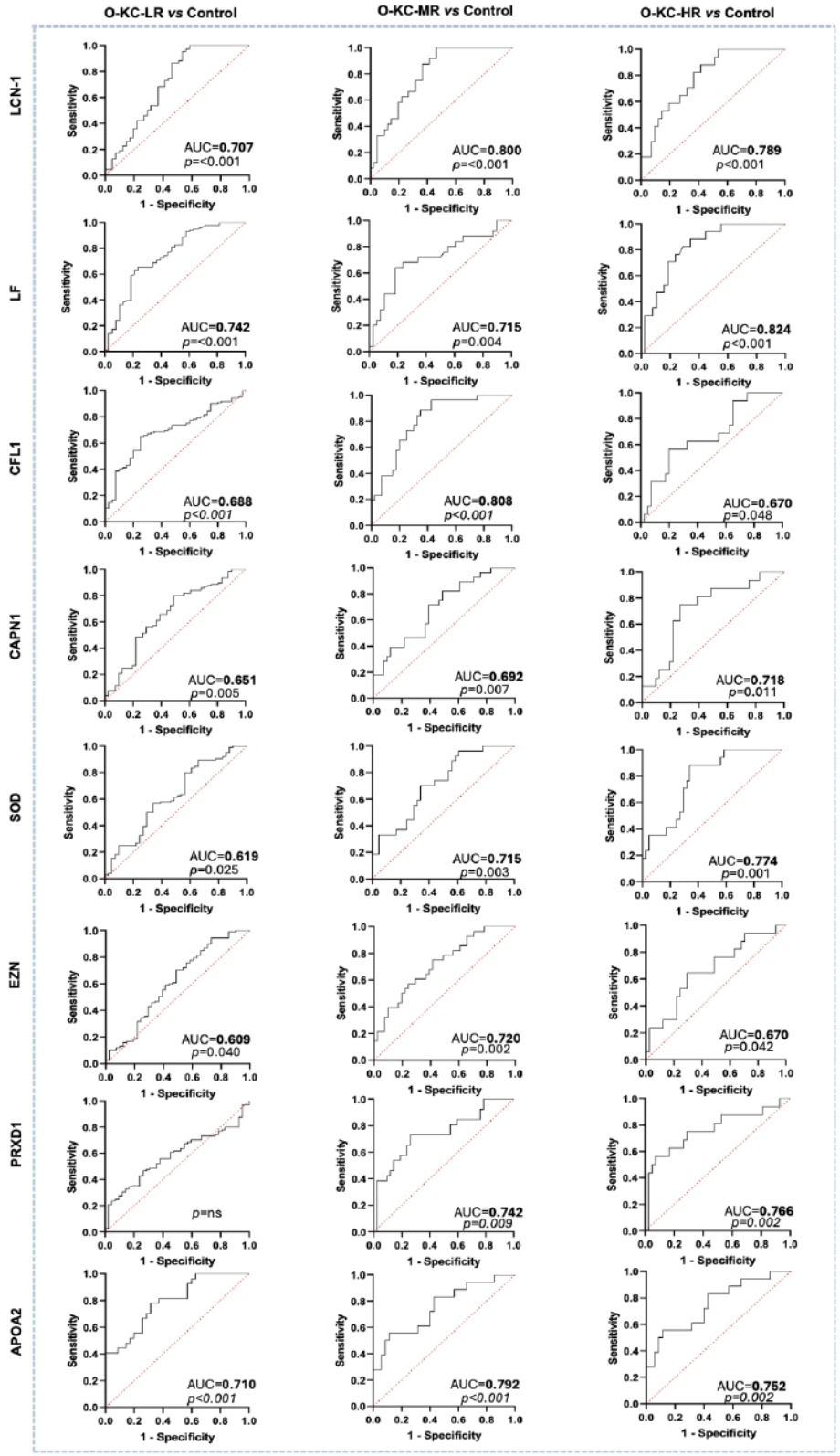


Figure S3. Receiver operating characteristic curve (ROC) analysis of dysregulated tear proteins in O-KC samples to predict with the highest sensitivity and specificity the alterations in the corneal biomechanical properties, as well as the risk associated with having a first-degree family member with KC.

Table S3. Cut-off values of the dysregulated tear proteins for each condition.

	O-KC-LR vs control			O-KC-MR vs control			O-KC-LR vs control		
	Sensitivity	Specificity	Cut-off	Sensitivity	Specificity	Cut-off	Sensitivity	Specificity	Cut-off
LCN-1	65%	64%	$< 4.56x10^4$	70%	70%	$< 2.79x10^4$	71%	68%	$< 3.20x10^4$
LF	70%	66%	$< 5.88x10^5$	72%	66%	$< 5.74x10^5$	82%	71%	$< 5.41x10^5$
CFL1	67%	70%	$< 1.27x10^3$	73%	75%	$< 1.20x10^3$	63%	68%	$< 1.31x10^3$
CAPN1	60%	63%	$< 2.51x10^3$	71%	60%	$< 2.64x10^3$	75%	73%	$< 2.29x10^3$
SOD1	58%	61%	$< 5.83x10^2$	70%	66%	$< 5.64x10^2$	71%	71%	$< 4.87x10^2$
EZN	60%	60%	$< 4.51x10^3$	61%	70%	$< 3.39x10^3$	65%	71%	$< 3.45x10^3$
PRXD1	ns	-	-	73%	71%	$< 5.72x10^3$	75%	71%	$< 5.82x10^3$
APOA2	66%	66%	$> 2.72x10^3$	70%	71%	$> 3.39x10^3$	72%	60%	$> 2.31x10^3$

Sample size: O-KC-LR (eyes of offspring of KC patients with low risk of ectasia development, n=114 eyes), **O-KC-MR** (eyes of offspring of KC patients with moderate risk of ectasia development, n=28 eyes), **O-KC-HR** (eyes of offspring of KC patients with a high risk of ectasia development, n=18 eyes).
Proteins: **LCN-1** (Lipocalin-1), **LF** (Lactoferrin), **CFL1** (Cofilin-1), **CAPN1** (Calpain-1 catalytic subunit), **SOD** (Superoxide Dismutase), **EZR** (Ezrin), **PRDX1** (Peroxiredoxin-1), **APOA2** (Apolipoprotein A-II).

Chapter 4

Clinical and molecular outcomes of the three-year follow-up of offspring of keratoconus patients

Maite López-López[1,2]*, Uxía Regueiro[1,2*#], Yaiza Pastoriza[1,2], Tania Alvite-Piñeiro[1,2], Isabel Lema[1,2,3#].

[1] Corneal Neurodegeneration Group (RENOIR). Clinical Neurosciences Research Laboratory (LINC), Health Research Institute of Santiago de Compostela (IDIS), Santiago de Compostela, Spain.
[2] Department of Surgery and Medical-Surgical Specialties. Faculty of Optics and Optometry, University of Santiago de Compostela (USC), Santiago de Compostela, Spain.
[3] Instituto Galego de Oftalmoloxía (INGO), Complexo Hospitalario Universitario de Santiago (CHUS), Santiago de Compostela, Spain.

* These authors have equally contributed to this work as First Authors.
[#] These authors have equally contributed to this work as Corresponding Authors.
- This manuscript has not yet been submitted to any scientific journal.

Author contribution. López-López M contributed to the conceptualization, design, formal analysis and investigation, writing and original draft preparation of this manuscript.

Abstract

Background: Keratoconus (KC) is a progressive corneal ectasia that remains one of the leading causes of corneal keratoplasty worldwide with limited visual recovery. The higher risk reported in first-degree relatives of KC patients coupled with the higher concordance of disease in monozygotic over dizygotic twins support the strong genetic component of KC disease. In addition, corneal biomechanical weakness constitutes a hallmark of early KC stages, so, the main purpose of this study was to analyze the corneal biomechanical and tomographical properties, as well as the evolution of LF expression (associated with biomechanical instability) during a three-year follow-up in young offspring of KC patients (O-KC).

Methods: This prospective cohort study included 80 young O-KC participants aged between 8 and 18. Corneal biomechanical-tomographical studies and tear fluid extraction for LF expression quantification were examined twice: at the baseline visit and during the second visit (three years later); in order to check the evolution of clinical-molecular markers and their association with biomechanical weakness and to assess the potential disease onset after 3 years. O-KC eyes were classified based on their biomechanical behavior (CBI index) as low, moderate, or high risk of ectasia development (O-KC-LR, O-KC-MR, and O-KC-HR respectively). Data analysis was performed using SPSS and GraphPad Prism, and LF expression was quantified by ELISA.

Results: 21% of the eyes within the O-KC-LR group at the beginning of the study progressed to moderate or high-risk states after 3 years follow-up. 39% of the O-KC-MR eyes progressed to a high-risk state, and also 39% from the O-KC-HR eyes exhibited a progressive impairment of corneal biomechanics evidenced by increasingly higher CBI values, or even tomographic markers compatible with corneal ectasia, after the follow-up. Biomechanical deterioration was associated with alterations in the deformation amplitude values (DAmax, DARatio max, and A1DA), time and velocity of corneal applanation, and mainly, abnormalities in the pachymetric progression indexes (Pachy slope and ARTh). No differences ($p>0.05$) were observed for LF expression between pre- and post- follow-up for either group of biomechanical decline; however, LF expression was statistically lower ($p<0.05$) in all study groups compared to the data reported from control subjects.

Conclusions: Our results support the vulnerability of KC offspring for corneal biomechanical weakness and disease development. Changes in corneal thickness progression seems to be the earliest detectable sign of corneal biomechanical decline, and LF downregulation is apparently related to KC family history but not with the early biomechanical decline.

Background

Keratoconus (KC) is a progressive corneal ectasia characterized by biomechanical instability, thinning, and protrusion of the corneal tissue.[1] The steep and sharply asymmetric final corneal shape induces high irregular astigmatism and increased magnitudes of higher-order aberrations, leading to a significant visual impairment.[2] KC affects all ethnicities and both sexes, and usually begins in adolescence (or even earlier) and progresses up to 30-40 years of age, causing a strong impact throughout the patient's life.[3]

Pediatric KC developed at younger ages (<12 years) has been described as a more aggressive condition, with a faster progression and often reaching more severe stages than when it develops in late adolescence.[4,5] Up to 28% of pediatric KC cases present with advanced disease severity at diagnosis, underlining the challenge of early detection and risk factor identification, as severe KC still ranks as one of the most frequent causes of corneal keratoplasty with limited visual recovery.[6]

The multifactorial nature of KC involves mechanical-environmental factors (such as eye rubbing and its underlying causes) which heavily influence its progression, and genetic factors which determine the predisposition and risk of developing the disease. Whereas KC tends to appear sporadically with no Mendelian patterns of inheritance to support its origin, KC relatives have shown between 15 to 67 times higher risk of developing the disease than the population with no family history of KC.[7] In addition, available data at present indicates that up to 26% of patients with KC report a positive family history of this disease, and the presence of two or more relatives with KC within the family has been associated with increased disease progression and severity.[8,9] In this sense, these findings suggest the influence of inheritance in KC etiopathogenesis, making family history one of the main risk factors associated with its development.

From a clinical view, the arrival and optimization of new tools to assess *in vivo* corneal biomechanical behavior allowed a further step in the clinical detection of the most subtle changes of the disease, determining that the reduction of corneal stiffness and strength constitute the earliest structural alterations in KC and promote tissue protrusion under the influence of intraocular pressure.[10,11] Under this assumption, the evaluation of the biomechanical behavior of the corneal tissue seems essential in the early screening of KC. From the molecular view, KC pathophysiology has been gradually unraveled thanks to the wide variety of studies focused on deeply understanding the biological bases of its pathogenesis. In this way, although the biochemical complexity of KC is not yet fully understood, processes linked to inflammation and oxidative stress appear to play a critical role in the cellular degeneration of the corneal tissue during the disease development.[12-15]

Based on the above, searching for specific biomarkers associated with biomechanical imbalance becomes imperative for in-depth understanding of KC disease and future

development of new therapeutic strategies. To this end, the main objective of this work was to analyze the corneal biomechanical and tomographical corneal properties, as well as the evolution of one molecular marker (Lactoferrin, LF) (previously associated with biomechanical instability) during a three-year follow-up in a sensitive population to ectasia development such as KC patient's offspring (O-KC).

Methods

Study design, clinical measurements, and participants

Study design

This prospective cohort study was performed following the principles of the Declaration of Helsinki of the World Medical Association. The chronological study design included a baseline ophthalmological visit (with corneal biomechanical-tomographical studies and tear fluid extraction for molecular analysis) and a second visit (three years later) repeating all procedures and checking the evolution of the clinical and molecular markers. Regarding sample size, a total of 160 eyes from 80 O-KC participants were involved. In terms of ethnicity, all participants in this study reported European ancestry. The ophthalmologic clinical protocol and the extraction of biological samples were approved by the Ethics Committee for Clinical Research of Galicia (2019/623). Study objectives, ophthalmologic procedures, collection of biological samples, and potential undesirable events associated with the biological sample extraction were described in the consent form requested from all study participants. All tests were performed by the same researchers. The ophthalmologic exploration included anamnesis, ocular health examination, corneal biomechanical and tomographical studies, and tear sample extraction using Schirmer Strips. Demographic data, as well as any information about ocular and medical history (allergies, asthma, rhinitis, atopic dermatitis, or other conditions that might be relevant to this study) were included in the anamnesis. In addition, family history of corneal ectasia or other ocular conditions was also documented.

Clinical measurements

The scanning of the biomechanical behavior of the corneal tissue was performed using the Corvis® ST device (Oculus, Wetzlar, Germany), a non-contact tonometer optimized to assess the dynamic response of the corneal tissue to an air puff. During the measurement cycle, the cornea undergoes a stress-strain process involving three stages of deformation. In this line, Corvis® ST uses an ultra-high-speed Scheimpflug camera to monitor corneal deformation and record all parameters related to the different corneal deformation processes, comparing them directly with the expected values and integrating highly specific indexes for the detection of the biomechanical anomalies related to the development of corneal ectasia. Three measurements were made three times per eye, and the average of the obtained values was calculated. The parameters studied included:

biomechanical corrected intraocular pressure (bIOP), time from the beginning of the air-puff until the first/second applanation (A1T/A2T), velocity of the corneal apex during the first/second applanation (A1V/A2V), time from the initiation of the air-puff until the highest corneal concavity (HCT), deformation amplitude (DA) at the first/second applanation (A1DA, A2DA), maximum deformation amplitude (DAmax), deformation amplitude at the highest corneal concavity (HCDA), deflection length at the first/second applanation (A1DLL/A2DLL), highest concavity deflection length (HCDLL), deflection amplitude at the fist/second applanation (A1DLA, A2DLA), deflection amplitude at maximum deformation (HCDLA), deflection area at the first/second applanation (A1DLAr, A2DLAr), deflection area at maximum deformation (HCDLAr), peak distance at the highest concavity (defined as the distance between two corneal peaks at the highest concavity, PD), DA Ratio Max (1 mm) and DA Ratio Max (2 mm) described as the maximum ratio of DA measured at 1 or 2 mm from the center of the cornea (with higher values suggesting less resistance to corneal deformation), integrated radius (IR), maximum value of the radius of curvature during the concave phase of the deformation (Max Inverse Radius), central corneal thickness (CCT), Ambrósio Relational Thickness horizontal (ARTh), changes of corneal thickness from the corneal center to the periphery averagely determined at 2.5mm from the apex (Pachy Slope), stiffness parameter at the first applanation (SP-A1), Corvis Biomechanical Index (CBI), and Stress-Strain Index (SSI).

Pentacam® HR (Oculus, Wetzlar, Germany) was used to analyze the corneal tomography. The parameters evaluated included the corneal central power (PDC), keratometry in the flattest meridian (K1), keratometry in the steeper meridian (K2), maximum dioptric power (Kmax), inferior-superior dioptric asymmetry (I-S asymmetry), maximum Ambrósio Relational Thickness (ARTmax), central corneal thickness (CCT), minimum thickness point (MTP), anterior and posterior surfaces elevation (AE and PE), total deviation value (BAD-D) and the Tomographic and Biomechanical Index (TBI).
Slit-lamp biomicroscopy evaluation was performed to determine the presence of ophthalmologic signs compatible with KC or other ocular surface conditions.

Study subjects

This study included 80 young O-KC recruited at the Instituto Galego de Oftalmoloxía (INGO) in Santiago de Compostela, Spain. The main inclusion criterion to be enrolled in the study was having a biological parent diagnosed with clinical KC, supported by slit-lamp examination and corneal topographical and tomographical exams. In addition, corneal features of these subjects could be compatible with normal corneal architecture, subclinical state of KC, or clinical manifestation of the disease. This study involved the same participants who were enrolled in our last work *"Tear proteomic analysis from offspring of keratoconus patients: new insights into corneal biomechanical weakness & disease risk stages"*. Moreover, inclusion requirements were Schirmer test >15mm in 5 minutes (min), conjunctival hyperemia <2 (Nathan Efron scale)[16], and at least 5 days without contact lenses, artificial tears, or eye drops. Evidence of other corneal diseases,

active ocular or systemic inflammation, anterior segment surgery, current treatment with local or systemic anti-inflammatory drugs, and/or some systemic diseases (such as renal, hepatic, or hematologic diseases) were considered exclusion criteria for the study.

Study groups

To address one of the main objectives of this study, focused on detecting biomechanical instability and higher risk of developing ectasia, the eyes of the O-KC participants were classified according to the CBI biomechanical index.[10] CBI index is calculated by combining the maximum inverse radius (MaxInverseRadius), the maximum DA ratio (2 mm), the horizontal thickness profile (ARTh), and the stiffness parameter at first applanation (SP-A1) in linear regression, obtaining an index with high accuracy (98.4% of sensitivity and 100% specificity) to detect the biomechanical alterations that could promote the ectasia development.

During the initial appointment, O-KC eyes were classified as follows: **(i)** Eyes of offspring of KC patients with low-risk of ectasia development [CBI<0.25] (**O-KC-LR** group), **(ii)** Eyes of offspring of KC patients with moderate-risk of ectasia development [CBI 0.25-0.50] (**O-KC-MR** group), and **(iii)** Eyes of offspring of KC patients with a high-risk of ectasia development [CBI >0.50] (**O-KC-HR** group).

After three years, the eyes were reclassified according to the updated CBI values. As a result, we differentiated between those eyes that maintained biomechanical values similar to the initial ones and those that showed a decline towards stages of higher biomechanical instability, discriminating between: **(i)** the O-KC-LR eyes that progressed to a moderate [**O-KC-LR_MR**] or high [**O-KC-LR_HR**] risk stages; **(ii)** the O-KC-MR that progressed to a high-risk stage [**O-KC-MR_HR**]; and **(iii)** the O-KC-HR that experienced a progression increasing their CBI value [**O-KC-HR_prog**].

Sample extraction and analysis

Sample extraction

Tear fluid samples were extracted using Schirmer strips (Tear Strips, Contacare Ophthalmics & Diagnostics, Gujarat, India). Strips were placed over the lower eyelid about 3mm from the lateral edge and were removed when the sample reached 15mm on the Schirmer scale (9µL), remaining in contact with the ocular surface for less than 5 min. Tear samples were extracted under suitable environmental conditions and without previous administration of drugs, artificial tears, or vital dyes. Immediately after collection, the strips were frozen and stored at −80°C until their analysis.

Sample processing

For tear analysis by ELISA, firstly, the Schirmer's strips were thawed cold for 30min. Subsequently, for protein extraction, Schirmer strips were cut and incubated for 1 hour (h) at room temperature (RT) in a 100µL solution of 100 mM ammonium bicarbonate. Samples were centrifuged for 20 min at 13000 x g, and the supernatant was placed in a new Eppendorf tube.

ELISA analysis

LF expression was measured in human tears using a commercial kit of Enzyme-Linked Immunosorbent Assay (ELISA) from FineTests® (LF_ELISA kit catalog number EH0396). The assay was carried out following the manufacturer's protocol using a 1:100000 dilution factor. Tear samples were assayed in duplicate, and mean expression values were reported as ng/mL. Curve Expert 1.4 and Microsoft Excel were used for curve and data analysis, and graphs were performed using GraphPad Prism 8.0 (San Diego, CA, USA).

To compare LF expression between O-KC groups and healthy controls, we referenced control data from our previous study ("*Tear proteomic analysis from offspring of keratoconus patients: new insights into corneal biomechanical weakness & disease risk stages*"). This last study, which employed the same ELISA kit and identical sample processing and analysis protocols, included control subjects matched for age and sex with the O-KC groups examined in this manuscript.

Statistical analysis

SPSS 29.0 (IBM, USA) for Mac and GraphPad Prism 8.0 (San Diego, CA, USA) were used for statistical analysis. Kolmogorov-Smirnov test was performed to confirm the normality of the quantitative variables. Categorical variables were represented as percentages. Mean ± standard deviation (SD) was used to represent continuous quantitative variables with a normal distribution, and variables with a non-normal distribution were presented as median [interquartile range, IQR]. Bivariate comparisons were performed using the chi-square test (for categorical variables), and t-student (parametric) or u-Mann-Whitney (non-parametric) test for continuous variables according to their normality. Comparisons between more than two groups were performed using the ANOVA or Kruskal-Wallis test depending on the normality. The paired samples t-test was used to evaluate comparisons after follow-up. $p<0.05$ value was considered statistically significant in all tests.

Results

Demographic and clinical data

A total of 160 eyes from 80 O-KC were included in this study. In the first visit all eyes were categorized based on the CBI index, obtaining the following three O-KC groups: **(i)**

114 eyes in the O-KC-LR group [CBI<0.25]; **(ii)** 28 eyes in the O-KC-MR group [CBI 0.25-0.50]; and **(iii)** 18 eyes in the O-KC-HR group [CBI>0.50].

As for demographic data, groups having moderate-high alterations in the corneal biomechanical properties showed slightly higher ages than the low-risk group. Specifically, the mean age was 10±3 years for O-KC-LR group, 13±2.5 years for O-KC-MR, and 16±3.7 years for O-KC-HR group. Regarding clinical variables, participants of the O-KC-MR and O-KC-HR groups showed a trend toward a higher percentage of allergic conditions than the low-risk group. No differences were observed regarding sex, eye itching, or eye rubbing. **Table 1** lists the demographic and clinical data among the O-KC groups.

Table 1. Demographic and clinical data among O-KC groups

Variables	O-KC LR	O-KC MR	$p^{\#1}$	O-KC HR	$p^{\#2}$	$p^{\#3}$
Age [years]	10±3.00	13±2.50	**0.010**	16±3.70	**0.002**	0.348
Sex [% male]	54.20	53.30	1.000	66.70	0.707	0.678
Allergic disease [%]	18.20	30.00	0.212	30.00	0.417	1.000
Eye itching [%]	24.50	24.00	0.958	18.80	0.759	1.000
Eye rubbing [%]	24.50	20.00	0.795	18.80	0.759	1.000

Sample size: O-KC-LR (59 O-KC participants), **O-KC-MR** (19 O-KC participants), **O-KC-HR** (10 O-KC participants).
[#1] **O-KC-LR compared to O-KC-MR** [#2] **O-KC-LR compared to O-KC-HR** [#3] **O-KC MR compared to O-KC-HR**

Assessment of the corneal biomechanical properties and tomographic profile of O-KC groups at the beginning of the study

Corneal biomechanics were assessed using the Corvis® ST device and the tomographic profile was determined using the Pentacam® HR. **Table 2** summarizes the values obtained for corneal strain behavior, pachymetry progression and stiffness, as well as the tomographic parameters of the three O-KC groups at the beginning of the study (first visit).

Table 2. Comparison of biomechanical data and tomographic parameters among O-KC groups in the first visit.

	Parameters	O-KC LR (n=114 eyes)	O-KC MR (n=28 eyes)	p#1	O-KC HR (n=18 eyes)	p#2	p#3
Corvis® ST	**bIOP** [mmHg]	16.24±1.88	15.84±2.20	0.364	15.15±1.90	0.053	0.290
	A1T [ms]	7.44±0.25	7.24±0.24	**0.005**	7.18±0.22	**0.003**	1.000
	A1V [m/s]	0.14±0.01	0.15±0.02	0.711	0.16±0.02	**0.049**	1.000
	A2T [ms]	22.01±0.32	22.20±0.47	0.205	22.14±0.30	1.000	1.000
	A2V [m/s]	-0.25±0.06	-0.27±0.03	1.000	-0.28±0.03	0.470	1.000
	HCT [ms]	17.29±0.52	17.44±'.52	1.000	17.25±0.54	1.000	1.000
	DAmax [mm]	1.06±0.09	1.12±0.10	**0.041**	1.15±0.09	**0.006**	1.000
	A1DA [mm]	0.15±0.01	0.14±0.01	**0.016**	0.15±0.01	0.536	0.124
	A2DA [mm]	0.42±0.06	0.42±0.04	0.752	0.39±0.05	0.092	0.079
	HCDA [mm]	0.86±0.09	0.91±0.09	0.064	0.97±0.10	**0.001**	0.643
	A1DLL [mm]	2.36±0.16	2.32±0.12	0.504	2.32±1.14	1.000	1.000
	A2DLL [mm]	3.21±0.67	3.01±0.86	1.000	2.85±0.83	0.659	1.000
	HCDLL [mm]	6.43±0.40	6.57±0.27	1.000	6.61±0.43	1.000	1.000
	A1DLA [mm]	0.10±0.01	0.09±0.01	**0.039**	0.10±0.01	0.956	0.140
	A2DLA [mm]	0.12±0.01	0.11±0.01	0.221	0.10±0.01	0.053	0.454
	HCDLA [mm]	0.86±0.09	0.92±0.09	**0.003**	0.97±0.10	**0.001**	0.076
	A1DLAr [mm]	0.20±0.03	0.18±0.02	**0.020**	0.20±0.02	0.414	0.064
	A2DLAr [mm]	0.26±0.05	0.25±0.08	0.316	0.25±0.05	0.244	0.856
	HCDLAr [mm]	3.07±0.45	3.31±0.46	**0.008**	3.57±0.53	**0.001**	0.121
	PD [mm]	4.92±0.27	5.09±0.19	**0.035**	5.11±0.26	0.059	1.000
	DARatio max [1mm]	1.52±0.05	1.55±0.04	**0.004**	1.58±0.05	**0.000**	0.073
	DARatio max [2mm]	4.06±0.32	4.36±0.30	**0.002**	4.76±0.52	**0.000**	**0.004**
	IR [mm^{-1}]	7.79±0.87	8.43±0.82	**0.022**	9.37±1.27	**0.000**	**0.018**
	MaxInverseRadius [mm^{-1}]	0.162±0.06	0.173±0.01	0.285	0.188±0.02	0.052	0.348
	CCT [µm]	549±33	519±24	**0.001**	509±30	**0.001**	1.000
	ARTh	685±161	529±137	**0.000**	418±108	**0.000**	0.276
	Pachy Slope [µm]	34±8	38±7	0.355	44±12	**0.000**	0.152
	SP-A1	100±12	87±13	**0.000**	81±13	**0.000**	1.000
	CBI	0.17±0.14	0.50±0.10	**0.001**	0.75±0.22	**0.001**	**0.001**
	SSI	0.99±0.15	0.96±0.14	1.000	0.83±0.15	**0.000**	0.062
Pentacam® XR	**PDC** [D]	43.28±1.22	43.01±1.28	0.537	45.97±5.52	**0.001**	**0.001**
	Kmax [D]	44.12±1.26	43.99±1.50	0.790	48.79±6.76	**0.001**	**0.001**
	I-S asymmetry [D]	-0.05±0.57	0.07±0.87	0.562	1.42±2.69	**0.001**	**0.001**
	ARTmax [µm]	455±91	401±68	**0.003**	287±79	**0.001**	**0.001**
	CCT [µm]	549±33	519±25	**0.001**	510±30	**0.001**	0.301
	MTP [µm]	546±32	516±24	**0.001**	504±30	**0.001**	0.191
	AE [µm]	3.00[2.00]	3.00[3.00]	0.965	4.50[7.00]	**0.001**	**0.001**
	PE [µm]	6.50[8.00]	7.00[11.00]	0.898	11.00[29.75]	**0.001**	**0.001**
	BAD-D	0.75[0.84]	1.31[0.90]	**0.028**	1.94[1.96]	**0.001**	**0.001**
	TBI	0.08[0.18]	0.20[0.47]	**0.001**	0.65[0.85]	**0.001**	**0.001**

Sample size: O-KC-LR (eyes of offspring of KC patients with low-risk of ectasia development, n=114 eyes), **O-KC-MR** (eyes of offspring of KC patients with moderate-risk of ectasia development, n=28 eyes), **O-KC-HR** (eyes of offspring of KC patients with a high-risk of ectasia development, n=18 eyes). **Corvis ST parameters: bIOP** [biomechanical corrected intraocular pressure], **A1T/A2T** [first/second applanation time], **A1V/A2V** [first/second applanation velocity], **HCT** [time to the highest concavity], **DAmax** [deformation amplitude], **A1DA/A2DA** [deformation amplitude at the fist/second applanation], **HCDA** [deflection amplitude at highest corneal concavity], **A1DLL/A2DLL** [first/second applanation deflection length], **HCDLL** [highest concavity deflection length], **A1DLA/A2DLA** [deflection amplitude at the fist/second applanation], **HCDLA** [deflection amplitude at maximum deformation], **A1DLAr/A2DLAr** [deflection area at the first/second applanation], **HCDLAr** [deflection area at maximum deformation], **PD** [peak distance at the highest concavity], **DAratio max 1mm** [maximum deformation amplitude ratio at 1mm], **DAratio max 2mm** [deformation amplitude ratio max 2mm], **IR** [integrated radius], **Max Inverse Radius** [maximum inverse radius], **CCT** [central corneal thickness], **ARTh** [Ambrósio Relational Thickness horizontal], **Pachy Slope** [changes of corneal thickness from the corneal center to the periphery], **SP-A1** [stiffness parameter at the first applanation], **CBI** [Corvis Biomechanical Index], and **SSI** [Stress-Strain Index].
Pentacam XR parameters: **PDC** [corneal central power], **K1** [keratometry in the flattest meridian], **K2** [keratometry in the steeper meridian], **Kmax** [maximum dioptric power], **I-S asymmetry** [inferior-superior dioptric asymmetry], **ARTmax** [maximum Ambrósio Relational Thickness], **CCT** [central corneal thickness], **MTP** [minimum thickness point], **AE/PE** [anterior and posterior surfaces elevation], **BAD-D** [total deviation value], and **TBI** [Tomographic and Biomechanical Index].
#1 O-KC-LR compared to O-KC-MR #2 O-KC-LR compared to O-KC-HR #3 O-KC MR compared to O-KC-HR.

Many differences were observed in the biomechanical assessment among O-KC groups. First, compared to the O-KC-LR group, O-KC-MR showed differential values for deformation parameters (DAmax, HCDLA, HCDLAr, PD, DARatiomax1mm, DARatiomax2mm, and IR), pachymetric metrics (CCT, and ARTh) and stiffness data (SP-A1), reflecting increased corneal deformation, reduced corneal thickness, and lower

corneal strength. As expected, in the O-KC-HR group, these differences increased, and several parameters (such as applanation velocity and time (A1T, A2V), maximal deformation at maximum concavity (HCDA), and stress-strain index (SSI)) highlighted a further deterioration of biomechanical stability.

When comparing the moderate and high-risk groups, DARatio max 1mm and DARatio max 2mm were the distinguishing parameters between both groups. These two parameters reach greater values in the O-KC-HR, describing less resistance for the cornea deformation (or a softer cornea) and a higher decline of the viscoelastic properties.

In agreement with the biomechanical findings, at the tomographic level variables related to central pachymetry (CCT), minimum corneal thickness point (MTP), and the maximum Ambrósio Relational Thickness value (ARTmax) differed when comparing the O-KC-LR and O-KC-MR groups; showing the O-KC-MR group lower values in all pachymetry parameters in comparison to the O-KC-LR. Regarding O-KC-HR, all variables studied including corneal curvature (PDC, K1, K2, Kmax), asymmetry (I-S asymmetry), pachymetry (ARTmax, CCT, MTP), anterior and posterior elevation (AE, PE), and ectasia risk index (BAD-D, TBI) showed statistical differences in comparison to the O-KC-LR group.

Lastly, tomographic analysis between O-KC-MR and O-KC-HR revealed higher values in the high-risk eyes for all morphological variables except for the pachymetric metrics. Predictably, the O-KC-HR showed steeper and asymmetrical corneas, with increased anterior and posterior elevation values, lower pachymetric thickness, and, consequently, higher values of ectasia-risk indexes.

Due to the differences observed in the age of three study groups, a correlation analysis was performed to determine whether any of the variables significantly different between O-KC groups would be associated with this factor. The intra-group correlation analysis showed no statistical associations between the age and the differential variables among O-KC groups (A1T, A1V, DAmax, A1DA, HCDA, A1DLA, HCDLA, A1DLar, HCDLAr, PD, DARatio max [1mm], DARatio max [2mm], IR, CCT, ARTh, Pachy Slope, SP-A1, CBI, and SSI).

Assessment of the corneal biomechanics and tomography after three years follow-up

To achieve one of the main objectives of this study, after three years all participants underwent further corneal biomechanics and tomography tests. This follow-up allowed differentiation among O-KC eyes that maintained their corneal biomechanical properties and those that progressed with corneal weakening. As a result, the 79% of the O-KC-LR eyes, the 61% of the O-KC-MR eyes, and the 61% of the O-KC-HR eyes maintained their

biomechanical properties, while the remaining ones suffered a biomechanical decline toward a corneal weakening trend.

In this way, study eyes were reclassified according to the updated CBI values. To guarantee precise outcomes, biomechanical and tomographical data were scrutinized exclusively for those eyes that exhibited a biomechanical deterioration in the three-year follow-up period. Based on this, we discriminate between the O-KC-LR eyes that progressed to moderate- or high-risk stages, the O-KC-MR that progressed to a high-risk stage, and the O-KC-HR that experienced an increase in their CBI values.

Characterization of the biomechanical and tomographical evolution on O-KC-LR cohort

Regarding the low-risk group, from the initial cohort that included 114 eyes, 18 eyes (16%) progressed to a moderate-risk [O-KC-LR_MR] and six eyes (5%) evolved to a high-risk stage [O-KC-LR_HR], representing a biomechanical decline after three years in the 21% of the eyes. **Table 3** shows the biomechanical and tomographical data of O-KC-LR that progressed into another risk group [O-KC-LR_MR or O-KC-LR_HR] after the follow-up.

Table 3. Comparison of biomechanical and topographical data of O-KC-LR progressive cases before and after three years follow-up.

		O-KC-LR_MR			O-KC-LR_HR		
	Parameters	**First visit** (n=18 eyes)	**Follow-up** (n=18 eyes)	$p^{\#1}$	**First visit** (n=6 eyes)	**Follow-up** (n=6 eyes)	$p^{\#2}$
Corvis® ST	**bIOP** [mmHg]	16.27±1.62	16.30±2.13	0.946	16.21±0.76	16.65±1.39	0.488
	A1T [ms]	7.41±0.25	7.37±0.31	0.537	7.31±0.08	7.26±0.19	0.390
	A1V [m/s]	0.15±0.01	0.14±0.02	**0.032**	0.15±0.01	0.14±0.02	0.122
	A2T [ms]	22.04±0.28	22.18±0.35	**0.030**	22.27±0.23	22.33±0.37	0.398
	A2V [m/s]	-0.26±0.03	-0.28±0.03	**0.003**	-0.28±0.03	-0.28±0.02	0.819
	HCT [ms]	17.20±0.53	17.73±0.32	**0.002**	17.01±0.66	17.44±0.43	0.088
	DAmax [mm]	1.08±0.09	1.08±0.09	0.937	1.18±0.11	1.10±0.08	0.129
	A1DA [mm]	0.14±0.01	0.14±0.01	0.336	0.16±0.03	0.14±0.01	0.251
	A2DA [mm]	0.42±0.04	0.43±0.04	0.395	0.40±0.04	0.39±0.05	0.696
	HCDA [mm]	1.07±0.09	1.08±0.09	0.937	0.95±0.07	0.91±0.05	0.129
	A1DLL [mm]	2.36±0.16	2.36±0.15	0.872	2.24±0.11	2.24±0.05	0.942
	A2DLL [mm]	3.13±0.72	3.14±0.61	0.977	3.01±0.75	2.72±0.30	0.551
	HCDLL [mm]	6.54±0.44	6.35±0.60	0.105	6.66±0.45	6.35±0.28	0.074
	A1DLA [mm]	0.10±0.01	0.10±0.01	0.234	0.09±0.01	0.10±0.01	0.260
	A2DLA [mm]	0.11±0.01	0.12±0.01	0.080	0.12±0.01	0.12±0.01	0.476
	HCDLA [mm]	0.88±0.09	0.87±0.10	0.346	0.95±0.07	0.91±0.05	0.159
	A1DLAr [mm]	0.20±0.02	0.19±0.03	0.191	0.19±0.02	0.17±0.02	0.170
	A2DLAr [mm]	0.26±0.06	0.26±0.05	0.893	0.26±0.04	0.25±0.03	0.769
	HCDLAr [mm]	3.18±0.47	3.09±0.58	0.312	3.48±0.45	3.23±0.25	0.108
	PD [mm]	4.99±0.27	4.89±0.33	**0.017**	5.12±0.22	4.96±0.12	0.117
	DARatio max [1mm]	1.53±0.05	1.54±0.04	0.375	1.50±0.06	1.55±0.02	0.127
	DARatio max [2mm]	4.13±0.31	4.19±0.28	0.389	3.96±0.46	4.21±0.14	0.246
	IR [mm^{-1}]	7.80±0.66	8.32±0.62	**0.002**	8.37±0.86	8.51±0.63	0.608
	MaxInverseRadius [mm^{-1}]	0.17±0.01	0.17±0.02	0.138	0.23±0.15	0.17±0.02	0.339
	CCT [µm]	544.65±17.18	542.45±19.94	0.374	525.00±11.49	518.14±12.16	0.081
	ARTh	632.91±121.44	546.48±57.06	**0.003**	567.69±153.52	450.45±79.71	**0.016**
	Pachy Slope [µm]	35.44±6.69	42.97±6.00	**0.001**	39.18±5.85	49.80±8.78	**0.008**
	SP-A1	96.45±13.13	95.51±13.53	0.745	95.08±5.98	89.90±7.16	0.092
	CBI	0.16±0.08	0.42±0.07	**0.001**	0.22±0.10	0.65±0.10	**0.001**
	SSI	0.98±0.15	0.94±0.12	0.079	0.88±0.16	0.89±0.13	0.928
Pentacam® XR	**PDC** [D]	43.17±1.01	42.90±0.92	0.075	43.34±0.51	43.04±0.69	0.054
	Kmax [D]	43.90±0.95	43.86±0.76	0.776	44.05±0.49	44.21±0.49	0.368
	I-S asymmetry [D]	0.03±0.65	-0.01±0.62	0.669	0.17±0.46	0.13±0.44	0.671
	ARTmax [µm]	436.00±52.87	438.80±55.69	0.836	445.28±73.87	428.00±85.52	0.459
	CCT [µm]	544.65±17.19	542.45±19.94	0.374	525.00±11.50	518.14±12.16	0.081
	MTP [µm]	541.50±16.20	538.15±19.15	0.196	523.71±13.41	513.42±14.52	0.068
	AE [µm]	3.00[1.00]	4.00[2.25]	0.174	3.00[2.00]	3.00[3.00]	0.270
	PE [µm]	5.00[3.25]	9.00[5.75]	**0.013**	6.00[8.00]	4.00[7.00]	0.102
	BAD-D	0.86±0.40	0.89±0.47	0.744	1.10±0.65	1.21±0.62	0.281
	TBI	0.13±0.15	0.18±0.24	0.378	0.20±0.21	0.16±0.21	0.451

Sample size: O-KC-LR_MR (eyes of offspring of KC patients with low-risk of ectasia development at the beginning of the study but progressed to moderate-risk states after 3 years of follow-up.n=18 eyes). **O-KC-LR_HR** (eyes of offspring of KC patients with low-risk of ectasia development at the beginning of the study but progressed to high-risk states after 3 years of follow-up.n=6 eyes).

Corvis ST parameters: bIOP [biomechanical corrected intraocular pressure], **A1T/A2T** [first/second applanation time], **A1V/A2V** [first/second applanation velocity], **HCT** [time to the highest concavity], **DAmax** [deformation amplitude], **A1DA/A2DA** [deformation amplitude at the fist/second applanation], **HCDA** [deflection amplitude at highest corneal concavity], **A1DLL/A2DLL** [first/second applanation deflection length], **HCDLL** [highest concavity deflection length], **A1DLA/A2DLA** [deflection amplitude at the fist/second applanation], **HCDLA** [deflection amplitude at maximum deformation], **A1DLAr/A2DLAr** [deflection area at the first/second applanation], **HCDLAr** [deflection area at maximum deformation], **PD** [peak distance at the highest concavity], **DAratio max 1mm** [maximum deformation amplitude ratio at 1mm], **DAratio max 2mm** [deformation amplitude ratio max 2mm], **IR** [integrated radius], **Max Inverse Radius** [maximum inverse radius], **CCT** [central corneal thickness], **ARTh** [Ambrósio Relational Thickness horizontal], **Pachy Slope** [changes of corneal thickness from the corneal center to the periphery], **SP-A1** [stiffness parameter at the first applanation], **CBI** [Corvis Biomechanical Index], and **SSI** [Stress-Strain Index].

Pentacam XR parameters: **PDC** [corneal central power], **K1** [keratometry in the flattest meridian], **K2** [keratometry in the steeper meridian], **Kmax** [maximum dioptric power], **I-S asymmetry** [inferior-superior dioptric asymmetry], **ARTmax** [maximum Ambrósio Relational Thickness], **CCT** [central corneal thickness], **MTP** [minimum thickness point], **AE/PE** [anterior and posterior surfaces elevation], **BAD-D** [total deviation value], and **TBI** [Tomographic and Biomechanical Index].

[#1] O-KC-LR compared to O-KC-LR_MR [#2] O-KC-LR compared to O-KC-LR_HR.

The evolution of CBI toward moderate-risk values was observed along with changes in some biomechanical parameters such as corneal applanation time and velocity (A1V, A2T, A2V), distance between the two corneal concavity peaks (PD), integrated area under the radius of curvature during the concave phase (IR) and pachymetric progression

parameters (ARTh, PachySlope). Regarding the evolution of O-KC-LR eyes towards high-risk values, alterations in the pachymetric progression parameters stand out. In fact, it is noteworthy that all cases of O-KC-LR that experienced any biomechanical decline showed alterations in pachymetric progression values (ARTh and PachySlope), suggesting that higher faster increase thickness toward the periphery (ARTh lower values) and higher differences in corneal thickness from the center to the periphery (PachySlope) underlying the biomechanical decline and the CBI progression.

Characterization of the biomechanical and tomographical evolution on O-KC-MR cohort

Cohort defined as O-KC-MR at the beginning of the study included 28 eyes showing a CBI index between 0.25 and 0.50 points. After three years, 11 eyes (39%) progressed to CBI index >0.50 suggestive of high biomechanical instability and, therefore, a high-risk for ectasia development [O-KC-MR_HR].

Along with CBI increase, alterations in corneal applanation time and velocity (A1T, A2T, and A2V), time until the highest concavity (HCT), deformation amplitude at the first applanation (A1DA), maximum ratio of deformation amplitude measured at 1 or 2 mm from the center of the cornea (DARatio max 1mm and DARatio max 2mm), integrated radius (IR), pachymetric progression (ARTh and PachySlope), and corneal stiffness (SP-A1) were observed. Specifically, higher and quick corneal deformation, less corneal resistance, higher differences in corneal thickness from the center to the periphery, and higher-faster increase in thickness toward the periphery supported the CBI increase in the O-KC-MR progressive cases.

Regarding corneal morphology, no differences were observed for any of the tomographic parameters evaluated. **Table 4** displays the biomechanical and tomographical parameters of O-KC-MR progressive cases before and after three years of follow-up.

Table 4. Comparison of biomechanical and tomographical data of O-KC-MR progressive cases before and after three years follow-up.

	Parameters	O-KC-MR_HR		
		First visit (n=11 eyes)	Follow-up (n=11 eyes)	p[#1]
Corvis® ST	**bIOP** [mmHg]	15.12±1.87	14.35±2.00	0.112
	A1T [ms]	7.15±0.28	7.00±0.20	**0.001**
	A1V [m/s]	0.16±0.02	0.15±0.01	0.467
	A2T [ms]	22.22±0.37	22.45±0.30	**0.006**
	A2V [m/s]	-0.28±0.03	-0.30±0.02	**0.001**
	HCT [ms]	17.14±0.62	17.70±0.35	**0.024**
	DAmax [mm]	1.16±0.10	1.15±0.08	0.776
	A1DA [mm]	0.14±0.01	0.13±0.01	**0.016**
	A2DA [mm]	0.42±0.05	0.40±0.03	0.392
	HCDA [mm]	1.16±0.10	1.15±0.08	0.776
	A1DLL [mm]	2.25±0.13	2.25±0.10	1.000
	A2DLL [mm]	3.10±1.07	3.23±0.70	0.747
	HCDLL [mm]	6.66±0.33	6.42±0.21	0.020
	A1DLA [mm]	0.09±0.01	0.09±.0.01	1.000
	A2DLA [mm]	0.11±0.01	0.12±0.01	0.025
	HCDLA [mm]	0.95±0.08	0.93±0.06	0.382
	A1DLAr [mm]	0.18±0.02	0.17±0.02	0.309
	A2DLAr [mm]	0.24±0.06	0.25±0.04	0.567
	HCDLAr [mm]	3.41±0.48	3.35±0.28	0.618
	PD [mm]	5.17±0.22	5.08±0.11	0.051
	DARatio max [1mm]	1.56±0.04	1.60±0.04	**0.023**
	DARatio max [2mm]	4.42±0.28	4.71±0.37	**0.003**
	IR [mm^{-1}]	8.83±0.97	9.81±1.30	**0.001**
	MaxInverseRadius [mm^{-1}]	0.18±0.01	0.19±0.03	0.367
	CCT [µm]	509.90±27.36	510.81±28.58	0.470
	ARTh	599.88±175.37	449.71±63.66	**0.007**
	Pachy Slope [µm]	34.23±7.82	47.57±8.48	**0.001**
	SP-A1	84.85±11.42	78.21±9.93	**0.017**
	CBI	0.42±0.10	0.80±0.10	**0.001**
	SSI	0.91±0.15	0.90±0.12	0.815
Pentacam® XR	**PDC** [D]	42.61±1.89	42.00±1.95	0.068
	Kmax [D]	43.70±1.99	43.70±2.00	0.502
	I-S asymmetry [D]	0.22±0.62	-0.08±0.80	0.025
	ARTmax [µm]	385.63±76.36	397.72±121.28	0.555
	CCT [µm]	509.90±27.36	510.81±28.58	0.470
	MTP [µm]	504.72±26.42	505.18±28.35	0.777
	AE [µm]	2.00[2.00]	1.00[5.00]	0.694
	PE [µm]	4.00[5.00]	6.00[6.00]	0.094
	BAD-D	1.50±0.79	1.40±0.90	0.356
	TBI	0.32±0.33	0.40±0.30	0.208

Sample size: O-KC-MR_HR (eyes of offspring of KC patients with moderate-risk of ectasia development at the beginning of the study but progressed to high-risk states after 3 years of follow-up n=11 eyes).

Corvis ST parameters: bIOP [biomechanical corrected intraocular pressure], **A1T/A2T** [first/second applanation time], **A1V/A2V** [first/second applanation velocity], **HCT** [time to the highest concavity], **DAmax** [deformation amplitude], **A1DA/A2DA** [deformation amplitude at the fist/second applanation], **HCDA** [deflection amplitude at highest corneal concavity], **A1DLL/A2DLL** [first/second applanation deflection length], **HCDLL** [highest concavity deflection length], **A1DLA/A2DLA** [deflection amplitude at the fist/second applanation], **HCDLA** [deflection amplitude at maximum deformation], **A1DLAr/A2DLAr** [deflection area at the first/second applanation], **HCDLAr** [deflection area at maximum deformation], **PD** [peak distance at the highest concavity], **DAratio max 1mm** [maximum deformation amplitude ratio at 1mm], **DAratio max 2mm** [deformation amplitude ratio max 2mm], **IR** [integrated radius], **Max Inverse Radius** [maximum inverse radius], **CCT** [central corneal thickness], **ARTh** [Ambrósio Relational Thickness horizontal], **Pachy Slope** [changes of corneal thickness from the corneal center to the periphery], **SP-A1** [stiffness parameter at the first applanation], **CBI** [Corvis Biomechanical Index], and **SSI** [Stress-Strain Index].

Pentacam XR parameters: PDC [corneal central power], **K1** [keratometry in the flattest meridian], **K2** [keratometry in the steeper meridian], **Kmax** [maximum dioptric power], **I-S asymmetry** [inferior-superior dioptric asymmetry], **ARTmax** [maximum Ambrósio Relational Thickness], **CCT** [central corneal thickness], **MTP** [minimum thickness point], **AE/PE** [anterior and posterior surfaces elevation], **BAD-D** [total deviation value], and **TBI** [Tomographic and Biomechanical Index].

[#1] O-KC-MR compared to O-KC-MR_HR.

Characterization of the biomechanical and tomographical evolution on O-KC-HR cohort

The O-KC-HR cohort included 18 eyes from offspring of KC patients with CBI values > 0.50 in the first visit, indicating a high biomechanical risk for ectasia development. Of them, seven eyes (39%) exhibited a progressive impairment of corneal biomechanics after the three-years follow-up [O-KC-HR_prog], evidenced by increasingly higher CBI values which could even be accompanied by tomographic alterations compatible with corneal ectasia.

Table 5 shows the biomechanical and tomographical data of O-KC-HR progressive cases at baseline and at the three-year follow-up. Comparative analysis evidenced differences in corneal velocity (A2V), highest concavity time (HCT), deformation amplitude in the first applanation of the cornea (A1DA), highest concavity deflection length (HCDLL), peak distance (PD), and pachymetric progression (ARTh, PachySlope) before and after follow-up in the O-KC-HR_prog eyes. In terms of corneal morphology, progressive O-KC-HR eyes reported statistically lower values for minimum corneal thickness, while the remaining metrics (curvature, asymmetry, elevation, and KC indexes) had similar values to the initial ones.

Table 5. Comparison of biomechanical and tomographical data of O-KC-HR progressive cases before and after three-years follow-up.

	Parameters	O-KC-HR_prog		
		First visit (n=7 eyes)	Follow-up (n=7 eyes)	p[#1]
Corvis® ST	**bIOP** [mmHg]	15.17±1.17	14.91±0.74	0.546
	A1T [ms]	7.17±0.15	7.05±0.06	0.104
	A1V [m/s]	0.16±0.02	0.16±0.01	0.965
	A2T [ms]	22.22±0.34	22.35±0.17	0.146
	A2V [m/s]	-0.28±0.03	-0.31±0.02	**0.023**
	HCT [ms]	17.06±0.50	17.69±0.37	**0.028**
	DAmax [mm]	1.17±0.07	1.19±0.05	0.561
	A1DA [mm]	0.14±0.01	0.13±0.01	**0.013**
	A2DA [mm]	0.39±0.04	0.41±0.05	0.237
	HCDA [mm]	1.30±0.07	1.18±0.05	0.561
	A1DLL [mm]	2.33±0.10	2.30±0.08	0.463
	A2DLL [mm]	3.07±0.87	3.22±0.58	0.610
	HCDLL [mm]	6.83±0.34	6.49±0.31	**0.005**
	A1DLA [mm]	0.10±0.01	0.10±0.01	0.668
	A2DLA [mm]	0.11±0.01	0.12±0.01	0.270
	HCDLA [mm]	1.00±0.10	0.98±0.05	0.463
	A1DLAr [mm]	0.20±0.02	0.19±0.01	0.725
	A2DLAr [mm]	0.26±0.05	0.28±0.03	0.266
	HCDLAr [mm]	3.71±0.51	3.51±0.30	0.136
	PD [mm]	5.19±0.17	5.06±0.11	**0.042**
	DARatio max [1mm]	1.57±0.03	1.61±0.04	0.150
	DARatio max [2mm]	4.60±0.37	4.80±0.33	0.348
	IR [mm^{-1}]	8.95±0.50	9.93±0.71	0.063
	MaxInverseRadius [mm^{-1}]	0.18±0.01	0.19±0.02	0.169
	ARTh	451.92±59.43	370.76±60.08	**0.004**
	Pachy Slope [µm]	42.72±3.60	53.91±5.43	**0.001**
	SP-A1	80.01±13.65	75.35±6.15	0.326
	CBI	0.69±.0.13	0.88±0.07	**0.001**
	SSI	0.82±0.13	0.84±0.08	0.800
Pentacam® XR	**PDC** [D]	43.84±1.59	43.99±1.18	0.826
	Kmax [D]	45.37±1.47	46.10±3.20	0.350
	I-S asymmetry [D]	0.38±1.72	0.96±2.75	0.253
	ARTmax [µm]	311.71±45.86	302.57±74.82	0.526
	CCT [µm]	510.28±19.24	500.29±9.21	0.077
	MTP [µm]	504.14±15.42	493.00±7.63	**0.046**
	AE [µm]	3.00[2.00]	3.000[8.00]	0.528
	PE [µm]	3.00[9.00]	3.00[7.00]	0.343
	BAD-D	2.11±1.08	2.53±2.33	0.421
	TBI	0.51±0.38	0.66±0.24	0.146

Sample size: O-KC-HR_prog (eyes of offspring of KC patients with high-risk of ectasia development at the beginning of the study but with increasing CBI index after 3 years of follow-up n=7 eyes).

Parameters: bIOP [biomechanical corrected intraocular pressure], **A1T/A2T** [first/second applanation time], **A1V/A2V** [first/second applanation velocity], **HCT** [time to the highest concavity], **DAmax** [deformation amplitude], **A1DA/A2DA** [deformation amplitude at the fist/second applanation], **HCDA** [deflection amplitude at highest corneal concavity], **A1DLL/A2DLL** [first/second applanation deflection length], **HCDLL** [highest concavity deflection length], **A1DLA/A2DLA** [deflection amplitude at the fist/second applanation], **HCDLA** [deflection amplitude at maximum deformation], **A1DLAr/A2DLAr** [deflection area at the first/second applanation], **HCDLAr** [deflection area at maximum deformation], **PD** [peak distance at the highest concavity], **DAratio max 1mm** [maximum deformation amplitude ratio at 1mm], **DAratio max 2mm** [deformation amplitude ratio max 2mm], **IR** [integrated radius], **Max Inverse Radius** [maximum inverse radius], **CCT** [central corneal thickness], **ARTh** [Ambrósio Relational Thickness horizontal], **Pachy Slope** [changes of corneal thickness from the corneal center to the periphery], **SP-A1** [stiffness parameter at the first applanation], **CBI** [Corvis Biomechanical Index], and **SSI** [Stress-Strain Index].

[#1] O-KC-HR compared to O-KC-HR_prog.

Tear LF concentrations in O-KC groups with biomechanical decline.

LF tear concentration was measured by ELISA in the O-KC groups that progressed to a higher ectasia risk state after the three-year follow-up. As a result, no differences for LF expression were observed between pre- and post- follow-up period for either group. However, compared to the LF levels previously reported in controls, LF expression was

significantly lower in all O-KC groups regardless of biomechanical deterioration [**Figure 1**].

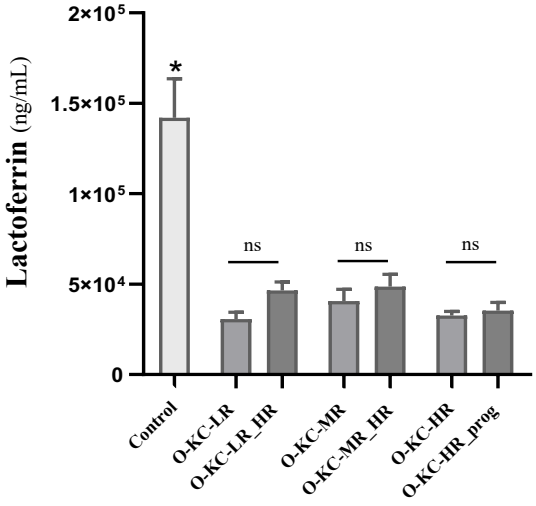


Figure 1. Tear LF levels in O-KC groups with biomechanical decline after three-years follow-up compared to the control data previously reported. **p* <0.05.

Discussion

Although KC genesis remains incompletely described, genetic-hereditary contributions are well documented in this pathology.[17–19] In this line, the susceptibility of KC first-degree family members has been suggested by different ways. Firstly, clinical observations of common abnormalities in corneal biomechanics and morphology of these subjects frequently resembling subclinical KC states flagged their possible susceptibility to disease development.[8,20–22] A recent study involving biological parents of KC patients evidenced that their corneal biomechanics and tomography indicators showed significant differences compared with healthy controls without KC offspring, emphasizing the importance of biomechanical and tomographical assessment for the prediction of KC onset.[17]

Besides that, some genetic variants have been identified in familial studies of KC that seem to create a high susceptibility genome in which external factors could potentially lead to disease development.[23–26] In this regard, it has been estimated that first-degree relatives of KC patients have 15-67 times greater risk for disease development, becoming the most susceptible population for KC onset.[7] However, although the susceptibility of offspring of KC patients seems conclusive, no study has determined the early biomechanical, tomographic, and molecular changes responsible for and triggering the disease onset.

Currently, the concept of screening corneal ectasia goes beyond the detection of mild or subclinical cases, focusing on the ability to detect the biomechanical weakness

susceptibility of the corneal tissue and the associated risk of ectasia development if any additional structural impact is added.[27] On this basis, the main objective of this work was to detect the earliest clinical and molecular alterations that would lead to an increased risk of KC disease or even to disease development.

Given the central role of biomechanical assessment for detecting structural weakness, which constitutes an early hallmark of corneal ectasias,[28] all eyes of the study participants were categorized based on their corneal biomechanical behavior. For such categorization, we used the CBI index, which has 98.4% sensitivity and 100% specificity to detect the biomechanical alterations that could promote ectasia development, scoring the results in a range between low and high risk of ectasia development.[10]

Overall, descriptive analysis of demographic and clinical data at baseline found that age was slightly higher in the biomechanically compromised groups. These differences were expected due to the disease's own evolutionary course, which usually arises at puberty and progresses until the third decade of life.[28]

As expected, differences in the biomechanical and tomographical scans were showed among groups at the first visit. Thus, the O-KC-MR and O-KC-HR groups evidenced increased corneal deformation, reduced corneal thickness, and lower corneal strength than the O-KC-LR. Along with these results, tomographic imaging highlighted corneal thickness and pachymetric progression as the most significant features of corneal morphology that differentiated the low-risk group from all others. In this sense, our results showed that the pachymetric parameters had statistically lower values in the moderate and high-risk groups compared to the low-risk, associating reduced corneal thickness and abnormal pachymetric progression with biomechanical decline and high ectasia risk.

Given the nature of CBI's calculation, the pachymetry findings were already predictable since, by definition, CBI is derived from a logistic regression analysis that considers corneal deformation parameters together with corneal thickness and progression.[10] Corneal thinning is one of the defining clinical features of KC disease, aggravated with disease severity.[1] Previous studies reported that central corneal thickness correlates with some of the parameters assessed in corneal biomechanical scanning,[29] consistent with our results, which suggest that silent alterations in pachymetric progression or the existence of morphologically thinner corneas are subject to higher deformation processes and, therefore, altered biomechanical behavior. Corneal thickness has a strong genetic component, with heritability estimates ranging between 0.68 and 0.95, and several identified genomic loci that account for its variability.[30-34] Therefore, in the proposed genetic signature predisposing to the development of the disease, phenotype towards a lower pachymetry could be determinant and carefully considered, especially in those cases with a preceding history of KC.

Pachymetry's relevance was also supported by biomechanical follow-up, where alterations in the Pachy Slope and ARTh indices underlay all cases that progressed with

increased CBI values. Roughly a quarter of the study eyes evolved to an enhanced risk of ectasia development, and most of the biomechanical differences observed in the progressive cases after three years were related to corneal applanation time and velocity, highest concavity, deformation amplitude parameters, stiffness data, and, above all, pachymetric progression. Interestingly, the follow-up analysis did not show differences for static pachymetric variables such as CCT or MTP; however, alterations in Pachy Slope and ARTh indexes, which provide information about the spatial thickness distribution across the entire cornea were observed in all cases with CBI progression.

Pachy Slope defines the corneal thickness variability from the center to the periphery. Higher values indicate higher thickness differences between the corneal center and periphery and less smoothness in pachymetric progression.[35] The Pachy Slope pattern has been well described in both healthy and KC eyes, exhibiting higher values in the ecstatic eyes and having reported a good ability to recognize the pachymetric progression impairment of the KC corneas.[36] On the other hand, ARTh results from the division between corneal thickness at the thinnest point and pachymetric progression index, with lower values representing a faster corneal thickness increase from the center toward the periphery.[10] Previous studies have demonstrated the ARTh effectivity in distinguishing between healthy and KC eyes, as well as its highly sensitivity for screening the fellow eye of unilateral KC.[35,37,38] In our study, changes in Pachy Slope and ARTh were observed in all cases that progressed toward higher CBI values, emphasizing the relevance of pachymetric progression assessment over fixed values of corneal thickness. Additionally, the assessment of pachymetric progression parameters also allows us to discern between those corneas that are naturally thinner, and those that may be undergoing a pathological process.

Regarding molecular analysis of LF, the under-expression of this iron-binding glycoprotein in biological samples from KC patients has been widely reported. In addition, our latest study also demonstrated a stronger reduction of LF tear levels in a O-KC cohort of participants compared to controls.[39,40] This reduction was observed even in offspring of KC patients with no apparent biomechanical or tomographic abnormalities, suggesting the involvement of this protein in the earliest disease risk stages. Based on the inherent properties of LF, it has been it has been hypothesized that its dysregulation could impact on the inflammatory and oxidative cellular environment involved in cell degeneration and damage in KC disease.[41] In this sense, our study aimed to determine whether the biomechanical and tomographical changes observed in the follow-up would run together with alterations in LF levels. The results showed no differences for LF expression in subjects evolving with biomechanical deterioration between before and after follow-up; however, LF levels in these subjects remained lower than previously reported LF expression data in age- and sex-matched control subjects, proposing that although there is no direct relationship with biomechanical impairment, LF plays an important role in the susceptibility of KC offspring to disease development.

In summary, this study supports the susceptibility of KC offspring to disease development and demonstrates the usefulness of corneal biomechanical tools in the detection and monitoring of KC-risk stages. Furthermore, alterations in the pachymetric progression seem to be the earliest detectable changes associated with corneal biomechanical decline and the higher risk for ectasia development. LF dysregulation appears to respond to the inherent KC family history but not to the corneal biomechanical weakness. However, studies with larger sample sizes are needed to obtain more robust and accurate conclusions.

References

1. Belin MW, Asota IM, Ambrosio R, Khachikian SS. What's in a name: keratoconus, pellucid marginal degeneration, and related thinning disorders. Am J Ophthalmol. 2011;152(2):157-162.

2. Martínez-Abad A, Piñero DP. New perspectives on the detection and progression of keratoconus. J Cataract Refract Surg. 2017;43(9):1213-1227.

3. Flockerzi E, Xanthopoulou K, Goebels SC, et al. Keratoconus staging by decades: a baseline ABCD classification of 1000 patients in the Homburg Keratoconus Center. Br J Ophthalmol. 2021;105(8):1069-1075.

4. Ertan A, Muftuoglu O. Keratoconus clinical findings according to different age and gender groups. Cornea. 2008;27(10):1109-1113.

5. Léoni-Mesplié S, Mortemousque B, Touboul D, et al. Scalability and severity of keratoconus in children. Am J Ophthalmol. 2012;154(1):56-62.e1.

6. Gordon-Shaag A, Millodot M, Kaiserman I, et al. Risk factors for keratoconus in Israel: a case-control study. Ophthalmic Physiol Opt. 2015;35(6):673-681.

7. Santodomingo-Rubido J, Carracedo G, Suzaki A, Villa-Collar C, Vincent SJ, Wolffsohn JS. Keratoconus: An updated review. Cont Lens Anterior Eye. 2022;45(3):101559.

8. Awwad ST, Yehia M, Mehanna CJ, et al. Tomographic and Refractive Characteristics of Pediatric First-Degree Relatives of Keratoconus Patients. Am J Ophthalmol. 2019;207:71-76.

9. Naderan M, Rajabi MT, Zarrinbakhsh P, Naderan M, Bakhshi A. Association between Family History and Keratoconus Severity. Curr Eye Res. 2016;41(11):1414-1418.

10. Vinciguerra R, Ambrósio R, Elsheikh A, et al. Detection of Keratoconus With a New Biomechanical Index. J Refract Surg. 2016;32(12):803-810.

11. Roy AS, Shetty R, Kummelil MK. Keratoconus: a biomechanical perspective on loss of corneal stiffness. Indian J Ophthalmol. 2013;61(8):392-393.

12. Lema I, Duran J. Inflammatory molecules in the tears of patients with keratoconus. Ophthalmology. 2005;112(4):654-659.

13. Toprak I, Kucukatay V, Yildirim C, Kilic-Toprak E, Kilic-Erkek O. Increased systemic oxidative stress in patients with keratoconus. Eye (Lond). 2014;28(3):285-289.

14. Navel V, Malecaze J, Pereira B, et al. Oxidative and antioxidative stress markers in keratoconus: a systematic review and meta-analysis. Acta Ophthalmol. Published online 2020.

15. Malfeito M, Regueiro U, Pérez-Mato M, Campos F, Sobrino T, Lema I. Innate Immunity Biomarkers for Early Detection of Keratoconus. Ocul Immunol Inflamm. 2019;27(6).

16. Efron N. Grading scales for contact lens complications. Ophthalmic Physiol Opt. 1998;18(2):182–186.

17. Li J, Zhang BN, Jhanji V, Wang X, Li D, Du X. Parental Corneal Tomographic and Biomechanical Characteristics of Patients With Keratoconus. Am J Ophthalmol. 2023;256:146-155.

18. Tuft SJ, Hassan H, George S, Frazer DG, Willoughby CE, Liskova P. Keratoconus in 18 pairs of twins. Acta Ophthalmol. 2012;90(6):482-486.

19. Weed KH, MacEwen CJ, McGhee CNJ. The variable expression of keratoconus within monozygotic twins: Dundee University Scottish Keratoconus Study (DUSKS). Contact Lens and Anterior Eye. 2006;29(3):123-6.

20. Kaya V, Utine CA, Altunsoy M, Oral D, Yilmaz OF. Evaluation of corneal topography with Orbscan II in first-degree relatives of patients with keratoconus. Cornea. 2008;27(5):531-534.

21. Ionescu IC, Corbu CG, Nicula C, et al. The importance of corneal biomechanics in assessing first degree family members of keratoconus patients. Rom J Ophthalmol. 2018;61:149-154.

22. Kara N, Altinkaynak H, Baz O, Goker Y. Biomechanical evaluation of cornea in topographically normal relatives of patients with keratoconus. Cornea. 2013;32(3):262-266.

23. Ionescu IC, Corbu CG, Tanase C, et al. Overexpression of Tear Inflammatory Cytokines as Additional Finding in Keratoconus Patients and Their First Degree Family Members. Mediators Inflamm. 2018;2018:4285268.

24. Khaled ML, Bykhovskaya Y, Gu C, et al. PPIP5K2 and PCSK1 are Candidate Genetic Contributors to Familial Keratoconus. Sci Rep. 2019;9(1):19406.

25. Shinde V, Sobreira N, Wohler ES, et al. Pathogenic alleles in microtubule, secretory granule and extracellular matrix-related genes in familial keratoconus. Hum Mol Genet. 2021;30(8):658-671.

26. Bykhovskaya Y, Rabinowitz YS. Update on the genetics of keratoconus. Exp Eye Res. 2021;202:108398.

27. De Stefano VS, Dupps WJ. Biomechanical Diagnostics of the Cornea. Int Ophthalmol Clin. 2017;57(3):75-86.

28. Godefrooij DA, de Wit GA, Uiterwaal CS, Imhof SM, Wisse RPL. Age-specific Incidence and Prevalence of Keratoconus: A Nationwide Registration Study. Am J Ophthalmol. 2017;175:169-172.

29. Masiwa LE, Moodley V. A review of corneal imaging methods for the early diagnosis of pre-clinical Keratoconus. J Optom. 2020;13(4):269-275.

30. Dimasi DP, Burdon KP, Craig JE. The genetics of central corneal thickness. Br J Ophthalmol. 2010;94(8):971-976.

31. Wang Y, Xu L, Wang S, et al. Heritability of Corneal Parameters in Nuclear Families With Keratoconus. Transl Vis Sci Technol. 2022;11(7):13.

32. Zheng Y, Ge J, Huang G, et al. Heritability of central corneal thickness in Chinese: the Guangzhou Twin Eye Study. Invest Ophthalmol Vis Sci. 2008;49(10):4303-4307.

33. Toh T, Liew SHM, MacKinnon JR, et al. Central corneal thickness is highly heritable: the twin eye studies. Invest Ophthalmol Vis Sci. 2005;46(10):3718-3722.

34. Lu Y, Vitart V, Burdon KP, et al. Genome-wide association analyses identify multiple loci associated with central corneal thickness and keratoconus. Nat Genet. 2013;45(2):155-63.

35. Yang K, Xu L, Fan Q, Zhao* D, Ren* S. Repeatability and comparison of new Corvis ST parameters in normal and keratoconus eyes. Sci Rep. 2019;9(1):15379.

36. Yang K, Xu L, Fan Q, et al. Evaluation of new Corvis ST parameters in normal, Post-LASIK, Post-LASIK keratectasia and keratoconus eyes. Sci Rep. 2020;10(1):5676.

37. Miao YY, Ma XM, Qu ZX, et al. Performance of Corvis ST Parameters Including Updated Stress-Strain Index in Differentiating Between Normal, Forme-Fruste, Subclinical, and Clinical Keratoconic Eyes. Am J Ophthalmol. 2024;258:196-207.

38. Peyman A, Sepahvand F, Pourazizi M, Noorshargh P, Forouhari A. Corneal biomechanics in normal and subclinical keratoconus eyes. BMC Ophthalmol. 2023;23(1):459.

39. Lema I, Brea D, Rodríguez-González R, Díez-Feijoo E, Sobrino T. Proteomic analysis of the tear film in patients with keratoconus. Mol Vis. 2010;16:2055-61.

40. Balasubramanian SA, Pye DC, Willcox MD. Levels of lactoferrin, secretory IgA and serum albumin in the tear film of people with keratoconus. Exp Eye Res. 2012;96(1):132-7.

41. Regueiro U, López-López M, Varela-Fernández R, Otero-Espinar FJ, Lema I. Biomedical Applications of Lactoferrin on the Ocular Surface. Pharmaceutics. 2023 Mar 7;15(3):865.

Introduction

Justification and hypothesis

Objectives

Methodology

WP1. Clinical & molecular study of KC disease

WP2. Clinical & molecular study of KC at-risk stages

WP3. Human LF as a therapeutic strategy for KC

Discussion

Conclusions

WP3. Human LF as a therapeutic strategy for KC

Human LF is an iron-binding mammalian glycoprotein that represents one of the major protein components of the tear fluid. Its multifactorial nature implies its role in multiple biological processes via antioxidant, anti-inflammatory, immunomodulatory, antibacterial, or antiviral properties. Several studies have reported LF dysregulation in the tear fluid of KC patients, and it has been suggested that lower LF concentrations may influence the reduced antioxidant capacity and increased immune-inflammatory status of corneal tissue cells in KC patients. In addition, previous studies of our group demonstrated that the overexpression of TLR2 constitutes a sensible and specific biomarker for KC disease, which could promote the inflammatory microenvironment observed in the corneal tissue of KC patients. On this basis, **Chapter 5** aims to demonstrate the interrelationship of LF and TLR2 with disease severity, as well as the immunomodulatory capacity of LF on TRL2 expression as a therapeutic approach for KC disease.

Chapter 5

Immunomodulatory effect of human lactoferrin on toll-like receptors 2 expression as therapeutic approach for keratoconus

Uxía Regueiro [1,2,*,†], **Maite López-López** [1,2,†], Rubén Varela-Fernández [1,3], Tomás Sobrino [4], Elio Diez-Feijoo [1,2,5] and Isabel Lema [1,2,5,*]

[1] Corneal Neurodegeneration Group (RENOIR), Clinical Neurosciences Research Laboratory (LINC), Health Research Institute of Santiago de Compostela (IDIS), Santiago de Compostela, Spain
[2] Department of Surgery and Medical-Surgical Specialties, Faculty of Optics and Optometry, University of Santiago de Compostela (USC), Santiago de Compostela, Spain
[3] Department of Pharmacology, Pharmacy and Pharmaceutical Technology, University of Santiago de Compostela (USC), Santiago de Compostela, Spain
[4] NeuroAging Laboratory (NEURAL), Clinical Neurosciences Research Laboratory (LINC), Health Research Institute of Santiago de Compostela (IDIS), Santiago de Compostela, Spain
[5] Galician Institute of Ophthalmology (INGO), Complexo Hospitalario Universitario de Santiago (CHUS), Santiago de Compostela, Spain

† These authors have equally contributed to this work as First Authors.
* These authors have equally contributed to this work as Corresponding Authors.

Published in: *International Journal of Molecular Science* 2022;23:12350.

Journal Citations Reports (JCR) Metrics: 2022
Journal Impact Factor (JIF): 5.60
JIF Quartile: Q1
Journal Position: 66/285 *Biochemistry & Molecular Biology*
JCR abbreviation: *Int J Mol Sci*
ISSN: 1661-6596

Author contribution. López-López M contributed to the conceptualization, design, formal analysis and investigation, writing and original draft preparation of this manuscript.

Open Access license details are provided in **Annex 4**.

International Journal of
Molecular Sciences

MDPI

Article

Immunomodulatory Effect of Human Lactoferrin on Toll-like Receptors 2 Expression as Therapeutic Approach for Keratoconus

Uxía Regueiro [1,2,*,†], Maite López-López [1,2,†], Rubén Varela-Fernández [1,3], Tomás Sobrino [4], Elio Diez-Feijoo [1,2,5] and Isabel Lema [1,2,5,*]

1 Corneal Neurodegeneration Group (RENOIR), Clinical Neurosciences Research Laboratory (LINC), Health Research Institute of Santiago de Compostela (IDIS), 15706 Santiago de Compostela, Spain
2 Department of Surgery and Medical-Surgical Specialties, Faculty of Optics and Optometry, University of Santiago de Compostela (USC), 15705 Santiago de Compostela, Spain
3 Department of Pharmacology, Pharmacy and Pharmaceutical Technology, University of Santiago de Compostela (USC), 15705 Santiago de Compostela, Spain
4 NeuroAging Laboratory (NEURAL), Clinical Neurosciences Research Laboratory (LINC), Health Research Institute of Santiago de Compostela (IDIS), 15706 Santiago de Compostela, Spain
5 Galician Institute of Ophthalmology (INGO), Conxo Provincial Hospital, 15706 Santiago de Compostela, Spain
* Correspondence: uxia.regueiro.lorenzo@sergas.es (U.R.); mariaisabel.lema@usc.es (I.L.); Tel.: +34-981951086 (U.R. & I.L.)
† These authors contributed equally to this work.

Abstract: Keratoconus (KC) is a corneal disorder whose etiology shares a close relationship with Lactoferrin (LTF) dysregulation and Toll-like Receptors 2 (TLR2) overexpression. This study shows how these two important biomarkers are clinically and molecularly interrelated, increasing knowledge about KC pathophysiology, and opening the door to future therapies. In this prospective clinical study, serum and tear LTF concentrations were quantified in 90 KC patients and 60 controls. A correlation analysis with multiple blood and tear immunoinflammatory mediators, and KC-associated tomographic parameters, was performed. An in vitro study using HEK-Blue^{TM}hTLR2 cell cultures was also conducted to determine the expression and functionality of TLR2 under the influence of LTF treatment. As a result, a LTF decreased was observed in KC patients compared to controls ($p < 0.0001$), evidencing the strong correlation with TLR2 overexpression at systemic and ocular surface level, with inflammatory mediator upregulation and with KC severity. In stimulated cell cultures, TLR2 expression was decreased using 2 mg/mL of LTF. The levels of secreted embryonic alkaline phosphatase (SEAP) and interleukin-8 (IL-8) were also reduced in supernatants after LTF treatment. As conclusions, the dysregulation of LTF and TLR2 in the ocular surface of KC patients contributes to KC severity by maintaining a detrimental chronic immune–inflammatory state. The immunomodulatory properties of LTF on TLR2 expression suggest its potential as a therapeutic approach for KC.

Keywords: keratoconus; lactoferrin; ocular surface disorders; Toll-like receptors

check for updates

Citation: Regueiro, U.; López-López, M.; Varela-Fernández, R.; Sobrino, T.; Diez-Feijoo, E.; Lema, I. Immunomodulatory Effect of Human Lactoferrin on Toll-like Receptors 2 Expression as Therapeutic Approach for Keratoconus. *Int. J. Mol. Sci.* **2022**, *23*, 12350. https://doi.org/10.3390/ijms232012350

Academic Editors: Murat Dogru and Takashi Kojima

Received: 6 September 2022
Accepted: 8 October 2022
Published: 15 October 2022

Publisher's Note: MDPI stays neutral with regard to jurisdictional claims in published maps and institutional affiliations.

Copyright: © 2022 by the authors. Licensee MDPI, Basel, Switzerland. This article is an open access article distributed under the terms and conditions of the Creative Commons Attribution (CC BY) license (https://creativecommons.org/licenses/by/4.0/).

1. Introduction

Lactoferrin, also named lactotransferrin (LTF), is an iron-binding mammalian glycoprotein that belongs to the transferrin family. This multifunctional glycoprotein is present in many fluids (such as tears, saliva, serum, milk, etc.) and exocrine secretions that recover mucosal sites considered as portals of entry and/or invasion of pathogens, contributing to the primary innate-immune defensive system [1–3]. It has an approximated molecular weight of 80 kDa and a highly conserved three-dimensional structure with iron-binding sites. Although its ability to bind Fe3+ ions allows it to play a predominant role in regulating free iron levels in body fluids, the major functions of LTF are related to antioxidant,

antibacterial, and antiviral activities [4]. It can be found as an iron-free protein (apo-LTF) or a fully iron-loaded protein (holo-LTF), showing the ability to bind to a greater variety of molecules in the apo state [5].

On the ocular surface, LTF is secreted mainly by the lacrimal gland, but the epithelial cells of the cornea and conjunctiva also produce detectable amounts [6]. It represents 25% of the total tear proteins [7] and provides essential protection in the ocular surface tissues due to its anti-inflammatory, immunomodulatory, and antimicrobial iron-binding role [8]. Previous studies have found variations with aging and several inflammatory ocular diseases, such as dry eye or vernal conjunctivitis, being however invariable with the sex [9]. In this line, patients with keratoconus (KC) have shown a lower concentration of LTF in tear fluid than control subjects; moreover, this tear LTF reduction in KC seems to be related to the disease development [10,11]. In advanced KC, the presence of Fleischer's ring (iron deposits around the base of the cone, localized in the epithelial basement membrane) is a clear indicator of altered iron metabolism, which may contribute to an oxidative microenvironment and cell damage, or even death processes. However, despite recent advances in understanding the LTF impact on cellular behavior, it is still unclear which pathways are activated and how this affects the epithelial and immune cell responses [12]. LTF constitutes a promising diagnostic and therapeutic target for numerous diseases; in fact, more and more research is focusing on using LTF as an active targeting ligand for drug delivery systems [13].

KC is a primary corneal ectasia that course with weakening, thinning, protrusion, and chronic degeneration of the corneal tissue; leading to a significant loss of vision and a reduction in quality of life [14,15]. The multifactorial etiology of KC is associated with environmental, biomechanical, genetic, and biochemical mechanisms that share a close relationship with the primary innate immune defensive system. In this line, the overexpression of Toll-like receptor 2 (TLR2) in blood monocytes and neutrophils, as well as in corneal and conjunctival epithelial cells of KC patients, was recently demonstrated [16,17]. TLR2 is an immune innate transmembrane protein that detects the presence of exogenous and/or endogenous agents associated with cell damage [18], promoting an inflammatory response and involving the molecular drivers which may cause tissue degradation in KC. The systemic innate immune TLR2 overexpression observed in patients with KC was correlated with the increase in inflammatory mediators and NF-kB factors in serum [16]. Furthermore, a study conducted in subclinical KC patients demonstrated that corneal and conjunctival TLR2 are suitable biomarkers for early detection of the disease [17].

Based on all these previous findings, which evidenced the LTF role in KC and the importance of TLR2 in the disease development; our hypothesis supports that both mediators may be intimately associated, leading to the development and maintenance of a detrimental status in KC. Therefore, the main purpose of this study was to measure serum and tear LTF concentrations in KC patients and examine their relationship with the disease's immune–inflammatory status, and KC severity. Furthermore, an in vitro study with a stimulated HEK-Blue^{TM} human TLR2 (hTLR2) cell culture was also conducted to determine the immunomodulatory capacity of LTF on TLR2 expression.

2. Results

2.1. Clinical Study

Blood sample analysis involved 20 control subjects (55% males; mean age, 30.5 ± 7.6 years) and 40 patients with KC (55% males; mean age, 33.1 ± 10.9 years). No sex- and age-related statistical differences were detected between these controls and KC patients ($p = 0.609$ and $p = 0.276$, respectively). Serum LTF concentrations were statistically lower in KC patients than in control subjects (446 ± 331 ng/mL vs. 1187 ± 282 ng/mL, respectively) ($p < 0.0001$) Figure 1.

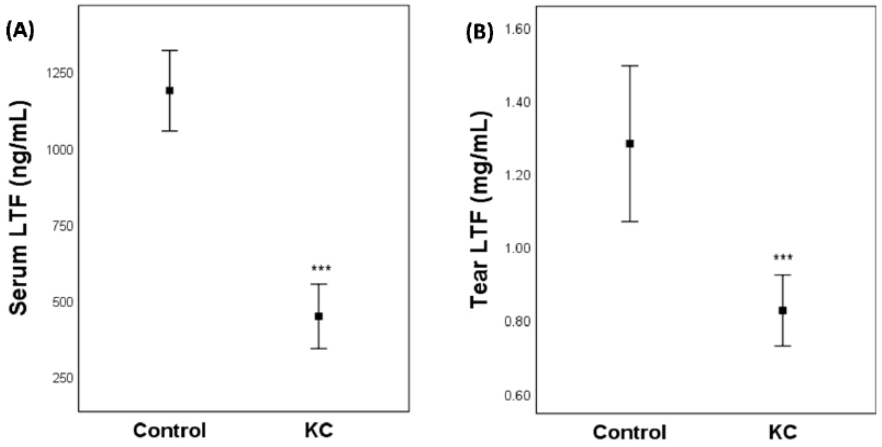


Figure 1. Serum (**A**) and tear (**B**) LTF concentrations in control subjects and KC patients. Statistical differences with regard to controls: *** $p < 0.0001$. Sample size: (**A**) controls = 20 eyes, KC = 40 eyes; (**B**) controls = 40 eyes, KC = 50 eyes. Abbreviations: KC, keratoconus; LTF, lactoferrin.

Tear fluid evaluation involved 40 control subjects (46% males; mean age, 29.4 ± 6.7 years) and 50 patients with KC (66% males; mean age, 33.2 ± 9.4 years). No sex- and age-related statistical differences were detected between these controls and KC patients ($p = 0.063$ and $p = 0.105$, respectively). LTF concentrations in tear fluid were also statistically reduced in KC patients compared to controls (0.83 ± 0.34 mg/mL vs. 1.28 ± 0.64 mg/mL, respectively) ($p < 0.0001$), as shown in Figure 1. In addition, tears analysis of KC patients revealed that there were no differences in LTF levels based on the presence or absence of ocular itching (0.83 ± 0.34 mg/mL vs. 0.82 ± 0.36 mg/mL, respectively) ($p = 0.925$), and based on the presence or absence of ocular rubbing (0.84 ± 0.23 mg/mL vs. 0.82 ± 0.41 mg/mL, respectively) ($p = 0.809$).

No differences were observed between the participants with or without allergic diseases for both serum and tear LTF concentrations (721 ± 487 ng/mL vs. 665 ± 462 ng/mL ($p = 0.648$), and 0.94 ± 0.40 mg/mL vs. 1.01 ± 0.50 mg/mL ($p = 0.305$); (respectively).

The bivariate correlation analysis showed a strong negative correlation between serum LTF concentrations and TLR2 expression in monocytes and neutrophils. Moreover, a strong negative correlation was also observed between serum LTF concentrations and serum inflammatory mediators such as IL-1β, IL-6, TNF-α, and MMP-9 (all $p < 0.0001$). Figure 2 shows the Pearson's coefficients of the bivariate correlation study, representing it by scatter plots.

Moreover, a negative correlation between tear LTF concentrations and TLR2 expression in corneal and conjunctival epithelial cells was found. In this regard, a negative correlation was also observed between tear LTF concentrations and the KC severity parameters: high I-S asymmetry, coma, coma-like, and posterior elevation values. The Pearson's coefficients of this bivariate correlation analysis are shown in Table 1.

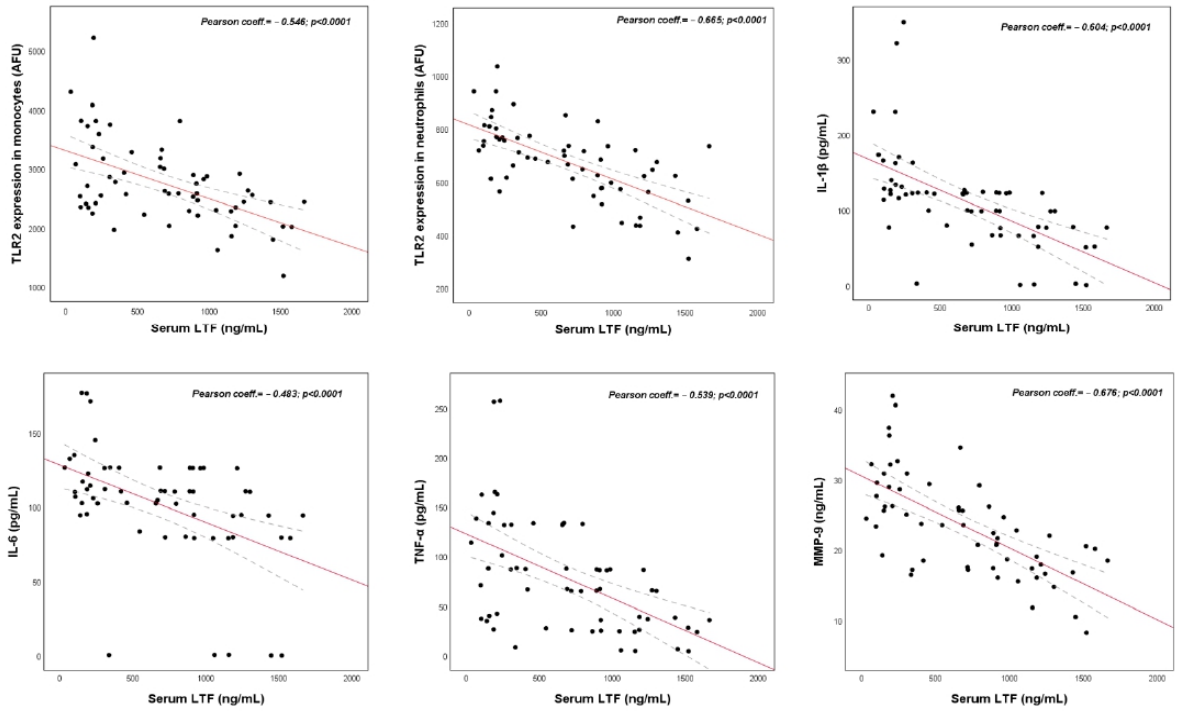


Figure 2. Scatter plots between serum LTF levels and immune–inflammatory biomarkers studied in blood samples showed a strong negative correlation for all of them. Abbreviations: AFU, arbitrary fluorescence units; IL, interleukin; LTF, lactoferrin; MMP-9, matrix metalloproteinase 9; TLR2, Toll-like receptor 2; TNF-α, tumor necrosis factor-alpha. Legend: the black dots represent the study cases, the grey dotted lines represent the mean confidence intervals, and the red line represents the linear fit line.

Table 1. Correlations (Pearson's coefficients) between tear LTF concentrations and ocular markers (TLR2 expression in corneal and conjunctival epithelial cells, and other corneal topographic, aberrometric, and tomographic parameters).

Tear LTF/Ocular Markers	Pearson's Coefficient, *p* Value
Tear LTF/TLR2 cornea	r = −0.289, **=0.007**
Tear LTF/TLR2 conjunctiva	r = −0.266, **=0.01**
Tear LTF/I-S asymmetry	r = −0.282, **=0.008**
Tear LTF/Coma	r = −0.314, **=0.003**
Tear LTF/Coma-like	r = −0.330, **=0.002**
Tear LTF/Post. elevation	r = −0.227, **=0.04**

Abbreviations: LTF, lactoferrin; TLR2, Toll-like receptor 2; I-S, paracentral infero-superior dioptric difference.

2.2. In Vitro Study

HEK-Blue^{TM}hTLR2 cell cultures, a line specifically designed for monitoring TLR2 agonists and antagonists, were used in this study as a first approach to assess the immunomodulatory effect of LTF on TLR2 expression. Figure 3A shows a 20× magnification brightfield microscopy image of HEK-Blue^{TM}hTLR2 and HEK-Blue^{TM}Null1 cell cultures.

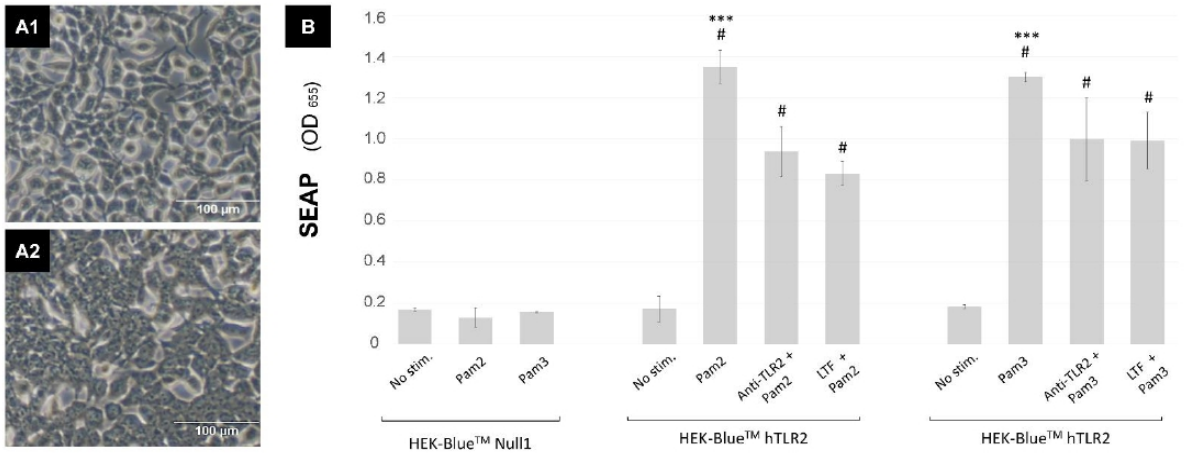


Figure 3. (**A**) Brightfield microscopy image of HEK-Blue^{TM} cells at a 20x magnification; (**A1**) transfected with hTLR2 (HEK-Blue^{TM}hTLR2) and (**A2**) without hTLR2 (HEK-Blue^{TM}Null1). (**B**) SEAP concentrations measured by QUANTI-Blue^{TM} assay in the supernatant of unstimulated, stimulated, neutralized, and immunomodulated HEK-Blue^{TM} cell cultures; statistical differences regarding to: # $p < 0.0001$ HEK-Blue^{TM}Null1 & Unstimulated HEK-Blue^{TM}hTLR2, *** $p < 0.005$ LTF & Anti-hTLR2-IgA. Abbreviations: Anti-TLR2, Anti-hTLR2-IgA; LTF, lactoferrin; No stim., unstimulated; OD, optical density; Pam2, Pam2CSK4; Pam3, Pam3CSK4; SEAP, secreted embryonic alkaline phosphatase; TLR2, Toll-like receptor 2.

TLR2 functionality after stimulation, neutralization, and immunomodulation was firstly determined by measuring SEAP production in cell culture supernatants by QUANTI-Blue^{TM} assay, as shown in Figure 3B. As result, statistical differences were found between stimulated HEK-Blue^{TM}hTLR2 (with Pam2CSK4 or Pam3CSK4) and unstimulated HEK-Blue^{TM}hTLR2 ($p < 0.0001$), as well as between stimulated HEK-Blue^{TM}hTLR2 (with Pam2CSK4 or Pam3CSK4) and unstimulated or stimulated HEK-Blue^{TM}Null1 ($p < 0.0001$); demonstrating that the stimulation with both synthetic lipopeptides TLR2 agonists (Pam2CSK4 or Pam3CSK4) causes SEAP overexpression in the supernatant of HEK-Blue^{TM}hTLR2 cell cultures. The pre-incubation with Anti-hTLR2-IgA reduces SEAP concentrations ($p < 0.001$ regarding Pam2CSK4, and $p = 0.004$ regarding Pam3CSK4) in the supernatant of HEK-Blue^{TM}hTLR2, proving the neutralizing role of this TLR2 antagonist. Likewise, the immunomodulatory action of 2 mg/mL of human LTF was also demonstrated; so, the pre-incubation with LTF reduces SEAP levels in the supernatant of HEK-Blue^{TM}hTLR2 ($p < 0.001$ regarding Pam2CSK4, and $p = 0.004$ regarding Pam3CSK4). No statistical differences were found between the pre-incubation with Anti-hTLR2-IgA and with LTF. Supplementary data includes information about HEK-Blue^{TM}hTLR2 pre-incubation with several LTF concentrations for the selection of the suitable dose of LTF, Figure S1.

TLR2 protein expression after stimulation, neutralization, and immunomodulation of HEK-Blue^{TM} cell cultures was evaluated by flow cytometry, immunohistochemistry, and western blot (WB) Figure 4. Flow cytometry results, presented in Figure 4A, showed that: (1) HEK-Blue^{TM}hTLR2 stimulation with both TLR2 agonists (Pam2CSK4 & Pam3CSK4) triggers the TLR2 protein overexpression (statistical differences were found between unstimulated HEK-Blue^{TM}hTLR2 and Pam2CSK4 ($p < 0.0001$) or Pam3CSK4 ($p < 0.0001$) stimulated HEK-Blue^{TM}hTLR2 cell cultures); (2) the pre-incubation with Anti-hTLR2-IgA or with 2 mg/mL of LTF reduces the TLR2 expression in the stimulated HEK-Blue^{TM}hTLR2 cell cultures (statistical differences were found between Anti-hTLR2-IgA and Pam2CSK4 ($p < 0.0001$) or Pam3CSK4 ($p = 0.009$), and between LTF and Pam2CSK4 ($p = 0.049$) or Pam3CSK4 ($p = 0.014$)); (3) there are differences between the neutralization provided by

Int. J. Mol. Sci. **2022**, *23*, 12350

Anti-hTLR2-IgA and the immunomodulation provided by LTF in HEK-Blue™hTLR2 cell cultures (being $p < 0.0001$ for Pam2CSK4 group and $p = 0.785$ for Pam3CSK4 group). These results are in accordance with QUANTI-Blue™'s assay findings.

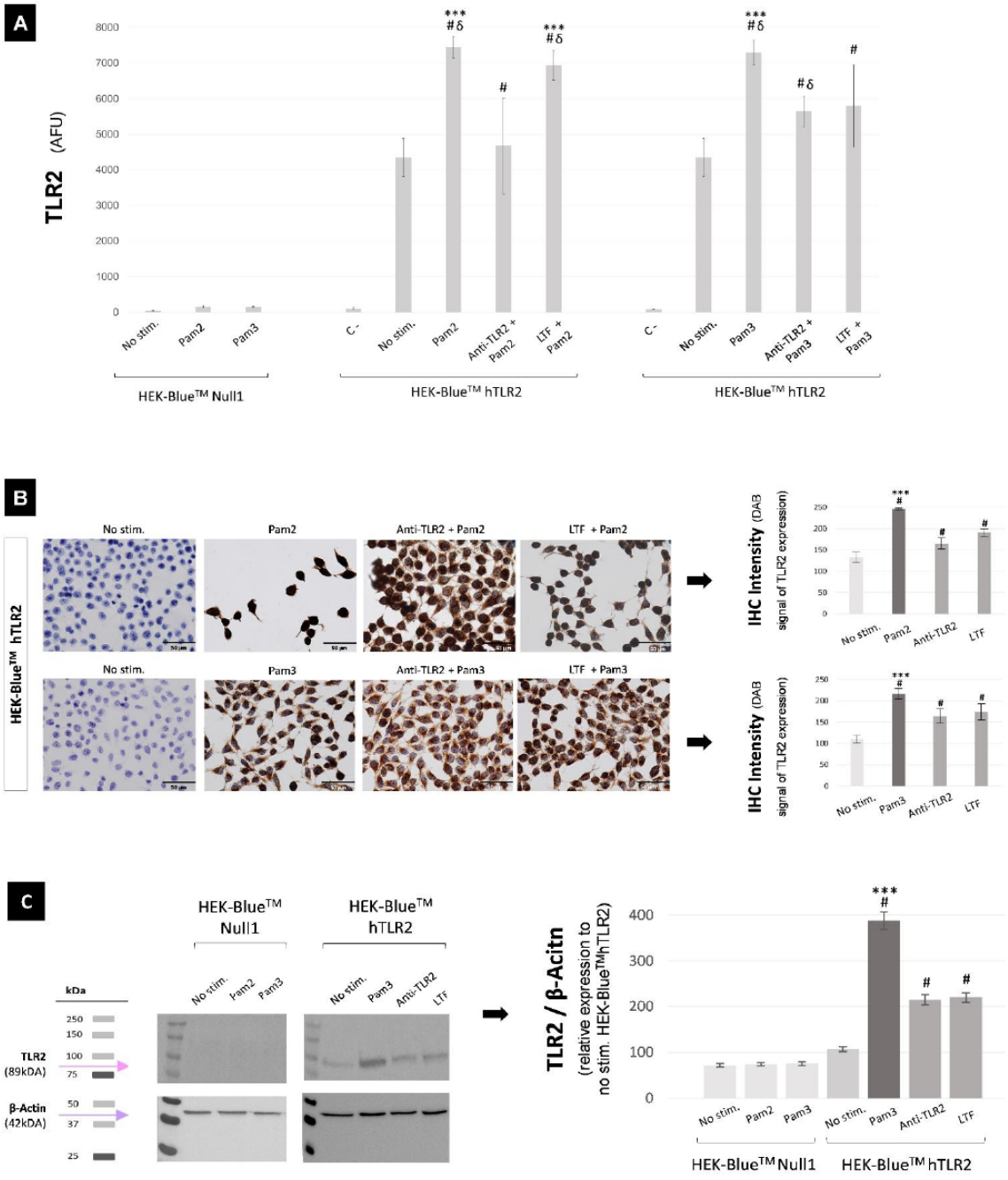


Figure 4. TLR2 protein expression in unstimulated, stimulated, neutralized, and immunomodulated HEK-Blue™ cell cultures, measured by flow cytometry (**A**), immunohistochemistry (**B**), and WB (**C**).

(**A**) Statistical differences with regard to: # $p < 0.0001$ HEK-Blue^{TM}Null1 and unlabeled cells (negative control), δ $p < 0.001$ unstimulated cells, *** $p < 0.05$ all groups. (**B**) Microscopic images of HEK-Blue^{TM}hTLR2 cells at a 40× magnification, and quantification of the intensity of staining; statistical differences with regard to: # $p < 0.0001$ unstimulated HEK-Blue^{TM}hTLR2, *** $p < 0.0001$ LTF and Anti-hTLR2-IgA. Legend: scale bars represent 50 µm. (**C**) WB revealed membrane and quantitative results analysis; statistical differences with regard to: # $p < 0.0001$ HEK-Blue^{TM}Null1 and unstimulated HEK-Blue^{TM}hTLR2, *** $p < 0.0001$ LTF and Anti-hTLR2-IgA. The uncropped blots are shown in Figure S2. Abbreviations: Anti-TLR2, Anti-hTLR2-IgA; C-, negative control (unlabeled cells in flow cytometry); IHC, immunohistochemistry; LTF, lactoferrin; No stim., unstimulated; Pam2, Pam2CSK4; Pam3, Pam3CSK4; TLR2, Toll-like receptor 2; WB, western blot.

The immunohistochemical assay carried out in HEK-Blue^{TM}hTLR2 cell culture confirms the high TLR2 expression in Pam2CSK4 and Pam3CSK4 stimulated cells (shown by dark brown staining), as well as the low TLR2 expression in unstimulated cells (without brown staining), Figure 4B. Comparing the Anti-hTLR2-IgA pre-incubated cell cultures and the stimulated ones, it is possible to observe a lightening of the dark brown staining, indicating that Anti-hTLR2-IgA pre-incubation contributes to TLR2 neutralization. Likewise, pre-incubation with LTF also showed a lightening of the dark brown staining seen in the stimulated cell cultures, being significantly more noticeable for the Pam3CSK4 stimulated group. Moreover, there were fewer color differences between Anti-hTLR2-IgA and LTF in the Pam3CSK4 stimulated group compared with the Pam2CSK4 stimulated group. These findings were corroborated by the quantification of the staining intensity, which was also consistent with the flow cytometer results.

The WB study was limited to the HEK-Blue^{TM} cell cultures stimulated with Pam3CSK4 because they showed better Anti-hTLR2-IgA neutralization and LTF immunomodulation capacities, Figure 4C. As a result, once again it was observed that: (1) the stimulation with TLR2 agonist triggered TLR2 overexpression ($p < 0.0001$); (2) the pre-incubation with TLR2 antagonist contributed to TLR2 neutralization ($p < 0.0001$); and (3) the pre-incubation with LTF led to TLR2 immunomodulation ($p < 0.0001$).

Finally, TLR2 functionality was determined by measuring IL-8 concentrations in the supernatants of unstimulated, stimulated, neutralized, and immunomodulated HEK-Blue^{TM} cell cultures, Figure 5. As we expect, IL-8 concentration was increased after stimulation with Pam2CSK4 or Pam3CSK4 in HEK-Blue^{TM}hTLR2 ($p < 0.0001$ and $p < 0.0001$, respectively). Pre-incubation with Anti-hTLR2-IgA or with 2 mg/mL of LTF in HEK-Blue^{TM}hTLR2 reduced IL-8 concentrations compared to stimulated cells ($p = 0.002$ regarding Pam2CSK4 and $p < 0.0001$ regarding Pam3CSK4, for Anti-hTLR2-IgA; $p = 0.009$ regarding Pam2CSK4 and $p < 0.0001$ regarding Pam3CSK4, for LTF). In addition, HEK-Blue^{TM}hTLR2 cells stimulated with Pam3CSK4 expressed more IL-8 than HEK-Blue^{TM}hTLR2 cells stimulated with Pam2CSK4 ($p < 0.0001$). No statistical differences were found between IL-8 concentrations of pre-incubated Anti-hTLR2-IgA and LTF HEK-Blue^{TM}hTLR2 cells (being $p = 0.442$ for Pam2CSK4 group, and $p = 0.168$ for Pam3CSK4 group).

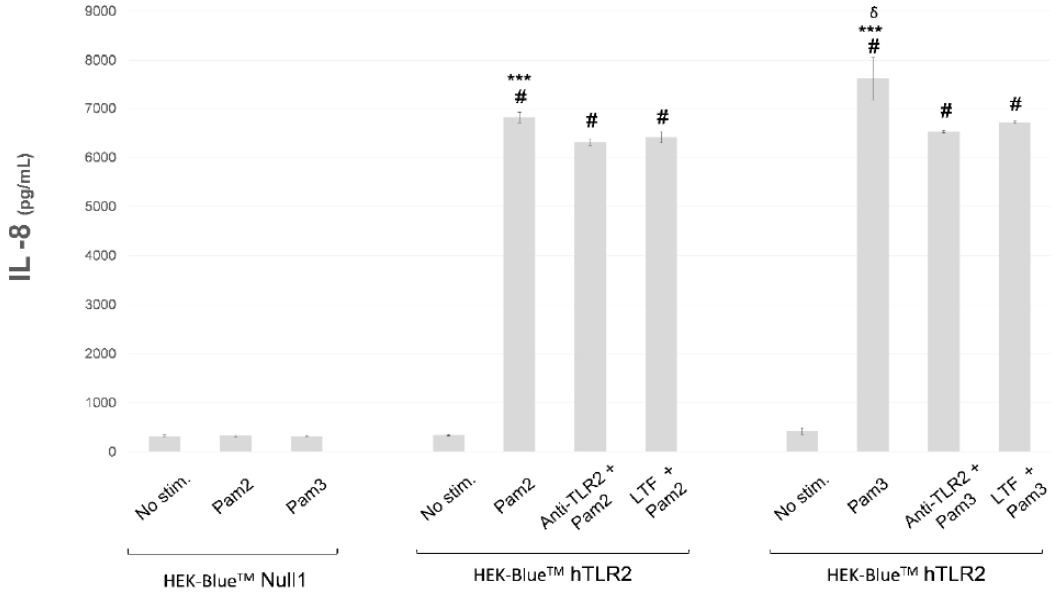


Figure 5. IL-8 concentrations were measured by ELISA in the supernatant of unstimulated, stimulated, neutralized, and immunomodulated HEK-Blue^{TM} cell cultures. Statistical differences with regard to: # $p < 0.0001$ HEK-Blue^{TM}Null1 and unstimulated HEK-Blue^{TM}hTLR2, *** $p < 0.0001$ Anti-TLR2 and LTF, δ $p < 0.0001$ Pam2CSK4 HEK-Blue^{TM}hTLR2. Abbreviations: Anti-TLR2, Anti-hTLR2-IgA; IL-8, interleukin 8; LTF, lactoferrin; No stim., unstimulated; Pam2, Pam2CSK4; Pam3, Pam3CSK4; TLR2, Toll-like receptor 2.

3. Discussion

This translational study aimed to examine LTF levels in serum and tear fluid of KC patients, as well as to assess its relationship with the systemic and local immune–inflammatory environment and the clinical status observed in KC. Remarkably, serum and tear LTF concentrations were found to be lower in KC patients than in control subjects. Moreover, the lower serum LTF concentrations observed in KC patients were strongly correlated with the increase in immune–inflammatory biomarkers, such as TLR2 and cytokines, in blood samples. Likewise, the lower tear LTF concentrations in KC patients were also correlated with increased immune biomarkers at the ocular surface and with high quantitative corneal parameters associated with the disease severity. In addition, the in vitro study performed in HEK-Blue^{TM}hTLR2 cell cultures confirmed the immunomodulatory role of LTF on the expression and functionality of TLR2.

LTF is an iron-binding protein of the transferrin family that plays an important defensive action due to its multifunctionality [8]. In plasma, LTF derives from neutrophils and its normal concentration is very low (0.5–2 µg/mL), especially when compared to LTF concentration in the tear fluid (1–2 mg/mL) [19]. This is evidence of the important role that LTF plays on the ocular surface, since it constitutes a high percentage of the total tear proteins [7]. In this study, we compared serum LTF concentrations in patients with KC and control subjects. As a result, we observed that serum LTF levels were 2.6 times significantly lower in KC patients than in controls. In these patients, reduced serum LTF levels were strongly correlated with the TLR2 overexpression in blood monocytes and neutrophils. Furthermore, these low LTF levels found in KC patients were also correlated with the overexpression of several serum inflammatory mediators (IL-1β, IL-6, TNF-α, MMP-9). These results show that the systemic immune–inflammatory alteration observed in patients with KC is closely related to low levels of LTF.

To check what was happening at the ocular level, in this study we also evaluated whether the LTF concentration in tears correlated with the immune alteration of the ocular surface in KC patients. In this way, we observed that tear LTF levels were 1.54 times significantly lower in KC patients than in control subjects. Moreover, the tear LTF levels in KC patients were negatively correlated with the TLR2 overexpression in corneal and conjunctival epithelial cells and with some quantitative topographic, aberrometric, and tomographic parameters related to the KC severity (I-S asymmetry, coma, coma-like, and posterior elevation). All of these findings provide evidence for the LTF role in the development and progression of KC.

Mainly due to its iron uptake capacity, showing an iron affinity 300 times higher than transferrin, LTF plays an anti-inflammatory, immunomodulatory, and antimicrobial iron-binding defensive role [8]. Iron is an important electron transfer mediator which is required for essential cellular functions such as respiration, oxygen transport, DNA synthesis, energy production, and cell proliferation [20]. In a ferrous state, iron acts as an electron donor, while in a ferric state, it acts as an acceptor. Although iron is necessary for many biological processes, excessive amounts of iron are toxic and lead to oxidative stress and synthesis of highly reactive radicals, producing tissue damage [21]. In this regard, a characteristic biomicroscopic sign present in corneas with moderate or advanced KC disease is the Fleischer ring. The Fleischer ring consists of iron deposits in the epithelial basement membrane, localized surrounding the base of the cone in keratoconic corneas. Gass et al. [22] suggested five possible sources for iron accumulation in the keratoconic corneal tissue: tears, blood plasma, breakdown of blood in perilimbal tissues, aqueous humor, and breakdown of intracellular cytochromic enzymes. However, the study conducted by Barraquer-Somers et al. [23] about different patterns and causes of iron deposition in corneal buttons, concludes that the tear film is likely the main source of iron accumulation, justifying it with the relative tear pooling mechanism on an irregular surface as responsible of the iron lines formation. Clearly, an altered iron metabolism occurs in keratoconic corneas, and this iron deposition may lead to an oxidative microenvironment and cell damage or death cell processes such as ferroptosis [24,25]. Knowing that tear iron transport among tissues is carried out by iron-binding proteins [26], the reduced tear and serum LTF levels observed in KC could contribute to iron filtration and accumulation in the corneal epithelial tissue. Similarly, other tear iron-binding proteins like serotransferrin have been shown also to be downregulated in KC patients [25], adding another contributing factor to iron deposition in corneal tissue. In this line, it could be possible to hypothesize that the oxidative microenvironment, the cell damage, and the ferroptosis induced by the iron deposition may affect the limbal cellular niche. Subsequently, it could affect the cells populations that share a common location in the palisades of Vogt at the limbal region, including the limbal stem cells (LSCs), the corneal stromal stem cells (SSCs), and the limbal stromal fibroblasts. According to this hypothesis, iron dyshomeostasis could influence the proper functioning of LSCs in the task of epithelial renewal, and the proper role of corneal stromal cells in the task of producing collagen fibrils, which collectively could induce the tissue degradation that leads to KC pathogenesis. However, further studies are needed to refine our current understanding of whether and how iron deposits in the epithelial basement membrane cause damage, by oxidative or ferroptosis processes, to the corneal epithelial cells and the surrounding ones.

The LTF involvement in other pathophysiological mechanisms of the KC disease is also uncertain. In this regard, our study focused on the immunomodulatory activity of LTF and its possible relationship with the innate immune predictive biomarkers recently discovered for KC, specifically the Toll-like receptors (TLRs). TLRs are immune innate transmembrane proteins that detect the presence of exogenous and/or endogenous agents associated with cell damage [18], triggering an inflammatory response and promoting molecular drivers which may cause tissue degradation. Overexpression of TLR2 and Toll-like receptor 4 (TLR4) in corneal and conjunctival epithelial cells was found in patients with clinical KC, subclinical KC, first-degree relatives (without abnormal clinical–topographic–

aberrometric–tomographic parameters) of KC patients, and even patients with pellucid marginal degeneration (another sort of corneal ectasia) when compared to healthy control participants [17,27,28]. TLR2 & TLR4 biomarkers showed a great potential to monitor early KC changes, and demonstrated relevant roles as predictive, diagnostic, and prognostic targets for corneal ectatic disorders. Moreover, this overexpression was also observed at the blood level (in monocytes and neutrophils), showing a clear association with inflammatory serum biomarkers [16]. Both receptors acquired significant importance in the pathophysiology of the disease, however, TLR2 seems to be slightly more involved in KC. To the best of our knowledge, this is the first study that examines the relationship between TLR2 expression and LTF levels in KC patients at both systemic and ocular levels.

Regarding the immunomodulatory capacity of LTF, it has been described that it promotes the modulation of signaling molecules associated with the immune innate and adaptative response balancing [12,29]. In this linen, LTF has shown a linked activity with pathogen-associated molecular patterns involved in the TLR4 pathway. Concretely, LTF interferes with CD14-LPS interaction, resulting in the inhibition of LPS-induced TLR4 activation. This LTF interaction modulates the immunoinflammatory process mainly by preventing the release of proinflammatory cytokines and limiting the recruitment of immune cells to inflammatory sites, as well as their activation [30,31]. However, LTF is also able to promote the recruitment and maturation of immune B and T cells [29,32]. An extensive in vitro overview of the LTF interactions has demonstrated that LTF may promote or inhibit TLR4 activation, being able to moderately activate it by direct interaction and to attenuate it by CD14-LPS interaction. In addition, the NF-κB activation guided by LTF could be done by both MyD88-dependent or -independent pathways [33]. These findings suggest that LTF modulation on TLR4 pathways might be present in KC patients, but there are no studies evaluating this issue. About TLR2 modulation, there is no information about the LTF impact or about how it affects the immune cell responses. Nevertheless, after proving the association between low LTF concentrations and TLR2 overexpression at both systemic (blood samples) and local (tear fluid & ocular surface) levels in KC patients, our in vitro study with cell cultures aimed to determine the LTF's immunomodulatory capacity on TLR2.

A fundamental hurdle in the study of the molecular-based mechanisms that lead to the development and progression of KC is the absence of a consolidated in vitro or in vivo model. In this study, we carried out an initial in vitro approach with a specifically designed cell line (HEK-Blue^{TM}hTLR2) for monitoring TLR2 agonists and antagonists, in order to find out how LTF contributes to TLR2 modulation. As a result, we confirmed that the use of LTF downregulates the expression and functionality of TLR2. More specifically, in stimulated HEK-Blue^{TM}hTLR2 cell cultures, TLR2 protein expression was statistically reduced using 2 mg/mL of human LTF. Moreover, the amount of SEAP and IL-8 released into the supernatant in response to the LTF immunomodulation was likewise reduced. The use of HEK-Blue^{TM}hTLR2 cell line allowed us to obtain a precise, specific, and direct demonstration that LTF immunomodulation involves the NF-kB-mediated TLR2 signaling pathway, confirming the successful and functional interaction between LTF and TLR2, and providing a stronger demonstration of the TLR2 immunomodulation by the human LTF. Undoubtedly, a deeper study about LTF modulatory properties of TLR2's immune–inflammatory response in a corneal epithelial cell line will be needed as the next step in future studies to understand in more detail the specific molecular process. This finding provides clear evidence that human LTF modulates the immune–inflammatory process mediated by the NF-κB-dependent TLR2 signaling pathway, preventing the overexpression of innate immune receptors, minimizing the release of pro-inflammatory cytokines, and limiting the enhancement of the chronic immune–inflammatory state. The ability to reduce the chronic immune–inflammatory microenvironment in KC corneas will help to minimize the cascade of molecular events (involving interleukins and metalloproteases (MMPs)) that trigger the corneal tissue degradation characteristic of the pathophysiology of the disease.

All these findings indicate a successful and functional interaction between LTF and TLR2 pathways; nevertheless, a deeper study of LTF modulatory properties on TLR2's immune–inflammatory response in a corneal epithelial cell line is needed to understand in more detail the specific molecular process.

The use of LTF in the development of therapies to treat KC has been taken into account in recent studies. Agwa et al. [13] highlighted the safety properties provided by LTF as a natural protein that plays a vital role in many physiological processes. This work supports the idea that the structure of LTF constitutes an advantage for administration efficiency, facilitating the design of a wide range of delivery systems [13]. Recently, two types of chitosan-based nanoparticles have been proposed as novel topical ophthalmic drug delivery systems which incorporate LTF as a pharmacological alternative for KC therapy [34]. Similarly, Pastori et al. [35] proposed the use of LTF-loaded therapeutic contact lenses to exert antioxidant activity on epithelial cells to reduce oxidative stress and to provide an effective device against the KC progression. However, none of these therapeutic approaches has yet been tested in a clinical setting. The findings observed in our study could impact on biotechnology development, opening the way for going a step further with dual LTF and TLR2-blocking therapeutic approach, or as a method to better target KC treatment. The use of LTF as a therapeutic agent would help to improve not only defensive and iron uptake capacities, preventing iron accumulation, increased oxidative stress, and avoiding cellular damage; but it would also improve the immune function on the KC ocular surface.

We have identified limitations to the clinical study. All participants should be included in both blood and tear collection to correlate serum and tear levels of LTF, rather than using two separate cohorts.

In conclusion, this study evidence that serum and tear LTF levels in KC patients strongly correlate with the disease's immune, inflammatory, and clinical status. Furthermore, the in vitro study confirmed that human LTF could indeed immunomodulate TLR2 expression in a functional manner, suggesting a potential therapeutic approach for future research.

4. Materials and Methods

4.1. Clinical Study

A total of 90 KC patients and 60 age- and gender-matched healthy controls were enrolled. Participants underwent a clinical exam with blood and tear collection. The main inclusion criterion was the KC diagnosis supported by slit-lamp, topographic, aberrometric and tomographic examination, following the KC diagnostic standards outlined in the literature [36–39]. Inclusion criteria for the healthy control participants included normal clinical parameters without biomicroscopic signs of KC, no alterations in the slit-lamp examination, no irregular astigmatisms in the tomographic evaluation that could suggest a subclinical state of the disease, and no family history of KC. Common inclusion criteria for both groups: (1) Schirmer $\geq$ 15 mm in 5 min; (2) conjunctival hyperemia < 2 (Nathan Efron scale) [40]; (3) at least 1 week without contact lenses and/or no instillation of eye drops. Exclusion criteria for both groups: (1) existence of active systemic or ocular inflammation, and/or current treatment with systemic or local anti-inflammatory drugs; (2) hepatic, renal, hematologic, and/or immunologic diseases, disorders of thyroid function, uncontrolled diabetes, and infections in the days preceding to the sample collection; (3) dry eye; (4) solid tumors or surgery interventions, since they may interfere with the results of the study of molecular markers. All clinical examinations were performed by the same researcher, and the molecular determinations were carried out in a laboratory blinded to clinical data.

4.1.1. Blood Sample Extraction and Analysis

Blood samples were extracted by venipuncture and collected in EDTA-anticoagulated tubes. These samples were used to measure serum concentrations of LTF. For the determination of LTF serum levels, blood samples were centrifuged for 15 min at 3000$\times$ *g* and

stored at −80 °C. LTF levels were measured using commercial ELISA kits following the manufacturer's instructions (Assaypro LLC, St. Charles, MO, USA). The intra-assay and inter-assay coefficient of variation (CV) was less than 8%.

4.1.2. Tear Sample Collection and Analysis

Schirmer strips (Contacare Ophthalmics Diagnostics, Guajarat, India) were used to collect the tear fluid from the temporal area of the lower eyelid. Tear collection was carried out with adequate environmental conditions, without previous administration of drugs, vital dyes, or other eye drops; gloves were used to avoid contamination of the samples. One strip was used for each participant, collecting 15 mm on the strip's scale. Samples were frozen at −80 °C until the molecular evaluation. These samples were used to evaluate the concentrations of LTF in the tear fluid. LTF levels were measured using a commercial ELISA kit following the manufacturer's instructions (Assaypro LLC, St. Charles, MO, USA). The intra-assay and inter-assay CV were less than 8%.

4.1.3. LTF Correlation Study with Immune, Inflammatory and Clinical Variables

All participants enrolled in this clinical study had also previously participated in other studies conducted by our group. Therefore, our database (*Corneal Ocular Pathology Line (2019/623)*) collects information about their clinical status and a wide range of systemic and local immunoinflammatory variables. In this line, LTF correlation analysis was elaborated using previously collected information about: (1) TLR2 expression in blood monocytes and neutrophils, and in corneal and conjunctival epithelial cells; (2) serum inflammatory mediators (interleukin-1β (IL-1β), interleukin-6 (IL-6), matrix metalloproteinase 9 (MMP9), and tumor necrosis factor-alpha (TNF-α)); (3) clinical considerations like the presence of ocular itching and/or rubbing, and corneal topographic, aberrometric and tomographic parameters (paracentral infero-superior dioptric difference (I-S), coma, coma-like, and posterior elevation). Assessment methodology and data obtained for these collected variables have been previously published [6,7]. Briefly, TLR2 expression in blood monocytes and neutrophils (from blood samples), and TLR2 expression in corneal and conjunctival epithelial cells (from ocular surface cellular samples collected by superficial scraping with ophthalmic surgical lancets) were analyzed using FACSAria iiu flow cytometer (BD Biosciences, Franklin Lakes, NJ, USA) with FACSDiva software (BD Biosciences, Franklin Lakes, NJ, USA). TLR2 proteins were marked with fluorescein isothiocyanate (FITC) anti-TLR2-conjugated monoclonal antibodies (Immunostep, Salamanca, Spain). The mean expression of TLR2 was reported as arbitrary fluorescence units (AFU). For the determination of IL-1β, IL-6, MMP9, and TNF-α serum levels, blood samples were centrifuged for 15 min at 3000× *g* and stored at −80 °C. MMP-9 concentrations were measured by ELISA kit following the manufacturer's instructions (GE Healthcare, UK). IL-1β, IL-6, and TNF-α levels were analyzed using an immunodiagnostic IMMULITE 1000 System (Siemens Healthcare Global, CA, USA). Finally, TOPCON CA-100 topographer-aberrometer and Orbscan IIz tomographer were used to compile the corneal quantitative parameters.

4.2. In Vitro Study

In vitro research was performed using the HEK-Blue™ hTLR2 cell line, a cell culture specifically designed for studying the stimulation, neutralization, and immunomodulation of TLR2. HEK-Blue™ hTLR2 cell line from InvivoGen (Cat.#hkb-htlr2, InvivoGen, Toulouse, France) was obtained by co-transfection of hTLR2 and secreted embryonic alkaline phosphatase (SEAP) reporter genes into human embryonic kidney 293 (HEK293) cells. The SEAP reporter gene is placed under the control of the IFN-β minimal promoter, fused to NF-kB and AP-1-binding sites; so, when a TLR2 ligand activates NF-kB and AP-1, the production of SEAP is induced. HEK-Blue™ Null1, the parental cell line of HEK-Blue™ hTLR2, was used as negative control. HEK-Blue™ Null1 (Cat.#hkb-null1, InvivoGen, Toulouse, France) was obtained by transfection of SEAP reporter genes into HEK293 cells, without hTLR2-reported genes.

Both HEK-Blue™ cell lines were seeded, cultured, maintained and propagated according to the manufacturer's instructions. At 48 h before starting the experiments, cells were cultured at a density of 3×10^5, 1×10^5, or 4×10^4 cells/well in respectively 12-, 24-, or 96-well plates (depending on the experiment). As a rule, each experiment of the in vitro study comprised at least three replicates for each measurement.

4.2.1. Experimental Design

To achieve TLR2 overexpression, HEK-Blue™ cell cultures were incubated for 18 h with Pam2CSK4 (10 ng/mL, InvivoGen, Toulouse, France) or Pam3CSK4 (100 ng/mL, InvivoGen, Toulouse, France), both synthetic lipopeptides TLR2 agonists. An IgA monoclonal antibody to human TLR2 (Anti-hTLR2-IgA, 10 µg/mL, InvivoGen, Toulouse, France) was used to neutralize TLR2 expression. The neutralizing protocol was performed following the manufacturer's instructions; briefly, HEK-Blue™ cells were pre-incubated for 1 h with Anti-hTLR2-IgA and then stimulated with Pam2CSK4 or Pam3CSK4 for 18 h. To assess the immunomodulatory activity of LTF, HEK-Blue™ cell cultures were pre-incubated with different concentrations (0.01–2 mg/mL) of human LTF (L1294, Sigma, St. Louise, MO, USA), following the same method carried out for neutralizing. 2 mg/mL of human LTF was the dose that achieved the best neutralization capacity, shown in Figure S1, and so it was used for the in vitro TLR2 immunomodulation study. TLR2 overexpression, neutralization, and immunomodulation were first determined by measuring SEAP production with QUANTI-Blue™ assay. Flow cytometry, immunohistochemistry, WB, and ELISA experiments were then performed to validate the expression and functionality of TLR2.

4.2.2. QUANTI-Blue™

QUANTI-Blue™ (rep-qbs, InvivoGen, Toulouse, France) is a colorimetric enzyme assay developed to detect SEAP in cell supernatant. The supernatant of unstimulated, stimulated, neutralized, and immunomodulated HEK-Blue™ cell cultures were collected for SEAP quantification by QUANTI-Blue™ assay. The measurements were carried out in 96-well plates, and SEAP levels were quantified using a spectrophotometer (Synergy 2, BioTek, USA) at a 655 nm wavelength, according to the provided instructions.

4.2.3. Flow Cytometry

The unstimulated, stimulated, neutralized, and immunomodulated HEK-Blue™ cell cultures were trypsinized (trypsin-EDTA, Gibco, Gaithersburg, MD, USA) and removed from the 24-well plates in which they were seeded. After 5 min centrifugation at 200× *g*, the cell pellet was resuspended in D-PBS (ATCC, Virginia, USA) and incubated for 20 min with FITC anti-TLR2-conjugated monoclonal antibodies (5 µL, Immunostep, Salamanca, Spain). TLR2 expression was evaluated using FACSAria iiu flow cytometer (BD Biosciences, Franklin Lakes, NJ, USA) with FACSDiva software (BD Biosciences, Franklin Lakes, NJ, USA). To avoid that the background from the antibody may interfere with the study, samples were washed with D-PBS and centrifuged before being analyzed. Unlabeled and thus non-fluorescent cells, as well as HEK-Blue™ Null1 cells, were used as both negative controls. TLR2 expression was reported as AFU.

4.2.4. Immunohistochemistry

Immunohistochemistry was automatically performed using an AutostainerLink 48 immunostainer (Dako-Agilent, Santa Clara, CA, USA). Briefly, the slides were incubated at room temperature (RT) in: (1) mouse monoclonal antibody to TLR2 (ab9100) (Abcam, Cambridge, UK) at 1:100 for 30 min; (2) EnVision®+ Dual Link System-HRP (dextran polymer conjugated with horseradish peroxidase and affinity-isolated goat anti-mouse and goat anti-rabbit immunoglobulins) (Dako-Agilent, K4065) for 20 min; (3) DAB+ substrate-chromogen solution (1 mL of substrate buffer solution containing hydrogen peroxide and 20 µL of 3,3′-diaminobenzidine tetrahydrochloride chromogen solution) for 10 min; and (4) EnVision FLEX hematoxylin for 15 min. The intensity of each TLR2 staining was

quantified by ImageJ (Rasband, WS, USA) by measuring the inverted DAB signal and by calculating the average with at least thirteen cells for each image.

4.2.5. Western Blot

The unstimulated, stimulated, neutralized, and immunomodulated HEK-Blue™ cell cultures were trypsinized and removed from the 12-well plates in which they were seeded. After centrifugation, the cell pellets were resuspended in RIPA lysis buffer (Thermo Scientific, Waltham, MA, USA) with protease inhibitor (Roche, Suiza) and shacked for 15 min on ice. The lysates were collected and centrifuged at 21,000× *g* for 30 min at 4 °C, and the supernatants were collected and stored at −80 °C. To prepare samples for WB, the total concentration of proteins was quantified using a micro BCA protein assay kit (Thermo Scientific, Waltham, MA, USA) according to the manufacturer's instructions. Each sample was aliquoted with 15 µg of total proteins, combined with 4× loading buffer, and denatured in a 95 °C metal bath for 10 min. Samples were run on SDS-PAGE 10% protein gel using a fixed voltage of 140 V. Proteins were electro-transferred to a PVDF membrane (Amersham™ Hybond 0.45, USA) using a Trans-Blot semi-dry system (Bio-Rad, Hercules, CA, USA) with a limited voltage of 25 V and 180 mA for 1 h 40 min. Post-blot membranes were blocked for 45 min with 3% bovine serum albumin (BSA, Sigma, St. Louise, MO, USA) (3% BSA diluted in Tris chloride Buffered Saline with Tween® 20 (TBST)), and then incubated overnight at RT in agitation with 1:500 rabbit polyclonal Anti-TLR2 target protein (A11225, ABclonal, Woburn, MA, USA) and with 1:2000 rabbit polyclonal Anti-β-actin control protein (Abcam, UK), both diluted in 3% BSA-TBST. TLR2 has a molecular weight of 89 kDa, while β-actin weighs 42 kDa. After overnight incubation, membranes were washed three times in TBST and incubated again for 1 h at RT in agitation with 1:5000 HRP-conjugated goat anti-rabbit IgG secondary antibody (Dako, Denmark) diluted in 3% BSA-TBST. Finally, membranes were washed in TBST, and revealed with Pierce™ ECL Western Blotting Substrate (Thermo Fisher, Lexington, MA, USA). ChemiDoc™ MP imaging system (Bio-Rad, Hercules, CA, USA) was used for band detection. Results were analyzed by ImageJ (Rasband, WS, USA) by measuring the mean grey value of protein bands delimited in ROIs. Relative expression of TLR2 to β-actin was calculated for each sample, and each group sample average was normalized to the control.

4.2.6. ELISA

The supernatant of unstimulated, stimulated, neutralized, and immunomodulated HEK-Blue™ cell cultures seeded in 24-well plates, was collected for IL-8 quantification. IL-8 concentrations were quantified using an ELISA kit (EK0413, Boster, Pleasanton, CA, USA) according to the manufacturer's instructions.

4.3. Statistical Analysis

SPSS 20.0 for Windows (IBM, NY, USA) was used to conduct the statistical analysis. A Kolmogorov–Smirnov test was used to verify the normality of a quantitative variable. Results were expressed as mean (±standard deviation (SD)) for continuous quantitative variables with normal distribution, and as percentages for categorical variables. Bivariate comparisons were made with Student's *t* test (normal continuous variables), and with the χ2 test (categorical variables). Graphic representations of the comparisons between normal continuous variables were made using error bars. An ANOVA test was used to make comparisons among more than two study groups following a DMS post hoc test. Bivariate correlations for normal distribution were analyzed using Pearson's coefficients and represented by scatter plots. A p value less than 0.05 was considered significant in all tests. The statistical EPIDAT 3.1 software was used for calculating the sample size of the clinical study. This determination was based on preliminary published studies of TLR2 levels [6,7]; accepting a confidence level of 95% ($\alpha = 0.05$) and 75% power ($\beta = 0.25$) of at least 20 control eyes and 40 eyes with KC would be necessary.

Supplementary Materials: The supporting information can be downloaded at: https://www.mdpi.com/article/10.3390/ijms232012350/s1.

Author Contributions: Conceptualization, U.R. and I.L.; methodology, U.R. and T.S.; formal analysis and investigation, U.R. and M.L.-L.; resources, T.S., E.D.-F. and I.L.; writing—original draft preparation, U.R.; writing—review and editing, M.L.-L., R.V.-F., T.S., E.D.-F. and I.L.; supervision, I.L.; funding acquisition, U.R., M.L.-L., R.V.-F., T.S. and I.L. All authors have read and agreed to the published version of the manuscript.

Funding: This project has been awarded grants from the Spanish Ministry of Economy and Competitiveness (I.L.: PI18/00159, Instituto de Salud Carlos III); Xunta de Galicia (Consellería de Economía e Industria: IN607A2018/3 & T.S.: IN607D 2020/09), and the European Union program ERFD. T.S. (CPII17/00027) is recipient of a research contract from the Miguel Servet Program (National Institute of Health Carlos III). Similarly, U.R. recognizes the support from Xunta de Galicia (Galician Innovation Agency GAIN: IN606B-2021/001) postdoctoral fellowship, and M.L.L. recognizes the support from Spanish Research Network on Cerebrovascular Diseases INVICTUS PLUS (RD16/0019/0001) fellowship. R.V.F. acknowledge the financial support of the FIDIS (Health Research Institute of Santiago de Compostela Foundation). The funders had no role in the study design, data collection and analysis, decision to publish, or preparation of the manuscript.

Institutional Review Board Statement: The clinical study was conducted in accordance with the Declaration of Helsinki of the World Medical Association (2008) and approved by the Ethics Committee of Research at Servizo Galego de Saúde (2015/436 and 2019/623).

Informed Consent Statement: Informed consent was obtained from all subjects involved in the study. Written informed consent has been obtained from the patient(s) to publish this paper.

Data Availability Statement: Not applicable.

Acknowledgments: Pathological Anatomy Service (Immunohistochemical Laboratory of the Santiago de Compostela Hospital Complex) has collaborated in the immunohistochemical assay of this project.

Conflicts of Interest: The authors declare no conflict of interest. The funders had no role in the design of the study; in the collection, analyses, or interpretation of data; in the writing of the manuscript; or in the decision to publish the results.

References

1. González-Chávez, S.A.; Arévalo-Gallegos, S.; Rascón-Cruz, Q. Lactoferrin: Structure, function and applications. *Int. J. Antimicrob. Agents* **2009**, *33*, 301.e1–301.e8. [CrossRef] [PubMed]
2. Sánchez, L.; Calvo, M.; Brock, J.H. Biological role of lactoferrin. *Arch. Dis. Child.* **1992**, *67*, 657–661. [CrossRef] [PubMed]
3. Vorland, L.H. Lactoferrin: A multifunctional glycoprotein. *APMIS* **1999**, *107*, 971–981. [CrossRef] [PubMed]
4. Zhang, Y.; Lu, C.; Zhang, J. Lactoferrin and Its Detection Methods: A Review. *Nutrients* **2021**, *13*, 2492. [CrossRef] [PubMed]
5. Steijns, J.M.; van Hooijdonk, A.C. Occurrence, structure, biochemical properties and technological characteristics of lactoferrin. *Br. J. Nutr.* **2000**, *84*, 11–17. [CrossRef]
6. Santagati, M.G.; La Terra Mulè, S.; Amico, C.; Pistone, M.; Rusciano, D.; Enea, V. Lactoferrin expression by bovine ocular surface epithelia: A primary cell culture model to study lactoferrin gene promoter activity. *Ophthalmic. Res.* **2005**, *37*, 270–278. [CrossRef]
7. Kijlstra, A.; Jeurissen, S.H.; Koning, K.M. Lactoferrin levels in normal human tears. *Br. J. Ophthalmol.* **1983**, *67*, 199–202. [CrossRef]
8. Wang, J.; Tian, Z. Recent advances in lactoferrin research and development during the past two years (2007–2009): In lieu of a preface of the Special Issue Lactoferrin. *Biometals* **2010**, *23*, 355–357. [CrossRef]
9. Flanagan, J.L.; Willcox, M.D. Role of lactoferrin in the tear film. *Biochimie* **2009**, *91*, 35–43. [CrossRef]
10. Lema, I.; Brea, D.; Rodríguez-González, R.; Díez-Feijoo, E.; Sobrino, T. Proteomic analysis of the tear film in patients with keratoconus. *Mol. Vis.* **2010**, *16*, 2055–2061.
11. Balasubramanian, S.A.; Pye, D.C.; Willcox, M.D. Levels of lactoferrin, secretory IgA and serum albumin in the tear film of people with keratoconus. *Exp. Eye Res.* **2012**, *96*, 132–137. [CrossRef] [PubMed]
12. Dierick, M.; Vanrompay, D.; Devriendt, B.; Cox, E. Lactoferrin, a versatile natural antimicrobial glycoprotein that modulates the host's innate immunity. *Biochem. Cell Biol.* **2021**, *99*, 61–65. [CrossRef] [PubMed]
13. Agwa, M.M.; Sabra, S. Lactoferrin coated or conjugated nanomaterials as an active targeting approach in nanomedicine. *Int. J. Biol. Macromol.* **2021**, *167*, 1527–1543. [CrossRef] [PubMed]
14. Belin, M.W.; Asota, I.M.; Ambrosio, R., Jr.; Khachikian, S.S. What's in a name: Keratoconus, pellucid marginal degeneration, and related thinning disorders. *Am. J. Ophthalmol.* **2011**, *152*, 157–162.e1. [CrossRef]

15. Wagner, H.; Barr, J.T.; Zadnik, K. Collaborative Longitudinal Evaluation of Keratoconus (CLEK) Study: Methods and findings to date. *Cont. Lens Anterior Eye* **2007**, *30*, 223–232. [CrossRef]
16. Sobrino, T.; Regueiro, U.; Malfeito, M.; Vieites-Prado, A.; Pérez-Mato, M.; Campos, F.; Lema, I. Higher Expression of Toll-Like Receptors 2 and 4 in Blood Cells of Keratoconus Patiens. *Sci. Rep.* **2017**, *7*, 12975. [CrossRef]
17. Malfeito, M.; Regueiro, U.; Pérez-Mato, M.; Campos, F.; Sobrino, T.; Lema, I. Innate Immunity Biomarkers for Early Detection of Keratoconus. *Ocul. Immunol. Inflamm.* **2019**, *27*, 942–948. [CrossRef]
18. Takeda, K.; Akira, S. Toll-like receptors in innate immunity. *Int. Immunol.* **2005**, *17*, 1–14. [CrossRef]
19. Hanstock, H.G.; Edwards, J.P.; Walsh, N.P. Tear Lactoferrin and Lysozyme as Clinically Relevant Biomarkers of Mucosal Immune Competence. *Front. Immunol.* **2019**, *10*, 1178. [CrossRef]
20. Camaschella, C. Iron-deficiency anemia. *N. Engl. J. Med.* **2015**, *372*, 1832–1843. [CrossRef]
21. Papanikolaou, G.; Pantopoulos, K. Iron metabolism and toxicity. *Toxicol. Appl. Pharmacol.* **2005**, *202*, 199–211. [CrossRef] [PubMed]
22. Gass, J.D.M. The Iron Lines of the Superficial Cornea: Hudson-Stahli Line, Stocker's Line and Fleischer's Ring. *Arch. Ophthalmol.* **1964**, *71*, 348–358. [CrossRef] [PubMed]
23. Barraquer-Somers, E.; Chan, C.C.; Green, W.R. Corneal epithelial iron deposition. *Ophthalmology* **1983**, *90*, 729–734. [CrossRef]
24. Volatier, T.L.A.; Figueiredo, F.C.; Connon, C.J. Keratoconus at a Molecular Level: A Review. *Anat. Rec.* **2020**, *303*, 1680–1688. [CrossRef]
25. López-López, M.; Regueiro, U.; Bravo, S.B.; Chantada-Vázquez, M.D.P.; Varela-Fernández, R.; Ávila-Gómez, P.; Hervella, P.; Lema, I. Tear Proteomics in Keratoconus: A Quantitative SWATH-MS Analysis. *Investig. Ophthalmol. Vis. Sci.* **2021**, *62*, 30. [CrossRef]
26. Loh, A.; Hadziahmetovic, M.; Dunaief, J.L. Iron homeostasis and eye disease. *Biochim. Biophys. Acta* **2009**, *1790*, 637–649. [CrossRef]
27. Regueiro, U.; López-López, M.; Hervella, P.; Sobrino, T.; Lema, I. Corneal and conjunctival alteration of innate immune expression in first-degree relatives of keratoconus patients. *Graefes Arch. Clin. Exp. Ophthalmol.* **2021**, *259*, 459–467. [CrossRef]
28. Regueiro, U.; Pérez-Mato, M.; Hervella, P.; Campos, F.; Sobrino, T.; Lema, I. Toll-like receptors as diagnostic targets in pellucid marginal degeneration. *Exp. Eye Res.* **2020**, *200*, 108211. [CrossRef]
29. Telang, S. Lactoferrin: A Critical Player in Neonatal Host Defense. *Nutrients* **2018**, *10*, 1228. [CrossRef]
30. Elass, E.; Masson, M.; Mazurier, J.; Legrand, D. Lactoferrin inhibits the lipopolysaccharide-induced expression and proteoglycan-binding ability of interleukin-8 in human endothelial cells. *Infect. Immun.* **2002**, *70*, 1860–1866. [CrossRef]
31. Legrand, D.; Mazurier, J. A critical review of the roles of host lactoferrin in immunity. *Biometals* **2010**, *23*, 365–376. [CrossRef] [PubMed]
32. Kruzel, M.L.; Zimecki, M.; Actor, J.K. Lactoferrin in a Context of Inflammation-Induced Pathology. *Front. Immunol.* **2017**, *8*, 1438. [CrossRef]
33. Ando, K.; Hasegawa, K.; Shindo, K.; Furusawa, T.; Fujino, T.; Kikugawa, K.; Nakano, H.; Takeuchi, O.; Akira, S.; Akiyama, T.; et al. Human lactoferrin activates NF-kappaB through the Toll-like receptor 4 pathway while it interferes with the lipopolysaccharide-stimulated TLR4 signaling. *FEBS J.* **2010**, *277*, 2051–2066. [CrossRef] [PubMed]
34. Varela-Fernández, R.; García-Otero, X.; Díaz-Tomé, V.; Regueiro, U.; López-López, M.; González-Barcia, M.; Lema, M.I.; Otero-Espinar, F.J. Design, Optimization, and Characterization of Lactoferrin-Loaded Chitosan/TPP and Chitosan/Sulfobutylether-β-cyclodextrin Nanoparticles as a Pharmacological Alternative for Keratoconus Treatment. *ACS Appl. Mater. Interfaces* **2021**, *13*, 3559–3575. [CrossRef]
35. Pastori, V.; Tavazzi, S.; Lecchi, M. Lactoferrin-loaded contact lenses counteract cytotoxicity caused in vitro by keratoconic tears. *Cont. Lens. Anterior Eye.* **2019**, *42*, 253–257. [CrossRef] [PubMed]
36. Fam, H.B.; Lim, K.L. Corneal elevation indices in normal and keratoconic eyes. *J. Cataract. Refract. Surg.* **2006**, *32*, 1281–1287. [CrossRef]
37. Alió, J.L.; Shabayek, M.H. Corneal higher order aberrations: A method to grade keratoconus. *J. Refract. Surg.* **2006**, *22*, 539–545. [CrossRef]
38. Rao, S.N.; Raviv, T.; Majmudar, P.A.; Epstein, R.J. Role of Orbscan II in screening keratoconus suspects before refractive corneal surgery. *Ophthalmology* **2002**, *109*, 1642–1646. [CrossRef]
39. Krachmer, J.H.; Feder, R.S.; Belin, M.W. Keratoconus and related noninflammatory corneal thinning disorders. *Surv. Ophthalmol.* **1984**, *28*, 293–322. [CrossRef]
40. Efron, N. Contact lens wear is intrinsically inflammatory. *Clin. Exp. Optom.* **2017**, *100*, 3–19. [CrossRef]

Supplementary material & data

Chapter 5

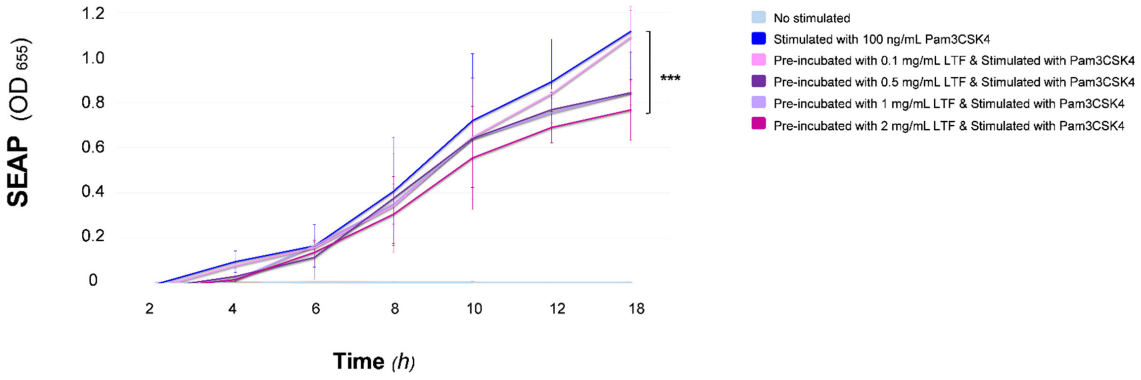


Figure S1. LTF dose test. Statistical differences: ***p<0.0001 between cells stimulated with 100ng/mL Pam3CSK4 and cells pre-incubated with 2mg/mL LTF. Abbreviations: LTF, lactoferrin; Pam3, Pam3CSK4; SEAP, secreted embryonic alkaline phosphatase.

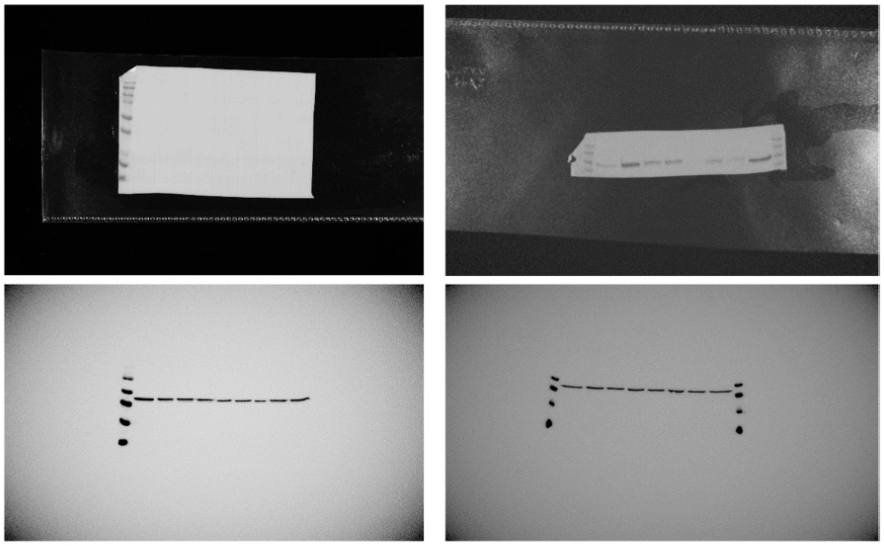


Figure S2. Uncropped blots in the same order as in Figure 4C.

Introduction

Justification and hypothesis

Objectives

Methodology

WP1. Clinical & molecular study of KC disease

WP2. Clinical & molecular study of KC at-risk stages

WP3. Human LF as a therapeutic strategy for KC

Discussion

Conclusions

Discussion

To address the central hypothesis of this thesis, a sequence of interconnected studies provided the necessary context to achieve all the specific objectives stated. In this line, the first and second work packages contemplated complementary purposes: **WP1** encompassed two studies focused on the search for protein biomarker networks in the tear fluid of KC patients, shedding light on the pathophysiological cascades of the disease and laying the groundwork for subsequently identifying, by **WP2** studies, the molecular markers and biological mechanisms involved in the KC earliest stages and the susceptibility to KC development in young offspring of KC patients. Additionally, the potential benefit of restoring LF levels as a therapeutic strategy for KC disease represent the main purpose of **WP3.**

Tear proteomics in KC disease

The quantitative and qualitative proteomic approaches followed in the first two chapters of the present thesis showed a high coverage of the tear proteome by identifying and quantifying more than 200 proteins in this biofluid. Our results showed that the KC patient's tear fluid protein composition had remarkable differences regarding the healthy control proteome, differing in more than one-third of the total proteins identified. Beyond differences in the global tear proteomic profile, alterations in the relative expression of 18 proteins were also observed in the tear samples of KC patients. In this way, both dysregulated and KC tear-specific expressed proteins were associated with cellular structural organization, oxidative stress, iron transport and homeostasis, and inflammatory processes, findings that are consistent with that reported in previous studies, where high levels of oxidative stress, chronic inflammatory events and alterations in cellular structure have been postulated as central mechanisms in the KC pathophysiology.[12,17,217,218]

In terms of cellular structure integrity and cytoskeletal organization, overexpression of CFL1, PLS3, and TUBA1C were observed in the tear samples of KC patients. All of them are involved in the regulation, organization and dynamics of the actin and tubulin cytoskeleton. Besides that, down-regulation of latexin (LXN), a potent inhibitor of the adenylyl cyclase-associated protein 1 and 2 (CAP1, CAP2) was also observed. Considering that CAP1 and CAP2 directly regulates filament dynamics and actin polymerization, [219] our results clearly pointed out alterations in actin assembly, cell morphology and communication.

CFL1 is an actin depolymerization factor involved in cell motility, cell division, membrane and cytoskeletal organization.[220] Overexpression of this protein and also of the

CFL1 gene was previously observed in the stromal fibroblasts of KC corneas, and the identification of CFL1 as a new mechanotransduction player suggests a possible impact of CFL dysregulation on corneal tissue weakness in KC disease.[221,222] PLS3 is an actin cross-linker and clustering protein which participates in all F-actin dynamics-dependent processes, such as cell motility and division, focal adhesion, neurotransmission or vesicle trafficking.[223] Although no previous studies have reported associations between PLS3 and KC disease, strong overexpression of this protein could be related to the disruption of actin filament junctions and the necessity of stimulating and regenerating these connections in the keratoconic corneal tissue. Finally, TUBA1C belongs to the tubulin family, which are a major component of the microtubules.[224] Previous studies showed an increase in tubulin-family proteins expression in the epithelial cells of KC corneas, proposing that the up-regulation of these proteins may be related to their increased synthesis to cope with the epithelial corneal thinning.[218]

Morphological changes observed in KC corneas reflect a complex structural alteration in which there is not only a loss of cell density, but also a disorganization of the fibers and a tissue framework failure. In this sense, we also observed a down-regulation of Rho GDP-dissociation inhibitor 1 (coding by *ARHGDIA* gene), which is actively involved in the control of Rho proteins homeostasis. Rho GTPases are the major regulators of cell shape, contractility, mechanics, adhesion, and migration.[225] Besides that, Rho proteins also control the actin filament assembly and the cytoskeletal responses through diverse effectors and constitute one of the central mechanotransduction paths in the cornea.[226] Previous studies have reported altered RhoA expression in severe KC corneal epithelium,[227] also it has been demonstrated that an increase in the oxidative stress levels can reduce Rho expression and impact on cellular mechanics, inducing less strength and stiffness.[228] Considering that structural weakening is the main hallmark of corneal stroma and epithelium during KC disease, promoting the tissue protrusion and ectasia onset, the Rho pathway could be involved in the cell-cell adhesion disruption and actin disorganization during KC pathophysiology.

Moreover, the qualitative analysis identified a 13-keratin cluster that were only expressed in tear samples from KC patients. Keratins (KRT) constitute the main components of the outermost layer of the epidermis, some of them are expressed also by the corneal epithelial cells; however, they do not belong to the natural composition of the tear fluid. Previous studies suggesting that the presence of KRTs in the tear fluid of KC patients could be the consequence of eyelid filtration due to the eye rubbing,[229] nevertheless, six of the KRT that we identified are expressed by corneal epithelial cells,[230] so its detection may be associated with corneal epithelial cell death and degeneration.

Regarding oxidative stress, the redox imbalance was evidenced by the down-regulation of proteins with essential protective roles against oxidative damage, such as heat-shock family proteins, PRDXs, and some metal-binding proteins like serotransferrin or hemopexin. TF was the highest under-expressed protein in the KC tear samples. It is the main iron-binding protein in the body, having a central function in controlling iron

homeostasis and preventing the harmful effects of free iron.[231] Increased levels of unbound free iron imply a potential toxic impact in tissues due to its ability to produce reactive species through different reactions such as Fenton's reaction, so, the internalization, storage, and export of cellular iron is strictly regulated to maintain the right intracellular iron levels. In addition, it has been described that free iron tends to accumulate in tissues leading to cellular damage and tissue injury.[232] In the same line of our results in tear samples, previous studies reported the under-expression of TF in the stromal cells of KC corneas, and certain polymorphisms of the *TF* gene has been associated with increased risk of KC.[233] Considering that TF down-regulation was observed in iron overload conditions with high levels of free iron,[234] and one of the main histologic characteristics of the KC is the iron deposition in the epithelial basement membrane (Fleischer ring), down-regulation of iron-binding proteins may contribute to the iron filtration, oxidative microenvironment, and epithelial cell damage in KC.

In the same line, the shot-gun analysis revealed two clusters of peptidyl-prolyl cis-trans isomerases (PPIases) and aldehyde-dehydrogenases (ALDHs) that were only expressed in the KC tears. PPIases and ALDHs are involved in the cellular protection against oxidative damage, regulating the cellular apoptosis by oxidative damage and neutralizing and removing the aldehyde radicals respectively.[235,236] In this context, the expression of these proteins in the tears of KC patients could be related to the antioxidant demand in the epithelial cells of a tissue under chronic oxidative damage.

The immune-inflammatory involvement was suggested through the dysregulation of several proteins such as annexin A1, annexin A2, α1-acid-glycoprotein, or S100A4, which are actively involved in inflammatory processes.[237–240] The inflammatory-related nature of KC has been extensively described as a chronic inflammatory state, without the classic signs of inflammation (heat, redness, swelling, pain), but with the prolonged contribution of imbalances between pro- and anti-inflammatory molecules that exacerbate its pathogenic processes.[241] Moreover, ongoing oxidative stress drives the activation of chronic inflammatory pathways, and most of the time these processes give feedback to each other. In this sense, oxidative stress and inflammation seem to act synergistically during KC pathophysiology, perhaps leading to the final cell degeneration and death.

Lastly, we found the under-expression of vitamin D-binding protein in the tear sample of KC patients. This protein is crucial for transporting vitamin D throughout the body, ensuring adequate levels, and preventing its deficiency. Vitamin D is a potent immunomodulator that also plays an important anti-inflammatory role on the ocular surface. Previous studies reported Vitamin D deficiency in blood samples of KC patients, and its low levels have been associated with elevated collagen degradation markers and disease progression.[242–244] Under normal conditions, levels of vitamin D in the tear fluid are higher than in plasma,[245] so, the observed deficit in blood may agree with our results in tears. Interestingly, vitamin D supplementation in adolescent patients with KC has shown potential beneficial effects by improving copper metabolism and thus increasing

endogenous CXL and antioxidant capacity, which may constitute an additional non-invasive and inexpensive therapeutic alternative.[246]
In summary, the results obtained with the quantitative and qualitative analysis of the tear proteome of KC patients strengthened the involvement of biological processes previously associated with the disease, such as inflammation, oxidative stress, immunity, and alterations in cellular structure and organization. In addition, the down-regulation of essential proteins in iron transport and homeostasis and its link with the activation of oxidative stress and inflammatory processes could highlight another fundamental pathway in the pathogenesis of the disease.

Tear proteomics in KC risk-stages and biomechanical weakness

Following the analysis of the biomarker networks and biological pathways that remain during the pathophysiological process and the development of the disease, the next step aimed to find out which of these factors played a decisive role in the disease susceptibility as well as in the onset of corneal biomechanical instability, trying to get closer to the molecular drivers that trigger the downstream molecular alterations.

Even though KC presents a complex pattern of inheritance, sometimes following an autosomal dominant/recessive mode or emerging spontaneously without any associated Mendelian pattern, it has been reported that first-degree relatives of KC patients have between 15-67 times higher risk than the population without a family history of corneal ectasia for KC development.[9] In the same way, most studies looking for the KC risk factors have found a strong influence of family history on disease onset, considering it one of the most relevant risk factor for its possible development.[9] Based on the above, the purpose of the **WP2** was to determine the proteomic alterations in the tears of offspring of KC patients (O-KC), who are associated with **(1)** higher susceptibility to disease development related to the presence of a parent diagnosed with the disease, and **(2)** higher biomechanical instability of corneal tissue that is critical in the earliest stages of corneal ectasia. In addition, a three-year follow-up study was performed to assess the biomechanical, tomographical, and molecular changes linked to preliminary disease onset in a cohort of O-KC participants progressing to subclinical or clinical KC stages.

To this end, we combine biomechanical and tomographical assessments with a complete tear proteomic study by LC-MS/MS in O-KC participants and in control subjects with no family history of any corneal ectasia. To reduce the intra-group variability associated with the genetic-hereditary complexity of the KC disease, the group of O-KC was sub-classified according to the results obtained in the corneal biomechanical examination. The biomechanical subcategorization of the study group allowed us to know not only those markers associated with the highest risk for the disease, but also those that might underlie the earliest biomechanical deterioration. It is worth mentioning that all control subjects were required to exhibit normal corneal biomechanical behavior to be included in the study.

Among all eyes included in the O-KC group, 18% showed moderate alterations in the corneal dynamics, indicating a moderate risk of ectasia development (O-KC-MR group), and 11% showed high alterations in the biomechanical exam, pointing out a high-risk of ectasia development (O-KC-HR). This implied that almost one-third of O-KC eyes showed moderate or high alterations of corneal biomechanical behavior, which agrees with previous studies, which have reported significantly higher biomechanical impairment in the corneas of first-degree relatives of KC patients compared to control subjects.[63,64]

The tomographic exam revealed that corneal thickness and pachymetric progression differed significantly among the groups categorized by their biomechanical alteration; showing thinner corneas, a faster increase in corneal thickness towards the periphery (lower ARTh values), and higher differences in corneal thickness from the center to the periphery (PachySlope) as biomechanical behavior worsened. Abnormalities in corneal tomographic features of KC relatives were also documented in previous studies, including corneal central steepening, asymmetric topographic patterns, and increased videokeratoscopy indices suggestive in some cases of subclinical disease states.[62,247–249] In this way, Jie Li et al [250] recently reported that parents of KC patients also showed steeper and thinner corneas, with biomechanical indices reflecting less stiffness and altered pachymetric progression, demonstrating from a complementary approach the potential heritability of tomographical and biomechanical traces.

The three-year follow-up study also revealed on one hand that the 26% of the O-KC eyes worsening their CBI index after the follow-up period, and on the other hand that alterations in pachymetric progression seemed to be the earliest detectable changes associated with the cases with biomechanical decline over the follow-up. Considering that pachymetric features are determined as one of the most highly heritable human traits, with a heritability range between 0.68 and 0.95, [251–253] and also that our study sample has a direct family history of KC where reduced corneal thickness is critical, our results suggest that in an at-risk endophenotype, slight and silent variations in corneal thickness and pachymetric progression could precede and stimulate the alterations in the corneal biomechanical behavior.

Returning to the initial study of O-KC participants, the LC-MS/MS analysis of the tear samples showed that 15 proteins had significantly differential expression between the O-KC groups and the control. In this line, the main biological pathways of these proteins explain a potential impact on mechanobiology, intercellular communication, and the cell cycle processes. Associated with these pathways, we also observed dysregulation of pivotal proteins in oxidative defense, which suggested that oxidative damage could induce and exacerbate cellular damage and disruption of tissue homeostasis at the earliest stages.

The evidence of oxidative damage in KC corneal cells seems already unquestionable; however, some genetic studies suggested its involvement in familial KC.[10] In this way,

our results have gone a step further, determining that the dysregulation of essential proteins in redox homeostasis, such as LF, SOD1, or PRDX1, is related not only to the progressive biomechanical deterioration but is also detectable in the at-risk subjects even before the biomechanical decline can be sensed with clinical tools. In this sense, the under-expression of LF, SOD1, and PRDX1 was sharply observed in all O-KC groups and was pronounced in those groups exhibiting higher biomechanical impairment.

The lower expression of LF in KC tear samples has been previously reported,[14,16] being considered by its antioxidant and anti-inflammatory nature as a potential therapeutic strategy for KC disease. Nevertheless, changes in LF expression in the samples of KC relatives in had not been reported to date. In this line, our results suggest that the potential of LF as a diagnostic and therapeutic target could be even more promising after observing that the decrease in its expression precedes even biomechanical alterations, having the highest sensitivity and specificity to discriminate between controls and biomechanically and tomographically healthy O-KC (O-KC-LR), and also the best AUC values to detect eyes at high-risk of developing ectasia (O-KC-HR). Similarly, the relationship between SOD1 and KC disease has been well-documented. The *SOD1* gene has been associated with familial KC through a deletion within intron 2 that segregates in affected family members. Given that SOD1 is one of the crucial antioxidant proteins of the human cornea, its under-expression has been related to antioxidant deficiency and the rise of free radicals and oxidative damage in KC corneal cells. However, as mentioned above about LF, our results have gone far beyond showing that SOD1 under-expression begins in those O-KC even without biomechanical or topographical alterations and becomes progressively evident as corneal properties worsen, emphasizing not only the involvement of SOD1 in corneal biomechanical decline but also in the at-risk endophenotype.

Along with oxidative damage, the underlying cellular mechanobiology impairment is recognized as the promoter of the subsequent corneal biomechanical weakness in KC.[226] Cell-cell communication processes and cellular response to stimuli are controlled by complex signaling pathways with multiple effectors. Based on what is directly observable in histological studies, corneal structural integrity progressively deteriorates as KC progresses, showing alterations in superficial epithelial cell differentiation, abnormalities in basal epithelial density, loss of its smoothness and regularity, and a complete stromal destructuring.[254–256] While in-depth corneal histological studies of relatives of KC patients are lacking, biomicroscopic examinations suggest that certain characteristic KC signs, like Fleischer's ring and visible corneal nerves, are more prevalent in these relatives compared to the general population.[257]

Our study on O-KC tear proteomics evidenced the dysregulation of five proteins (CFL1, CAPN1, EZN, ACNT4, and ACTG) that are involved in cell morphology and migration, cell-cell adhesion, cell-substrate binding, F-actin crosslinking, or cytoskeleton remodeling, and participate in central mechanotransduction and cell adhesion paths like RhoA, β-catenin, or mTOR signaling cascades.[258–261] The dysregulation of that proteins could contribute to the onset of biomechanical decline and cell-cell communication

weakness. In fact, the under-expression of these proteins was consistently higher in the O-KC groups with moderate or high alterations in corneal biomechanics. Alterations in CFL1 and CAPN1 were previously observed in KC stromal and epithelial cells, being recognized as possible underlying factors of stromal thinning and structural failure.[218,221] Despite the lack of data on dysregulation of these proteins in KC family members, their link with the disease pathophysiology support their potential contribution to KC risk.

Similarly, we observed the down-regulation of ACTN4 and ACTG in the tear samples of O-KC group with moderate-risk of ectasia development, two proteins that represent important factors in actin filament composition and F-actin crosslinking. Consistent with these findings, previous studies had already reported the down-regulation of β-actin expression in KC epithelium and stroma and human antigen R (HuR) mRNA stabilizing factor, which directly modulates β-actin gene expression.[218,262,263] The main functions of β-actin in the corneal stroma are to provide mechanical support and transmit signals from the cytoplasm to the surroundings; so, it has been proposed that the low levels of β-actin in KC stroma can compromise the cytoskeletal functions, mainly owing to a loss of β-actin stress fibers, and even could lead to keratocytes apoptosis.[262] No specific information is reported on ACTN4 and ACTG expression in KC relatives; however, pathogenic alleles in cytoskeletal and extracellular matrix-related genes have been previously associated with KC families, so our findings in O-KC participants could be associated with early alterations in actin filaments assembly and cross-linking. [264]

Considering all these findings, a deeper understanding over how initial oxidative stress imbalances impact cellular mechanobiology and tissue dysfunction is critical for unraveling the complex molecular networks involved in the early KC at-risk stages and susceptibility.

Proteomic overlap between KC and KC at-risk stages

WP1 and **WP2** were designed with complementary purposes. Firstly, **WP1** aimed to identify those proteomic markers and pathways that could be involved in the pathophysiology of clinical KC by focusing on patients with a well-defined KC diagnosis. Secondly, **WP2** was geared towards discovering the biomarkers and pathways underlying KC susceptibility and the early corneal biomechanical weakness by examining young O-KC, considered the most vulnerable population for KC development. In this sense, the networked layout of our studies also allowed the identification of overlapping markers and main pathways between clinical KC and KC at-risk stages, evidencing that most of the dysregulated proteins in both groups were closely associated, evolutionarily linked, or shared common biological functions.

The first matching finding between the proteomic tear analysis in KC patients and KC offspring was the dysregulation of iron-binding proteins. In this sense, the KC tear samples showed a marked under expression of TF and HPX, two critical proteins against

iron and heme toxicity.[265,266] At the same time, analysis of tear fluid from the offspring of KC patients revealed the lower expression of LF and HPX, being the LF a transferrin-family glycoprotein with very similar functionality to TF, high affinity for ferric ions,[107,267] and which low levels have been previously reported in the tear fluid of patients with KC.[14,16] While iron is essential for a wide range of cellular functions, its homeostasis must be tightly regulated. Excessive levels of free iron are highly harmful to cells and tissues due to their involvement in the catalysis of some reactions (such as Fenton or Haber/Weiss) and the consequent generation of reactive species that damage the cellular components and can even lead to ferroptosis cell death.[232,268] In this line, LF and TF, as iron-binding proteins, provide free-iron overload protection by reducing the quantity of unbounded iron available in the extracellular space, and therefore, prevents the activation of damaging reactions.

Oxidative damage in the KC corneal cells has been noticed in a wide number of studies,[87] and the Fleischer's ring, one of the most distinctive signs of the KC semiology, evidence the iron homeostasis failure in the epithelial tissue during the disease. Although different origins have been proposed for the accumulated iron in the Fleischer ring, some studies have concluded that the tear film is possibly the main source of that iron ions.[269] In this line and given the close relationship between iron dysregulation and oxidative damage, the dysregulation of iron-binding proteins in KC offspring, even in subjects without clinical disease and further associated with biomechanical impairment, points to a central contribution of iron dyshomeostasis on the oxidative damage to corneal cells in the earliest and at-risk stages of KC development.

Along with iron-binding proteins, the dysregulation of CFL1 was also observed in both KC and O-KC studies. CFL1 protein acts as an actin depolymerization factor participating in F-actin reorganization and cytoskeletal dynamics.[270] Besides that, CFL1 is a downstream mediator of RhoA pathway, whose activity is controlled upon phosphorylation by two LIM kinases (LIMK1 and LIMK2) which are simultaneously under the control of the small Rho GTPases.[271] The RhoA pathway is a highly conserved mechanotransduction path in the corneal tissue, critical for cellular migration, cellular shape regulation, cellular adhesion, stress fiber formation, and also having a key role in the actin cytoskeleton response to mechanical stimulus.[272–276] Rho GTPases are redox-sensitive,[277] and previous studies demonstrated the direct impact of oxidative stress in the cellular biomechanical weakness and focal adhesions through the Rho signaling, in a way that increased reactive species lead to decreased cell stiffness by reducing the RhoA expression and down-regulating the α-actin and cytoskeletal membrane-linker proteins.[228]

CFL1 dysregulation has been previously reported in KC corneal stromal cells,[221] and our results identified CFL1 dysregulation in both KC tear samples and also in the offspring of KC patients even without alterations in corneal biomechanical behavior. These findings could suggest the potential Rho signaling involvement in the early corneal tissue instability.

Besides that, our studies also revealed the differential expression of other effectors of the Rho signaling in the tear samples of KC and KC offspring, such as the Rho GDP-dissociation inhibitor 1 and the membrane-linker protein EZN, respectively. Rho GDP-dissociation inhibitor 1 is a potent regulator of the activation-inactivation cycle of Rho small GTPases, and EZN is a cross-linker between cortical actin filaments and the plasma membrane, being activated by phosphorylation of Rho kinases and also contributes to the regulation of Rho GTPase activity by interacting with Rho-related proteins.[278,279] Consistent with our findings, previous studies reported the overexpression of RhoA in the epithelial cells of severe KC,[227] and in the same line, the dysregulation of another mechanotransduction paths, such as the Hippo, TGF β, or Wnt signaling, also has been described in KC disease.[280,281]

As well, a number of master cytoskeletal and cell-cell adhesion proteins were dysregulated in both KC and KC offspring studies, such as PLS3, TUBA1C, CAPN1, ACNT4, and ACTG. All these results seem to fit together providing new insights into the molecular mechanisms that may underlie the early tissue instability and biomechanical decline at the earliest and at-risk KC stages.

Briefly, as a whole, **WP1** and **WP2** findings suggested similar biomarkers but common paths involved in clinical KC, KC at-risk stages, and also corneal biomechanical weakness. The biomarker network identified in those studies points toward an alteration in cell structure, integrity and communication exacerbated by chronic oxidative damage that could originate from different ways such as iron dyshomeostasis or inflammatory-immune imbalance.

LF in KC disease and its potential as a therapeutic target

The background on the LF involvement in the KC pathophysiology as well as the emerging insights into its participation in the at-risk stages and corneal biomechanical decline provided by the studies developed in the **WP2** of this thesis supported the potential LF as a promising therapeutic strategy for KC disease.

In the **WP3** we confirmed that tear and serum LF levels in KC samples were drastically reduced compared to control subjects. Additionally, lower tear LF levels strongly correlated with immune biomarkers at the ocular surface and with higher clinical quantitative corneal parameters associated with disease severity in KC patients. Moreover, the reduced serum LF concentration in KC patients correlated with increased immune-inflammatory biomarkers, such as TLR2, previously reported as a biomarker with a strong diagnostic and prognostic value in corneal ectasias.[77]

As mentioned above, LF is an iron-binding protein belonging from the transferrin family and having strong iron uptake capacity, with an iron affinity 300 times higher than transferrin.[282] This property confers an important antioxidant, anti-inflammatory, immunomodulatory, and antimicrobial iron-binding defensive function.[107] Based on the

immunomodulatory role of LF, confirmed by its ability to modulate signaling molecules associated with the innate and adaptative immune system, [283] the *in vitro* approach of the last work package of this thesis was focused on evaluate the LF therapeutic action.

TLRs are transmembrane proteins that constitute important effectors of the innate immunity cascades, detecting the presence of exogenous and/or endogenous agents associated with cell damage, and triggering an inflammatory response which may cause tissue degradation.[284] This fundamental concept underpins the hypothesis that TLR activation contributes to the inflammatory response associated with KC pathophysiology.[99] The overexpression of TLR2 was observed in blood, corneal, and conjunctival epithelial cells of KC and subclinical KC patients, healthy first-degree relatives of KC patients, and even in other corneal ectasias like pellucid marginal degeneration in comparison to the control subjects.[77,99–101] Additionally, TLR2 showed a promising value for early diagnosis, monitoring, and prognosis of corneal ectatic disorders.[77]

LF has been proposed as an endogenous ligand of TLRs capable of modulating its activation. However, while the interactions between LF and TLR4 have been well-described, our knowledge of LF's influence on TLR2 receptors remains largely unexplored.

Given the link between TLR2 overexpression and LF low concentrations observed in the **WP3**, and also considering the potential benefits of LF as an immunomodulatory and anti-inflammatory molecule, we designed an *in vitro* approach focused on determining how LF contributes to TLR2 modulation and consequently to validate its capacity as a potential therapeutic strategy.

Our findings demonstrated that LF treatment downregulates the expression and functionality of TLR2 in the cell cultures. More precisely, stimulated HEK-Blue™ hTLR2 cell cultures reduced its TLR2 protein expression when 2 mg/mL of human LF was added in a similar way to that obtained with the Anti-hTLR2-IgA, and therefore, evidencing its power for TLR modulation. Besides that, LF also affected the functionality of TRL2, with lower levels of SEAP and IL-8 in the supernatants of TRL2 LF-treated cell cultures.

Although a deeper understanding of the specific molecular crosstalk underlying the TLR2 modulation by LF is needed, our results demonstrated the capacity of LF to modulate the immune-inflammatory processes mediated by the TLR2 signaling pathway, reducing the release of proinflammatory cytokines, and limiting the chronic inflammatory-immunological stage, becoming a promising therapeutic strategy for KC disease.

From a therapeutical point of view, LF has been described as a successful targeting ligand for nanomedicine applications.[285] In this sense, our group has driven the design and optimization of effective LF delivery systems to the ocular surface as a potential approach

for KC therapy.[169–171] Some of the nanosystems developed for LF release and topical ophthalmic delivery included the chitosan nanoparticles, PLGA nanospheres, and nanostructured lipid carriers; three pharmacological alternatives with different materials and properties that enable exploring different interaction pathways between the molecule and the target tissue, providing a wide range of possibilities to obtain a controlled and efficient LF release in the ocular surface.[169–171] In a complementary way, Pastori et al[286,287] proposed using LF-loaded contact lenses as an effective device against KC progression. In light of our results, this study supports the use of LF as a therapeutic agent, encouraging the ongoing biopharmaceutical studies, and boosting their clinical applicability even in the earliest stages of the disease.

Although all the studies included in this compendium provide new insights into the pathophysiology and genesis of KC, some limitations have been identified. First of all, **Chapter 1** and **Chapter 2** were carried out in a small cohort of KC and control subjects, which didn't allow the stratification of the eyes according to disease severity. In this light, a larger sample size would enable the elucidation of those markers and pathways intertwined as the disease progresses, a task on which we are currently working. Also relative to the sample size, the categorization of the O-KC eyes in **Chapter 3** and **Chapter 4** led to an uneven distribution of participants across the study groups, with a substantially higher sample in the low-risk group than in the others (which was expected due to the incidence of the disease in this population). To address this limitation, equalizing the sample size across all study groups could provide greater consistency in our results. In addition, the inherent limitations of the corneal biomechanics methodology also influence our results, thus, the availability of new tools that allow focal analysis of corneal tissue and its biomechanical properties will lead to more exhaustive studies of the molecular factors that directly impact corneal structural weakness.

Finally, regarding **Chapter 5**, we used a commercial cell line specifically designed for studying the stimulation, neutralization, and immunomodulation of TLR2, which constitutes a useful first approach for exploring the potential immunomodulatory role of LF. However, studies in corneal epithelial cell lines are needed to mimic the pathophysiological process during KC disease, and, at the same time, an *in vivo* model suitable for studying KC disease will be essential to assess the traslationality of our results.

Introduction

Justification and hypothesis

Objectives

Methodology

WP1. Clinical & molecular study of KC disease

WP2. Clinical & molecular study of KC risk-stages

WP3. Human LF as a potential therapeutic approach

Discussion

Conclusions

Conclusions

WP1. Clinical & molecular study of KC disease.

Chapter 1

1. SWATH-MS quantification analysis revealed the dysregulation of 18 proteins in the tear samples of KC patients compared to controls.

2. Gene ontology and interaction network analysis between dysregulated proteins highlighted the impact of these proteins on inflammation, oxidative stress, and cellular structure processes.

3. The marked down-regulation of transferrin and hemopexin in tear samples from KC patients underscored the potential role of iron dyshomeostasis in the disease pathogenesis.

Chapter 2

4. Shot-gun qualitative proteomic analysis identified a total of 232 proteins in the tear samples of KC and control subjects.

5. The KC tear proteome composition differed from the control tear proteome in more than one-third of the total proteins identified.

6. The proteins only identified in the KC tear samples and dysregulated proteins resulting from spectral counting semi-quantification described once again the oxidative and iron transport imbalance in KC samples.

WP2. Clinical & molecular study of KC-risk stages.

Chapter 3

7. The vulnerability of the offspring of KC patients for disease development was supported by 29% of eyes within this group showing CBI values compatible with moderate-high risk for disease development.

8. SWATH-MS analysis determined the dysregulation of 15 proteins in O-KC groups, even in those without corneal biomechanical weakness.

9. Among dysregulated proteins, LCN1, LF, SOD1, EZN, and CAPN1 showed high sensitivity and specificity to discriminate between controls and O-KC groups, and also to detect moderate-high alterations in the corneal biomechanical properties.

10. LRA analysis determined three specific protein panels with high sensitivity-specificity for discriminating between the control and O-KC groups with different biomechanical weakness.

11. Dysregulated proteins were associated with oxidative stress, cell-adhesion, cytoskeleton organization, and mechanotransduction paths such as RhoA, mTOR, or E-cadherin/N-cadherin signaling.

12. Oxidative stress and cell structural alterations appear to begin long before the onset of clinical signs and even before alterations in the corneal biomechanics that can be detected with the current tools.

Chapter 4

13. After 3-year follow-up, a significant percentage of O-KC eyes had worsened its corneal biomechanical scores (21% in the O-KC-LR group, 29% in the O-KC-MR group, and 39% in the O-KC-HR group), indicating increased tissue instability, and thus higher risk for KC.

14. Changes in corneal thickness progression seems to be the earliest detectable sign of corneal biomechanical decline.

15. No differences were observed for LF expression between before and after follow-up in either group progressing toward further biomechanical weakening; however, LF values remained consistently lower than those obtained for the control group.

WP3. Human LF as therapeutic strategy for KC.

Chapter 5

16. Serum and tear LF concentration were statistically reduced in patients with KC compared to controls.

17. LF lower concentration was strongly correlated with KC severity markers, proinflammatory mediators' upregulation, and TLR2 overexpression at the systemic and ocular surface levels.

18. The treatment with 2mg/mL of LF reduced the expression and functionality of TLR2 in stimulated HEK-Blue™ hTLR2 cell cultures, supporting the potential of LF as a therapeutic strategy for KC disease.

Bibliography

1. Romero-Jiménez M, Santodomingo-Rubido J, Wolffsohn JS. Keratoconus: a review. Contact lens & anterior eye. 2010;33(4):157-166.

2. Belin MW, Asota IM, Ambrosio R, Khachikian SS. What's in a name: keratoconus, pellucid marginal degeneration, and related thinning disorders. Am J Ophthalmol. 2011;152(2):157-162.

3. Rabinowitz YS. Keratoconus. Surv Ophthalmol. 1998;42(4):297-319.

4. Scarcelli G, Besner S, Pineda R, Yun SH. Biomechanical characterization of keratoconus corneas ex vivo with Brillouin microscopy. Invest Ophthalmol Vis Sci. 2014;55(7):4490-4495.

5. Komninou MA, Seiler TG, Enzmann V. Corneal biomechanics and diagnostics: a review. Int Ophthalmol. 2024 Mar 13;44(1):132.

6. Kymes SM, Walline JJ, Zadnik K, Sterling J, Gordon MO, Collaborative Longitudinal Evaluation of Keratoconus Study Group. Changes in the quality-of-life of people with keratoconus. Am J Ophthalmol. 2008;145(4):611-617.

7. Wagner H, Barr JT, Zadnik K. Collaborative Longitudinal Evaluation of Keratoconus (CLEK) study: methods and findings to date. Contact Lens and Anterior Eye. 2007;30(4):223-232.

8. Bykhovskaya Y, Rabinowitz YS. Update on the genetics of keratoconus. Exp Eye Res. 2021;202.

9. Santodomingo-Rubido J, Carracedo G, Suzaki A, Villa-Collar C, Vincent SJ, Wolffsohn JS. Keratoconus: An updated review. Cont Lens Anterior Eye. 2022;45(3):101559.

10. Shinde V, Sobreira N, Wohler ES, et al. Pathogenic alleles in microtubule, secretory granule and extracellular matrix-related genes in familial keratoconus. Hum Mol Genet. 2021;30(8):658-671.

11. Wang Y, Rabinowitz YS, Rotter JI, Yang H. Genetic epidemiological study of keratoconus: evidence for major gene determination. Am J Med Genet. 2000;93(5):403-409.

12. Lema I, Duran J. Inflammatory molecules in the tears of patients with keratoconus. Ophthalmology. 2005;112(4):654-659.

13. Lema I, Sobrino T, Duran JA, Brea D, Diez-Feijoo E. Subclinical keratoconus and inflammatory molecules from tears. British Journal of Ophthalmology. 2009;93(6):820-824.

14. Lema I, Brea D, Rodríguez-González R, Díez-Feijoo E, Sobrino T. Proteomic analysis of the tear film in patients with keratoconus. Mol Vis. 2010;16:2055-2061.

15. Balasubramanian SA, Mohan S, Pye DC, Willcox MD. Proteases, proteolysis and inflammatory molecules in the tears of people with keratoconus. Acta Ophthalmol. 2012;90(4):303-309.

16. Balasubramanian SA, Pye DC, Willcox MD. Levels of lactoferrin, secretory IgA and serum albumin in the tear film of people with keratoconus. Exp Eye Res. 2012;96(1):132-137.

17. Chwa M, Atilano SR, Reddy V, Jordan N, Kim DW, Kenney MC. Increased stress-induced generation of reactive oxygen species and apoptosis in human keratoconus fibroblasts. Invest Ophthalmol Vis Sci. 2006;47(5):1902-1910.

18. Gomes JA, Tan D, Rapuano CJ, Belin MW, Ambrósio R, Guell JL. Global Consensus on Keratoconus and Ectatic Diseases. Cornea. 2015;34(4):359-369.

19. Esporcatte LPG, Salomão MQ, Neto AB da C, Machado AP, Lopes BT, Ambrósio R. Enhanced Diagnostics for Corneal Ectatic Diseases: The Whats, the Whys, and the Hows. Diagnostics. 2022;12(12):3027.

20. Moshirfar M, Tukan AN, Bundogji N, et al. Ectasia After Corneal Refractive Surgery: A Systematic Review. Ophthalmol Ther. 2021;10(4):753-776.

21. Peris-Martinez C, Lanzagorta-Aresti A, Aviñó-Martinez J. Ectasias corneales naturales. In: Del Buey Sayas MA, Peris-Martinez C, eds. Biomecánica y Arquitectura Corneal. Elsevier.Barcelona; 2014:153-164.

22. Lee BW, Jurkunas U V., Harissi-Dagher M, Poothullil AM, Tobaigy FM, Azar DT. Ectatic Disorders Associated With a Claw-shaped Pattern on Corneal Topography. Am J Ophthalmol. 2007;144(1):154-156.

23. Jinabhai A, Radhakrishnan H, O'Donnell C. Pellucid corneal marginal degeneration: A review. Contact Lens and Anterior Eye. 2011;34(2):56-63.

24. Kayazawa F, Nishimura K, Kodama Y, Tsuji T, Itoi M. Keratoconus with Pellucid Marginal Corneal Degeneration. Archives of Ophthalmology. 1984;102(6):895-896.

25. Godefrooij DA, de Wit GA, Uiterwaal CS, Imhof SM, Wisse RPL. Age-specific Incidence and Prevalence of Keratoconus: A Nationwide Registration Study. Am J Ophthalmol. 2017;175:169-172.

26. Ertan A, Muftuoglu O. Keratoconus clinical findings according to different age and gender groups. Cornea. 2008;27(10):1109-1113.

27. Krachmer JH, Feder RS, Belin MW. Keratoconus and related noninflammatory corneal thinning disorders. Surv Ophthalmol. 1984;28(4):293-322.

28. Léoni-Mesplié S, Mortemousque B, Touboul D, et al. Scalability and severity of keratoconus in children. Am J Ophthalmol. 2012;154(1):56-62.

29. Gordon-Shaag A, Millodot M, Kaiserman I, et al. Risk factors for keratoconus in Israel: a case-control study. Ophthalmic Physiol Opt. 2015;35(6):673-681.

30. Lin KK, Chen YW, Yeh CT, et al. Comparing the natural progression and clinical features of keratoconus between pediatric and adult patients. Sci Rep. 2022;12(1):8278.

31. Vincent AL, Weiser BA, Cupryn M, Stein RM, Abdolell M, Levin A V. Computerized corneal topography in a paediatric population with Down syndrome. Clin Exp Ophthalmol. 2005;33(1):47-52.

32. Robertson I. Keratoconus and the Ehlers-Danlos syndrome: a new aspect of keratoconus. Med J Aust. 1975;1(18):571-573.

33. Elder MJ. Leber congenital amaurosis and its association with keratoconus and keratoglobus. J Pediatr Ophthalmol Strabismus. 1994;31(1):38-40.

34. Weed KH, MacEwen CJ, McGhee CNJ. The variable expression of keratoconus within monozygotic twins: Dundee University Scottish Keratoconus Study (DUSKS). Contact Lens and Anterior Eye. 2006;29(3):123-126.

35. Tuft SJ, Hassan H, George S, Frazer DG, Willoughby CE, Liskova P. Keratoconus in 18 pairs of twins. Acta Ophthalmol. 2012;90(6):482-486.

36. Bykhovskaya Y, Margines B, Rabinowitz YS. Genetics in Keratoconus: where are we? Eye and Vision. 2016;3(1):16.

37. Li X, Bykhovskaya Y, Haritunians T, et al. A genome-wide association study identifies a potential novel gene locus for keratoconus, one of the commonest causes for corneal transplantation in developed countries. Hum Mol Genet. 2012;21(2):421-429.

38. Rong SS, Ma STU, Yu XT, et al. Genetic associations for keratoconus: A systematic review and meta-Analysis. Sci Rep. 2017;7(1):4620.

39. McComish BJ, Sahebjada S, Bykhovskaya Y, et al. Association of Genetic Variation with Keratoconus. JAMA Ophthalmol. 2020;138(2):174-181.

40. Lu Y, Vitart V, Burdon KP, et al. Genome-wide association analyses identify multiple loci associated with central corneal thickness and keratoconus. Nat Genet. 2013;45(2):155-163.

41. Choquet H, Melles RB, Yin J, et al. A multiethnic genome-wide analysis of 44,039 individuals identifies 41 new loci associated with central corneal thickness. Commun Biol. 2020;3(1):301.

42. Khawaja AP, Rojas Lopez KE, Hardcastle AJ, et al. Genetic Variants Associated with Corneal Biomechanical Properties and Potentially Conferring Susceptibility to Keratoconus in a Genome-Wide Association Study. JAMA Ophthalmol. 2019;137(9):1005-1012.

43. Karolak JA, Ginter-Matuszewska B, Tomela K, et al. Further evaluation of differential expression of keratoconus candidate genes in human corneas. PeerJ. 2020;8:e9793.

44. Kabza M, Karolak JA, Rydzanicz M, et al. Collagen synthesis disruption and downregulation of core elements of TGF-β, Hippo, and Wnt pathways in keratoconus corneas. European Journal of Human Genetics. 2017;25(5):582-590.

45. Héon E, Greenberg A, Kopp KK, et al. VSX1: A gene for posterior polymorphous dystrophy and keratoconus. Hum Mol Genet. 2002;11(9):1029-1036.

46. Abu-Amero KK, Al-Muammar AM, Kondkar AA. Genetics of Keratoconus: Where Do We Stand? J Ophthalmol. 2014;2014:641708.

47. Khaled ML, Bykhovskaya Y, Yablonski SER, et al. Differential expression of coding and long noncoding rnas in keratoconus-affected corneas. Invest Ophthalmol Vis Sci. 2018;59(7):2717-2728.

48. Sharif R, Khaled ML, McKay TB, Liu Y, Karamichos D. Transcriptional profiling of corneal stromal cells derived from patients with keratoconus. Sci Rep. 2019;9(1):12567.

49. Li X, Rabinowitz YS, Tang YG, et al. Two-stage genome-wide linkage scan in keratoconus sib pair families. Invest Ophthalmol Vis Sci. 2006;47(9):3791-3795.

50. Czugala M, Karolak JA, Nowak DM, et al. Novel mutation and three other sequence variants segregating with phenotype at keratoconus 13q32 susceptibility locus. European Journal of Human Genetics. 2012;20(4):389-397.

51. Bykhovskaya Y, Li X, Epifantseva I, et al. Variation in the lysyl oxidase (LOX) gene is associated with keratoconus in family-based and case-control studies. Invest Ophthalmol Vis Sci. 2012;53(7):4152-4157.

52. Hughes AE, Bradley DT, Campbell M, et al. Mutation altering the miR-184 seed region causes familial keratoconus with cataract. Am J Hum Genet. 2011;89(5):628-633.

53. Lapeyre G, Fournie P, Vernet R, et al. Keratoconus Prevalence in Families: A French Study. Cornea. 2020;39(12):1473-1479.

54. Olivo-Payne A, Abdala-Figuerola A, Hernandez-Bogantes E, Pedro-Aguilar L, Chan E, Godefrooij D. Optimal management of pediatric keratoconus: challenges and solutions. Clin Ophthalmol. 2019;13:1183.

55. Awwad ST, Yehia M, Mehanna CJ, et al. Tomographic and Refractive Characteristics of Pediatric First-Degree Relatives of Keratoconus Patients. Am J Ophthalmol. 2019;207:71-76.

56. Naderan M, Rajabi MT, Zarrinbakhsh P, Naderan M, Bakhshi A. Association between Family History and Keratoconus Severity. Curr Eye Res. 2016;41(11):1414-1418.

57. Jamali H, Beigi V, Sadeghi-Sarvestani A. Consanguineous Marriage as a Risk Factor for Developing Keratoconus. Med Hypothesis Discov Innov Ophthalmol. 2018;7(1):17-21.

58. Rabinowitz YS, Maumenee IH, Lundergan MK, Puffenberger E, Francomano CA, et al. Molecular genetic analysis in autosomal dominant keratoconus. Cornea. 1992;11(4):302-308.

59. Kriszt Á, Losonczy G, Berta A, Vereb G, Takács L. Segregation analysis suggests that keratoconus is a complex non-mendelian disease. Acta Ophthalmol. 2014;92(7):e562-e568.

60. Kaya V, Utine CA, Altunsoy M, Oral D, Yilmaz OF. Evaluation of corneal topography with Orbscan II in first-degree relatives of patients with keratoconus. Cornea. 2008;27(5):531-534.

61. Shneor E, Frucht-Pery J, Granit E, Gordon-Shaag A. The prevalence of corneal abnormalities in first-degree relatives of patients with keratoconus: a prospective case-control study. Ophthalmic & Physiological Optics. 2020;40(4):442.

62. Karimian F, Aramesh S, Rabei HM, Javadi MA, Rafati N. Topographic evaluation of relatives of patients with keratoconus. Cornea. 2008;27(8):874-878.

63. Kara N, Altinkaynak H, Baz O, Goker Y. Biomechanical evaluation of cornea in topographically normal relatives of patients with keratoconus. Cornea. 2013;32(3):262-266.

64. Ionescu IC, Corbu CG, Nicula C, et al. The importance of corneal biomechanics in assessing first degree family members of keratoconus patients. Rom J Ophthalmol. 2018;61:149-154.

65. Crawford AZ, Zhang J, Gokul A, McGhee CNJ, Ormonde SE. The enigma of environmental factors in keratoconus. Asia-Pacific Journal of Ophthalmology. 2020;9(6):549-556.

66. Gordon-Shaag A, Millodot M, Shneor E, Liu Y. The genetic and environmental factors for keratoconus. Biomed Res Int. 2015;2015:795738.

67. Shneor E, Millodot M, Blumberg S, Ortenberg I, Behrman S, Gordon-Shaag A. Characteristics of 244 patients with keratoconus seen in an optometric contact lens practice. Clin Exp Optom. 2013;96(2):219-224.

68. McMonnies CW. Mechanisms of rubbing-related corneal trauma in keratoconus. Cornea. 2009;28(6):607-615.

69. Weed KH, MacEwen CJ, Giles T, Low J, McGhee CNJ. The Dundee University Scottish Keratoconus study: demographics, corneal signs, associated diseases and eye rubbing. Eye. 2008;22(4):534-541.

70. Carlson AN. Expanding our understanding of eye rubbing and keratoconus. Cornea. 2010;29(2):245.

71. Balasubramanian SA, Pye DC, Willcox MD. Effects of eye rubbing on the levels of protease, protease activity and cytokines in tears: relevance in keratoconus. Clin Exp Optom. 2013;96(2):214-218.

72. Rabinowitz YS. The genetics of keratoconus. Ophthalmol Clin North Am. 2003;16(4):607-620.

73. Kenney MC, Brown DJ. The cascade hypothesis of keratoconus. Cont Lens Anterior Eye. 2003;26(3):139-146.

74. Shetty R, Sharma A, Pahuja N, et al. Oxidative stress induces dysregulated autophagy in corneal epithelium of keratoconus patients. PLoS One. 2017;12(9):1-20.

75. Chwa M, Atilano SR, Hertzog D, Zheng H, Langberg J, et al. Hypersensitive response to oxidative stress in keratoconus corneal fibroblasts. Invest Ophthalmol Vis Sci. 2008;49(10):4361-4369.

76. Atilano S, Lee D, Fukuhara P, et al. Corneal Oxidative Damage in Keratoconus Cells due to Decreased Oxidant Elimination from Modified Expression Levels of SOD Enzymes, PRDX6, SCARA3, CPSF3, and FOXM1. J Ophthalmic Vis Res. 2019;14(1):62-70.

77. Malfeito M, Regueiro U, Pérez-Mato M, Campos F, Sobrino T, Lema I. Innate Immunity Biomarkers for Early Detection of Keratoconus. Ocul Immunol Inflamm. 2019;27(6): 942-948.

78. di Martino E, Ali M, Inglehearn CF. Matrix metalloproteinases in keratoconus - Too much of a good thing? Exp Eye Res. 2019;182:137-143.

79. Spoerl E, Zubaty V, Raiskup-Wolf F, Pillunat LE. Oestrogen-induced changes in biomechanics in the cornea as a possible reason for keratectasia. Br J Ophthalmol. 2007;91(11):1547-1550.

80. Sies H. Oxidative stress: A concept in redox biology and medicine. Redox Biol. 2015;4:180-183.

81. Shinde V, Hu N, Mahale A, et al. RNA sequencing of corneas from two keratoconus patient groups identifies potential biomarkers and decreased NRF2-antioxidant responses. Sci Rep. 2020;10(1):9907.

82. Behndig A, Karlsson K, Johansson BO, Brännström T, Marklund SL. Superoxide dismutase isoenzymes in the normal and diseased human cornea. Invest Ophthalmol Vis Sci. 2001;42(10):2293-2296.

83. Nozik-Grayck E, Suliman HB, Piantadosi CA. Extracellular superoxide dismutase. Int J Biochem Cell Biol. 2005;37(12):2466-2471.

84. Tekin S, Seven E. Assessment of serum catalase, reduced glutathione, and superoxide dismutase activities and malondialdehyde levels in keratoconus patients. Eye (Lond). 2022;36(10):2062-2066.

85. Udar N, Atilano SR, Brown DJ, et al. SOD1: a candidate gene for keratoconus. Invest Ophthalmol Vis Sci. 2006;47(8):3345-3351.

86. Caglayan M, Kocamış SI, Sarac O, et al. Investigation of Heme Oxygenase 2 Enzyme Protein Expression in Keratoconus and Normal Human Corneal Epithelium: An Immunohistochemical Study. Curr Eye Res. 2019;44(1):25-29.

87. Navel V, Malecaze J, Pereira B, et al. Oxidative and antioxidative stress markers in keratoconus: a systematic review and meta-analysis. Acta Ophthalmol. 2021;99(6):e777-e794.

88. Peris-Martínez C, Piá-Ludeña JV, Rog-Revert MJ, Fernández-López E, Domingo JC. Antioxidant and Anti-Inflammatory Effects of Oral Supplementation with a Highly-Concentrated Docosahexaenoic Acid (DHA) Triglyceride in Patients with Keratoconus: A Randomized Controlled Preliminary Study. Nutrients. 2023;15(5):1300.

89. Liskova P, Dudakova L, Krepelova A, Klema J, Hysi PG. Replication of SNP associations with keratoconus in a Czech cohort. PLoS One. 2017;12(2):e0172365.

90. Klotz LO, Sánchez-Ramos C, Prieto-Arroyo I, Urbánek P, Steinbrenner H, Monsalve M. Redox regulation of FoxO transcription factors. Redox Biol. 2015;6:51-72.

91. Hawiger J, Zienkiewicz J. Decoding inflammation, its causes, genomic responses, and emerging countermeasures. Scand J Immunol. 2019;90(6):e12812.

92. Alió JL, García CH. Fisiopatología. In: Alió JL, Carreras B, Ruíz JM, eds. Inflamaciones Oculares. Edika Med. Barcelona; 1995:3-44.

93. Ferrari G, Rama P. The keratoconus enigma: A review with emphasis on pathogenesis. Ocul Surf. 2020;18(3):363-373.

94. Erdinest N, Wajnsztajn D, London N, Solomon A. Ocular surface inflammation and ectatic corneal disorders. Curr Opin Allergy Clin Immunol. 2023;23(5):430-437.

95. Ionescu C, Corbu CG, Tanase C, et al. Inflammatory Biomarkers Profile as Microenvironmental Expression in Keratoconus. Dis Markers. 2016;2016:1243819.

96. Shetty R, Ghosh A, Lim RR, et al. Elevated expression of matrix metalloproteinase-9 and inflammatory cytokines in keratoconus patients is inhibited by cyclosporine A. Invest Ophthalmol Vis Sci. 2015;56(2):738-750.

97. Sawaguchi S, Twining SS, Yue BYJT, Wilson P, Sugar J, Chan SK. Alpha-1 proteinase inhibitor levels in keratoconus. Exp Eye Res. 1990;50(5):549-554.

98. Hori J. Mechanisms of immune privilege in the anterior segment of the eye: what we learn from corneal transplantation. J Ocul Biol Dis Infor. 2008;1(2-4):94-100.

99. Sobrino T, Regueiro U, Malfeito M, Vieites-Prado A, Pérez-Mato M, et al. Higher expression of Toll-like receptors 2 and 4 in blood cells of keratoconus patiens. Sci Rep. 2017;7(1):12975.

100. Regueiro U, Pérez-Mato M, Hervella P, Campos F, Sobrino T, Lema I. Toll-like receptors as diagnostic targets in pellucid marginal degeneration. Exp Eye Res. 2020;200:108211.

101. Regueiro U, López-López M, Hervella P, Sobrino T, Lema I. Corneal and conjunctival alteration of innate immune expression in first-degree relatives of keratoconus patients. Graefe's Arch Clin Exp Ophthmol.2021;259(2):459-467.

102. Takeda K, Akira S. Toll-like receptors in innate immunity. Int Immunol. 2005;17(1):1-14.

103. Anderson K V. Toll signaling pathways in the innate immune response. Curr Opin Immunol. 2000;12(1):13-19.

104. O'Neill LA, Bryant CE, Doyle SL. Therapeutic targeting of Toll-Like receptors for infectious and inflammatory diseases and cancer. Pharmacol Rev. 2009;61(2):177-197.

105. Kanzler H, Barrat FJ, Hessel EM, Coffman RL. Therapeutic targeting of innate immunity with Toll-like receptor agonists and antagonists. Nat Med. 2007;13(5):552-559.

106. Lee SJ, Lee S. Toll-like receptors and inflammation in the CNS. Curr Drug Targets Inflamm Allergy. 2002;1(2):181-191.

107. Regueiro U, López-López M, Varela-Fernández R, Otero-Espinar FJ, Lema I. Biomedical Applications of Lactoferrin on the Ocular Surface. Pharmaceutics. 2023;15(3):865.

108. Versura P, Bavelloni A, Grillini M, Fresina M, Campos EC. Diagnostic performance of a tear protein panel in early dry eye. Mol Vis. 2013;19:1247-1257.

109. Jenssen H, Hancock REW. Antimicrobial properties of lactoferrin. Biochimie. 2009;91(1):19-29.

110. Legrand D, Mazurier J. A critical review of the roles of host lactoferrin in immunity. Biometals. 2010;23(3):365-376.

111. Chaerkady R, Shao H, Scott SG, Pandey A, Jun AS, Chakravarti S. The keratoconus corneal proteome: loss of epithelial integrity and stromal degeneration. J Proteomics. 2013;87:122-131.

112. García B, García-Suárez O, Merayo-Lloves J, et al. Differential Expression of Proteoglycans by Corneal Stromal Cells in Keratoconus. Invest Ophthalmol Vis Sci. 2016;57(6):2618-2628.

113. Bykhovskaya Y, Gromova A, Makarenkova HP, Rabinowitz YS. Abnormal regulation of extracellular matrix and adhesion molecules in corneas of patients with keratoconus. Int J Keratoconus Ectatic Corneal Dis. 2016;5(2):63-70.

114. Wojcik KA, Blasiak J, Szaflik J, Szaflik JP. Role of biochemical factors in the pathogenesis of keratoconus. Acta Biochim Pol. 2014;61(1):55-62.

115. Khaled ML, Helwa I, Drewry M, Seremwe M, Estes A, Liu Y. Molecular and Histopathological Changes Associated with Keratoconus. Biomed Res Int. 2017;2017:7803029.

116. Bilgihan K, Hondur A, Sul S, Ozturk S. Pregnancy-induced progression of keratoconus. Cornea. 2011;30(9):991-994.

117. Naderan M, Jahanrad A. Topographic, tomographic and biomechanical corneal changes during pregnancy in patients with keratoconus: a cohort study. Acta Ophthalmol. 2017;95(4):e291-e296.

118. Wang C, Li AL, Pang Y, Lei YQ, Yu L. Changes in intraocular pressure and central corneal thickness during pregnancy: a systematic review and Meta-analysis. Int J Ophthalmol. 2017;10(10):1573-1579.

119. Grandas OH, Mountain DJH, Kirkpatrick SS, et al. Effect of hormones on matrix metalloproteinases gene regulation in human aortic smooth muscle cells. J Surg Res. 2008;148(1):94-99.

120. Sherwin T, Brookes NH. Morphological changes in keratoconus: pathology or pathogenesis. Clin Exp Ophthalmol. 2004;32(2):211-217.

121. Meek KM, Tuft SJ, Huang Y, Gill PS, Hayes S, et al. Changes in collagen orientation and distribution in keratoconus corneas. Invest Opthalmol Vis Sci. 2005;46(6):1948-1956.

122. Hollingsworth JG, Bonshek RE, Efron N. Correlation of the appearance of the keratoconic cornea in vivo by confocal microscopy and in vitro by light microscopy. Cornea;24(4):397-405.

123. Belin MW, Jang HS, Borgstrom M. Keratoconus: Diagnosis and Staging. Cornea. 2022;41(1):1-11.

124. Shneor E, Piñero DP, Doron R. Contrast sensitivity and higher-order aberrations in Keratoconus subjects. Sci Rep. 2021;11(1):12971.

125. Antunes-Foschini RMS, Coutinho JVAL, Rocha EM, Bicas HEA. Oculomotor Status, Binocular Vision, and Stereoacuity in a Series of Keratoconus Subjects. Invest Ophthalmol Vis Sci. 2018;59(5):1869-1877.

126. De Stefano VS, Dupps WJ. Biomechanical Diagnostics of the Cornea. Int Ophthalmol Clin. 2017;57(3):75-86.

127. Padmanabhan P, Elsheikh A. Keratoconus: A Biomechanical Perspective. Curr Eye Res. 2023;48(2):121-129.

128. Luce DA. Determining in vivo biomechanical properties of the cornea with an ocular response analyzer. J Cataract Refract Surg. 2005;31(1):156-162.

129. Fontes BM, Junior RA, Jardim D, Velarde GC, Nosé W. Ability of corneal biomechanical metrics and anterior segment data in the differentiation of keratoconus and healthy corneas. Arq Bras Oftalmol. 2010;73(4):333-337.

130. Luz A, Lopes B, Hallahan KM, et al. Discriminant Value of Custom Ocular Response Analyzer Waveform Derivatives in Forme Fruste Keratoconus. Am J Ophthalmol. 2016;164:14-21.

131. Ambrósio R, Ramos I, Luz A, et al. Dynamic ultra-high speed Scheimpflug imaging for assessing corneal biomechanical properties. Rev Bras Oftalmol. 2013;72(2):99-102.

132. Esporcatte LPG, Salomão MQ, Lopes BT, et al. Biomechanical diagnostics of the cornea. Eye and Vision. 2020;7:9.

133. Lopes BT, Ramos I de C, Salomão MQ, Canedo ALC, Ambrósio R. Horizontal pachymetric profile for the detection of keratoconus. Rev Bras Oftalmol. 2015;74(6):382-385.

134. Song P, Yang K, Li P, et al. Assessment of Corneal Pachymetry Distribution and Morphologic Changes in Subclinical Keratoconus with Normal Biomechanics. Biomed Res Int. 2019;2019:1748579.

135. Vinciguerra R, Ambrósio R, Elsheikh A, et al. Detection of Keratoconus With a New Biomechanical Index. J Refract Surg. 2016;32(12):803-810.

136. Sedaghat MR, Momeni-Moghaddam H, Ambrósio R, et al. Diagnostic Ability of Corneal Shape and Biomechanical Parameters for Detecting Frank Keratoconus. Cornea. 2018;37(8):1025-1034.

137. Ren S, Xu L, Fan Q, Gu Y, Yang K. Accuracy of new Corvis ST parameters for detecting subclinical and clinical keratoconus eyes in a Chinese population. Sci Rep. 2021;11(1):4962.

138. Shen Y, Han T, Jhanji V, et al. Correlation Between Corneal Topographic, Densitometry, and Biomechanical Parameters in Keratoconus Eyes. Transl Vis Sci Technol. 2019;8(3):12.

139. Eliasy A, Chen KJ, Vinciguerra R, et al. Determination of Corneal Biomechanical Behavior in-vivo for Healthy Eyes Using CorVis ST Tonometry: Stress-Strain Index. Front Bioeng Biotechnol. 2019;7:105.

140. Elham R, Jafarzadehpur E, Hashemi H, et al. Keratoconus diagnosis using Corvis ST measured biomechanical parameters. J Curr Ophthalmol. 2017;29(3):175-181.

141. Miao YY, Ma XM, Qu ZX, et al. Performance of Corvis ST Parameters Including Updated Stress-Strain Index in Differentiating Between Normal, Forme-Fruste, Subclinical, and Clinical Keratoconic Eyes. Am J Ophthalmol. 2024;258:196-207.

142. Martínez-Abad A, Piñero DP. New perspectives on the detection and progression of keratoconus. J Cataract Refract Surg. 2017;43(9):1213-1227.

143. Zhang X, Munir SZ, Sami Karim SA, Munir WM. A review of imaging modalities for detecting early keratoconus. Eye. 2021;35(1):173.

144. Alió JL, Shabayek MH. Corneal higher order aberrations: a method to grade keratoconus. Journal of refractive surgery. 2006;22(6):539-545.

145. Shajari M, Jaffary I, Herrmann K, et al. Early Tomographic Changes in the Eyes of Patients With Keratoconus. J Refract Surg. 2018;34(4):254-259.

146. MA, Hadid M, Izquierdo L. A Systematic Review of Subclinical Keratoconus and Forme Fruste Keratoconus. J Refract Surg. 2020;36(4):270-279.

147. de Sanctis U, Loiacono C, Richiardi L, Turco D, Mutani B, Grignolo FM. Sensitivity and specificity of posterior corneal elevation measured by Pentacam in discriminating keratoconus/subclinical keratoconus. Ophthalmology. 2008;115(9):1534-1539.

148. Khachikian SS, Belin MW. Posterior elevation in keratoconus. Ophthalmology. 2009;116(4):816.

149. Ambrósio R, Caiado ALC, Guerra FP, et al. Novel pachymetric parameters based on corneal tomography for diagnosing keratoconus. J Refract Surg. 2011;27(10):753-758.

150. Hashemi H, Beiranvand A, Yekta A, Maleki A, Yazdani N, Khabazkhoob M. Pentacam top indices for diagnosing subclinical and definite keratoconus. J Curr Ophthalmol. 2016;28(1):21-26.

151. Belin MW, Villavicencio OF, Ambrósio RR. Tomographic parameters for the detection of keratoconus: suggestions for screening and treatment parameters. Eye Contact Lens. 2014;40(6):326-330.

152. Shetty R, Rao H, Khamar P, et al. Keratoconus Screening Indices and Their Diagnostic Ability to Distinguish Normal From Ectatic Corneas. Am J Ophthalmol. 2017;181:140-148.

153. Bamdad S, Sedaghat MR, Yasemi M, Vahedi A. Sensitivity and Specificity of Belin Ambrosio Enhanced Ectasia Display in Early Diagnosis of Keratoconus. J Ophthalmol. 2020;2020:7625659.

154. Ambrósio R, Lopes BT, Faria-Correia F, et al. Integration of Scheimpflug-Based Corneal Tomography and Biomechanical Assessments for Enhancing Ectasia Detection. J Refract Surg. 2017;33(7):434-443.

155. Krumeich JH, Daniel J, Knalle A. Live-epikeratophakia for keratoconus. J Cataract Refract Surg. 1998;24(4):456-463.

156. Belin MW, Duncan JK. Keratoconus: The ABCD Grading System. Klin Monbl Augenheilkd. 2016;233(6):701-707.

157. Ortiz-Toquero S, Perez S, Rodriguez G, de Juan V, Mayo-Iscar A, Martin R. The influence of the refractive correction on the vision-related quality of life in keratoconus patients. Quality of Life Research. 2016;25(4):1043-1051.

158. Amorim-de-Sousa A, Macedo-de-Araújo R, Fernandes P, Queirós A, González-Méijome JM. Multifocal Electroretinogram in Keratoconus Patients without and with Scleral Lenses. Curr Eye Res. 2021;46(11):1732-1741.

159. Moschos MM, Nitoda E, Georgoudis P, Balidis M, Karageorgiadis E, Kozeis N. Contact lenses for keratoconus- current practice. Open Ophthalmol J. 2017;11:241-251.

160. Macedo-de-Araújo RJ, van der Worp E, González-Méijome JM. A one-year prospective study on scleral lens wear success. Cont Lens Anterior Eye. 2020;43(6):553-561.

161. Macedo-De-Araújo RJ, Faria-Ribeiro M, McAllinden C, Van Der Worp E, González-Méijome JM. Optical Quality and Visual Performance for One Year in a Sample of Scleral Lens Wearers. Optom Vis Sci. 2020;97(9):775-789.

162. Wollensak G, Spoerl E, Seiler T. Riboflavin/ultraviolet-A-induced collagen crosslinking for the treatment of keratoconus. Am J Ophthalmol. 2003;135(5):620-627.

163. Randleman JB, Khandelwal SS, Hafezi F. Corneal cross-linking. Surv Ophthalmol. 2015;60(6):509-523.

164. Ng ALK, Chan TC, Cheng AC. Conventional versus accelerated corneal collagen cross-linking in the treatment of keratoconus. Clin Exp Ophthalmol. 2016;44(1):8-14.

165. O'Brart DPS. Corneal collagen crosslinking for corneal ectasias: a review. Eur J Ophthalmol. 2017;27(3):253-269.

166. Arnalich-Montiel F, Alió del Barrio JL, Alió JL. Corneal surgery in keratoconus: which type, which technique, which outcomes? Eye and Vision. 2016;3(1):2.

167. Parker JS, Van Dijk K, Melles GR. Treatment options for advanced keratoconus: a review. Surv Ophthalmol. 2015;60(5):459-480.

168. McMonnies CW. Eye rubbing type and prevalence including contact lens "removal-relief" rubbing. Clin Exp Optom. 2016;99(4):366-372.

169. Varela-Fernández R, García-Otero X, Díaz-Tomé V, et al. Design, Optimization, and Characterization of Lactoferrin-Loaded Chitosan/TPP and Chitosan/Sulfobutylether-β-cyclodextrin Nanoparticles as a Pharmacological Alternative for Keratoconus Treatment. ACS Appl Mater Interfaces. 2021;13(3):3559-3575.

170. Varela-Fernández R, García-Otero X, Díaz-Tomé V, et al. Mucoadhesive PLGA Nanospheres and Nanocapsules for Lactoferrin Controlled Ocular Delivery. Pharmaceutics. 2022;14(4):799.

171. Varela-Fernández R, García-Otero X, Díaz-Tomé V, et al. Lactoferrin-loaded nanostructured lipid carriers (NLCs) as a new formulation for optimized ocular drug delivery. Eur J Pharm Biopharm. 2022;172:144-156.

172. Li Q, Weng J, Mohan RR, et al. Hepatocyte growth factor and hepatocyte growth factor receptor in the lacrimal gland, tears, and cornea. Invest Ophthalmol Vis Sci. 1996;37(5):727-739.

173. Vesaluoma M, Teppo AM, Grönhagen-Riska C, Tervo T. Release of TGF-β1 and VEGF in tears following photorefractive keratectomy. Curr Eye Res. 1997;16(1):19-25.

174. Stern ME, Gao J, Siemasko KF, Beuerman RW, Pflugfelder SC. The role of the lacrimal functional unit in the pathophysiology of dry eye. Exp Eye Res. 2004;78(3):409-416.

175. Pflugfelder SC, Stern ME. Biological Functions of Tear Film. Exp Eye Res. 2020;197:108115.

176. Willcox MDP, Argüeso P, Georgiev GA, et al. TFOS DEWS II Tear Film Report. Ocular Surface. 2017;15(3):366-403.

177. Gipson IK, Argüeso P. Role of mucins in the function of the corneal and conjunctival epithelia. Int Rev Cytol. 2003;231:1-49.

178. Spurr-Michaud S, Argüeso P, Gipson I. Assay of mucins in human tear fluid. Exp Eye Res. 2007;84(5):939-950.

179. Gipson IK. Distribution of mucins at the ocular surface. Exp Eye Res. 2004;78(3):379-388.

180. Zhou L, Zhao SZ, Koh SK, et al. In-depth analysis of the human tear proteome. J Proteomics. 2012;75(13):3877-3885.

181. Ponzini E, Santambrogio C, De Palma A, Mauri P, Tavazzi S, Grandori R. Mass spectrometry-based tear proteomics for noninvasive biomarker discovery. Mass Spectrom Rev. 2022;41(5):842-860.

182. Nishtala K, Pahuja N, Shetty R, Nuijts RMMA, Ghosh A. Tear biomarkers for keratoconus. Eye Vis (Lond). 2016;3(1):19.

183. Winiarczyk M, Biela K, Michalak K, Winiarczyk D, Mackiewicz J. Changes in Tear Proteomic Profile in Ocular Diseases. Int J Environ Res Public Health. 2022;19(20):13341.

184. Bajkowska D, Szelachowska M, Buczyńska A, Krętowski AJ, Siewko K. Tears as a Source of Biomarkers in the Diagnosis of Graves' Orbitopathy. Biomolecules. 2022;12(11):1620.

185. Azkargorta M, Soria J, Acera A, Iloro I, Elortza F. Human tear proteomics and peptidomics in ophthalmology: Toward the translation of proteomic biomarkers into clinical practice. J Proteomics. 2017;150:359-367.

186. Król-Grzymała A, Sienkiewicz-Szłapka E, Fiedorowicz E, Rozmus D, Cieślińska A, Grzybowski A. Tear Biomarkers in Alzheimer's and Parkinson's Diseases, and Multiple Sclerosis: Implications for Diagnosis (Systematic Review). Int J Mol Sci. 2022;23(17):10123.

187. Georgiev GA, Eftimov P, Yokoi N. Structure-function relationship of tear film lipid layer: A contemporary perspective. Exp Eye Res. 2017;163:17-28.

188. Cwiklik L. Tear film lipid layer: A molecular level view. Biochim Biophys Acta. 2016;1858(10):2421-2430.

189. Sorkhabi R, Ghorbanihaghjo A, Taheri N, Ahoor MH. Tear film inflammatory mediators in patients with keratoconus. Int Ophthalmol. 2015;35(4):467-472.

190. Jun AS, Cope L, Speck C, Feng X, Lee S, et al. Subnormal cytokine profile in the tear fluid of keratoconus patients. PLoS One. 2011;6(1):e16437.

191. Martínez-Pérez L, Viso E, Touriño R, Gude F, Rodríguez-Ares MT. Clinical evaluation of meibomian gland dysfunction in patients with keratoconus. Cont Lens Anterior Eye. 2022;45(3):101495.

192. Zhou W, Yu H, Feng Y. Decrease in Tear Film Lipid Layer Thickness in Patients with Keratoconus. J Clin Med. 2022;11(18):5252.

193. Carracedo G, Recchioni A, Alejandre-Alba N, et al. Signs and Symptoms of Dry Eye in Keratoconus Patients: A Pilot Study. Curr Eye Res. 2015;40(11):1088-1094.

194. Karamichos D, Zieske JD, Sejersen H, Sarker-Nag A, Asara JM, Hjortdal J. Tear metabolite changes in keratoconus. Exp Eye Res. 2015;132:1-8.

195. Sağlik A, Koyuncu İ, Soydan A, Sağlik F, Gönel A. Tear Organic Acid Analysis After Corneal Collagen Crosslinking in Keratoconus. Eye Contact Lens. 2020;46 Suppl 2:S122-S128.

196. Wisse RP, Kuiper JJ, Gans R, Imhof S, Radstake TR, Van der Lelij A. Cytokine expression in keratoconus and its corneal microenvironment: a systematic review. Ocul Surf. 2015;13(4):272-283.

197. Lema I, Durán JA, Ruiz C, Díez-Feijoo E, Acera A, Merayo J. Inflammatory response to contact lenses in patients with keratoconus compared with myopic subjects. Cornea. 2008;27(7):758-763.

198. Fodor M, Kolozsvári BL, Petrovski G, et al. Effect of contact lens wear on the release of tear mediators in keratoconus. Eye Contact Lens. 2013;39(2):147-152.

199. Fodor M, Vitályos G, Losonczy G, et al. Tear Mediators NGF along with IL-13 Predict Keratoconus Progression. Ocul Immunol Inflamm. 2021;29(6):1090-1101.

200. Kolozsvári BL, Petrovski G, Gogolák P, Rajnavölgyi É, Tóth F, et al. Association between mediators in the tear fluid and the severity of keratoconus. Ophthalmic Res. 2014;51(1):46-51.

201. Acera A, Vecino E, Rodríguez-Agirretxe I, Aloria K, Arizmendi JM, et al. Changes in tear protein profile in keratoconus disease. Eye. 2011;25(9):1225-1233.

202. Balmus IM, Alexa AI, Ciuntu RE, et al. Oxidative stress markers dynamics in keratoconus patients' tears before and after corneal collagen crosslinking procedure. Exp Eye Res. 2020;190:107897.

203. Mazzotta C, Traversi C, Mellace P, et al. Keratoconus Progression in Patients With Allergy and Elevated Surface Matrix Metalloproteinase 9 Point-of-Care Test. Eye Contact Lens. 2018;44 Suppl 2:S48-S53.

204. Pásztor D, Kolozsvári BL, Csutak A, Berta A, Hassan Z, et al. Tear mediators in corneal ectatic disorders. PLoS One. 2016;11(4):e0153186.

205. Monti C, Zilocchi M, Colugnat I, Alberio T. Proteomics turns functional. J Proteomics. 2019;198:36-44.

206. Chantada-Vázquez MDP, García Vence M, Serna A, Núñez C, Bravo SB. SWATH-MS Protocols in Human Diseases. Methods Mol Biol. 2021;2259:105-141.

207. Gillet LC, Navarro P, Tate S, et al. Targeted data extraction of the MS/MS spectra generated by data-independent acquisition: a new concept for consistent and accurate proteome analysis. Mol Cell Proteomics. 2012;11(6):O111.016717.

208. Wuen Ma JY, Sze YHON, Bian JF, Lam TC. Critical role of mass spectrometry proteomics in tear biomarker discovery for multifactorial ocular diseases (Review). Int J Mol Med. 2021;47(5):83.

209. von Thun und Hohenstein-Blaul N, Funke S, Grus FH. Tears as a source of biomarkers for ocular and systemic diseases. Exp Eye Res. 2013;117:126-137.

210. Fam HB, Lim KL. Corneal elevation indices in normal and keratoconic eyes. J Cataract Refract Surg. 2006;32(8):1281-1287.

211. Efron N. Contact lens wear is intrinsically inflammatory. Clin Exp Optom.2017;100(1):3-19.

212. Bonzon-Kulichenko E, Pérez-Hernández D, Núñez E, et al. A robust method for quantitative high-throughput analysis of proteomes by 18O labeling. Mol Cell Proteomics. 2011;10(1):M110.003335.

213. Perez-Hernandez D, Gutiérrez-Vázquez C, Jorge I, et al. The intracellular interactome of tetraspanin-enriched microdomains reveals their function as sorting machineries toward exosomes. J Biol Chem. 2013;288(17):11649-11661.

214. Shevchenko A, Wilm M, Vorm O, Mann M. Mass spectrometric sequencing of proteins from silver-stained polyacrylamide gels. Anal Chem. 1996;68(5):850-858.

215. Redestig H, Fukushima A, Stenlund H, et al. Compensation for systematic cross-contribution improves normalization of mass spectrometry-based metabolomics data. Anal Chem. 2009;81(19):7974-7980.

216. Lambert JP, Ivosev G, Couzens AL, et al. Mapping differential interactomes by affinity purification coupled with data-independent mass spectrometry acquisition. Nat Methods. 2013;10(12):1239-1245.

217. Olofsson EM, Marklund SL, Pedrosa-Domellöf F, Behndig A. Interleukin-1alpha downregulates extracellular-superoxide dismutase in human corneal keratoconus stromal cells. Mol Vis. 2007;13:1285-1290.

218. Joseph R, Srivastava OP, Pfister RR. Differential epithelial and stromal protein profiles in keratoconus and normal human corneas. Exp Eye Res. 2011;92(4):282-298.

219. Liang Y, Van Zant G. Aging stem cells, latexin and longevity. Exp Cell Res. 2008;314(9):1962.

220. Ostrowska Z, Moraczewska J. Cofilin - a protein controlling dynamics of actin filaments. Postepy Hig Med Dosw (Online). 2017;71(0):339-351.

221. Lee JE, Oum BS, Choi HY, Lee SU, Lee JS. Evaluation of differentially expressed genes identified in keratoconus. Mol Vis. 2009;15:2480.

222. Domingues C, Geraldo AM, Anjo SI, et al. Cofilin-1 Is a Mechanosensitive Regulator of Transcription. Front Cell Dev Biol. 2020;8:678.

223. Wolff L, Strathmann EA, Müller I, et al. Plastin 3 in health and disease: a matter of balance. Cell Mol Life Sci. 2021;78(13):5275.

224. Kristensson MA. The Game of Tubulins. Cells. 2021;10(4):745.

225. Toksoz D, Merdek KD. The Rho small GTPase: functions in health and disease. Histol Histopathol. 2002;17(3):915-927.

226. Thomasy SM, Leonard BC, Greiner MA, Skeie JM, Raghunathan VK. Squishy matters - Corneal mechanobiology in health and disease. Prog Retin Eye Res. 2024;99:101234.

227. Amit C, Padmanabhan P, Narayanan J. Deciphering the mechanoresponsive role of β-catenin in keratoconus epithelium. Sci Rep. 2020;10(1):21382.

228. Sun S, Wong S, Mak A, Cho M. Impact of oxidative stress on cellular biomechanics and rho signaling in C2C12 myoblasts. J Biomech. 2014;47(15):3650-3656.

229. Balasubramanian SA, Wasinger VC, Pye DC, Willcox MD. Preliminary identification of differentially expressed tear proteins in keratoconus. Mol Vis. 2013;19:2124-2134.

230. Dyrlund TF, Poulsen ET, Scavenius C, et al. Human cornea proteome: Identification and quantitation of the proteins of the three main layers including epithelium, stroma, and endothelium. J Proteome Res. 2012;11(8):4231-4239.

231. Gomme PT, McCann KB. Transferrin: Structure, function and potential therapeutic actions. Drug Discov Today. 2005;10(4):267-273.

232. Lieu PT, Heiskala M, Peterson PA, Yang Y. The roles of iron in health and disease. Mol Aspects Med. 2001;22(1-2):1-87.

233. Wójcik KA, Synowiec E, Jiménez-García MP, et al. Polymorphism of the transferrin gene in eye diseases: Keratoconus and fuchs endothelial corneal dystrophy. Biomed Res Int. 2013;2013:247438.

234. Bartnikas TB. Known and potential roles of transferrin in iron biology. Biometals. 2012;25(4):677-686.

235. McClements L, Annett S, Yakkundi A, Robson T. The Role of Peptidyl Prolyl Isomerases in Aging and Vascular Diseases. Curr Mol Pharmacol. 2015;9(2):165-179.

236. Stagos D, Chen Y, Cantore M, Jester JV, Vasiliou V. Corneal aldehyde dehydrogenases: multiple functions and novel nuclear localization. Brain Res Bull. 2010;81(2-3):211-218.

237. Han PF, Che X Da, Li HZ, Gao YY, Wei XC, Li PC. Annexin A1 involved in the regulation of inflammation and cell signaling pathways. Chinese Journal of Traumatology. 2020;23(2):96.

238. Dallacasagrande V, Hajjar KA. Annexin A2 in Inflammation and Host Defense. Cells. 2020;9(6):1-14.

239. Ceciliani F, Lecchi C. The Immune Functions of α1 Acid Glycoprotein. Curr Protein Pept Sci. 2019;20(6):505-524.

240. Ambartsumian N, Klingelhöfer J, Grigorian M. The Multifaceted S100A4 Protein in Cancer and Inflammation. Methods Mol Biol. 2019;1929:339-365.

241. McMonnies CW. Inflammation and keratoconus. Optom Vis Sci. 2015;92(2):e35-e41.

242. Akkaya S, Ulusoy DM. Serum Vitamin D Levels in Patients with Keratoconus. Ocul Immunol Inflamm. 2020;28(3):348-353.

243. Zarei-Ghanavati S, Yahaghi B, Hassanzadeh S, Mobarhan MG, Hakimi HR, Eghbali P. Serum 25-hydroxyvitamin D, selenium, zinc and copper in patients with keratoconus. J Curr Ophthalmol. 2020;32(1):26-31.

244. Aslan MG, Fındık H, Okutucu M, et al. Serum 25-Hydroxy Vitamin D, Vitamin B12, and Folic Acid Levels in Progressive and Nonprogressive Keratoconus. Cornea. 2021;40(3):334-341.

245. Sethu S, Shetty R, Deshpande K, et al. Correlation between tear fluid and serum vitamin D levels. Eye and Vision. 2016;3(1):22.

246. Vitar RML, Fonteyne P, Knutsson KA, et al. Vitamin D Supplementation Impacts Systemic Biomarkers of Collagen Degradation and Copper Metabolism in Patients With Keratoconus. Transl Vis Sci Technol. 2022;11(12):16.

247. Rabinowitz YS, Garbus J, McDonnell PJ. Computer-assisted corneal topography in family members of patients with keratoconus. Archives of ophthalmology. 1990;108(3):365-371.

248. Levy D, Hutchings H, Rouland JF, Guell J, Burillon C, et al. Videokeratographic anomalies in familial keratoconus. Ophthalmology. 2004;111(5):867-874.

249. Steele TM, Fabinyi DC, Couper TA, Loughnan MS. Prevalence of Orbscan II corneal abnormalities in relatives of patients with keratoconus. Clin Exp Ophthalmol. 2008;36(9):824-830.

250. Li J, Zhang BN, Jhanji V, Wang X, Li D, Du X. Parental Corneal Tomographic and Biomechanical Characteristics of Patients With Keratoconus. Am J Ophthalmol. 2023;256:146-155.

251. Dimasi DP, Burdon KP, Craig JE. The genetics of central corneal thickness. Br J Ophthalmol. 2010;94(8):971-976.

252. Landers JA, Hewitt AW, Dimasi DP, et al. Heritability of central corneal thickness in nuclear families. Invest Ophthalmol Vis Sci. 2009;50(9):4087-4090.

253. Toh T, Liew SHM, MacKinnon JR, et al. Central corneal thickness is highly heritable: the twin eye studies. Invest Ophthalmol Vis Sci. 2005;46(10):3718-3722.

254. Jongebloed WL, Worst JFG. The keratoconus epithelium studied by SEM. Doc Ophthalmol. 1987;67(1-2):171-181.

255. Efron N, Hollingsworth JG. New perspectives on keratoconus as revealed by corneal confocal microscopy. Clin Exp Optom. 2008;91(1):34-55.

256. Sykakis E, Carley F, Irion L, Denton J, Hillarby MC. An in-depth analysis of histopathological characteristics found in keratoconus. Pathology. 2012;44(3):234-239.

257. Kriszt Á, Losonczy G, Berta A, Takács L. Presence of Fleischer ring and prominent corneal nerves in keratoconus relatives and normal controls. Int J Ophthalmol. 2015;8(5):922-927.

258. Bernstein BW, Bamburg JR. ADF/Cofilin: A Functional Node in Cell Biology. Trends Cell Biol. 2010;20(4):187.

259. Wells A, Huttenlocher A, Lauffenburger DA. Calpain proteases in cell adhesion and motility. Int Rev Cytol. 2005;245:1-16.

260. Hoskin V, Szeto A, Ghaffari A, Greer PA, CÃtéc GP, Elliott BE. Ezrin regulates focal adhesion and invadopodia dynamics by altering calpain activity to promote breast cancer cell invasion. Mol Biol Cell. 2015;26(19):3464-3479.

261. Shao H, Wang JHC, Pollak MR, Wells A. α-actinin-4 is essential for maintaining the spreading, motility and contractility of fibroblasts. PLoS One. 2010;5(11): e13921.

262. Joseph R, Srivastava OP, Pfister RR. Downregulation of β-Actin Gene and Human Antigen R in Human Keratoconus. Invest Ophthalmol Vis Sci. 2012;53(7):4032-4041.

263. Srivastava OP, Chandrasekaran D, Pfister RR. Molecular changes in selected epithelial proteins in human keratoconus corneas compared to normal corneas. Mol Vis. 2006;12:1615-25.

264. Otey CA, Carpen O. Alpha-actinin revisited: a fresh look at an old player. Cell Motil Cytoskeleton. 2004;58(2):104-111.

265. Gao G, Li J, Zhang Y, Chang YZ. Cellular Iron Metabolism and Regulation. Adv Exp Med Biol. 2019;1173:21-32.

266. Vanacore R, Eskew JD, Sung L, Davis T, Smith A. Safe coordinated trafficking of heme and iron with copper maintain cell homeostasis: modules from the hemopexin system. Biometals. 2019;32(3):355-367.

267. Baker HM, Baker EN. Lactoferrin and iron: structural and dynamic aspects of binding and release. Biometals. 2004;17(3):209-216.

268. Jiang X, Stockwell BR, Conrad M. Ferroptosis: mechanisms, biology and role in disease. Nat Rev Mol Cell Biol. 2021;22(4):266-282.

269. Gass JDM. The Iron Lines of the Superficial Cornea: Hudson-Stahli Line, Stocker's Line and Fleischer's Ring. Archives of Ophthalmology. 1964;71(3):348-358.

270. Tanaka K, Takeda S, Mitsuoka K, et al. Structural basis for cofilin binding and actin filament disassembly. Nature Communications 2018 9:1. 2018;9(1):1-12.

271. Prunier C, Prudent R, Kapur R, Sadoul K, Lafanechère L. LIM kinases: cofilin and beyond. Oncotarget. 2017;8(25):41749.

272. Anderson S, DiCesare L, Tan I, Leung T, Sundarraj N. Rho-mediated assembly of stress fibers is differentially regulated in corneal fibroblasts and myofibroblasts. Exp Cell Res. 2004;298(2):574-583.

273. Anderson SC, Stone C, Tkach L, SundarRaj N. Rho and Rho-kinase (ROCK) signaling in adherens and gap junction assembly in corneal epithelium. Invest Ophthalmol Vis Sci. 2002;43(4):978-86.

274. Saito J, Morishige N, Chikama TI, Gu J, Sekiguchi K, Nishida T. Differential regulation of focal adhesion kinase and paxillin phosphorylation by the small GTP-binding protein Rho in human corneal epithelial cells. Jpn J Ophthalmol. 2004;48(3):199-207.

275. Yin J, Lu J, Yu FSX. Role of Small GTPase Rho in Regulating Corneal Epithelial Wound Healing. Invest Ophthalmol Vis Sci. 2008;49(3):900.

276. Kim A, Lakshman N, Petroll WM. Quantitative assessment of local collagen matrix remodeling in 3-D culture: the role of Rho kinase. Exp Cell Res. 2006;312(18):3683-3692.

277. Aaron Hobbs G, Zhou B, Cox AD, Campbell SL. Rho GTPases, oxidation, and cell redox control. Small GTPases. 2014;5:e28579.

278. DerMardirossian C, Bokoch GM. GDIs: Central regulatory molecules in Rho GTPase activation. Trends Cell Biol. 2005;15(7):356-363.

279. Kawaguchi K, Asano S. Pathophysiological Roles of Actin-Binding Scaffold Protein, Ezrin. Int J Mol Sci. 2022;23(6):3246.

280. Sarker-Nag A, Hutcheon AE, Karamichos D. Mitochondrial Profile and Responses to TGF-β Ligands in Keratoconus. Curr Eye Res. 2016;41(7):900-7.

281. You J, Corley SM, Wen L, et al. RNA-Seq analysis and comparison of corneal epithelium in keratoconus and myopia patients. Scientific Reports 2017 8:1. 2018;8(1):1-13.

282. Wang J, Tian Z. Recent advances in lactoferrin research and development during the past two years (2007-2009): in lieu of a preface of the Special Issue Lactoferrin. Biometals. 2010;23(3):355-357.

283. Dierick M, Vanrompay D, Devriendt B, Cox E. Lactoferrin, a versatile natural antimicrobial glycoprotein that modulates the host's innate immunity. Biochemistry and cell biology. 2021;99(1):61-65.

284. Kawai T, Akira S. TLR signaling. Cell Death Differ. 2006;13(5):816-825.

285. Agwa M, Sabra S. Lactoferrin coated or conjugated nanomaterials as an active targeting approach in nanomedicine. Int J Biol Macromol. 2021;167:1527-1543.

286. Pastori V, Tavazzi S, Lecchi M. Lactoferrin-loaded contact lenses counteract cytotoxicity caused in vitro by keratoconic tears. Cont Lens Anterior Eye. 2019;42(3):253-257.

287. Pastori V, Tavazzi S, Lecchi M. Lactoferrin-loaded contact lenses: eye protection against oxidative stress. Cornea. 2015;34(6):693-697.

Annexes

Annex 1
Clinical protocol

CÓDIGO: _____ **TELÉFONO: _____**

Sexo: Hombre [1] Mujer [2]

Edad: ____ años.

Edad de diagnóstico (en caso de ectasia corneal):_____ años.

Grupo: Control progenitor [1] Control hijo/a [2]
Familiar (hijo/a) [3] Qc [4]

Enfermedad alérgica: SI [1] NO [2] Cual/es:

Enfermedades generales o asociadas: SI [1] NO [2] Cual/es:

Enfermedades oculares asociadas: SI [1] NO [2] Cual/es:

Tratamientos en curso:
- Generales: SI [1] NO [2] Cual/es:
- Oculares: SI [1] NO [2] Cual/es:

Antedecentes familiares de Ectasia corneal: SI [1] NO [2]

Grado: Hermano/a [1] Padre/Madre [2] Ambos [3] Otros [4]

	OD	OI
Uso de LC:	Si [1] No [2]	Si [1] No [2]
T° sin ellas:	_____ horas	_____horas
Tipo de LC:	_____	_____
Picor ocular:	Si [1] No [2]	Si [1] No [2]
Frotamiento ocular:	Si [1] No [2]	Si [1] No [2]
Signos biomicrocópicos:	Si [1] No [2]	Si [1] No [2]
	Tipo: _____	_____
AVL:	Sin corrección:_____	Sin corrección:_____
	Con corrección:_____	Con corrección:_____
Corrección óptica**:	_____	_____

Tomografía corneal:

	OD	OI
PDC	_____ D	_____ D
K1	_____ D	_____ D
K2	_____ D	_____ D
dK	_____ D	_____ D
Kmax	_____ D	_____ D
I-S asymmetry	_____ D	_____ D
ARTmax	_____	_____

Aberrometría (RMS):

	OD	OI
Coma ($Z_3^{\pm 1}$)	_____µm	_____ µm
Coma-Like	_____µm	_____ µm

	OD	OI
Elevación anterior	_____mm	_____mm
Elevación posterior	_____mm	_____mm
Paquimetría central	_____µm	_____µm
Paquimetría mínima	_____µm	_____µm
BAD-D	_____	_____
TBI	_____.	_____

Biomecánica corneal:

bIOP	_____mmHg	_____mmHg
A1T	_____ms	_____ms
A1V	_____m/s	_____m/s
A2T	_____ms	_____ms
A2V	_____m/s	_____m/s
HCT	_____ms	_____ms
A1DA	_____mm	_____mm
A2DA	_____mm	_____mm
DAmax	_____mm	_____mm
HCDA	_____mm	_____mm
A1DLL	_____mm	_____mm
A2DLL	_____mm	_____mm
HCDLL	_____mm	_____mm
A1DLA	_____mm	_____mm
A2DLA	_____mm	_____mm
HCDLA	_____mm	_____mm
A1DLAr	_____mm^2	_____mm^2
A2DLAr	_____mm^2	_____mm^2
HCDLar	_____mm^2	_____mm^2
HCdArclenght	___mm	_____mm
PD	_____mm	_____mm
DARatio Max (1mm)	____mm	_____mm
DARatio Max (2mm)	____mm	_____mm
IR	_____mm^{-1}	_____mm^{-1}
Max Inv Radius	_____mm^{-1}	_____mm^{-1}
HC radius	_____mm	_____mm
CCT	_____ µm	_____ µm
ARTh	_____	_____
Pachy Slope	_____ µm	_____ µm
SP-A1	_____	_____
CBI	_____	_____
SSI	_____	_____

Recogida de lágrima Si No

Clasificación Agudeza visual Lejana:

0,05- o inferior	1	0,400-0,500	4	1,00 o superior	7
0,100-0,160	2	0,600-0,700	5		
0,200-0,300	3	0,800-0,900	6		

Clasificación de los Signos Biomicroscópicos:

Nervios Corneales Visibles	1	Varios	4
Estrías de Vogt	2	Incurvamiento Inferior	5
Anillo de Fleischer	3	Leucoma corneal	6

Annex 2

Ethics committee

XUNTA DE GALICIA
CONSELLERÍA DE SANIDADE
Secretaría Xeral Técnica

Comité de Ética de la Investigación
Santiago Lugo

galicia

DICTAMEN DEL COMITÉ DE ÉTICA DE LA INVESTIGACIÓN DE SANTIAGO-LUGO

Ana Estany Gestal, Secretaria del Comité de Ética de la Investigación de Santiago-Lugo,

CERTIFICA:

Que este Comité evaluó en su reunión del día 15 de enero de 2020 el estudio:

Título: Línea de investigación en patología ocular corneal
Versión: 1.0
Promotor/a: M.ª Isabel Lema Gesto
Investigador/a: M.ª Isabel Lema Gesto
Código de Registro: 2019/623

Y que este Comité, tomando en consideración la pertinencia del estudio, el conocimiento disponible, los requisitos legales aplicables y los Procedimientos Normalizados de Trabajo del Comité, emite un dictamen **FAVORABLE** para la realización del citado estudio.

Documento asinado dixitalmente por:
Ana Estany Gestal (20/01/2020 14:41)
https://sede.xunta.gal/cve?idcve=SAOC-M4G4-BOAH-OF4O-TCSQ-D157-9527-7164-09

NOTA: Se le recuerda que en el caso de que en este estudio se recluten pacientes, el equipo investigador debe tener disponible el Documento de Consentimiento Informado (Hojas de Información y Hojas de Firma) tanto en *galego* como en castellano en el momento de comenzar el reclutamiento.

Xacobeo 2021

XUNTA DE GALICIA
CONSELLERÍA DE SANIDADE
Secretaría Xeral Técnica

Comité de Ética de la Investigación
Santiago Lugo

galicia

DICTAMEN DEL COMITÉ DE ÉTICA DE LA INVESTIGACIÓN DE SANTIAGO-LUGO

Mª Mercedes Rodicio García, Vicesecretaria del Comité de Ética de la Investigación de Santiago-Lugo,

CERTIFICA:

Que este Comité evaluó en su reunión del día 19 de mayo de 2020 el estudio**:**

Título: Análisis proteómico lagrimal y estudio tomográfico corneal en hijos de pacientes con queratocono
Versión: V2
Promotor/a: M.ª Isabel Lema Gesto
Investigador/a: M.ª Isabel Lema Gesto; Pablo Herbella Lorenzo
Código de Registro: 2020/089 ILG-APET-2020-01

Y que este Comité, tomando en consideración la pertinencia del estudio, el conocimiento disponible, los requisitos legales aplicables y los Procedimientos Normalizados de Trabajo del Comité, emite un dictamen **FAVORABLE** para la realización del citado estudio.

NOTA: Se le recuerda que en el caso de que en este estudio se recluten pacientes, el equipo investigador debe tener disponible el Documento de Consentimiento Informado (Hojas de Información y Hojas de Firma) tanto en gallego como en castellano en el momento de comenzar el reclutamiento.

Xacobeo 2021

Lista de verificación para Tese con estudos observacionales. **EPIDEMIOLOXÍA STROBE**

Si/non/NA		**páxina**
Título e resumo		
SI	Indique, no título ou no resumo, o deseño do estudo	III
SI	Proporcione no resumo unha sinopse informativa e equilibrada do que se fixo e o que se atopou.	IV-IX
Introdución		
SI	Indique o fundamento científico da Investigación que se comunica	1-25
Obxectivos		
SI	Indique os obxectivos específicos, incluída calquera hipótese preespecificada	27-29
Material e métodos		
Deseño do estudo		
SI	Presente os elementos crave do deseño do estudo	32
Contexto		
SI	Describa o marco, os lugares e as datas relevantes, incluídos os períodos de recrutamento, exposición, seguimento e recolleita de datos.	32-33
Participantes		
SI	Para estudos de cohortes: proporcione os criterios de elixibilidade, así como as fontes e o método de selección dos participantes. Especifique os métodos de seguimento	32-33
SI	Estudos de casos e controis: proporcione os criterios de elixibilidade, así como as fontes e o proceso diagnóstico dos casos e o de selección dos controis. Proporcione as razóns para a elección de casos e controis.	32-33
N/A	Estudos transversais: proporcione os criterios de elixibilidade e as fontes e métodos de selección dos participantes	-
N/A	Estudos de cohortes apareados. Proporcione os criterios para a formación de parellas e o número de participantes con e sen exposición	-
N/A	Estudos de casos e controis apareados. Proporcione os criterios para a formación das parellas e o número de controis por cada caso	-
Variables		
SI	Defina claramente todas as variables: de resposta, exposicións, predictoras, confusoras e modificacoras do efecto. Se procede, proporcione os criterios diagnósticos	33-35
Fontes de datos/medidas		
SI	Para cada variable de interese, proporcione as fontes de datos e os detalles dos métodos de valoración (medida).	33-44

N/A	Si houbese máis dun grupo, especifique a comparabilidade dos procesos de medida	-
Sesgos		
SI	Especifique todas as medidas adoptadas para afrontar fontes potenciais de nesgo	34
Tamaño da mostra		
SI	Explique como se determinou o tamaño da mostra	33
Variables cuantitativas		
SI	Explique como se trataron as variables cuantitativas na análise. Se procede, explique como se categorizaron e por que	43
Métodos estatísticos		
SI	Especifique todos os métodos estatísticos, incluídos os empregados para controlar os factores de confusión	43
SI	Especifique todos os métodos utilizados para analizar subgrupos e interaccións	43
N/A	Explique o tratamento dos datos ausentes (missing data)	-
N/A	Estudo de cohortes: se procede, explique como se afrontan as perdas no seguimento	-
SI	Estudos de casos e controis: se procede, explique como se aparearon casos e controis	33
N/A	Estudos transversais: se procede, especifique como se ten en conta na análise a estratexia da mostraxe	-
SI	Describa as análises de sensibilidade	43
Resultados		
Participantes		
SI	Número de participantes en cada fase do estudo; por exemplo: cifras dos participantes potencialmente elixibles, os analizados para ser incluídos, os confirmados elixibles, os incluídos no estudo, os que tiveron un seguimento completo e os analizados	32
N/A	Razóns da perda de participantes en cada fase	-
N/A	Considere o uso dun diagrama de fluxo	-
Datos descritivos		
SI	Características dos participantes no estudo (p. ex., demográficas, clínicas, sociais) e información sobre exposicións e posibles factores de confusión	32-33
N/A	Número de participantes con datos ausentes en cada variable de interese	-
SI	Estudos de cohortes: resuma o período de seguimento (p. ex., promedio e total)	54
Datos das variables de resultado		
SI	Estudos de cohortes: describa o número de eventos do efecto, ou ben proporcione medidas resumo ao longo do tempo	54

SI	Estudos de casos e controis: describa o número de participantes en cada categoría de exposición, ou ben proporcione medidas resumo de exposición	47,48,57
N/A	Estudos transversais: describa o número de eventos do efecto, ou ben proporcione medidas resumo	-
Resultados principais		
N/A	Proporcione estimacións crúas (non axustadas) e, se procede, axustadas por factores de confusión, así como a súa precisión (p. ex., intervalos de confianza do 95%). Especifique os factores de confusión polos que se axusta e as razóns para incluílos	-
SI	Se categoriza variables continuas, describa os límites dos intervalos	94
N/A	Se fose pertinente, valore acompañar as estimacións do risco relativo con estimacións do risco absoluto para un período de tempo relevante	-
Outras análises		
SI	Describa outras análises efectuadas (de subgrupos, interaccións ou sensibilidade)	43
Discusión		
Resultados clave		
SI	Resuma os resultados principais dos obxectivos do estudo	60-70
Limitacións		
SI	Discuta as limitacións do estudo, tendo en conta posibles fontes de sesgo ou de imprecisión. Razoe tanto sobre a dirección como sobre a magnitude de calquera posible sesgo	70
Interpretación		
SI	Proporcione unha interpretación global prudente dos resultados considerando obxectivos, limitacións, multiplicidade de análises, resultados de estudos similares e outras probas empíricas relevantes	60-70
Xenerabilidade		
SI	Discuta a posibilidade de xeneralizar os resultados (validez externa)	60-70
Financiamento		
SI	Especifique o financiamento e o papel dos patrocinadores do estudo e, se procede, do estudo previo no que se basea o presente traballo	Pre-índice

Baseado na declaración STROBE. Lista de puntos esenciais que deben describirse na publicación de estudos observacionais

Annex 4

Open access license statement

This thesis by compendium includes the following three articles published under an Open Access license:

Article 1: Tear proteomics in keratoconus: a quantitative SWATH-MS analysis.

Authors: Maite López-López, Uxía Regueiro, Susana B. Bravo, María del Pilar Chantada-Vázquez, Rubén Varela-Fernández, Paulo Ávila-Gómez, Pablo Hervella, Isabel Lema.

Journal: Investigative Ophthalmology & Visual Science (IOVS).

Open Access License: Creative Common CC-BY-NC-ND. This work is licensed under a Creative Common Attribution-NonCommercial-NoDerivatives 4.0 International License, allowing the distribution and reproduction of the manuscript in any medium, as long as the original work is properly cited, not for commercial purposes, and not for altered content distribution. The following link provides more details about the journal's Open Access policy: https://arvojournals.org/SS/openaccess.aspx

Article 2: Shot-gun proteomics for the identification and profiling of the tear proteome of keratoconus patients.

Authors: Maite López-López, Uxía Regueiro, Susana B. Bravo, María del Pilar Chantada-Vázquez, Carmen Pena, Elío Díez-Feijoo, Pablo Hervella, Isabel Lema.

Journal: Investigative Ophthalmology & Visual Science (IOVS).

Open Access License: Creative Common CC-BY-NC-ND. This work is licensed under a Creative Common Attribution-NonCommercial-NoDerivatives 4.0 International License, allowing the distribution and reproduction of the manuscript in any medium, as long as the original work is properly cited, not for commercial purposes, and not for altered content distribution. The following link provides more details about the journal's Open Access policy: https://arvojournals.org/SS/openaccess.aspx

Article 3: Immunomodulatory effect of human lactoferrin on toll-like receptors 2 expression as a therapeutic approach for keratoconus.

Authors: Uxía Regueiro, Maite López-López, Rubén Varela-Fernández, Tomás Sobrino, Elio Diez-Feijoo, Isabel Lema.

Journal: International Journal of Molecular Science (IJMS).

Open Access License: Creative Common CC BY license. This work is licensed under a Creative Common CC BY license, which enables to distribute, remix, adapt, and build upon the material in any medium or format, so long as attribution is given to the creator. The license also allows for commercial use. For more details about the journal's Open Access policy: https://www.mdpi.com/openaccess

Keratoconus (KC) is a progressive corneal ectasia that leads to severe visual impairment and remains one of the leading causes of corneal keratoplasty worldwide. Family history is one of the main risk factors for its development, and corneal biomechanical weakness represents a hallmark of the early stages of this pathology, in which the corneal tissue progressively weakens as the disease progresses.
The molecular factors and pathways involved in the early and at-risk stages of the disease are still largely unknown. In this sense, this work focuses on identifying tear proteomic biomarkers and pathways related to corneal biomechanical weakness and KC at-risk stages. Furthermore, new insights into lactoferrin's involvement in the KC disease and its immunomodulatory capacity as a therapeutic approach are also provided.